

EFFECTS OF MODERATE STRESS-RELEASE DISTURBANCE  
ON THE SHEAR BEHAVIOUR OF LIGHTLY OVERCONSOLIDATED  
SIMULATED MARINE CLAY

by

MARK ROBERT JAMIESON

A thesis  
presented to the University of Manitoba  
in partial fulfillment of the requirements for the degree of  
Master of Science  
in  
Civil Engineering



National Library  
of Canada

Bibliothèque nationale  
du Canada

Canadian Theses Service    Service des thèses canadiennes

Ottawa, Canada  
K1A 0N4

The author has granted an irrevocable non-exclusive licence allowing the National Library of Canada to reproduce, loan, distribute or sell copies of his/her thesis by any means and in any form or format, making this thesis available to interested persons.

The author retains ownership of the copyright in his/her thesis. Neither the thesis nor substantial extracts from it may be printed or otherwise reproduced without his/her permission.

L'auteur a accordé une licence irrévocable et non exclusive permettant à la Bibliothèque nationale du Canada de reproduire, prêter, distribuer ou vendre des copies de sa thèse de quelque manière et sous quelque forme que ce soit pour mettre des exemplaires de cette thèse à la disposition des personnes intéressées.

L'auteur conserve la propriété du droit d'auteur qui protège sa thèse. Ni la thèse ni des extraits substantiels de celle-ci ne doivent être imprimés ou autrement reproduits sans son autorisation.

ISBN 0-315-54881-9

EFFECTS OF MODERATE STRESS RELEASE DISTURBANCE  
ON THE SHEAR BEHAVIOUR OF LIGHTLY OVERCONSOLIDATED  
SIMULATED MARINE CLAY

BY

MARK ROBERT JAMIESON

A thesis submitted to the Faculty of Graduate Studies of  
the University of Manitoba in partial fulfillment of the requirements  
of the degree of

MASTER OF SCIENCE

© 1989

Permission has been granted to the LIBRARY OF THE UNIVER-  
SITY OF MANITOBA to lend or sell copies of this thesis, to  
the NATIONAL LIBRARY OF CANADA to microfilm this  
thesis and to lend or sell copies of the film, and UNIVERSITY  
MICROFILMS to publish an abstract of this thesis.

The author reserves other publication rights, and neither the  
thesis nor extensive extracts from it may be printed or other-  
wise reproduced without the author's written permission.

## Abstract

The main objectives of this thesis were to examine the effects of moderate stress release disturbance on samples of lightly overconsolidated simulated marine clay and to search for a laboratory procedure that best recovers the in-situ undrained shear behaviour. Thirteen "samples" of illitic clay were consolidated one-dimensionally, stored either "drained" or "undrained" for one of three storage periods, reconsolidated using one of three reconsolidation procedures, and then subjected to undrained shearing. The results were then compared with those from five in-situ "control specimens" which had not been offloaded, stored or reconsolidated.

For samples stored either "drained" or "undrained", those stored for the shortest period of time and then reconsolidated to the in-situ stress state gave the best estimate of the in-situ undrained shear strength,  $c_u$  and stress-strain behaviour. For "samples" which were stored for longer periods and reconsolidated to a stress state different from the in-situ,  $c_u$  was underestimated. The decrease in  $c_u$  with an increase in storage time was larger for the "samples" which were stored "drained" rather than "undrained".

## Acknowledgements

The author wishes to express his sincere thanks to his advisor, Dr. J. Graham, for his advice, encouragement, and patience throughout the entire project and especially during the preparation of this thesis.

A special thanks is given to Dr. David Ho, whose help during the technical review and testing program was greatly appreciated.

The author also wishes to thank fellow graduate students Farbod Saadat, Alan Wan, Jian-Hua Yin, and especially Brian Lignau for their assistance throughout the program.

Special thanks is also given to the technical staff in the Civil Engineering Department, and in particular Narong Piamsalee, for their technical assistance during the experimental investigation.

Financial assistance in the form of NSERC funding is also acknowledged.

The author is deeply indebted to his parents for the continual support and encouragement throughout his graduate studies.

## Table of Contents

	<u>Page</u>
Abstract.....	i
Acknowledgements.....	ii
Table of Contents.....	iii
List of Symbols.....	v
List of Tables.....	viii
List of Figures.....	ix
 <u>Chapter</u>	
1. Introduction.....	1
1.1 General.....	1
1.2 Objectives.....	4
2. Literature Review and Pertinent Theory.....	2
2.1 Introduction.....	2
2.2 Review of Process Disturbance.....	2
2.3 Gassy Sediments.....	12
2.4 Recovering In-situ Undrained Shear Strength.....	19
3. Testing Program.....	23
3.1 Introduction.....	23
3.2 Sample Preparation and Test Procedures.....	25
3.2.1 Triaxial Consolidation.....	26
3.2.2 Back Pressuring.....	27
3.3 Design of the Current Testing Program.....	28
4. Consolidation, Unloading, Storage, and Reconsolidation Results.....	31
4.1 Introduction.....	31
4.2 Consolidation.....	32
4.2.1 Slurry Consolidation.....	32
4.2.2 Triaxial Consolidation.....	35
4.3 Unloading.....	39
4.4 Storage.....	42
4.5 Reconsolidation.....	47

	<u>Page</u>
5. Undrained Shear Test Results.....	51
5.1 Introduction.....	51
5.2 Stress-Strain Relationships.....	51
5.3 Effective Stress Paths.....	54
5.4 Porewater Pressure Generation.....	58
5.5 Elastic Modulus.....	61
6. Discussion and Comparison With Previous Work.....	63
6.1 Introduction.....	63
6.2 Soil Properties and Moisture Content Analysis.....	63
6.3 Undrained Shear Behaviour.....	68
6.3.1 Failure Envelopes.....	68
6.3.2 Influence of Storage and Reconsolidation Procedures on Undrained Shear Strength.....	70
6.3.3 Failure Axial Strains.....	73
6.3.4 Porewater Pressure Generation.....	74
6.4 End of Test - "Critical State".....	76
7. Conclusions and Suggestions for Further Research.....	78
7.1 Conclusions.....	78
7.2 Suggestions for Further Research.....	82
Bibliography.....	83
Tables.....	88
Figures.....	93
Appendix A High Pressure Testing.....	175

### List of Symbols

- A,  $\bar{B}$  - porewater pressure parameters (after Skempton 1954)
- $A_f$  - value of  $A = \Delta u / \Delta q$  at failure
- $A_u$  - value of  $A$  during undrained shear unloading
- $c'$  - effective cohesion
- $c_u$  - undrained shear strength
- CU - strain-controlled, consolidated, undrained compression test
- $e$  - voids ratio
- $E_{50}$  - elastic modulus to 50 % of maximum deviator stress in undrained shear
- $G_s$  - specific gravity
- $I_p$  - plasticity index
- $K_0$  - lateral coefficient of earth pressure at rest  
(=  $\sigma'_3 / \sigma'_1$ )
- $m$  - porewater pressure parameter (=  $\Delta u / \Delta p$ )
- OCR - overconsolidation ratio
- $p'$  - effective mean principle stress  
(=  $(\sigma'_1 + \sigma'_2 + \sigma'_3) / 3$ )
- $q$  - deviator stress (=  $\sigma_1 - \sigma_3$ )
- $u$  - porewater pressure
- $u_f$  - porewater pressure at failure
- $u_r$  - residual porewater pressure

- $u_{ri}$  - initial residual porewater pressure
- $u_{l/g}$  - liquid to gas saturation pressure
- $v$  - volumetric strain ( $= (\epsilon_1 + \epsilon_2 + \epsilon_3)/3$ )
- $V$  - specific volume ( $= 1 + e$ )
- $w$  - moisture content
- $w_l$  - liquid limit
- $w_p$  - plastic limit
- $\sigma_{cell}$  - cell pressure (i.e.  $\sigma_3$ )
- $\sigma_1', \sigma_3'$  - major and minor principal effective stresses
- $\sigma_{ps}'$  - residual effective stress after perfect sampling
- $\sigma_h$  - total horizontal stress
- $\sigma_h'$  - effective horizontal stress
- $\sigma_v$  - total vertical stress
- $\sigma_v'$  - effective vertical stress
- $\sigma_{vc}'$  - effective preconsolidation pressure
- $\sigma_{v0}'$  - in-situ effective vertical (overburden) pressure
- $\phi'$  - effective angle of shearing resistance
- $\epsilon_1, \epsilon_3$  - major and minor principal strains (i.e. axial and lateral strains in triaxial compression test)
- $\kappa_1$  - slope of reload line in  $\ln p', V$  space during triaxial consolidation
- $\kappa_2$  - slope of reload line in  $\ln p', V$  space during triaxial consolidation
- $\lambda_1$  - slope of normally consolidated line in  $\ln \sigma_v, V$  space during cylinder consolidation

- $\lambda_2$  - slope of normally consolidated line in  $\ln p', V$   
space during triaxial consolidation
- $\Delta p$  - change in total mean principal stress
- $\Delta u$  - change in porewater pressure

## List of Tables

<u>Table</u>	<u>Page</u>
3.1 Classification Results of Illitic Clay.....	88
4.1 Summary of Consolidation Results.....	89
4.2 Summary of Test Results During Storage and Reconsolidation.....	90
5.1 Summary of Undrained Shear Test Results.....	91
6.1 Water Contents Throughout Test.....	92

## List of Figures

<u>Figure</u>		<u>Page</u>
1.1 a,b	Typical Gravity and Pile Supported Seabed Structures (Hoeg 1986).....	93
2.1	Isotropic Unloading Behaviour of Saturated, Unsaturated and Gassy Soils (Sobkowicz and Morgenstern 1984).....	94
3.1	Schematic Diagram of Modelled In-situ Conditions.....	95
4.1 a,b	One-Dimensional Slurry Consolidation, $\text{Log}(\sigma_v)$ vs. $w$ .....	96
4.2 a,b	Triaxial Consolidation Samples T771, T772 $\text{log } p'$ vs. $V$ .....	97
4.2 c,d	Triaxial Consolidation Samples T773, T787 $\text{log } p'$ vs. $V$ .....	98
4.2 e,f	Triaxial Consolidation Samples T777, T774 $\text{log } p'$ vs. $V$ .....	99
4.2 g,h	Triaxial Consolidation Samples T775, T778 $\text{log } p'$ vs. $V$ .....	100
4.2 i,j	Triaxial Consolidation Samples T779, T789 $\text{log } p'$ vs. $V$ .....	101
4.2 k,l	Triaxial Consolidation Samples T781, T782 $\text{log } p'$ vs. $V$ .....	102
4.2 m,n	Triaxial Consolidation Samples T784, T788 $\text{log } p'$ vs. $V$ .....	103
4.3	Normalized Yield Locus of Illitic Clay, $q$ vs. $p'$ (Graham and Lau 1988).....	104
4.4	Typical Unload-Reload Zone of Anisotropic Clay $q$ vs. $p'$ (Graham and Houlsby 1983).....	105
4.5	Final Consolidation Points For Control Specimens of Kwok (1984), Lau (1986) and Author in $V$ vs. $\text{log } p'$ .....	106
4.6 a	Porewater Pressure Behaviour During Isotropic Unloading, Sample T777.....	107

4.6 b	Porewater Pressure Behaviour During Isotropic Unloading, Sample T774.....	108
4.6 c	Porewater Pressure Behaviour During Isotropic Unloading, Sample T775.....	109
4.6 d	Porewater Pressure Behaviour During Isotropic Unloading, Sample T778.....	110
4.6 e	Porewater Pressure Behaviour During Isotropic Unloading, Sample T779.....	111
4.6 f	Porewater Pressure Behaviour During Isotropic Unloading, Sample T789.....	112
4.6 g	Porewater Pressure Behaviour During Isotropic Unloading, Sample T781.....	113
4.6 h	Porewater Pressure Behaviour During Isotropic Unloading, Sample T782.....	114
4.6 i	Porewater Pressure Behaviour During Isotropic Unloading, Sample T784.....	115
4.6 j	Porewater Pressure Behaviour During Isotropic Unloading, Sample T788.....	116
4.7 a,b	Swelling Behaviour During Drained Storage v vs. log (time).....	117
4.8 a,b	Porewater Pressure Behaviour During Undrained Storage, u vs. log (time).....	118
4.9 a,b	Typical Volumetric Straining During Reconsolidation of Samples Stored Undrained Samples T784 and T788.....	119
4.10 a,b	Typical Volumetric Straining During Reconsolidation of Samples Stored Drained Samples T777 and T775.....	120
5.1 a,b	Undrained Stress-Strain and Porewater Pressure Results, Sample T771 (Control).....	121
5.2 a,b	Undrained Stress-Strain and Porewater Pressure Results, Sample T772 (Control).....	122
5.3 a,b	Undrained Stress-Strain and Porewater Pressure Results, Sample T773 (Control).....	123

5.4 a,b	Undrained Stress-Strain and Porewater Pressure Results, Sample T785 (Control).....	124
5.5 a,b	Undrained Stress-Strain and Porewater Pressure Results, Sample T787 (Control).....	125
5.6 a,b	Undrained Stress-Strain and Porewater Pressure Results, Sample T777.....	126
5.7 a,b	Undrained Stress-Strain and Porewater Pressure Results, Sample T774.....	127
5.8 a,b	Undrained Stress-Strain and Porewater Pressure Results, Sample T775.....	128
5.9 a,b	Undrained Stress-Strain and Porewater Pressure Results, Sample T778.....	129
5.10 a,b	Undrained Stress-Strain and Porewater Pressure Results, Sample T776.....	130
5.11 a,b	Undrained Stress-Strain and Porewater Pressure Results, Sample T779.....	131
5.12 a,b	Undrained Stress-Strain and Porewater Pressure Results, Sample T789.....	132
5.13 a,b	Undrained Stress-Strain and Porewater Pressure Results, Sample T781.....	133
5.14 a,b	Undrained Stress-Strain and Porewater Pressure Results, Sample T781*.....	134
5.15 a,b	Undrained Stress-Strain and Porewater Pressure Results, Sample T782.....	135
5.16 a,b	Undrained Stress-Strain and Porewater Pressure Results, Sample T784.....	136
5.17 a,b	Undrained Stress-Strain and Porewater Pressure Results, Sample T788.....	137
5.18	Effective Stress Path During Undrained Shear In $p'$ vs. $q$ Space, Sample T771 (Control).....	138
5.19	Effective Stress Path During Undrained Shear In $p'$ vs. $q$ Space, Sample T772 (Control).....	139
5.20	Effective Stress Path During Undrained Shear In $p'$ vs. $q$ Space, Sample T773 (Control).....	140

5.21	Effective Stress Path During Undrained Shear In $p'$ vs. $q$ Space, Sample T785 (Control).....	141
5.22	Effective Stress Path During Undrained Shear In $p'$ vs. $q$ Space, Sample T787 (Control).....	142
5.23	Effective Stress Path During Undrained Shear In $p'$ vs. $q$ Space, Sample T777.....	143
5.24	Effective Stress Path During Undrained Shear In $p'$ vs. $q$ Space, Sample T774.....	144
5.25	Effective Stress Path During Undrained Shear In $p'$ vs. $q$ Space, Sample T775.....	145
5.26	Effective Stress Path During Undrained Shear In $p'$ vs. $q$ Space, Sample T778.....	146
5.27	Effective Stress Path During Undrained Shear In $p'$ vs. $q$ Space, Sample T776.....	147
5.28	Effective Stress Path During Undrained Shear In $p'$ vs. $q$ Space, Sample T779.....	148
5.29	Effective Stress Path During Undrained Shear In $p'$ vs. $q$ Space, Sample T789.....	149
5.30	Effective Stress Path During Undrained Shear In $p'$ vs. $q$ Space, Sample T781.....	150
5.31	Effective Stress Path During Undrained Shear In $p'$ vs. $q$ Space, Sample T781*.....	151
5.32	Effective Stress Path During Undrained Shear In $p'$ vs. $q$ Space, Sample T782.....	152
5.33	Effective Stress Path During Undrained Shear In $p'$ vs. $q$ Space, Sample T784.....	153
5.34	Effective Stress Path During Undrained Shear In $p'$ vs. $q$ Space, Sample T788.....	154
5.35	Failure Envelope In $p'$ vs. $q$ Space For $\sigma'_{vc}=160$ kPa.....	155
5.36	Normalized Porewater Pressure Behaviour During Undrained Shear, in $\Delta u$ vs. $\Delta p$ Space Sample T771 (Control).....	156

5.37	Normalized Porewater Pressure Behaviour During Undrained Shear, In $\Delta u$ vs. $\Delta p$ Space Sample T772 (Control).....	157
5.38	Normalized Porewater Pressure Behaviour During Undrained Shear, In $\Delta u$ vs. $\Delta p$ Space Sample T773 (Control).....	158
5.39	Normalized Porewater Pressure Behaviour During Undrained Shear, In $\Delta u$ vs. $\Delta p$ Space Sample T785 (Control).....	159
5.40	Normalized Porewater Pressure Behaviour During Undrained Shear, In $\Delta u$ vs. $\Delta p$ Space Sample T787 (Control).....	160
5.41	Normalized Porewater Pressure Behaviour During Undrained Shear, In $\Delta u$ vs. $\Delta p$ Space Sample T777.....	161
5.42	Normalized Porewater Pressure Behaviour During Undrained Shear, In $\Delta u$ vs. $\Delta p$ Space Sample T774.....	162
5.43	Normalized Porewater Pressure Behaviour During Undrained Shear, In $\Delta u$ vs. $\Delta p$ Space Sample T775.....	163
5.44	Normalized Porewater Pressure Behaviour During Undrained Shear, In $\Delta u$ vs. $\Delta p$ Space Sample T778.....	164
5.45	Normalized Porewater Pressure Behaviour During Undrained Shear, In $\Delta u$ vs. $\Delta p$ Space Sample T776.....	165
5.46	Normalized Porewater Pressure Behaviour During Undrained Shear, In $\Delta u$ vs. $\Delta p$ Space Sample T779.....	166
5.47	Normalized Porewater Pressure Behaviour During Undrained Shear, In $\Delta u$ vs. $\Delta p$ Space Sample T789.....	167
5.48	Normalized Porewater Pressure Behaviour During Undrained Shear, In $\Delta u$ vs. $\Delta p$ Space Sample T781.....	168

5.49	Normalized Porewater Pressure Behaviour During Undrained Shear, In $\Delta u$ vs. $\Delta p$ Space Sample T781*.....	169
5.50	Normalized Porewater Pressure Behaviour During Undrained Shear, In $\Delta u$ vs. $\Delta p$ Space Sample T782.....	170
5.51	Normalized Porewater Pressure Behaviour During Undrained Shear, In $\Delta u$ vs. $\Delta p$ Space Sample T784.....	171
5.52	Normalized Porewater Pressure Behaviour During Undrained Shear, In $\Delta u$ vs. $\Delta p$ Space Sample T788.....	172
6.1	Graph Of The Undrained Shear Strength, $c_u$ vs. Specific Volume, $V$ During Shearing.....	173
6.2	Graph Of Effective Mean Pressure, $p'$ vs. Specific Volume, $V$ At The End Of Test.....	174
A.1	Schematic Diagram of High Pressure Triaxial Cell (Craig 1983).....	181
A.2	Predicted Isotropic Unloading Behaviour For In-situ Stress State of $\sigma'_v = \sigma'_h = 400$ kPa, $u = 2000$ kPa ( $\bar{B} = 1.0$ )....	182
A.3	Schematic Diagram of the Modified Pedestal Base Of High Pressure Triaxial Cell.....	183
A.4	Specific Volume, $V$ vs. Log (Time) During Consolidation Sample T790.....	184

## Chapter 1 - Introduction

### 1.1 General

The ongoing demand for energy resources has accelerated hydrocarbon recovery in nearshore and offshore waters in the last 20-30 years. The two most common types of seabed structures used as drilling platforms for the recovery of oil and natural gas are gravity structures and pile supported structures, as shown in Figs. 1.1a,b. Drilling platforms of the gravity structure type are supported on massive concrete footings which rest on the seabed. Applied loads resulting from wind, waves, or ice are resisted by the large mass of concrete and the large volume of foundation soil which it stresses. Drilling platforms on pile supported structures are supported by a tower configuration of steel members. Stability is provided from piles which penetrate into the seabed from the base of the tower. In both cases, economical and safe design of the foundation requires a good knowledge of the engineering properties of the supporting foundation soil and this can only be obtained through a thorough program of site investigation.

A properly conducted soil investigation requires a combination of both in-situ and laboratory testing to find the representative strength and settlement characteristics of the soil in question (Attwooll et al.1985; Jefferies et al.1985; Hoeg 1986). Both types of tests have their respective advantages and disadvantages, but the

disadvantages seem to be magnified when working in a marine environment (Richards 1984). Consequently, the design parameters obtained from either in-situ or laboratory testing may not be representative of the actual field conditions. Also, the costs of both in-situ and laboratory testing are very high, due mainly to the cost of mobilizing the drill-ships and the sophisticated equipment required for high quality testing (Sangrey 1972). Therefore, it is desirable to design an efficient and effective testing program.

Strength and compressibility determination from in-situ methods usually requires past knowledge of the material being investigated so that an empirical correlation can be made between the measured properties and actual field values. This correlation is not always available. With laboratory testing procedures the main problem is associated with the methods used to obtain samples and their treatment prior to testing. Clay specimens taken from the seabed are subjected to two types of disturbance which can significantly alter their in-situ particle structure, porewater pressure (pwp) distribution, and water content. First, a mechanical disturbance is introduced into the specimen when the sampling tube is inserted into the soil mass. Richards and Zuidberg (1986) indicated that recent advances in sampling technology have reduced the amount of mechanical disturbance introduced during the sampling process. However it can never be totally eliminated regardless of the technique employed. The second type of disturbance induced in the specimen is caused by the release of the confining pressure as the sample is lifted from its seabed

environment to the deck of the sampling ship. The release of stresses causes straining in the microstructure of the clay, and can change its strength and compressibility characteristics.

This project is a continuation of the work performed by Kwok (1984), Ambrosie (1985), and Lau (1986) which examined the disturbance of reconstituted clay samples due to pressure release alone. The undrained shear behavior of "control specimens" which have not been subjected to any pressure release or mechanical disturbance is compared with that of so called "samples" which have undergone pressure release disturbance but no mechanical disturbance. The quotation marks, " ", signifying the simulated "samples" and "control specimens" will be omitted in the following text. However, it should be remembered that these terms are defined here strictly for reconstituted test specimens used in this testing program.

The work described in the following text continues the earlier investigations of lightly overconsolidated clay (overconsolidation ratio, OCR=2). The previous projects on overconsolidated clay, (Kwok 1984 and Lau 1986) have been subject to some criticism for the value of the at-rest lateral coefficient of earth pressure,  $K_0 = \sigma'_h / \sigma'_v$  used for overconsolidated specimens. It has been shown that  $K_{0oc}$  (the value of  $K_0$  for an overconsolidated state) approaches 1.0 for OCR=2, from its normally consolidated value of  $K_{0nc} \approx 0.53$  for the type of soil used in this series of investigations (Brooker and Ireland 1965; Mayne and Kulhawy 1982; Kirkpatrick et al. 1986). The earlier projects of Kwok (1984) and Lau (1986) held  $K_0$  constant at

0.53 for both the normally consolidated and overconsolidated stress states. This was done at the time to remove one of the possible test variables from the test program. Subsequently however, it was considered necessary to use a more realistic value of  $K_0$ , and this forms the basis of the research work that will be reported in this thesis. The testing program from the earlier work has been duplicated in this program as far as possible so that direct comparisons can be made between results for  $K_{0oc} = 0.53$  used by the earlier researchers (Kwok 1984 and Lau 1986) and  $K_{0oc} = 1.0$  used in the present research.

## 1.2 Objectives

The main objective of this study is to find a laboratory procedure for effective reconsolidation of reconstituted samples of illitic clay which have experienced stress release and a subsequent storage period causing disturbance. The procedure should produce the best possible evaluation of the in-situ undrained shear behavior of the clay. Samples in this project were subjected to the same storage conditions and reconsolidation procedures as those used by Kwok (1984), Ambrosie (1985), and Lau (1986) which simulate the actual treatment of recovered specimens. This permits comparisons being drawn between the results of this and the earlier studies to find the effect of changing the value of  $K_{0oc}$  during the preparation of the specimens.

In addition, a limited number of samples were tested at

significantly higher pressure levels than in the previous projects to simulate sampling in deeper water. This high pressure testing has been performed to initiate a new technology at the University of Manitoba. The behavior of gassy soils and the cavitation of water within the sample and the testing equipment have been investigated in principle as potential problems during the pressure release stage.

The laboratory testing program for studying the stress release effects consisted of eighteen (18) - 76 mm diameter reconstituted specimens of illite clay tested in triaxial compression. Of the 18 specimens, two were considered less useful than the rest because accurate control of water contents during testing was lost. The tests therefore had to be repeated. Four of the remaining specimens were tested as control specimens to evaluate the in-situ behavior. The remaining 12 were tested as simulated samples, with 2 being tested at high pressure.

Chapter 2 of the thesis provides a review of the previous research that has investigated the effects of pressure release disturbance. Details of the testing program will be discussed in Chapter 3. Chapter 4 presents the results obtained from the consolidation, unloading, storage, and reconsolidation stages. The results of the undrained shear tests are presented in Chapter 5. Chapters 6 and 7 present a discussion and synthesis of the test data and conclusions drawn from the study. The high pressure testing will be discussed in Appendix A. All tables, figures, and appendices referred to in the text will be presented at the end of the thesis.

## Chapter 2 - Literature Review and Pertinent Theory

### 2.1 Introduction

Accurate estimations of the undrained shear strength,  $c_u$  of foundation soils are required for safe and cost-efficient foundation design for offshore structures. However, it is difficult to measure undrained strength correctly using either in-situ or laboratory testing methods. Test samples recovered from the seabed are inevitably subjected to two sorts of disturbance outlined in Chapter 1, that is mechanical disturbance and pressure release induced disturbance. This chapter presents a detailed review of pressure release disturbance which is the subject of this thesis.

### 2.2 Review of Process Disturbance

The amount of stress release disturbance induced during retrieval of samples depends mainly on the magnitude and nature of the stress change, that is, on the reduction and changes of the principal stress system (Kirkpatrick et al. 1986; Graham and Lau 1988). Therefore, the problem of stress release disturbance is seen not only in the offshore geotechnical industry but in onshore sampling and testing as well. This section reviews research on the effects of stress release on both onshore and offshore soils.

Removal of a test specimen from its in-situ environment will

inevitably cause the confining pressures to be released. There are two processes which lead to this pressure release. First, when the sampling tube is pushed into the clay, there is shear distortion produced around the outside surface of the specimen. This produces a thin shell of remoulded clay which will readily compress, allowing the rest of the sample to experience lateral expansion. As a result, there is a reduction in the effective stresses inside the sample (Graham and Lau 1988). Secondly, the total stresses acting on the sample are reduced to zero when the sample is extruded from the sampling tube for either visual classification and geological testing on board the ship (de Ruiter 1976; Young et al. 1983) or during installation of the specimen into a triaxial apparatus in the laboratory (Graham and Lau 1988).

In all cases, the reduction of the total confining stresses causes the specimen to attempt to swell, and negative porewater pressures or suction pressure will be introduced into the pore structure of the clay. If the sample has free access to water, in what is known as a "drained storage" condition, the negative porewater pressures will relax with time and eventually go to zero (Feng and Lui 1986). This relaxation of the negative porewater pressures is dependent mainly on the permeability of the clay. The other extreme of the drainage conditions is when the sample is subjected to a stress release and storage period with no access to water. That is, the specimen is subjected to an "undrained storage" condition. It has been found in this case as well that the negative porewater pressure

will often relax with time (Graham et al.1987). The reasons for the relaxation of negative porewater pressures appear to be different for the two cases. In the drained case, the suction in the sample will decrease due to intake of water into the sample. In the undrained case, where no water is available to enter the sample and alleviate the suction, it has been postulated that the relaxation may be due to slow changes in the microstructure of the clay (Kirkpatrick and Khan 1984; Graham et al.1987). However, Graham et al. also suggested that the relaxation of the suction may in part be due to diffusion of water through the sample membrane or around various seals while the specimen is in the triaxial apparatus. This is not then truly an undrained case. Kirkpatrick and Khan (1984) also noted that the amount of relaxation for a given time period was larger for a more permeable clay.

During unloading, the total stress system acting on the sample is reduced to zero. As a result of the effective stress principle, the value of the effective mean stress,  $p'$  after sampling is therefore equal in magnitude but opposite in sign to the negative porewater pressure generated (that is  $p' = p - u$ , with  $p=0$ ). It was once commonly believed that "perfect samples" held their in-situ  $p'$  values constant after experiencing a stress release by generating negative porewater pressures, where the term "perfect sample" was defined by Ladd and Lambe (1963) as one which is subjected only to the disturbance associated with the release of the in-situ shear stresses alone. However, this has been challenged by several researchers. Both Ladd

and Lambe (1963) and Skempton and Sowa (1963) reported decreases of 20% in  $p'$  after "perfect sampling" from test data on normally consolidated clay. More recently, Lau (1986) found  $p'$  to decrease as much as 15% after the release of the in-situ stresses, also from tests on normally consolidated clay.

In the general case, the in-situ stress state of a specimen before sampling is anisotropic, that is,  $\sigma'_v \neq \sigma'_h$ . The stress release associated with sampling causes the stress system to go to an isotropic state, that is  $\sigma'_v = \sigma'_h = -u$  (Skempton and Sowa 1963; Ladd and Bailey 1964; Kulkarni 1983; Graham et al. 1987). Ladd and Lambe (1963) presented the following equation to determine the residual isotropic effective stress,  $\sigma'_{ps}$  after perfect sampling for normally and lightly overconsolidated clays:

$$\sigma'_{ps} = \sigma'_{v0} [ K_0 + A_u ( 1 - K_0 ) ] \dots\dots\dots 2.1$$

where  $\sigma'_{v0}$  = in-situ vertical effective stress

$K_0$  = at rest lateral coefficient of earth pressure

$A_u$  = undrained pore pressure coefficient

$$= \frac{u - \sigma_h}{\sigma_v - \sigma_h} \dots\dots\dots 2.2$$

If the swelling of the sample is purely isotropic and elastic in nature then  $A_u$  would be 0.333 (Skempton and Sowa 1963) and  $\sigma'_{ps}$  would equal the in-situ  $p'$  value. Reconsolidating the sample to its in-situ effective stresses would then return the sample to its in-situ water content and soil fabric structure (Coatsworth 1986).

A number of researchers have used this equation to analyse stress release data (for example, Noorany and Seed 1965; Okumura 1977; Graham

and Lau 1988). Most values of  $A_u$  reported in the literature differ significantly from 0.333 (for example, Ladd and Lambe 1963 reported  $A_u$  values of -0.1 to 0.2 for a normally consolidated silty clay). However, in the earlier investigations of this continuing research project at the University of Manitoba, Kwok (1984) and Lau (1986) reported average values of  $A_u$  of 0.37 and 0.42 for illite clay with  $OCR=2$ . Also, Ladd and Lambe (1963) reported an  $A_u$  value of 0.3 for a heavily overconsolidated plastic clay. This suggests only small deviations from isotropic elastic material behaviour. Lau (1986) proposed that the deviations from isotropic elastic behaviour observed in his testing program may be due in part to an anisotropic elastic response of the soil material (Graham and Houlsby 1983).

In the investigation described in this thesis, the in-situ stress state prior to the release of the confining pressure is isotropic for the reasons outlined in Section 1.1. Equation 2.1 proposed by Ladd and Lambe (1963) will therefore not apply since the variable  $A_u$  is valid for unloading of shear stress only, which does not exist in the samples tested in this project prior to the unloading stage. The principal point to be remembered however, is that swelling that accompanies unloading should be primarily an elastic response with little plastic straining occurring.

Skempton and Sowa (1963) determined from an experimental investigation that a stress release will not significantly affect the undrained shear strength provided the water content is not changed and the associated strains in the microstructure of the clay are small.

Small strains of this nature would normally be associated with "elastic" strains. According to Coatsworth (1986), a laboratory procedure of reconsolidating a sample to its in-situ stress state would therefore return the sample to its in-situ water content and fabric structure. A subsequent undrained shear test would then give strengths representative of the actual values in the ground. Reconsolidation of a sample to its in-situ stress state has been found to successfully reproduce the in-situ undrained shear strength by a number of researchers, including Kirkpatrick and Khan (1984), Graham et al.(1987), Kirkpatrick et al.(1986), and Graham and Lau (1988).

To be successful in recovering the in-situ strengths, a qualitative analysis of the amount of disturbance induced in the sample must first be made in order to choose the correct reconsolidation procedure and this will be discussed in Section 2.4. There are three main factors which dictate the amount of stress release disturbance introduced into a sample during sampling. The first two are thought by Kirkpatrick et al.(1986) to be the most significant factors affecting the amount of disturbance in saturated soils. The first is the amount of reduction in the effective mean stress. They found that the higher the reduction in the in-situ  $p'$ , the more pronounced the stress release effects will be. The second significant variable is the degree of change in the principal stress system, which can be expressed by the change in the effective stress ratio,  $\sigma'_1 / \sigma'_3$ . The change from in-situ anisotropic stresses to an isotropic stress field will cause some rearrangement of the clay

microstructure (Graham and Lau 1988). This will change the stress-strain response of the clay during subsequent strength testing.

The last major cause of sample disturbance from pressure release is related to the amount of gas present in the pore structure of the clay. For samples recovered from large depths below the ocean surface where the total confining pressure is very high, this can be the most influential element in determining the amount of disturbance. Recovered samples which contain a large amount of gas in the pore structure of the clay have been observed to expand from both ends of the sampling tube. Also, large gaps along the length of the core and the odor of gas are frequently observed (McIver 1974). In many cases, the samples are damaged so badly that they can not be transferred to a triaxial cell for strength testing in an intact form.

### 2.3 Gassy Sediments

The research testing reported in the later sections of this thesis deals only with saturated soils. As part of the overall project in the University of Manitoba, however, the author was required to review the current understanding of gassy soil behaviour for possible future work. This work is placed on record in the following section.

The primary gases found in the interstitial water of marine sediments are methane  $\text{CH}_4$ , nitrogen  $\text{N}_2$ , and carbon dioxide  $\text{CO}_2$ , with other gases such as oxygen  $\text{O}_2$ , ammonia  $\text{NH}_3$ , hydrogen sulfide  $\text{H}_2\text{S}$ , and

ethane  $C_2H_6$  being found in specific locations (Kaplan 1974, McIver 1974, and Chace 1985). These gases are found primarily as free gas bubbles or dissolved in the interstitial water, but can occur as solid gas hydrates if the pressure is high and the temperature is low (Chace 1985).

Gas hydrates or clathrate hydrates are solid compounds resembling snow or low density ice in appearance that can exist well above the ice formation point (Hand et al. 1984; Hitchon 1974). They are compounds in which water forms a crystal lattice structure containing voids that can incorporate guest molecules such as methane (Miller 1974). Hitchon (1974) believes that natural gas hydrates in sedimentary basins are most likely formed through a reduction in temperature and not necessarily an increase in pressure. Therefore, they are most likely to exist in areas of extensive and relatively thick continuous permafrost. There is currently no conclusive method available for verifying the existence of gas hydrates in-situ (Stoll 1974; Hitchon 1974). However, Bryan (1974) stated that unusually high seismic velocities in gas rich sediments suggest the possible existence of gas hydrates.

It is believed that there are four main sources of the natural gases found in marine soils (Kaplan 1974). The first is from the atmosphere in which gases initially dissolved at the water surface make their way downward into the seabed. Oxygen and carbon dioxide are the main atmospheric gases that can be dissolved into the seawater. However, it is believed that this source accounts for only

a small amount of the total  $O_2$  and  $CO_2$  present. The second and most important process for gas generation is microbiological degradation of organic matter within the seabed. The dominant gases formed from this source are nitrogen and methane. Methane is the most abundant gas found throughout the world in marine soils and commonly comprises 80 - 100 % of the gases present. Thermocatalytic degradation of organic matter deep in the ocean bed is the third process in gas production. Small amounts of both  $CH_4$  and  $C_2H_6$  can be formed. The last major source of gases in marine soils is from submarine volcanic or geothermal processes. The major gas produced is  $CO_2$  but  $CH_4$ ,  $H_2$ ,  $N_2$ , and  $H_2S$  can also be produced and make their way up into seabed soils depending on the depth and type of the igneous source.

The amount of gas measured in recovered samples has been found to vary greatly (McIver 1974). When the sample is being raised to the ship, stress release occurs and gas can come out of solution. This has been evidenced by the presence of gas odor as the sampling tubes are opened and by the presence of large gaps along the length of the core caused by expanding gas. By the time the samples are sealed for gas measurement, a large amount of gas has often escaped. McIver reports that this is one of the reasons why the amount of gas measured in a recovered core is usually well below the theoretical amount that could be dissolved in the pore water.

The amount and state of gas present in the pore structure of a soil depends on the availability of that particular gas and its conditions of pressure and temperature. Based on ideal gas laws, the

theoretical amounts of free and dissolved gas can be calculated using the gas laws of Boyle, Charles, Henry, and Fick. Boyle's Law states that at a constant temperature, the volume of a gas,  $V$  is inversely proportional to the pressure,  $p$  acting on that gas, or

$$V \propto 1/p \dots\dots\dots 2.3$$

Therefore, the higher the pressure, the smaller the volume that the gas will occupy for a given temperature. Charles's Law states that the volume of a given quantity of gas is directly proportional to the absolute temperature,  $T$  ( $^{\circ}K$ ) for a constant pressure, or

$$V \propto T \dots\dots\dots 2.4$$

As the temperature reduces, the volume that a given mass of gas will occupy also decreases. Henry's law relates the equilibrium amount of gas dissolved in the pore fluid to pressure. It states that the equilibrium solubility of a gas,  $C_g$  in any solvent is directly proportional to the pressure of that gas,  $p_g$  over the solvent. The proportionality constant,  $k$  is called Henry's constant and depends on the type of gas and solvent and the temperature of the system. Henry's Law is written as

$$C_g = k * p_g \dots\dots\dots 2.5$$

Finally, Fick's Law relates the mass flow rate of gas through a soil medium to the pressure differential acting on that gas, or

$$v_a = -D * (\delta p / \delta y) \dots\dots\dots 2.6$$

where  $v_a$  = mass flow rate of the gas

$D$  = transmission constant with the same units as permeability

$p$  = absolute gas pressure

This equation applies to the rate at which the gas goes into solution in the pore fluid of the soil structure.

If a soil has a relatively large amount of gas dissolved in the pore fluid, and if the presence of the gas has a dominating influence on the loading or unloading behaviour of the soil, then the soil is defined as a gassy soil (Sobkowicz and Morgenstern 1984, 1987). Fig. 2.1, reproduced from Sobkowicz and Morgenstern (1984), shows the typical isotropic unloading behaviour of the three recognized classes of soil, that is saturated, unsaturated, and gassy soils. Initially, all three soil types follow the same unloading path when the porewater pressure is greater than the liquid to gas saturation pressure,  $u_{l/g}$ , (see curve I Fig. 2.1) where  $u_{l/g}$  is defined as the value of the minimum fluid pressure where a given volume of gas is completely dissolved in the porefluid. Its value depends on the volume of gas and the temperature and type of the gas and porefluid system. During this stage, Skempton's pore pressure coefficient,  $B = \Delta u / \Delta \sigma$  is equal to 1.0. Only at pressures less than  $u_{l/g}$  can free gas exist. The behaviour of each soil type changes as the porewater pressure is lowered below  $u_{l/g}$ .

Consider first, saturated soil. This is soil in which the entire volume of the void space is occupied by a fluid, in this case water, and there is no free gas present at any value of pressure above the cavitation point of the fluid. The unloading curve continues at  $\bar{B} = 1.0$  for porewater pressures less than  $u_{l/g}$  (curve LN). For fine

grained saturated soil, the pores are small enough to sustain high porewater tensions due to the attractive forces between the water molecules and clay particles and from any capillary forces developed. Therefore, there will be no cavitation of the pore water. The value of the effective stress is kept constant throughout the unloading. The porewater pressure of coarse grained soil does not decrease below approximately -100 kPa which is thought to be pressure at which cavitation of water takes place (Sobkowicz and Morgenstern 1984). The pore size is too large to develop high attractive or capillary forces and no further decrease in porewater pressure can be sustained (curve LM). (From a review and analysis of all available data to that time, Temperly and Chambers (1946) believed that the tension pressure at which cavitation takes place in the water medium itself is in the order of 40 atm. The 1 atm. value quoted by Sobkowicz and Morgenstern (1984) may be the pressure at which the water molecules "pull" away from the soil particle boundaries and the subsequent low pressure voids will fill with water vapor. The value of this "pull away" pressure is dependent on the adhesion force developed between the water molecule and the soil particles (Knapp et. al. 1970). This is also cavitation, by definition, since water vapor will be formed in the cavity created as the water molecules pull away from the soil particles.)

Next, consider an unsaturated soil, which is one where there is only a small amount of free gas present in the pore structure of the soil. Once the porewater pressure goes below  $u_1/g$ , the relatively

small amount of gas which was initially completely dissolved in the pore fluid will begin to exsolve. The porewater pressure will continue to decrease as the unloading continues but the rate at which it does so will be lower than the rate at which the total isotropic stress decreases, that is  $\bar{B} < 1.0$  (see curve K Fig. 2.1). The effective stress will always be positive, and will never reach zero.

Finally, consider the behaviour of gassy soil, where there is a large amount of gas present. Once the porewater pressure becomes equal to  $u_{1/g}$ , the large amount of gas that was dissolved in the pore fluid begins to exsolve at a very fast rate. From curve J, Fig. 2.1, it can be observed that the porewater pressure of the soil remains relatively constant for a considerable change in total stress. Therefore, the effective stress decreases at approximately the same rate as the total stress. At some point, the effective stress will reach zero, but the porewater pressure and the total stress will both be greater than zero, and equal to each other. The amount of gas present in the free and dissolved state will then follow the laws of Henry, Boyle and Charles. With a large amount of gas exsolving at very fast rates, the dynamics of the venting of the gas can cause the soil fabric to be completely disrupted. Triaxial test results will have little practical meaning since the specimen can be severely damaged or destroyed. Wide variations in the density of retrieved marine cores are commonly observed in actual sampling operations, and one cause of this is the effervescence (or initiation) and subsequent expansion of gas bubbles (Chace 1985). This causes the residual

effective pressure,  $\sigma_{ps}'$  to be greatly reduced from the in-situ effective stress (Okumura and Matsumoto 1981).

The formation of gas bubbles and their subsequent expansion can cause severe damage to a sample after retrieval. The offshore geotechnical testing industry considers this an extreme problem of pressure release disturbance. This, along with a number of other experimental problems must be overcome to achieve high quality testing of gassy soils. The primary goal of the laboratory testing described in this thesis is restricted to examining the pressure release disturbance of a fine grained saturated soil with isotropic unloading behaviour similar to that of curve ILN in Fig. 2-1.

#### 2.4 Recovering In-situ Undrained Shear Strength

Ladd and Bailey (1964) stated that the strengths of tube samples measured from unconsolidated undrained triaxial compression tests (UU tests) are often appreciably less than those of "perfect samples". This can lead to over-design of geotechnical structures. Improved techniques are therefore needed. It is commonly believed that consolidated undrained (CU) tests give improved results and the strengths determined are more representative of the in-ground strengths. However, the costs of this test are appreciably more. Currently, there are two established and apparently logical methods for consolidating disturbed samples that are to be used for measuring undrained shear strengths. These are the Bjerrum method and the

SHANSEP method (Coatsworth 1986).

The so-called Bjerrum method (Bjerrum 1973) is one in which the specimen is reconsolidated to its in-situ effective stress state. Any loss of suction (decrease in  $p'$ ) that the sample underwent during its retrieval and storage is corrected. If the swelling during the stress release is of an elastic nature, then the consolidation will return the sample to its in-situ water content and soil fabric. This method is best suited for samples which have undergone low to moderate amounts of disturbance. Researchers who have found this method to accurately represent the in-situ behaviour include Kirkpatrick et al. (1986) and Graham and Lau (1988).

The SHANSEP method is based on the findings of Ladd and Foott (1974) that laboratory tests on specimens with the same OCR but different preconsolidation pressures,  $\sigma_{VC}'$  exhibit similar strength and stress-strain characteristics when normalized with respect to  $\sigma_{VC}'$ . The method involves consolidating the sample under its in-situ  $K_{0nc}$  value to stresses greater than the in-situ  $\sigma_{VC}'$ . The sample will then become normally consolidated (NC) and the effects of disturbance will be somewhat alleviated. To obtain overconsolidated (OC) specimens, NC specimens are offloaded and allowed to swell until the desired OCR is reached. The specimens are then tested in undrained shear and the results for each particular specimen are normalized with respect to their specific  $\sigma_{VC}'$ . For a particular OCR value, clays which exhibit normalized behaviour will yield at a constant value of  $c_u/\sigma_{VC}'$  (Coatsworth 1986). This method works well for NC soils which exhibit

normalized behaviour. However, increased overconsolidation as a result of aging will not be represented in this type of test. Any bonded structure associated with the aging process will be broken as the consolidation pressures surpass the in-situ  $\sigma_{vc}'$ . This will cause a reduced stiffness (Mori 1981) and an underestimate of  $c_u$  (Coatsworth 1986).

The in-situ stress state in many clays is generally anisotropic. Both the methods previously mentioned require anisotropic reconsolidation of specimens. However, many commercial laboratories do not have the required equipment or technical ability to perform anisotropic consolidation. Therefore, it is generally desirable to use isotropic consolidation procedures to represent anisotropic in-situ behaviour. There are a number of researchers who have investigated a variety of isotropic consolidation procedures of samples. Both Kwok (1984) and Lau (1986) were relatively successful in recovering the in-situ  $c_u$  of remoulded samples which were originally consolidated anisotropically, ( $K_0 = 0.53$ ), by reconsolidating the samples isotropically to 0.6 times the effective vertical stress,  $\sigma_v'$ . Also, Henkel (1960) found from tests on remoulded clay that specimens anisotropically consolidated will follow a similar effective stress path during undrained compression as that of specimens consolidated isotropically to the same moisture content. Coatsworth (1986) presented a method which makes it possible to determine the isotropic consolidation pressure required to bring the specimen to the same water content as that which would be achieved by

anisotropic  $K_0$  consolidation. He also proposed a method to use isotropic swelling to represent anisotropic swelling during offloading to produce overconsolidated specimens. This offers advantages in the commercial testing industry.

However, these procedures only provide good measurements of undrained shear strengths in certain instances of overconsolidation ratios, stress levels, and amounts of disturbance, and are not generally successful. Moreover, they are not usually successful in recovering strain-dependent behaviour, reflected in such things as porewater pressure parameters and deformation moduli. Therefore, the effective stress paths that the specimens would follow during shear testing may not be the same as those that the clay would observe in the field loading application. Close examination of the literature showed that previous projects all had conceptual, experimental, or interpretive deficiencies applicable to specific conditions. No coherent, rational, and carefully researched method appeared to exist to guide the selection of a reconsolidation procedure to successfully recover the in-situ loading behaviour for a general soil case. The following chapters present results that provide solidly researched guidance for commercial users who are testing clays with low permeabilities and moderate pressure release disturbance.

## Chapter 3 - Testing Program

### 3.1 Introduction

The testing program described in this thesis was designed to extend the test conditions examined in earlier research programs by Kwok (1984) and Lau (1986) on the stress release disturbance of lightly overconsolidated simulated offshore samples. It was shown in Chapter 1 that these earlier programs have been subjected to some criticism because they used a constant value of  $K_0 = \sigma'_h / \sigma'_v = 0.53$  for both the normally consolidated and overconsolidated specimens. Natural lightly overconsolidated clays have  $K_{0oc} > K_{0nc}$  (Mayne and Kulhaway 1982 and Kirkpatrick et al. 1986).

The specimens tested in the project were formed with  $\sigma'_1 = 160$  kPa with  $K_{0nc} = 0.53$ , and then offloaded to  $\sigma'_1 = \sigma'_3 = 80$  kPa producing an overconsolidated clay specimen with  $OCR = 2.0$  and  $K_{0oc} = 1.0$ . These specimens can be expected to more correctly represent the behavior of lightly overconsolidated clay than those tested in the previous programs.

Test samples were created by removing stresses from specifically prepared triaxial specimens of clay while still in the cell. These samples were then allowed to sit under near-zero stresses for various periods of "storage" time before reconsolidation and undrained shearing. Samples have been tested with both totally free and totally restricted access to drainage during the storage period. This project

has also used the same storage times as in the previous work, namely 15 min., 1 day and 7 days.

Fig. 3.1 shows the equivalent field conditions of the in-situ stress states that were chosen for this project. The majority of the tests were conducted on specimens with an in-situ stress state of:

Vertical effective stress,  $\sigma_1' = 80$  kPa

Overconsolidation Ratio,  $OCR = 2.0$

Coefficient of lateral earth pressure,  $K_{0oc} = 1.0$

Porewater pressure,  $u = 500$  kPa.

with full saturation. In addition, a small number of samples were attempted to be consolidated to an in-situ stress state of:

$\sigma_1' = 400$  kPa

$OCR = 2.0$

$K_{0oc} = 1.0$

$u = 2000$  kPa

to initiate a new technology in the University of Manitoba geotechnical laboratories to simulate sampling in deeper water. However, equipment problems and time constraints were encountered and the tests performed were not as extensive as was desired. This high pressure testing will be reported briefly in Appendix A.

The soil used in this program is an illitic clay obtained in 1982 from Grundy County, Illinois for use in the earlier research projects by Kwok (1984), Ambrosie (1985), and Lau (1986). A new series of standard classification tests were performed on the clay with the results shown in Table 3.1. The specific gravity and liquid and

plastic limits were found to be 2.74, 62.5, and 29.9, respectively. It can be observed from the table that although the specific gravity value was fairly close to that of the earlier investigations, the liquid and plastic limits have increased almost monotonically with time. It is believed that this is due to an alteration in the chemical composition of the clay, probably due to oxidation. (It was observed by Dr. J. Graham - the adviser of the overall research program - that the clay had changed color from its original blue-grey to a brown-grey, particularly during the current investigation (pers. comm.)). Since the clay used in the present study has been slightly altered from that of the earlier projects, care must be taken when comparing the test results between the various programs. Additional indications of chemical changes in the clay will be discussed in the following text as they arose during the testing and subsequent analysis.

### 3.2 Sample Preparation and Test Procedures

The reconstituted samples used in this series of tests were cut from a large "cake" of soil. This cake was formed by initially preparing a slurry mixture with a water content ( $w$ ) of 120% (about  $2w_l$ ) and then consolidating it one dimensionally in a large diameter cell ( $\emptyset=254$  mm) to  $\sigma'_v = 70$  kPa. The cake was then extruded from the cell and three 76 mm diameter triaxial specimens were trimmed for placement into triaxial cells. The procedures for forming and

trimming the specimens are the same as those used by Kwok (1984), Ambrosie (1985), and Lau (1986). Detailed description of these processes will therefore not be repeated here. Full details were given by Lau (1986).

Once the specimens had been installed in the triaxial cells, the stresses were changed incrementally to the consolidation in-situ stresses that were required. Control specimens were then tested immediately in undrained shear, while samples were subjected to unloading, storage, and reconsolidation procedures before shearing. A brief description of these unloading, storage, and reconsolidation steps will be given in Section 3.3, and the reader can refer to Lau (1986) for further details. The procedures used at this stage have largely duplicated those used in earlier projects. The only exceptions involved the stress system at the end of triaxial consolidation and the use of back-pressure during consolidation. These two different procedures will be described in detail in the following sections.

### 3.2.1 Triaxial Consolidation

The initial stage of triaxial consolidation is the same process as was used in the earlier research. That is, each specimen was subjected to anisotropic consolidation ( $K_0 = 0.53$ ), with a first vertical stress of  $\sigma'_v = 50$  kPa. The specimens were loaded with 24 hour periods between successive load increments. A load increment

ratio of 1.15 was used until a final vertical stress of  $\sigma'_V = 160$  kPa was achieved. The specimens were then offloaded to produce overconsolidation. Mayne and Kulhaway (1982) and Kirkpatrick et al (1986) indicated that after offloading to produce a specimen with  $OCR = 2.0$ , the  $K_0$  value approaches 1.0 from its normal consolidation value of 0.53. The testing performed in the project described here deviates from the previous work at the University of Manitoba by changing  $K_{0OC}$  from 0.53 to 1.0 during this overconsolidation stage. The specimens were then allowed to sit for a 4 day period to allow stabilization of the clay interparticle contacts and the porewater pressure before further testing. This is also consistent with the earlier projects. Measurements of height and volume change were recorded throughout the consolidation process so that sample dimensions could be calculated at any time.

### 3.2.2 Back Pressuring

For low values of back-pressure (or porewater pressure), there is little change caused to the soil structure that can be directly attributed to the use of back pressure (Bishop and Henkel 1962). In relatively low pressure triaxial testing, say to 1 MPa, the primary function of back-pressure application is to dissolve any free gas present in the sample into its pore fluid. This improves the reliability of porewater pressure measurements. In the previous programs, all specimens were consolidated with atmospheric pressure in

the drainage leads. Any air expelled from the samples during consolidation was flushed away from the pedestal and its volume measured. After consolidation was complete, a back-pressure of 500 kPa was applied for one day to simulate the porewater pressures in the field. At the beginning of this new project, it was desired to have each sample subjected to back-pressure during the entire consolidation stage. This would eliminate the risk of losing precise volume control while attempting to remove any expelled air. Also, the effective stress state of the sample can be slightly altered during the application of the back-pressure. The one day time period may not be long enough to allow the sample to return to a "steady" state where very little volume change is occurring. The first five specimens were back pressured in the same way as in the previous research. The remaining 11 specimens were subjected to 200 kPa of back pressure for the entire consolidation stage. When consolidation was complete, the back-pressure was increased to 500 kPa for one day as before. Both processes gave good saturation values ( $\bar{B} > 0.98$ ). Two control tests were performed with 500 kPa back-pressure during the entire consolidation phase to check that the magnitude of the back-pressure did not affect the results.

### 3.3 Design of the Current Test Program

As in the previous projects, the purpose of the work was to study stress release disturbance alone without the mechanical disturbance

that usually accompanies sampling. As explained by Graham and Lau (1988), the use of reconstituted samples is therefore necessary if "sampling" effects independent of mechanical disturbance are to be identified. This program is completely consistent with the previous research except that the value of  $K_{0oc}$  during the overconsolidation stage has been changed. The objective is to compare the undrained shear behavior of simulated samples which have experienced stress release, with the behavior of in-situ control specimens, which have not experienced this stress release. The samples were subjected to the three separate processes of unloading, storage and reconsolidation after triaxial consolidation, which model field sampling and storage prior to testing. These three processes will be briefly explained in the following paragraphs. The reader is referred to Lau (1986) for a more detailed description.

As explained in Chapter 1, when a sample is lifted from its marine environment for laboratory testing, the total confining pressure is reduced to zero. This stress release has been modelled in the laboratory by reducing the consolidation stresses on a reconstituted "sample" with the drainage leads closed. With  $K_{0oc} = 1.0$  in this project, the unloading is purely isotropic. This contrasts with the earlier projects in which  $K_{0oc} = 0.53$  and shear unloading was required. The resulting porewater pressure changes have been measured with pressure transducers mounted on the cell base.

The samples were then allowed to sit for three different time periods with either totally free or totally restricted access to

drainage. This simulates the outer bounds of the possible drainage conditions during actual storage of real samples prior to laboratory triaxial testing. These are the same drainage conditions investigated in the earlier projects, so direct comparisons can be made with the earlier results. Also, the same storage times as in the previous projects were again investigated, that is 15 min., 1 day, and 7 days. Emphasis was placed on the 15 min. and 7 day times since these produce the upper and lower bounds of the differing shear behavior.

Laboratory reconsolidation procedures have been investigated for recovering the in-situ strength of the control specimens from the samples using consolidated undrained triaxial tests. Three different reconsolidation procedures were used consistent with the earlier research, that is isotropic reconsolidation to 0.6 and 1.0 times the in-situ vertical effective stress,  $\sigma_v'$  and anisotropic reconsolidation to  $1.0\sigma_v'$  with  $K_0 = 0.53$ . Back-pressure of 200 kPa was used throughout the reconsolidation process. The isotropic reconsolidation pressures were increased in one step to the desired values. In the case of the anisotropically reconsolidated samples, the vertical load was applied one day later to allow some stabilization of the porewater pressures generated in the samples, (Graham and Lau 1988). After a 3 to 4 day period when the porewater pressure changes had dissipated, the samples were then sheared undrained.

It is appreciated that the limited number of tests performed in this program severely limits the statistical value of the conclusions that can be drawn. However, in consultation with his advisors Dr. J.

Graham and Dr. D. Ho, it was decided to perform only one test with each of the controlled set of variables so that a qualitative appreciation of the important variables could be obtained.

## Chapter 4 - Consolidation, Unloading, Storage, and Reconsolidation Results

### 4.1 Introduction

As outlined in Chapter 3, a slurry mixture of illitic clay was consolidated one dimensionally in a large cylinder to form a "cake" of reconstituted soil. From each cake, three specimens could be trimmed for triaxial testing. A total of 7 "cakes" was prepared in the present program. Of the possible 21 specimens, only 17 were placed in triaxial cells, with 2 of these being part of the experimental high pressure testing. In addition, one triaxial specimen (the first) was prepared from a slurry mixture consolidated in a smaller cylinder. Each specimen was consolidated in triaxial compression as outlined in Section 3.2. Five of the specimens were used as in-situ control specimens and subjected to undrained shearing immediately after consolidation. The remaining 13 were subjected to unloading and various storage and reconsolidation processes. One control specimen and one low pressure sample were damaged during the triaxial portion of their tests and their results were considered questionable. These tests were therefore repeated. The data collected from these low pressure specimens as well as the results of the other 14 specimens will be discussed in this chapter. The results of the high pressure testing will be discussed separately in Appendix A.

## 4.2 Consolidation

There are two stages of consolidation in preparing specimens for shear testing. The first is one dimensional consolidation of the slurry mixture in cylinders, and the second is consolidation under almost  $K_0$ -conditions in triaxial cells. The results of each will be discussed in this section.

### 4.2.1 Slurry Consolidation

One dimensional consolidation of clay in first-time loading is commonly characterized by a straight line relationship between  $\log(\text{pressure})$  versus compression expressed in terms of voids ratio  $e$ , water content  $w$ , specific volume  $V$ , or vertical strain  $\epsilon$ . The slope of this straight line gives an indication to the compressibility of the clay. In the previous programs of this research, Kwok (1984), Ambrosie (1985), and Lau (1986) chose to plot this compressibility during slurry consolidation in terms of the  $\log(\text{vertical effective stress } \sigma'_v)$  versus water content,  $w$ . However, they chose the critical state parameter " $\lambda$ " to define this compressibility. In classical critical state soil mechanics,  $\lambda$  is the slope of  $\ln(p')$  versus voids ratio where  $p'$  is the effective mean pressure,  $(\sigma'_1 + 2\sigma'_3)/3$ . They designated this slope for the slurry consolidation as " $\lambda_1$ ". The author has chosen to adopt the same conventions to allow for convenient comparisons.

The duration of the load increments was generally one day. Due to this time constraint, complete dissipation of excess porewater pressures was not allowed during all of the load increments in any of the programs. During the first load increment, the "cakes" were consolidated for a period of three days to allow for partial dissipation of porewater pressure build-up. This procedure was adopted by Lau (1986), but not Kwok (1984) or Ambrosie (1985). As in all the previous projects, each "cake" was consolidated during the final load increment for a longer period until primary consolidation was complete. This allows complete dissipation of all excess porewater pressures at the end of slurry consolidation.

Curves of  $w$  vs.  $\text{Log}(\sigma'_v)$  are shown in Figs. 4.1a,b for the 8 slurry consolidations that were done. The slope,  $\lambda_1$ , has been measured through the one day consolidation values, and the numerical values are given in Table 4.1. This is not the true  $\lambda_1$ -value that would result if complete dissipation of excess porewater pressure was allowed during each load increment (Kwok 1984). However it still gives an indication as to the compressibility of the clay. As can be seen from Figs. 4.1a,b, the curves are not identical, although the slopes are fairly consistent.

It is believed that the differences in these curves are due to the incomplete dissipation of the excess porewater pressure built up during successive load increments. For samples such as T790-T792, it is believed that the excess porewater pressure during the early load increments did not dissipate as quickly as those in say the sample

T784-T786. In the first case, more of the initially high excess porewater pressures were carried over into subsequent loading stages, and the compressions during these load increments were therefore smaller. It is important to note, however, that aside from samples T771, T791 and T792, the consolidation points after the longer final load increment are all within 2.99 % of each other. The location of this final consolidation point is the main criterion for producing consistent "cakes" for subsequent testing, and it is considered less important that the paths of the samples in  $w$  vs.  $\text{Log } \sigma_v$  shown in Figs. 4.1a,b are not identical in this early stage of specimen preparation. Sample T771 was not allowed to reach porewater pressure equilibrium during the final consolidation stress because of constraints in the management of the program. The final water content shown in Table 4.1 was therefore higher than that of the other samples.

An average  $\lambda_1$  value of  $0.477 \pm 0.065$  (standard deviation) was observed in the present program. This is lower than equivalent values found by Kwok (1984) and Ambrosie (1985), who found 0.621 and 0.689, respectively, but close to the value found by Lau (1986) which was 0.513. Lau thought that the differences between his  $\lambda_1$  value and those found by Kwok and Ambrosie could be due to different consolidation techniques he used in the first load increment. The longer initial loading period of three days allowed part of the initial high porewater pressures to dissipate and the degree of consolidation at the end of the first load increment would be greater

than in the case of Kwok or Ambrosie. Therefore, less excess porewater pressure was carried over into subsequent loading stages and the resulting compressions would be smaller. This would cause the  $\lambda_1$  value to be smaller, that is the slope would be less steep. The author used the same techniques as Lau and got closely similar  $\lambda_1$ -values.

What is considered more important however, is the consistency of the water content of each "cake" at the final vertical stress. As calculated from Table 4.1, the average water content at "equilibrium" after 12-14 days under the final load increment is 50.6 %  $\pm$ 1.16 % (excluding "cake" T771). The "cakes" are therefore all close to the same water content. Closer examination of the water contents in Table 4.1 shows that the water content at the end of slurry consolidation increased almost monotonically as the program progressed. This could be another indication of chemical changes occurring in the clay with time that were reflected in the Atterberg limit values, as discussed in Section 3.1. In any event, the state of each "cake" at the end of each slurry consolidation is fairly consistent and the triaxial samples trimmed for each test all had voids ratios that were very near each other.

#### 4.2.2 Triaxial Consolidation

After completion of slurry consolidation, each "cake" was extruded and specimens were carefully trimmed for installation and

subsequent consolidation in triaxial cells. The stress paths of each specimen during this consolidation are shown in Figs. 4.2a-n, plotted as specific volume,  $V$  versus  $\log(p')$ . (curves of samples T776 and T785 were not included due to inaccurate specific volume measurements.) The critical state parameters, " $\lambda$ " and " $\kappa$ " (with respect to voids ratio  $e$  versus  $\ln(p')$ ) are again used to characterize the slopes of the virgin compression lines and the unload-reload lines, respectively.

First, consider the top portion of the curves of Figs. 4.2a-n between  $p' = 50$  and  $70$  kPa. Each specimen was offloaded at the end of the slurry consolidation. Therefore, this initial section of the curves is a reload line. The average slope of this line in  $e-\ln p'$  space has been designated as " $\kappa_1$ ", and was found to be  $0.118 \pm 0.009$  for the current project (see Table 4.1). This is only about 13% higher than the  $\kappa_1$  values of Kwok (1984), Ambrosie (1985), and Lau (1986) who found 0.103, 0.105, and 0.102, respectively. Consider next the straight line portion of the curves in Figs. 4.2a-n between  $p' = 70$  and  $110$  kPa. This is a virgin compression line and its slope in  $e-\ln p'$  space has been designated as " $\lambda_2$ ". For this research project,  $\lambda_2$  was found to be  $0.231 \pm 0.012$ . This compares very favorably with the values of Kwok, Ambrosie, and Lau, who found  $\lambda_2$  values of 0.226, 0.237, and 0.234, respectively.

Finally, consider the unloading line of Figs. 4.2a-n. The slope of this line in  $e-\ln p'$  space is characterized by " $\kappa_2$ ". From Table 4.1, the average  $\kappa_2$  was found to be  $0.020 \pm 0.006$  for the current

research. This can not be compared with the previous values of 0.048, 0.050, and 0.047 found by Kwok, Ambrosie, and Lau, respectively. The reasons for this are as follows. First, consider the yield locus of the clay in normalized deviator stress,  $q/\sigma_{VC}'$  versus  $p'/\sigma_{VC}'$  space as shown in Fig. 4.3 (from Graham and Lau 1988). This yield envelope was determined in the previous projects on stress release disturbance at the University of Manitoba using the same clay. The final stress state of the specimens of the current project is shown in the figure. It is obvious that at the final state of  $p' = 80$  kPa,  $q = 0$ , and  $OCR = 2.0$  used in this project, the specimens have gone outside the yield envelope defined by Graham and Lau (1988) for  $\sigma_{VC}' = 160$  kPa. Therefore, these specimens have yielded during offloading and some compressive plastic straining will have occurred allowing very little volumetric swelling. Those of Kwok and Lau were subjected to purely elastic strains during the offloading and no yielding would have occurred. This would be supported by an observation of the  $\kappa_2$ -value for the present study being less than that found in the earlier projects, which was found to be the case. This unload line would not technically be a purely elastic unload line, that is defined as a  $\kappa_2$ -line.

Second, it is likely that the clay has anisotropic elastic properties (Lau 1986). Then according to Wood and Graham (1987), the unload-reload region in  $V$ - $\ln p'$  space is not a line but rather a zone similar to that shown shaded in Fig. 4.4. The lower edge of this region corresponds to the yield locus of the clay. Each unload-reload

region is defined by the current preconsolidation pressure,  $\sigma_{VC}'$  and its shape is dictated by the anisotropic elastic properties of the clay. Since the offloading of the specimens in the previous projects was performed without yielding of the clay, the final consolidation points would all lie within the yield locus of their specific unload-reload regions in  $V$  vs.  $\ln(p')$  space. The specimens of the present project, however will have changed to different unload-reload regions in  $V$ - $\ln p'$  space as the overconsolidation progresses, with each region being defined by a slightly increasing  $\sigma_{VC}'$ . The shape of each yield locus will be approximately the same. (Subsequent isotropic consolidation to higher stresses would gradually modify the shape of the anisotropically determined yield envelope.) The final consolidation points of the specimens of the previous three projects are within the elastic zone of the unload-reload region and are therefore inside the yield envelope, while the specimens of the current project are on a newly formed yield envelope controlled by an isotropic mean stress  $p' = 80$  kPa. Fig. 4.5 shows the final consolidation points in  $V$  vs.  $\log(p')$  space of the control specimens for Kwok (1984) and Lau (1986), as well as those of the current project. The one-dimensional normally consolidated lines (1-D NCL) for the previous projects (taken from Graham and Lau 1988) and that of the current project are plotted. It also shows systematically possible traces of the yield loci through the earlier data and the present data. The observed change in the position of the 1-D NCL between the different projects is another indication of chemical

changes that have occurred in the clay during its storage in the laboratory over the last 6 or 7 years. The data of the current project lie on the top "hook" of the unload-reload region whereas the earlier data lie in a different part of their respective zone. However, note that the higher  $p'$ -values in the present series have produced higher  $V$ -values. This would be expected from the oxidation of the clay with time.

Due to the anisotropic behaviour of the specimens, a straight  $\kappa$ -line through any of the points is not representative of the behaviour of the clay. The "elastic wall" is not a  $\kappa$ -line but a region as stated earlier. Straight lines through any of these points would not be measuring comparable properties since the consolidation points are defined for different areas of the unload-reload region. It is therefore not a concern that the  $\kappa_2$  values are different in the different test series.

### 4.3 Unloading

After the samples were consolidated to the stress state of  $\sigma'_v = \sigma'_h = 80$  kPa and  $OCR = 2.0$ , they were subjected to isotropic unloading in the triaxial cells to a cell pressure of approximately 5 kPa with no access to drainage. The 5 kPa of cell pressure was used to ensure contact between the sample membrane and the specimen, and therefore to control the accuracy of the volume change readings. This procedure simulates the act of raising an actual sample from the

seabed to the ship and its later extrusion from the sampling tube. The samples in this project were unloaded incrementally and this process took about 10 minutes on average.

Figs. 4.6a-j show the changes in porewater pressure that accompanied the unloading of the cell pressure for all samples. During the unloading, the average  $\bar{B}$  values ( $= \Delta u / \Delta \sigma_{\text{cell}}$ ) taken through the points were found to be 98 - 100 % except for samples T778 and T784. These samples had  $\bar{B}$  values of 94 and 96 % respectively. The decrease in the  $\bar{B}$  value in these specimens could be associated with dissolved air in the porewater and drainage leads coming out of solution as the pressure is decreased. This dissolution of air would affect the porewater pressures developed in the drainage leads and the measured value would not be exact. No air was actually observed in these specimens.

The average mean effective stress,  $p'$  prior to unloading was 78.4 kPa. Immediately following the unloading, the average  $p'$  of the samples was found to be 66.2 kPa. This is a reduction of approximately 15 %. This average of 66.2 kPa, however includes the results of samples T778 and T784 which had individual reductions in  $p'$  of 38.5 and 40.2 % respectively. If these two samples are ignored, then the average  $p'$  after unloading would be 70.2 kPa which is a 9.2 % reduction. Both of these values, however are higher than the reduction in  $p'$  measured by Kwok (1984) and Lau (1986) for lightly overconsolidated samples ( $\text{OCR} = 2$ ) which were 3.5 and 3.8 %, respectively. The samples of Kwok and Lau were unloaded from an

in-situ  $p'$  of approximately 55 kPa.

However, consider the decrease in  $p'$  reported by Lau (1986) for the normally consolidated samples which were unloaded from an in-situ  $p'$  of approximately 110 kPa. He found the  $p'$  to decrease by 15%. It is evident that in the present project, the samples did not hold their in-situ  $p'$  values after unloading. However, it is obvious that the reduction in  $p'$  found in the present study was between the values reported by Kwok (1984) and Lau (1986) with in-situ  $p'$ -values of 55 kPa and Lau (1986) with an in-situ  $p'$ -value of 110 kPa. Since the testing procedures were almost identical, a possible reason for the  $p'$  reduction after unloading could be due to cavitation of the water in the drainage leads. As the negative pressure gets nearer to the presumed cavitation point of water (-100 kPa), the recorded porewater pressures may not be that which is occurring in the specimen. Since the negative porewater pressures that were attempted to be measured in the present project were closer to -100 kPa than the overconsolidated samples of Kwok (1984) and Lau (1986) but not as close as the normally consolidated samples of Lau (1986), it is considered systematic of the test procedures that the reduction in  $p'$  of 9.2 % found in the present project lies between the reduction values determined in the other projects.

Alternatively, there could have been a significantly large amount of air dissolved in the water in the drainage leads that came out of solution when the pressures were decreased. This could cause the porewater pressures measured in the drainage leads to be higher, that

is less negative, than those in the pore structure of the sample. Then the measured  $p'$  would be less than the actual value in the sample.

#### 4.4 Storage

After the unloading stage, the samples were subjected to various lengths of storage periods. This was to model the time lag that actual samples experience between the time they are retrieved and the time they are mounted in triaxial cells for strength testing. To be consistent with the three previous projects, the storage periods used were 15 minutes, 1 day and 7 days. The two extreme cases of drainage conditions were investigated, that is the samples either had totally free access to drainage (drained storage), or they were totally restricted from drainage (undrained storage).

First, consider the samples that were stored under drained conditions. Figs. 4.7a,b show the volumetric strain  $v=(2\epsilon_3+\epsilon_1)$  plotted against  $\log(\text{storage time})$ . The curves are all roughly the same shape with the curve being more complete as the storage time increases. There appear to be 3 sections in the curves, with the points of contraflexure at approximately 2 hours and 2 days. The second point of contraflexure at about 2 days is close to that found by Lau (1986) who reported an "equilibrium time" of 2 to 3 days.

The final volumetric strains measured during the drained storage periods are summarized in Table 4.2. The two samples stored for 15

minutes had final  $v$ -values of 0.18 and 0.27 % respectively, while the 1 day and 7 day samples had final  $v$ -values during the swelling of 3.95 % and 6.12, 7.81, and 8.28 % respectively. It can be observed that the final  $v$ -values found for samples stored for the same time period were fairly close to one another with one exception, sample T779 with  $v = 6.12$  %. It is seen in Fig. 4.7b that the final three data points of T779 deviate significantly from the smooth curve. It is unknown why this occurred. There were no technical problems detected during this period. However, the problem is considered to be isolated to the one sample and not characteristic of the general trend. If this deviation had not occurred, then the final  $v$  value would have been near 7.5 % from a manual projection of the curve which is consistent with the other two.

Consider next the samples which were stored under undrained conditions. The curves of the residual porewater pressure,  $u_r$  during the storage versus the  $\log(\text{storage time})$  are shown in Figs. 4.8a,b. There are two general trends that can be observed. In samples T782 and T784, the porewater pressure continued to decrease from the initial residual porewater pressure  $u_{r_i}$  at the beginning of the storage to a minimum and then began to rise. In samples T781 and T788, the porewater pressure continually increased from  $u_{r_i}$  once the storage period had begun. It is believed that the mechanism which causes the samples to continue a reduction in  $u_r$  immediately after unloading has to do with the "equalization time" of the pressure transducers. In samples T782 and T784, it took approximately 10

minutes before the measured porewater pressure began to rise. It is thought that during this time the transducers had not reached an "equilibrated" state and the measured porewater pressures were somewhat greater (that is, less negative) than the actual porewater pressures in the sample. Also it is possible that some gas exsolved from the water in the drainage leads during the unloading and affected the measured  $u_{rj}$ . It could then take some time for the porewater pressure in the drainage leads to equilibrate. This type of behaviour was observed in only one other project. Graham et al.(1987) found this to occur during the storage of their normally consolidated samples. They thought that it was due to entrapped air that was observed in the drainage leads. Porewater pressure relaxation with time has been observed by a number of researchers, for example Graham et al.(1987), and Kirkpatrick et al.(1986).

It can also be observed from Figs. 4.8a,b, that the curves are not completely "smooth". It is believed that one cause of this is due to the daily zero shift of the porewater pressure transducers with respect to the daily atmospheric pressure. During all other stages in the test, both the cell and porewater pressure transducers were rezeroed daily with respect to the atmospheric pressure so that the measured gauge pressure would be accurate. This was done by isolating each transducer and subjecting it to a column of water which was open to the atmosphere and equal in height to the midpoint of the specimen. This was performed on the porewater pressure transducer after the first day of storage for sample T782. Since the pressure in the water

immediately surrounding the transducer in its mounting block at this stage was less than the atmospheric pressure, this small amount of water slightly compressed once it was exposed to the higher atmospheric pressure and a small volume decrease in the measuring burette (.1 to .2 ml) was observed. This is most likely due to the compressibility properties of both pure water and any air dissolved within the water. Therefore, when the transducer was resubjected to the pressure in the drainage lead (that is, the porewater pressure in the sample), the mass of water in this space was slightly larger than that before the rezeroing process and the pressure was observed to increase slightly (2 to 3 kPa) which can be seen in Fig. 4.8a for time approximately 1400 minutes (that is, 1 day). Therefore, this practice was not repeated during the rest of the undrained storage periods. The fluctuations measured in pressure due to the daily atmospheric changes commonly were 0.5 to 1 kPa. It was considered more desirable to have this occur than to have small amounts of water entering into the drainage leads which would make the sample not totally undrained.

The general trend during storage was found to be that the residual porewater pressure increased from its value immediately after unloading. This is consistent with the results found by other researchers. Kirkpatrick et al.(1986) and Kwok (1986) found that the ratio of  $u_r / u_{rj}$  decreased to approximately 70 and 64.6 % respectively after 7 days of storage, (Kirkpatrick et al. did not measure directly the negative porewater pressures but instead

estimated them from the  $p'$  values and the saturation curves). This compares well with the 74.4 % value of  $u_r / u_{ri}$  found in the current project for the average of the 7 day storage samples. This and the other values of the ratio for the different lengths of storage period are shown in Table 4.2. It can be observed from the table and Fig. 4.8b that the final  $u_r / u_{ri}$  observed for sample T784, which was stored for one day, was greater than 1.0 (that is 1.259). The porewater pressure of this sample began to rise after about 10 minutes. It is speculated that the porewater pressure would continue to rise and surpass  $u_{ri}$  if the storage period had been longer which would be consistent with the general trend of the negative porewater pressures relaxing with time.

The reason for the relaxation of porewater pressures is unclear, but Graham et al.(1987) believed that it could be due to reorganization of the clay microstructure in response to the change from an anisotropic to an isotropic stress state in their project. A comparable reorganization of the soil particles in the samples of the present project could be due to one of two reasons. First, there was a reduction in the measured  $p'$ -value after unloading. Therefore, the specimen would be under different stress states before and after unloading. This could cause the changes in the microstructure of the clay that were suggested by Graham et al.(1987). However, as mentioned earlier, it is unclear if the  $p'$ -values measured after unloading are precise due to the possibility of cavitation. A possible alternative for the cause of this reorganization of the

fabric structure could be due to the change in state of the stress acting on the porewater from compression to tension. The suction in the water will be transferred to the individual soil particles. This could cause an elastic compression of the soil structure and the particles would be in a more dense form. The suction pressure would then decrease, that is the porewater pressure would rise with time as was observed. This possible explanation may not, however, be applicable for the relatively low negative pressure range (<100 kPa) which the samples are being subjected to.

Another possible explanation could be that water migrated through the sample membranes or around the seals and entered the drainage leads. This would cause an increase in the amount of porewater in the drainage leads and consequently, the porewater pressures would increase. However, the effect of this was checked in calibration testing at the beginning of the project and was found not to be a significant problem.

#### 4.5 Reconsolidation

The next step in the testing program was to reconsolidate the samples to one of three stress states. These stress states were consistent with the three earlier projects, that is 0.6 times the in-situ vertical effective stress,  $\sigma'_v$  with  $K_0 = 1.0$ ,  $1.0 \sigma'_v$  with  $K_0 = 1.0$ , and  $1.0 \sigma'_v$  with  $K_0 = 0.53$ . Since these reconsolidation procedures will be referred to frequently in the remainder of the

thesis, the following short-hand notation will be used:  $0.6\sigma'_v$ -iso,  $1.0\sigma'_v$ -iso, and  $1.0\sigma'_v$ -aniso, respectively. The main objective of this study is to determine which of the three reconsolidation procedures will give the best estimate of the undrained shear strength of the samples. The reconsolidation stresses were added in one load increment and the resulting porewater pressures in the sample were allowed to equilibrate for 4 - 5 days. The final axial and volumetric strains experienced during reconsolidation are shown in Table 4.2 along with the reconsolidation type of each sample.

The strains experienced during the reconsolidation are again shown to depend on both the storage conditions and reconsolidation procedures used on each sample (Graham and Lau 1988). Consider first the samples which were stored undrained. No volumetric expansion was allowed during the storage period, and consequently, the volumetric and axial strains experienced during the subsequent reconsolidation were found to be small. Figs. 4.9a,b show the specific volume,  $V$  of typical sample T784 and T788 plotted against the  $\log(\text{reconsolidation time})$ , where T784 and T788 were stored undrained for 1 day and 7 days respectively and both reconsolidated to  $0.6 \sigma'_v$  iso. Table 4.2 and Figs. 4.9a,b show that the length of storage time has little effect on the strains observed during reconsolidation if the sample are stored undrained. The other samples that were stored undrained had similar  $V$  vs.  $\log(\text{time})$  relationships during reconsolidation as those shown in Figs. 4.9a,b and have not been included here.

Next, consider the samples which were subjected to drained

storage. Figs. 4.10a,b show the curves of  $V$  vs.  $\log$  (reconsolidation time) for samples T777 and T775 which were stored under drained conditions for 15 minutes and 7 days respectively and both reconsolidated to  $1.0 \sigma'_v$  iso. It is observed from these curves and Table 4.2 that the length of the storage time has a significant effect on the strains experienced during the reconsolidation if the sample is stored under drained conditions. When a sample is stored for 15 minutes, there is very little time for it to swell and subsequently the volumetric expansion during the storage will be very small, as was observed in T777 (and in the specimens stored undrained in Fig. 4.9). When the sample was later subjected to its reconsolidation stresses, it expelled very little water and therefore the strains experienced during the reconsolidation were very small. However, if the sample was subjected to longer storage periods, as in the case of T775, there will be a greater volumetric expansion. When this sample was later reconsolidated, more water was expelled than in the case of the sample T777. The curves of  $V$  vs.  $\log$  (time) during the reconsolidation of the other samples which were stored under drained conditions were all similar to those in Fig. 4.10a,b and it was not considered helpful to include them in the thesis.

Consider next the effect of the reconsolidation procedure on the strains that the sample experienced during the reconsolidation stage. First, examine the strains experienced by sample T775, T779, and T789, which were all stored under drained conditions for 7 days. These samples were subjected to the three different reconsolidation

procedures, that is  $1.0 \sigma'_v$  iso,  $1.0 \sigma'_v$  aniso, and  $0.6 \sigma'_v$  iso, respectively. It is observed from Table 4.2, that the volumetric strains experienced by T775, which had the highest mean effective stress,  $p' = 80$  kPa, were much larger than those experienced by T779 and T789 which had  $p'$  values of 54.9 and 64 kPa respectively. This is to be expected, and is consistent with the findings of Lau (1986). Also, the axial strains experienced by T779 were much higher than those of T775 and T789. This is also to be expected, since there is a deviator stress,  $q$  of 37.6 kPa applied on T779 while no deviator stress was applied to T775 and T789. Finally, it is observed from Table 4.2 that sample T779 and T789 had very similar volumetric strains during reconsolidation and their  $p'$  values were very close to one another. Similarly, both T775 and T789 had no deviator stress applied during the reconsolidation and it was observed that the axial strains experienced by these two sample were very similar. These findings conform with the general trends observed for all samples in this project and are consistent with the findings of the earlier researchers on this project.

## Chapter 5 - Undrained Shear Test Results

### 5.1 Introduction

After the consolidation or the reconsolidation procedures of the control specimens and samples described in Chapter 4, the triaxial cells were transferred to strain controlled compression frames for undrained shear testing. These tests were performed at an axial deformation rate of 0.009 mm per minute (approximately 0.5 % strain per hour). This chapter presents the results of the shear tests from all test specimens. A summary of the results is shown in Table 5.1.

### 5.2 Stress-Strain Relationships

Curves of normalized deviator stress  $q / \sigma_{VC}'$ , normalized porewater pressure change  $\Delta u / \sigma_{VC}'$ , and effective stress ratio  $q / p'$  versus axial strain  $\epsilon_1$  are shown in Figs. 5.1 to 5.17 for all the specimens during undrained shearing. The definition of the failure point has been designated as the point at which the maximum  $q$  occurs. This is consistent with the definition adopted by Lau (1986). In general, all the stress-strain curves were similar in shape with all showing some reduction in shear resistance with post-peak straining.

The following general trends were observed with respect to the different storage and reconsolidation procedures. First, consider the behaviour of the samples which were stored undrained. It can be

observed from Figs. 5.13 to 5.17 that all three stress-strain curves show sharper, more distinct peaks for the samples that are stored for longer periods regardless of the reconsolidation procedure. These peaks occur at smaller axial strains for the samples stored for the longer time periods. However, there appears to be little effect of the duration of the storage period on the peak  $q$ -value for samples reconsolidated using the same procedure. This was evident in the strengths shown by samples T784 and T788 which had peak  $q$ -values of 82.3 and 81.1 kPa, and were stored for 1 and 7 days, respectively. These samples were reconsolidated to a  $p'$ -value of 48 kPa. This was also found by Skempton and Sowa (1963), Kirkpatrick and Khan (1986), and Graham et al. (1987). The other two samples stored undrained, T781 and T782 showed peak  $q$ -values of 68.9 and 75.8 kPa, respectively, and had  $p'$ -values during the reconsolidation of 80 and 55 kPa. The possible reasons for this decrease in peak- $q$  are as follows.

It is believed that for sample T781, the wrong proving ring serial number may have been recorded during the undrained shear testing and the calibration factor used in the calculations of the results (3.6779 N/div) would therefore be incorrect. There were only three different proving rings used in the present project and it is believed that the correct calibration factor was 4.6642 N/div as opposed to 3.6779 N/div. The shear results of this sample based on the new calibration factor are given in Table 5.1 under T781\* and the stress-strain curve is shown in Fig. 5.14. The original data sheets have been carefully re-examined, but unfortunately there is no way of

confirming the correct calibration factor. However, the results of the present program would be more consistent and agree better with the conclusions found by earlier researchers if the proving ring had the higher calibration factor. Significant anomalies result with the use of the lower factor. With the new calibration factor, the peak  $q$ -value changes to 91.3 kPa which is much closer to the values obtained for the control specimens. This would also fit into the belief that the samples consolidated with a higher  $p'$ -value should show a higher strength. The results of this sample compared with the others will be done by considering both results except where specified. It has been thought more responsible to identify this difficulty openly, than to make assumptions covertly that can be neither confirmed nor denied. For T782, it is thought that the small decrease in strength compared with T784 and T788 which had slightly higher  $p'$  during reconsolidation, is due to experimental scatter.

Next, consider the samples which were subjected to drained storage. It is seen from Figs. 5.6 to 5.12 that for samples reconsolidated using the same procedure, the peak  $q$ -values decrease with an increase in the storage time. The peak  $q / p'$ -values are approximately independent of the storage periods. It was also found that the  $\epsilon_1$ -value at the peaks of  $q$  and  $q / p'$  increased with increasing storage time. The opposite was found for samples stored undrained.

The results from samples which were reconsolidated using the same procedures will now be examined. It was found that samples stored for

15 minutes (T777 and T781\*) had peak  $q$  and  $q / p'$  values very close to each other for the drained and the undrained storage, respectively. However, for samples which were stored for seven days, it was generally found that the strength for the samples stored drained was slightly lower than those stored undrained. These were the same conclusions found by Graham et al.(1987). Also, it is observed from Table 5.1 that for different storage times, the reduction in the peak strengths is much larger for samples stored under drained conditions than that for those stored undrained.

Finally, consider the value of the axial strains at failure for the control specimens compared with the samples. For the control specimens, it was found that  $\epsilon_1$  at failure ranged from 2.67-3.48 % (Table 5.1). The samples which were reconsolidated to  $1.0 \sigma'_v$ -aniso had axial strains at failure slightly lower, that is 2.32-2.78 %. For both of the isotropic reconsolidation procedures, it was found that the samples stored for 15 minutes or 1 day had  $\epsilon_1$ -values at failure similar to those of the control specimens, 2.38-3.57 %, while the samples stored for 7 days had significantly larger  $\epsilon_1$ -values at failure than the in-situ control specimens, 3.16-4.43 %.

### 5.3 Effective Stress Paths

The effective stress paths followed by all test specimens during undrained shearing are shown in Figs. 5.18 to 5.34 in deviator stress,  $q$  versus effective mean stress,  $p'$ . There are 2 general shapes that

were observed (see for example Figs. 5.23 and 5.34 for samples T777 and T788). Each of the curves had 3 basic components with the first 2 of these being roughly similar for all test specimens. Consider first the lower portion of the curves in the low  $q$  range. As  $q$  increases on the specimens, the curves follow an almost straight line which was inclined slightly to the left (that is  $\Delta p' / \Delta q < 0$ ). Most of the curves then show a bend towards the right and a second nearly straight line ensues until peak  $q$  occurs. This section is either vertical or slightly inclined to the right for most specimens. The third section, which is again nearly straight, then occurs after failure when the  $q$  begins to decrease from its peak value as the sample moves towards critical state. The 2 different general shapes are evident from the direction that this third section takes immediately after the peak  $q$  occurs.

The direction that this third section follows after failure depends on the porewater pressure generation after the peak  $q$ -value is obtained. If the porewater pressure continues to rise after failure, as in sample T781 (see Fig. 5.13a), then the third section of the  $q$ - $p'$  curve turns towards the left and slopes down to the left as in Fig. 5.30. For a sample such as T788 (Figs. 5.17a and 5.34), the porewater pressure decreases after failure and hence the third section of the curve turns towards the right and slopes down. Note, however that the general slope and direction of this third section in  $p',q$  planes is similar for all specimens. The difference in the shape of the curves is evident only in the direction that the curve moves

immediately following failure. The exceptions to this behaviour were found in samples T776 and T779 (Figs. 5.27 and 5.28) which showed significantly different stress paths from that of all other test specimens. It was observed that the samples which were consolidated to  $1.0\sigma'_v$  iso best modelled the shape of the in-situ effective stress path.

It is observed from Figs. 5.23 to 5.34 and Table 5.1 that the reconsolidation procedure affected the direction in which the curve moved after failure. For the samples consolidated to  $1.0\sigma'_v$  iso, the curves all moved to the left after failure. This was also the behaviour observed for the control specimens. For the other 2 reconsolidation procedures,  $0.6\sigma'_v$  iso and  $1.0\sigma'_v$  aniso, the curves moved to the right with only two exceptions. Sample T776 (Fig. 5.27) moved to the right, but the results of this sample were considered undependable due to a loss in the accurate control of the water content of the sample. Sample T779 (Fig. 5.28) showed a stress path significantly different from all other test specimens and its behaviour has been considered an individual exception. Finally, T784 (Fig. 5.33) did not move either to the right or left, but rather followed back down the second section of its  $q$ - $p'$  curve. This may be due to its short storage period. If this sample had been stored for a longer period, then it may have showed a larger movement as was the case in T788 which was stored for 7 days with the same reconsolidation procedure.

Now compare the peak  $q$ -values shown in Table 5.1 and Fig. 5.35.

Consider the undrained shear strength, (expressed as  $q_{\text{peak}} = 2 c_u$ ) of the 5 in-situ control specimens. It is evident that the  $q_{\text{peak}}$  found for specimens T785 and T787 were slightly lower than those of T771, T772, and T773. The first two were subjected to a porewater pressure of 500 kPa during the entire triaxial consolidation stage. The other three were consolidated under 200 kPa of back pressure with it being raised to 500 kPa for one day prior to the undrained shear test. The samples were also consolidated in this same manner. However, the discrepancy is not large, and the  $q_{\text{peak}}$ -values of the samples will be compared to that of the average value obtained from all control specimens.

The average  $q_{\text{peak}}$ -value found for the five control specimens was 86.7 Pa. It is evident from Table 5.1 and Fig. 5.35, which shows the  $p'$  vs.  $q$  failure points for all test specimens, that several samples had strengths which were close to this value. First, the samples which were stored drained and then reconsolidated to  $1.0\sigma'_v$  iso, that is T777, T774 and T775 which had peak  $q$ -values of 91.7, 89.8, and 80.5 kPa respectively. The strengths of these samples were found to be 5.8 and 3.6 % higher and 7.2 % lower, respectively than the average of the control specimens. Also, the samples which were stored undrained and reconsolidated isotropically to either  $1.0\sigma'_v$  or  $0.6\sigma'_v$  (considering T781\*) had strengths close to that of the average in-situ strength. Samples T781\* ( $1.0\sigma'_v$  iso), T784 ( $0.6\sigma'_v$  iso) and T788 ( $0.6\sigma'_v$  iso) had peak  $q$ -values of 91.3, 82.3 and 81.1 kPa, which showed changes in strength of +5.1 to +6.5 %. The remaining samples

showed decreases in the in-situ strength ranging from -15.4 to -38.7 %. This would be unacceptable in commercial testing. The failure envelope in  $p'$  vs.  $q$  space (Fig. 5.35) will be discussed in more detail in Section 6.3.1.

#### 5.4 Porewater Pressure Generation

Curves of the normalized change in porewater pressure  $\Delta u / \sigma_{vc}'$  versus the axial strain  $\epsilon_1$  are shown in Figs. 5.1a to 5.15a for all test specimens during the undrained shear testing. As discussed in Section 5.2, different porewater pressure behavior was observed depending on the reconsolidation procedure. For the in-situ control specimens and the samples reconsolidated to  $1.0\sigma_v'$  iso, the porewater pressure continued to slowly rise after failure was reached. For the samples reconsolidated to either  $0.6\sigma_v'$  iso or  $1.0\sigma_v'$  aniso, it was observed that the porewater pressure either stayed constant (as was observed in T779 and T784), or decreased after failure. The specimens which showed an increase in porewater pressure after failure demonstrate a tendency to compress during undrained shear. This "compressive" behavior was also observed by Lau (1986) for his normally consolidated (NC) test specimens. In contrast, the specimens which showed a decrease in the porewater pressure after the failure was reached have demonstrated a tendency to dilate or expand. Lau's overconsolidated specimens also showed this type of dilative behavior.

The values of the porewater pressure parameter at failure

$A_f = \Delta u_f / \Delta(\sigma_1 - \sigma_3)_f$  are shown in Table 5.1. It is observed that the control specimens T785 and T787 had slightly higher  $A_f$ -values (0.45 and 0.42, respectively) than those of the other 3 controls (0.35 to 0.39). This may be due to the different porewater pressure conditions during consolidation as explained in Section 3.2.2. These  $A_f$ -values are significantly higher than those reported by Kwok (1984) and Lau (1986) who found it to vary between 0.12 and 0.20. However, this is to be expected since their specimens had been consolidated to a different (anisotropic) stress state. The samples which gave the best estimate of the in-situ  $A_f$ -values were T777, T774, and T789 (0.38, 0.43, and 0.40, respectively), which were reconsolidated to 1.0 iso, 1.0 iso, and 0.6 iso, respectively. The first 2 of these also gave the best estimate of the in-situ undrained shear strength. The  $A_f$ -value increased with increasing storage time for samples which were stored drained and reconsolidated using the same procedure. This was also found by Lau (1986).

Curves of the normalized change in porewater pressure  $\Delta u / \sigma_{vc}'$  versus the normalized change in total mean stress  $\Delta p / \sigma_{vc}'$  are shown for all specimens in Figs. 5.36 to 5.52. It was observed that all curves had an initial straight line section. The control specimens and the samples which were reconsolidated to  $1.0\sigma_v'$  iso (Figures 5.36 to 5.43, 5.48, and 5.49) then showed a slight bend to the right before taking a sudden hook to the left. In contrast, the samples which were reconsolidated to either  $0.6\sigma_v'$  iso or  $1.0\sigma_v'$  aniso (Figures 5.44, 5.46, 5.46, and 5.50 to 5.52) showed a sharp hook to the right following the

initial straight line section (excluding T776, Figure 5.45). It was evident that the porewater pressure behavior of the samples reconsolidated to  $1.0\sigma'_v$  iso was very similar to that of the in-situ control specimens, while that of the other specimens was quite different.

The slopes of the initial straight line sections has been designated as "m", and the values are shown for all specimens in Table 5.1. It was observed that the m-values of control specimens T771 and T785, which were 1.257 and 1.782 respectively, are significantly different from the other three controls which had m-values ranging from 1.508 to 1.566. Specimen T771 was consolidated to  $\sigma'_v = 80$  kPa,  $K_0 = 0.8$  and  $OCR = 1.0$ , which was slightly different from all other specimens which had a  $K_0$ -value of 1.0 at the final consolidation stress. Specimen T785 had a significantly higher water content at the end of triaxial consolidation than the other specimens (see Table 4.1). Therefore, these 2 specimens are at slightly different  $p' - q - V$  states than the others. The m-values of the samples will be compared to those of the remaining 3 in-situ control specimens, T772, T773, and T787. The m-values of the control specimens found by Kwok (1984) and Lau (1986) were 0.82 to 1.56 and 0.86 to 1.34 respectively. These are significantly lower than those found in the present study. However, this is again to be expected since the specimens were consolidated to different stress states.

It is evident from Table 5.1 that the samples which were consolidated to  $1.0\sigma'_v$  iso gave the best estimates of the in-situ

behavior. This was especially true for T777, which was stored drained for 15 minutes and had an  $m$ -value of 1.546. Sample T788, which was stored undrained for 7 days and then reconsolidated to  $0.6\sigma'_v$  iso also showed an  $m$ -value (1.507) that was close to in-situ value. It was also observed that as the storage time increased, so too did the  $m$ -value. This was also found by Lau (1986).

Considering both porewater pressure parameters  $m$  and  $A_f$ , it was observed that samples T777 and T774 gave the best estimate of the in-situ behavior. These samples were stored drained for 15 minutes and 1 day respectively, then both reconsolidated to  $1.0\sigma'_v$  iso. Some of the other samples had either the  $m$  or  $A_f$ -values close to that of the in-situ behavior, however only T777 and T774 had both values comparable to that of the control specimens. It should be remembered that these samples also gave the best estimate of the in-situ undrained shear strength.

### 5.5 Elastic Modulus

The elastic secant modulus  $E_{50}$  has been used to evaluate the early elastic portion of the  $q$  vs.  $\epsilon_1$  curves. This  $E_{50}$  value was obtained for each test from the slope of the  $q$  vs.  $\epsilon_1$  curve between the start of shearing and 50 % of the maximum deviator stress (Graham 1974). This parameter was also used by Lau (1986) to evaluate the early elastic portion of his stress-strain curves. The  $E_{50}$ -values as well as the relative stiffness  $E_{50} / c_u$  for all specimens are shown

in Table 5.1.

As seen from the table, the  $E_{50}$ -values for the in-situ control specimens show considerable scatter and therefore, no firm interpretation can be made. This was also found in the results of Lau (1986). From the table, it is seen that samples which had a shorter duration of storage period showed a larger  $E_{50}$ -value than those with a longer storage period. This was also observed by Lau (1986) who thought that this indicated that the samples with the shorter storage time were subjected to less disturbance during the offloading and subsequent storage. It is difficult to determine which reconsolidation procedure gave the best estimate of the in-situ  $E_{50}$ -value due to the variability found in the values calculated for the control specimens.

## Chapter 6 - Discussion and Comparison With Previous Work

### 6.1 Introduction

The project discussed in this thesis investigated the disturbance caused by effects of moderate stress release on the undrained shear behaviour of reconstituted clay specimens. The primary goal of the research was to determine a laboratory procedure for the treatment of samples which best estimates the "in-situ" undrained shear strength and stress-strain behaviour. An outline of the program and test procedures was given in Chapter 3. Detailed test results were given in Chapters 4 and 5 which also included some analysis of the data. This chapter examines more general topics raised by the research.

### 6.2 Soil Properties and Moisture Content Analysis

Classification tests, consisting of Atterberg limits and specific gravity tests, were performed on the illitic clay to monitor any chemical changes that might have occurred with time and altered the clay properties. Classification test results of the present investigation as well as those from Wu et al.(1983), Kwok (1984), Ambrosie (1985), and Lau (1986), all on the same clay, were presented in Table 3.1. As discussed in Section 3.1, it can be seen that the liquid limit  $w_L$  has increased monotonically with time, although the

plastic limit  $w_p$  and the specific gravity  $G_s$  have not been significantly altered. Over the 6 years that the clay has been stored in the laboratory, it was observed to change color from an original blue-grey to a brown-grey. Therefore, the chemical composition of the clay has been somewhat altered, probably by oxidation. It was also observed during the present tests, that the water content of the "cakes" at the end of slurry consolidation increased almost monotonically by small amounts as the program progressed. In any case, the clay used in the present investigation was slightly different in its chemistry compared with that used in the earlier projects. Therefore, care must be taken when comparing the results with the earlier investigations. It can be expected that strength would likely be unaffected by this process whereas water contents, specific volumes and stress-strain parameters ( $A_f$ ,  $m$ ,  $E_{50}$ , etc.) might show some changes.

Table 6.1 shows the moisture contents of each specimen during five different stages in the testing program. The moisture content at the beginning and end of slurry consolidation and at the end of the undrained shear testing were obtained directly from oven dried samples of the slurry and soil trimmings. These can therefore be considered accurate. The remaining three sets of water contents were calculated from volume change measurements recorded throughout each test. The volume change can be measured with good precision ( $\pm 0.05$  ml) and therefore can be considered accurate. However, there were small discrepancies between the moisture contents measured at the ends of

the tests from oven dried samples and those calculated from the volume change readings. These discrepancies were commonly 1 to 2 %. This used to be a common problem in triaxial testing at the University of Manitoba. It has been determined to be due to the procedure used for installing specimens into triaxial cells.

Most triaxial testing performed at the University of Manitoba is done on saturated soils. When a rubber membrane is placed around a specimen to isolate it from the cell liquid, water is flushed up between the side of the specimen and the membrane to expell any trapped air. This gives good saturation and improves the porewater pressure response. It is believed that the soil on the outside of the specimen (which is overconsolidated at this stage) absorbs a small amount of water during this flushing process. Therefore, the average water content in the specimen will be slightly higher than that measured from oven-dried samples prior to installation and the water content close to the outside of the specimen will be even higher. This difference was calculated at the end of the test and water contents throughout the test were adjusted appropriately. The water contents shown in Table 6.1 for the beginning of the triaxial test gives both the original value from oven dried sample at the end of one dimensional slurry consolidation, and the adjusted water content for the beginning of the triaxial consolidation.

The moisture content of each slurry mixture except the first was measured just prior to it being poured into the large cylinder for one dimensional consolidation. The intended water content was 120 %. As

can be seen from Table 6.1, the water contents range from 117.1 to 119.0 %, excluding sample T772 to T774. These are close to the desired value. It is believed that the small differences were due to a small volume of dissolved air originally in the porewater that was removed during the mixing process by a vacuum pump, as well as the extraction of water vapor. Slurry mixture T772 to T774 had a water content significantly less than the others (103.8 %). This was due to a measurement error during initial mixing. However, as can be seen from Table 6.1, the water content at the end of the slurry consolidation is not significantly different from the others.

Consider next the water contents of each specimen after slurry consolidation and prior to triaxial consolidation. It can be seen that T771 had a much higher water content (55.99 %) than the rest of the specimens. This was due to the time management problem discussed in Section 4.2.1. Specimens T791 and T792 were part of the high pressure testing program and their calculated water contents until the stage that the tests were terminated have been included for comparison.

The average water content at this end of slurry consolidation stage was found to be  $50.14 \% \pm 0.86 \%$ , excluding T771, T791, and T792. The variability compares favorably with that of Lau (1986), who found a standard deviation of 0.7 % at this stage. However, it can be seen from Table 6.1, that as the program progressed with time, the water content at the end of the slurry consolidation showed a generally increasing trend with some exceptions. This could again indicate

chemical changes which slightly altered the clay properties. The next column in the table shows the calculated water contents just prior to triaxial consolidation. These were back-calculated from the measured water content from oven dried samples at the end of triaxial shearing and the recorded volume changes measured throughout the consolidation, storage, and reconsolidation procedures, as was discussed earlier in this section. The difference in water content at this stage between the two estimates of water content range from 0.64 to 2.59 %.

Water contents of the specimens at the end of triaxial consolidation were calculated from the initial water contents and volume change readings recorded during consolidation processes. It is observed that there is considerable scatter in the results. The average water content was 42.05 %  $\pm$  1.20 %. The scatter is higher than that found by Lau (1986), who had a standard deviation of 0.4 %. It is believed that this is again in part due to the chemical changes that have occurred in the clay during the present program. The water content of T771 (42.17 %), is close to that of the others, even though the water content at the end of the slurry consolidation was much higher than the rest. Therefore, this sample is consolidated to approximately the same V-state as the others.

The moisture contents of the samples at the end of drained storage are also shown in Table 6.1. It can be seen that those samples stored for seven days showed a large increase in the moisture content, (for example T775 where the water content changed from 39.59 to 47.90 % after storage). Those which were stored for

15 minutes or 1 day showed much smaller increases in the water content as would be expected, (for example T777, which was stored drained for 15 minutes and had an increase of water content from 41.63 to 41.84 %). This trend of increasing change in water content with an increase in storage time was also observed by Lau (1986).

The net changes occurring in moisture content from the end of the consolidation period to the end of the reconsolidation period can be obtained by comparing the values in the fifth and seventh rows of Table 6.1. For the samples stored under drained conditions, it appears that those stored for longer periods show a larger net change in water content regardless of the reconsolidation procedure. See for example T777, T774, and T775 which were stored for 15 minutes, 1 day and 7 days, respectively and reconsolidated under  $1.0\sigma'_v$  iso. The net increases in water content in this case from the end of the consolidation to the end of reconsolidation were 0, 1.93, and 2.13 % respectively. This trend can also be observed in T778 and T779 (see Table 6.1). The same conclusion was reached by Lau (1986). However, for the samples stored undrained, there seems to be no systematic variation in moisture contents between these two stages (see also Graham et al.1987).

### 6.3 Undrained Shear Behaviour

#### 6.3.1 Failure Envelopes

The three previous M. Sc. projects at the University of Manitoba on stress release effects, identified a well-defined failure envelope. Fig. 5.35 shows this envelope in  $p'$ - $q$  space along with the failure  $p'$ - $q$  points from the present investigation. The previous overconsolidated envelope for samples stored drained for 15 minutes or stored undrained had  $c'_{uoc} = 16$  kPa with  $\phi' = 18^\circ$ . For samples stored drained for 7 days, the cohesion intercept decreased to 11 kPa with the same friction angle. The normally consolidated envelope was defined by  $c'_{unc} = 0$  and  $\phi = 25^\circ$ . It is observed that the control specimens in the present testing program show a fairly good agreement with the higher overconsolidated envelope. The scatter in the results is unfortunate, but is similar to that found by the three previous researchers.

It is seen that the present data from samples stored undrained or drained for short periods (15 minutes or 1 day) agree fairly well with the 15 minute or undrained envelope defined by the previous researchers. The samples which were stored undrained show reasonably good agreement of failure  $p'$  and  $q$  values of the control specimens. It appears that the duration of the storage time has little effect on the undrained shear strength. This was the same conclusion found by Graham et al.(1987). It was stated in Section 5.2 that the peak  $q$ -value for samples stored drained depended on the duration of the storage period. This can also be seen in Fig. 5.35 which shows that the failure envelope of the 7 day samples is below that of the control specimens and the 15 minute and 1 day samples. The present data agree

fairly well with the 7 day envelope defined by previous researchers.

It must be noted that the definition of overconsolidation could cause some problems in the examination of the present data. The conventional definition of overconsolidation is the ratio (OCR) of the maximum past vertical effective stress  $\sigma_{VC}'$  to the present vertical effective stress  $\sigma_{V0}'$ . However, critical state soil mechanics states that an overconsolidated soil can be changed to a normally consolidated one by yielding of that soil. Therefore, an overconsolidated soil can only exist inside the yield locus or state boundary surface. It was observed in Section 4.2.2 that during the offloading of the specimens in the present program to produce overconsolidation, they were yielded and the yield locus was expanded. Therefore, using the second definition, the specimens of the present program would technically be considered normally consolidated. However, the conventional definition of overconsolidation was adopted in the earlier projects and was therefore continued in the present investigation. This helps explain the unusual porewater pressure responses that will be dealt with in Section 6.3.4.

### 6.3.2 Influence Of Storage And Reconsolidation Procedures

#### On Undrained Shear Strength

This research investigated the effects of a number of different storage conditions and reconsolidation procedures on the undrained shear strength of samples which had been unloaded to "zero" total

applied stresses. Samples were subjected to both drained and undrained storage. Also, the duration of the storage period was varied to determine its effect on undrained shear behaviour. Three reconsolidation procedures were investigated with the objective of finding the procedure to best reproduce the "in-situ" behaviour. Five control specimens were tested without offloading to represent the in-situ behaviour. The results of the storage and reconsolidation stages were given in Chapter 4, and the results of the undrained shear tests were presented in Chapter 5.

As shown in Chapter 5, the samples which best recovered the in-situ shear strength were those which were either 1) stored undrained and reconsolidated to either  $1.0\sigma'_v$  iso or  $0.6\sigma'_v$  iso or 2) those stored drained for 15 minutes or 1 day and then reconsolidated to  $1.0\sigma'_v$  iso. It should be pointed out that in the second case, the reconsolidation procedure takes the specimens back to their in-situ stress state. The second of these conclusions is similar in principle to that found by Lau (1986) who found that drained storage for a short period followed by reconsolidation to the in-situ stress state was successful in recovering the in-situ shear strength. In his case however, the "in-situ" stress state was anisotropic, not isotropic as in the present case. Kwok (1984) found that for samples stored undrained, the shear strength did not depend on the length of the storage period for any given reconsolidation procedure. The present research supports these general conclusions, but adds a new dimension to them since the "in-situ" stresses were different than those tested

previously.

For samples stored drained, the longer the duration of the storage time, the lower the the strength. This was discussed in Chapter 5 and is also evident in Fig. 6.1 which shows the undrained shear strength  $c_u$  vs. specific volume  $V$  for all the various procedures that were examined. It can be seen that for the different reconsolidation procedures,  $c_u$  is larger for samples stored for shorter periods. Longer drained storage periods allow more water to be taken in, that is, the strains that these samples are subjected to during the storage period are larger. This must cause irrecoverable disruption of the soil structure since, regardless of the reconsolidation procedure, the in-situ  $c_u$  could not be recovered.

Fig. 6.1 also shows that the reconsolidation procedure with the highest  $p'$ -value produced samples with the highest strength. This is much the same conclusion found by Lau (1986). It can be seen from the figure that the samples reconsolidated to  $1.0\sigma'_v$  iso ( $p' = 80$  kPa) showed the highest strengths, while the other 2 procedures of  $0.6\sigma'_v$  iso and  $1.0\sigma'_v$  aniso with  $p'$ -values of 55 and 42 kPa, respectively had strengths lower than the first, but similar to each other. It is also observed that the sample reconsolidated to  $0.6\sigma'_v$  iso displayed the lowest  $V$  after reconsolidation. This would not be expected since the highest  $p'$ -value should give the lowest  $V$ .

Consider now the shape of the effective stress paths of the specimens in  $p'$ - $q$  space. It was observed in Section 5.3 and from Figs. 5.18 to 5.34 that samples reconsolidated to  $1.0\sigma'_v$  iso (or

reconsolidation to the "in-situ" stress state) best recovered the "in-situ" shape. Lau (1986) also found that reconsolidating a sample to its in-situ stress state best reproduced the shape of the in-situ  $p'$ - $q$  effective stress path, but remember again in his case, the in-situ state was anisotropic. The other two reconsolidation procedures had different shapes of the curve after the peak resistance occurred compared with the "in-situ" shapes from the control specimens. This may be due to reconsolidation to  $p'$ -values different from the in-situ value.

### 6.3.3 Failure Axial Strains

Section 5.2 examined the vertical strain at failure  $\epsilon_{1f}$  for all specimens. For samples stored undrained, it was found that the failure strains were smaller for the longer periods of storage. This was also found by Kwok (1984). For samples stored drained, the values of  $\epsilon_{1f}$  increased with an increase in storage time. (Lau (1986) found no systematic variation in  $\epsilon_{1f}$  with time for his samples stored drained). The samples which were reconsolidated to  $1.0\sigma'_v$  aniso showed failure strains which were slightly lower than those from the "control specimens" (2.32-2.78 % versus 2.67-3.48 %, respectively). This could be due the change in stress state from an in-situ isotropic state to an anisotropic stress state. For the samples reconsolidated using either of the two isotropic reconsolidation procedures, the  $\epsilon_{1f}$ -values for those stored for either 15 minutes or 1 day were very close to the

in-situ values (2.38-3.57 %). Those samples stored for 7 days had  $\epsilon_{1f}$ -values higher than the in-situ values (3.16-4.43 %). These were for both drained and undrained storage. It can be seen that the anisotropic reconsolidation procedure under-estimated the  $\epsilon_{1f}$ -value while the other two generally over-estimated it. Both Kwok (1984) and Lau (1986) found that all reconsolidation procedures over-estimated the value of  $\epsilon_1$  at failure. This was also generally found in the present investigation except for the anisotropic reconsolidation procedure. These findings influence the stiffness parameters such as  $E_{50}$  that can be interpreted from the stress-strain results.

#### 6.3.4 Porewater Pressure Generation

Section 5.4 presented the results of the porewater pressure generation during undrained shear. The values of  $A_f$  and  $m$  were presented in Table 5.1. It was observed that the in-situ value of  $A_f$  ranged from 0.35 to 0.42. There were 3 samples which gave a good estimate of these values. These were all reconsolidated isotropically, with 2 of these being reconsolidated to the in-situ stresses and stored drained for short periods. The anisotropically reconsolidated samples did not in this case produce  $A_f$ -values close to the in-situ value. This again is similar in principle to the findings of Lau (1986), who found that the samples reconsolidated to the in-situ stress state produced the best estimate of the in-situ  $A_f$ . In most cases in the present study, the  $A_f$ -value measured from samples

was higher than the in-situ value from the control specimens. This was also found by Lau (1986) who indicated that this was due to the particle reorientation during unloading, storage, and reconsolidation which causes the specimens to generate larger porewater pressures. For the small number of samples in this study which showed a smaller  $A_f$ , the opposite of this would be true. It was also found that the value of  $A_f$  for samples stored drained increased with an increase in the storage time. Lau (1986) also observed this and thought that this indicated that the longer storage period produced more disturbance of the samples.

The initial slope of the  $\Delta u / \sigma'_{VC}$  vs.  $\Delta p / \sigma'_{VC}$  curves (designated as "m"), was also used to evaluate the porewater pressure generation. Again, it was found that the samples stored drained for short periods and then reconsolidated to the in-situ stress state produced the best estimate of m. There was one other sample which gave a good estimate of the in-situ m-value, sample T788 which was stored undrained for 7 days and then reconsolidated to  $0.6\sigma'_v$  iso. This is thought to be an isolated occurrence. As the storage time increased, the m-value also increased. This was also observed by Lau (1986). In summary, the samples stored for short periods and reconsolidated to the in-situ stresses gave the best estimates of both of the in-situ  $A_f$  and m-values.

#### 6.4 End Of Test - "Critical State"

Fig. 6.2 shows the state of all samples in  $V$  vs.  $\log p'$  space at the end of undrained shearing. The states were interpreted from the measured data at the end of shear testing. The samples can be considered to be at a state that is only a fair approximation of the classical definition of critical state where  $\delta u / \delta \epsilon_1 = \delta q / \delta \epsilon_1 = 0$  (see Figs. 5.1 to 5.17). These formal conditions were clearly not fully met by the samples in the present study, especially the samples which were stored for 7 days drained and reconsolidated to either  $0.6 \sigma'_V$  iso or  $1.0 \sigma'_V$  aniso (see Figs. 5.10 to 5.12 and 6.2). However, it is evident that the data in Fig. 6.2 approach in principle what could be interpreted as a "Critical State Model" (Wroth and Houlsby 1980). The critical state line (CSL) shown in the figure is a best fit line with slope  $\lambda_2 = 0.231$  which was measured from the anisotropic consolidation of the triaxial specimens prior to unloading, storage, reconsolidation, and shearing. The line shows a fairly good agreement, with a few exceptions. The conclusions that can be drawn from this is that the Critical State Model permits a good understanding of the particular processes that have been explored in the testing program.

Fig. 6.2 also shows some final evidence of chemical changes that have occurred in the clay since the entire stress release project was initiated approximately 7 years ago. Note the shift in the CSL found in the present program from that determined by Graham and Lau (1988).

This shift is similar in magnitude to that observed in Fig. 4.5 for the 1-D NCL. This similarity in shift is encouraging when considering the comparability between the present investigation and the previous projects.

## Chapter 7 - Conclusions and Suggestions for Further Research

### 7.1 Conclusions

The following principal conclusions have been drawn from the testing performed in this thesis project. It was determined that to accurately recover the in-situ undrained shear strength of reconstituted samples which have undergone moderate stress release and are subjected to drained storage, they should first be stored for as short a time as possible before testing and then reconsolidated to their in-situ stress state ( $1.0 \sigma'_V$  iso in this study). If the samples have no access to drainage during the storage period, then again they should be stored for as short a time as possible and reconsolidated to  $1.0 \sigma'_V$  iso, although the length of storage time does not have as great an effect on the strength as was found for the samples which were stored drained. These conclusions are very similar in principle (though clearly different in detail) to those found from earlier programs. Criticisms of the choice of  $K_{0oc} = K_{0nc}$  in the earlier work, while justified, do not mean that the earlier conclusions can be disregarded.

The following more specific and less principle conclusions have been drawn from the results presented in this thesis:

1. One-dimensional slurry consolidation of illitic clay in the large steel cylinder continued to provide consistent specimens within

each "cake" and between successive "cakes" in terms of small variations in moisture content. The average moisture content at the end of slurry consolidation was found to be 50.6 % with a standard deviation of 1.16 %.

2. For identical loading conditions, the  $\lambda_1$ -values for one-dimensional cylinder consolidation ranged from 0.356 to 0.565 with an average of 0.477 and standard deviation of 0.065.
3. During triaxial consolidation, the  $\kappa_1$ -values for reloading ranged from 0.101 to 0.133 with an average of 0.118 and a standard deviation of 0.009.
4. The  $\lambda_2$ -values during triaxial consolidation ranged from 0.214 to 0.274 with an average of 0.231 and a standard deviation of 0.012.
5. The  $\kappa_2$ -values during triaxial consolidation varied from 0.012 to 0.70 with an average of 0.020 and a standard deviation of 0.006.
6. During isotropic unloading of test samples, the porewater pressures decreased by 94 to 100 % of the corresponding decrease in total stress (that is  $\bar{B} = 94-100$  %).
7. For samples stored under drained conditions, the amount of volume increase experienced was found to increase with the length of storage time. The samples stored for 15 minutes showed final volumetric strain increases of 0.18 and 0.27 %, while the samples stored for 1 and 7 days exhibited much greater increases of 3.95 % and 6.12 to 8.28 %, respectively.
8. For the samples stored under undrained conditions, a general trend of increasing residual porewater pressure with time immediately

after unloading was observed. Final values of the ratio  $u_r / u_{r_i}$  were found to be 79.2 % (15 minute storage), 125.9 % (1 day storage), and 89.7 and 50.1 % (7 day storage periods).

9. For samples stored undrained and reconsolidated using the same procedure, the length of storage time had no apparent effect on the strains observed during reconsolidation.
10. For samples stored drained and then reconsolidated using the same procedure, an increase in both the axial and volumetric strains during reconsolidation was observed for samples stored for longer periods. Also, an increase in the porewater pressure parameters  $m$  and  $A_f$  was observed for longer storage periods. This is due to a higher degree of sample disturbance from stress release caused by longer duration storage periods.
11. For samples stored under identical conditions, higher volumetric strains were found for samples reconsolidated to higher  $p'$ -values. Also, higher axial strains were observed for samples reconsolidated anisotropically (with some shear stress) compared with those reconsolidated isotropically.
12. The failure envelope of  $c'_{OC}=16$  kPa and  $\phi'_{OC}=18^\circ$  for the control specimens and 15 minute samples and  $c'_{OC}=11$  kPa and  $\phi'_{OC}=18^\circ$  for the 7 day samples established in the preceding research was found to apply for the current project.
13. For samples stored undrained, all 3 reconsolidation procedures produced undrained shear strengths similar to the in-situ shear strength of the control specimens for all storage periods.

However, those reconsolidated isotropically and stored for the shortest time period did seem to give the best estimate of the in-situ strength. It is unfortunate that some experimental error and scatter were observed for the samples stored undrained and it is difficult to make a firm interpretation.

14. For samples which were stored drained, those reconsolidated to  $1.0 \sigma'_v$  iso (which is also the in-situ stress state prior to unloading) which were stored for either 15 minutes or 1 day best recovered the in-situ  $c_u$ . They over estimated the in-situ value by 6 and 4 %, respectively. The samples reconsolidated to  $1.0 \sigma'_v$  aniso underestimated the in-situ  $c_u$  value by 17 and 31 % for storage times of 15 minutes and 7 days, respectively, while the sample stored for 7 days and reconsolidated to  $0.6 \sigma'_v$  iso underestimated  $c_u$  by 34 %.
15. In general, all 3 reconsolidation procedures overestimated the in-situ  $A_f$  value for samples stored drained while it was underestimated for samples stored undrained regardless of the reconsolidation procedure. Significant variability was observed for the axial strain at failure ( $\epsilon_{1f}$ ), porewater pressure parameter  $m$ , and modulus  $E_{50}$  and it is difficult to draw any firm conclusions.
16. The data from the present program seemed to fit into a generalized Critical State Model which permits a good understanding of soil behaviour.

## 7.2 Suggestions For Further Research

1. Further research should be conducted on samples with higher in-situ effective stresses and OCR values, which are now common occurrences in the offshore geotechnical industry.
2. A better understanding of gassy soil behaviour is required and a theroretically and practically sound testing program must be implemented to help contribute to this understanding.
3. Further work is required to compare and evaluate research such as that described in this thesis with the effects of sample disturbance due to stress release on real offshore clay samples.

REFERENCES

- Ambrosie, A. W., 1985. Effects of stress-release disturbance on the shear behaviour of simulated offshore normally consolidated clay samples. M. Sc. Thesis, University of Manitoba.
- Atkinson, J. H. and Bransby, P. L., 1978. The mechanics of soils - an introduction to critical state soil mechanics. Publ. McGraw-Hill Book Co. Ltd., England.
- Attwooll, W. J., Fujioka, M. R., and Kittridge, J. C., 1985. Laboratory and in-situ testing of marine soils in Iran and Indonesia. Strength Testing of Marine Sediments; Lab and In-situ Measurements. American Society of Testing of Materials, Special Technical Publication 883, Eds. Chaney, R. C. and Demars, K. R., pp. 440-453.
- Bishop, A. W. and Henkel, D. J., 1962. Measurements of soil properties in the triaxial test. Publ. Edward Arnold, London, England. 2nd Ed.
- Bjerrum, L., 1973. Problems of soil mechanics and construction on soft clays. State of the Art Report to Session IV, 8th International Conference on Soil Mechanics and Foundation Engineering, Moscow, 1973. Vol. 3, pp. 1-53.
- Brooker, E. W. and Ireland, H. O., 1965. Earth pressures at rest related to stress history. Canadian Geotechnical Journal (C. G. J.), Vol. II, No. 1, February 1965, pp. 1-15.
- Bryan, G. M., 1974. In-situ indication of gas hydrate. Natural Gases in Marine Sediments, Ed. I. R. Kaplan. Publ. Plenum Press, New York, pp. 299-308.
- Chace, A. B. Jr., 1985. Pressure release disturbance in simulated marine cores as indicated by a laboratory gamma-ray densitometer. Strength Testing of Marine Sediments: Laboratory and In-situ Measurements, ASTM STP 883, Eds. Chaney, R. C. and Demars, K. R., pp. 154-165.
- Coatsworth, A. M., 1986. A rational approach to consolidated undrained triaxial testing. Site investigation Practice: Assessing BS 5930 Geological Society, Engineering Special Publication No. 2, Ed. A. B. Hawkins, pp. 167-175.
- Craig, R. F., 1983. Soil Mechanics. Publ. Van Nostrand Reinhold (UK) Co. Ltd. Molly Millars Lane, Wokingham, Berkshire, England. Third Ed., p. 113.

- de Ruiter, J., 1976. North Sea site investigation - the role of the geotechnical consultant. *Offshore Soil Mechanics*. Eds. Philip George and David Wood, Cambridge University Engineering Department, pp. 62-78.
- Feng, G.-D. and Lui, Z., 1986. The adhesive force of marine clay. *Marine Geotechnology and Nearshore and Offshore Structures*, ASTM STP 923, Eds. R. C. Chaney and H. Y. Fang. Philadelphia, pp. 267-280.
- Fredlund, D. G., 1976. Density and compressibility characteristics of air-water mixture. *C. G. J.* Vol. 13, No. 4, Nov., pp. 386-396.
- Graham, J. and Houlsby, G. T., 1983. Anisotropic elasticity of a natural clay. *Geotechnique* Vol. 33, No. 2, June, pp. 165-180.
- Graham, G., Kwok, C. K. and Ambrosie, R. W., 1987. Stress release, undrained storage, and reconsolidation in simulated underwater clay. *C. G. J.* Vol. 24, No. 2, May, pp. 279-288.
- Graham, G. and Lau, S. L.-K., 1988. Influence of stress-release disturbance, storage, and reconsolidation procedures on the shear behaviour of reconstituted underwater clay. *Geotechnique*, Vol. 38, No. 2, June, pp. 279-300.
- Hand, J. H., Katz, D. L., and Verma, V. K., 1974. Review of gas hydrates with implications for ocean sediments. *Natural Gases in Marine Sediments*, Ed. I. R. Kaplan. Plenum Press, New York, pp. 179-194.
- Henkel, D. J., 1960. The shear strength of saturated remoulded clays. *ASCE - Research Conf. on Shear Strength of Remoulded Soils*, Boulder, Colorado, 1960, pp. 533-554.
- Hitchon, Brian, 1974. Occurrence of natural gas hydrates in sedimentary basins. *Natural Gases in Marine Sediments*, Ed. I. R. Kaplan. Plenum Press, New York, pp. 195-234.
- Hoeg, K., 1986. Geotechnical issues in offshore engineering. *Marine Geotechnology and Nearshore and Offshore Structures*, ASTM STP 923, Eds. R. C. Chaney and H. Y. Fang. Philadelphia, pp. 7-50.
- Jefferies, M. G., Ruffell, J. P., Crooks, J. H. A., and Hughes, J. M. O., 1985. Some aspects of the behavior of Beaufort Sea clays. *Strength Testing of Marine Sediments, Laboratory and In-situ Measurements*, ASTM STP 883, pp. 487-514.
- Kaplan, I. R., 1974. Introduction. *Natural Gases in Marine Sediments*, Plenum Press, New York, pp. 1-10.

- Kirkpatrick, W. M. and Khan, A. J., 1984. The reaction of clays to sampling stress relief. *Geotechnique*, Vol. 34, No. 1, March, pp. 29-42.
- Kirkpatrick, W. M., Khan, A. J., and Mirza, A. A., 1986. The effects of stress relief on some overconsolidated clays. *Geotechnique*, Vol. 36, No. 4, Dec., pp. 511-525.
- Knapp, Robert T., Daily, James W., and Hammitt, Frederick G., 1970. *Cavitation*. McGraw-Hill Book Co., New York, pp. 51-93.
- Kulkarni, R. P., 1983. The strength of "perfect samples" of Bombay marine clay. *Irrigation and Power*, Vol. 40, No. 3, July, pp. 265-270.
- Kwok, C. K., 1984. Effects of stress-release disturbance on the shear behavior of simulated overconsolidated clay samples. M. Sc. Thesis, University of Manitoba, Winnipeg, Manitoba, Canada.
- Ladd, C. C. and Bailey, W. A., 1964. Correspondence on "The behavior of saturated clays during sampling and testing" by Skempton, A. W. and Sowa, V. A. *Geotechnique* Vol. 14, No. 4, pp. 353-358.
- Ladd, C. C. and Foott, R., 1974. New design procedures for stability on soft clays. *Journal of Geotechnical Engineering Division, Proceedings American Society of Civil Engineers*, Vol. 100, GT7, July, pp. 763-786.
- Ladd, C. C. and Lambe, T. W., 1963. The strength of "undisturbed" clay determined from undrained tests. *ASTM - Symposium on Laboratory Shear Testing of Soils*, Ottawa. STP 361.
- Lau, S. L.-K., 1986. Effects of stress-release disturbance on the shear behavior of simulated offshore clays subjected to drained storage. M. Sc. Thesis, University of Manitoba, Winnipeg, Manitoba, Canada.
- Mayne, P. W. and Kulhawy, F. H., 1982.  $k_0$ -OCR relationships in soil. *ASCE - Geotechnical Division*, June, pp. 851-872.
- McIver, R. D., 1974. Hydrocarbon gas (methane) in canned deep sea drilling project core samples. *Natural Gases in Marine Sediments*, Ed. I. R. Kaplan. Plenum Press, New York, pp. 63-69.
- Miller, S. L., 1974. The nature and occurrence of clathrate hydrates. *Natural Gases in Marine Sediments*, Ed. I. R. Kaplan. Plenum Press, New York, pp. 151-177.
- Mori, H., 1981. General report on session 7 - soil exploration and sampling. *Proc. 10th Int. Conf. on Soil Mechanics and Foundation*

- Engineering, Stockholm, Sweden, 1981, Vol 4, pp. 399-413.
- Noorany, I. and Seed, H. B., 1965. In-situ strength characteristics of soft clays. ASCE - Journal of Soil Mechanics and Foundation Division, Vol. 91, No. sm2, pp. 49-80.
- Okumura, T., 1977. Stress change of soil samples taken from sea floor. 9th International Conference on Soil Mechanics and Foundation Engineering, Tokyo. Specialty Session 2, Soil Sampling, 1977, pp. 141-145.
- Okumura, T. and Matsumoto, K., 1981. Marine auto sampler and sample quality. Proc. 10th Int. Conf. of SMFE, Stockholm, Sweden, 1981, Vol. 2, pp. 537-540.
- Richards, A. F., 1984. Modelling and consolidation of marine soils. Seabed Mechanics, IUTAM, pp. 3-8.
- Richards, A. F. and Zuidberg, H. M., 1986. Sampling and in-situ geotechnical investigations offshore. Marine Geotechnology and Nearshore/Offshore Structures, Eds. R. C. Chaney and H. Y. Fang. ASTM - STP 923, Philadelphia, pp. 51-73.
- Sangrey, D. A., 1972. Obtaining strength profiles with depth for marine deposits using undisturbed samples. Underwater Soil Sampling, Testing and Construction Control, ASTM STP 501, pp. 106-121.
- Skempton, A. W., 1954. The por pressure coefficients A and B. Geotechnique, Vol. 4, No. 4, pp. 143-147.
- Skempton, A. W. and Sowa, V. A., 1963. The behavior of saturated clays during sampling and testing. Geotechnique, Vol. 13, No. 4, pp. 269-290.
- Sobkowicz, J. C. and Morgenstern, N. R., 1984. The undrained equilibrium behavior of gassy sediments. C. G. J., Vol. 21, No. 3, August, pp. 439-448.
- Sobkowicz, J. C. and Morgenstern, N. R., 1987. An experimental investigation of transient pore pressure behavior in soils due to gas exsolution. Prediction and Performance in Geotechnical Engineering, Calgary, June, 1987, pp. 267-275.
- Stoll, R. D., 1974. Effects of gas hydrates in sediments. Natural Gases in Marine Sediments, Ed. I. R. Kaplan. Plenum Press, New York, pp. 235-248.
- Temperley, H. N. V. and Chambers, L. G., 1946. The behavior of water under hydrostatic tension: I. The Proceedings of the Physical

Society, Vol. 58, Jan.-Nov., pp. 420-435.

- Wroth, C. P. and Houlsby, G. T., 1980. A critical state model for predicting the behaviour of clays. Proc. of Workshop on Limit Equilibrium, Plasticity, and Generalized Stress-Strain in Geotechnical Engineering, McGill University, Montreal, pp. 592-627.
- Wood, D. M. and Graham, J., 1987. Anisotropic yielding and elasticity of Winnipeg clay. Symposium on Yielding, Damage, and Failure of Anisotropic Soils, Grenoble, France, 1987.
- Young, A. G., Quiros, G. W. and Ehlers, C. J., 1983. Effects of offshore sampling and testing on undrained soil shear strength. Proceedings of the 15th Offshore Technology Conference, Houston, Texas, Vol. 1, 1983, pp. 193-216.

AUTHOR	LL	PL	PI	SPECIFIC GRAVITY
JAMIESON (1989)	62.5	29.9	32.6	2.74
LAU (1986)	59.5	25.9	33.6	2.74
AMBROSIE (1985)	57.9	25.1	32.8	2.73
KWOK (1984)	57.2	25.7	31.5	2.73
WU et al. (1983)	54.4	26.1	28.3	--

TABLE 3.1 CLASSIFICATION RESULTS OF ILLITIC CLAY

SAMPLE No.	$\lambda_1$	W/C - END OF SLURRY CONS. (%)	$K_1$	$\lambda_2$	$K_2$	W/C - END OF TX. CONS. (%)
T771	0.565	58.58	0.218	0.274	0.070	43.25
T772	0.389	49.74	0.123	0.214	0.018	41.40
T773	0.389	50.63	0.115	0.220	0.019	41.80
T774	0.389	51.11	0.113	-	0.015	41.13
T775	0.356	51.12	0.101	0.224	0.031	41.54
T776	0.356	-	-	-	-	-
T777	0.356	51.91	0.133	0.219	0.020	41.63
T778	0.511	51.16	0.125	0.225	0.020	41.99
T779	0.511	51.51	0.110	0.222	0.012	42.24
T781	0.505	49.20	0.116	0.245	0.022	41.21
T782	0.505	52.44	0.121	0.236	0.017	42.73
T784	0.512	51.49	0.109	0.241	0.032	43.56
T785	0.512	50.93	-	-	-	43.78
T787	0.468	51.60	-	-	0.015	42.76
T788	0.468	52.08	0.128	0.242	0.017	42.59
T789	0.468	52.19	0.122	0.250	0.025	42.64
T790	0.506	-	-	-	-	-
T791	0.506	52.85	-	-	-	-
T792	0.506	53.17	-	-	-	-

NOTE: WATER CONTENTS AT END OF TRIAXIAL CONS. ARE CALCULATED FROM VOLUME CHANGE MEASUREMENTS USING THE WATER CONTENT AT THE END OF TRIAXIAL CONSOLIDATION (OR END OF SHEARING) FROM OVEN DRIED SAMPLES AS A BASE

TABLE 4.1 SUMMARY OF CONSOLIDATION RESULTS

SAMPLE NO.	STORAGE			RECONSOLIDATION		
	STORAGE TIME	DRAINED	UNDRAINED	TYPE	v (%)	v (%)
		VOLUMETRIC SWELLING v (%)	$u_r/u_{ri}$			
T777	15 MIN	0.27	--	1.0	0.24	0.17
T774	1 DAY	3.95	--	1.0	3.57	1.23
T775	7 DAY	8.28	--	1.0	7.33	2.24
T778	15 MIN	0.18	--	1.0	-0.60	0.26
T779	7 DAY	6.12	--	1.0	4.53	3.94
T789	7 DAY	7.81	--	0.6	4.54	2.14
T781	15 MIN	--	0.792	1.0	-0.02	0.11
T782	7 DAY	--	0.897	1.0	-0.64	0.20
T784	1 DAY	--	1.259	0.6	0.12	0.43
T788	7 DAY	--	0.501	0.6	-1.14	0.02

NOTE: POSITIVE RECONSOLIDATION STRAINS ARE COMPRESSIVE

TABLE 4.2 SUMMARY OF TEST RESULTS DURING STORAGE AND RECONSOLIDATION

SAMPLE No.	PEAK q (kPa)	p' AT FAIL. (kPa)	PEAK q/p'	p' END OF TEST (kPa)	C <sub>i</sub> AT PEAK q (%)	A <sub>f</sub> AT PEAK q	m	B UNLOADING (%)	E <sub>50</sub> (MPa)	E <sub>50</sub> /C <sub>u</sub>
T771	86.6	68.9	1.278	59.7	2.67	0.35	1.257	---	20.1	464
T772	93.6	75.4	1.276	65.6	3.48	0.37	1.566	---	98.6	2107
T773	88.6	72.9	1.250	62.4	2.76	0.39	1.508	---	9872.0	233000
T785	83.1	72.9	1.163	66.4	3.31	0.45	1.782	---	164.0	3947
T787	81.6	77.4	1.059	67.8	2.85	0.42	1.508	---	187.8	4603
T777	91.7	75.6	1.252	64.1	2.38	0.38	1.546	0.993	263.4	5745
T774	89.8	72.1	1.250	64.7	3.57	0.43	1.597	1.000	124.7	2777
T775	80.5	63.9	1.272	60.0	4.18	0.52	1.593	0.992	92.9	2308
T778	71.7	61.8	1.157	58.9	2.32	0.14	0.993	0.937	128.0	3570
T776	64.1	45.9	1.520	42.0	2.54	0.61	1.438	---	17.4	634
T779	54.9	45.8	1.205	43.2	2.55	0.83	2.196	1.008	26.8	836
T789	57.3	44.9	1.310	44.5	4.43	0.40	1.694	0.995	69.8	2436
T781	68.9	70.7	0.991	64.1	3.14	0.44	1.479	0.990	124.1	3602
T781*	91.3	78.1	1.185	70.5	3.14	0.35	1.160	0.990	177.2	3882
T782	75.8	62.4	1.265	54.0	2.78	0.13	1.143	0.984	84.3	2224
T784	82.3	67.7	1.219	60.5	3.26	0.31	1.357	0.956	179.1	4352
T788	81.1	61.9	1.371	59.0	3.16	0.19	1.507	1.001	130.7	3223

TABLE 5.1 SUMMARY OF UNDRAINED SHEAR TEST RESULTS

SAMPLE	START OF SLURRY CONS. (ODS)		WATER CONTENTS (%)		END OF SLURRY CONS. (ODS)		END OF TRIAXIAL CONS. (Cal)		END OF TRIAXIAL STORAGE (Cal)		END OF RECONS. (ODS)		STORAGE TIME/TYPE		RECONS. TYPE	
T771	--		55.99	58.58	43.25	--	43.25	--	43.25	--	43.25	--	--			--
T772	103.8		48.47	49.74	41.40	--	41.40	--	41.40	--	41.40	--	--			--
T773	103.8		48.92	50.63	41.80	--	41.80	--	41.80	--	41.80	--	--			--
T785	117.9		50.93	--	43.78	--	43.78	--	43.78	--	43.78	--	--			--
T787	119.0		50.73	51.60	42.76	--	42.76	--	42.76	--	42.76	--	--			--
T777	117.9		49.86	51.91	41.63	41.84	41.63	41.84	41.63	41.84	41.63	15 MIN	- D	1.0	ISO	
T774	103.8		49.13	51.11	39.62	42.65	39.62	42.65	39.62	42.65	41.55	1 DAY	- D	1.0	ISO	
T775	117.9		49.17	51.12	39.59	47.90	39.59	47.90	39.59	47.90	41.72	7 DAY	- D	1.0	ISO	
T778	118.0		50.22	51.16	41.99	42.15	41.99	42.15	41.99	42.15	42.65	15 MIN	- D	1.0	ANISO	
T776	117.9		50.05	--	--	--	--	--	--	--	43.50	7 DAY	- D	1.0	ANISO	
T779	118.0		50.87	51.51	42.24	47.21	42.24	47.21	42.24	47.21	43.44	7 DAY	- D	1.0	ANISO	
T789	119.0		51.41	52.19	42.64	48.84	42.64	48.84	42.64	48.84	44.23	7 DAY	- D	0.6	ISO	
T781	117.1		49.98	49.20	41.21	41.21	41.21	41.21	41.21	41.21	41.21	15 MIN	- U	1.0	ISO	
T782	117.1		50.23	52.44	42.73	42.73	42.73	42.73	42.73	42.73	42.73	7 DAY	- U	1.0	ANISO	
T784	117.9		51.26	51.49	43.56	43.56	43.56	43.56	43.56	43.56	43.56	1 DAY	- U	0.6	ISO	
T788	119.0		50.81	52.08	42.59	42.59	42.59	42.59	42.59	42.59	43.54	7 DAY	- U	0.6	ISO	

NOTE: ODS - MEASURED FROM OVEN DRIED SAMPLES  
 Cal - CALCULATED FROM VOLUME CHANGE MEASUREMENTS  
 D - DRAINED STORAGE  
 U - UNDRAINED STORAGE  
 ISO - ISOTROPIC RECONSOLIDATION  
 ANISO - ANISOTROPIC RECONSOLIDATION

TABLE 6.1 WATER CONTENTS OF SAMPLES THROUGHOUT TEST

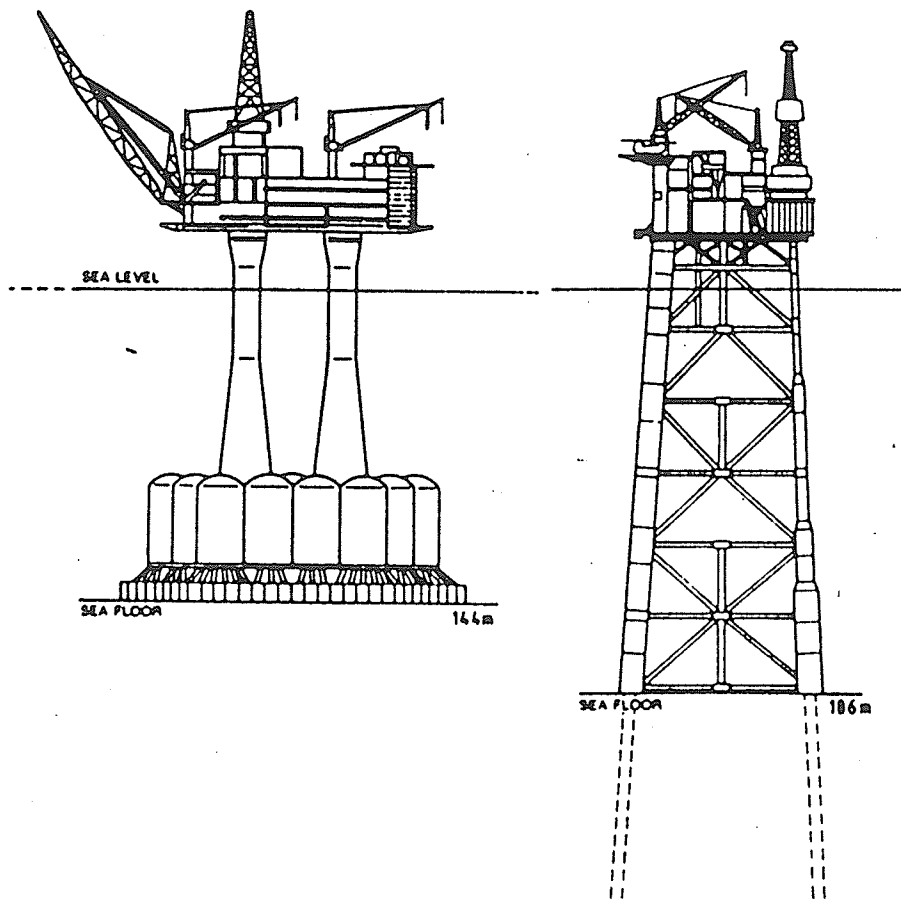


FIGURE 1.1 a,b TYPICAL GRAVITY AND PILE SUPPORTED SEABED STRUCTURES  
HOEG (1986)

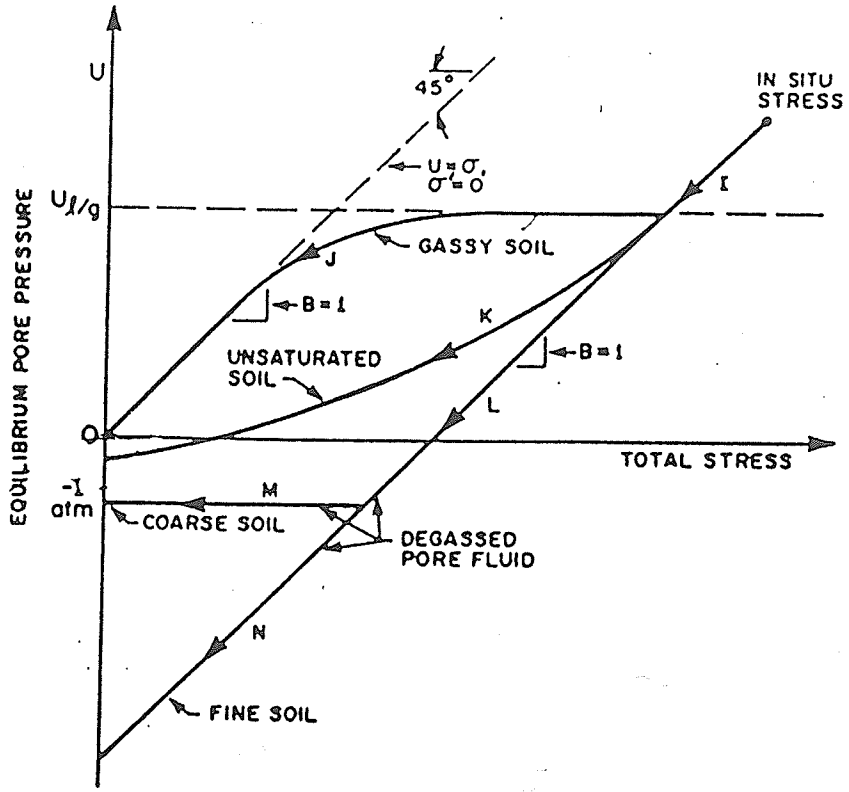


FIGURE 2.1 ISOTROPIC UNLOADING BEHAVIOUR OF SATURATED (1), UNSATURATED (2), AND GASSY (3) SOILS; (SOBKOWICZ AND MORGENSTERN 1984)

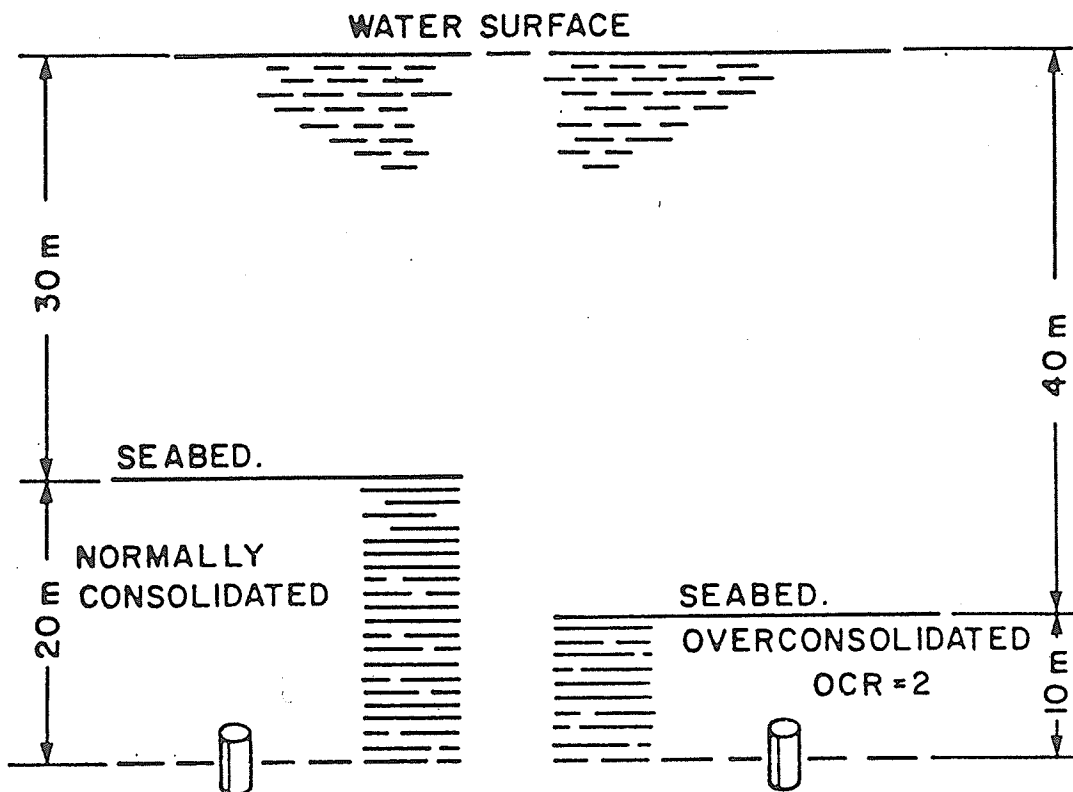


FIGURE 3.1 SCHEMATIC DIAGRAM OF MODELLED IN-SITU FIELD CONDITIONS.

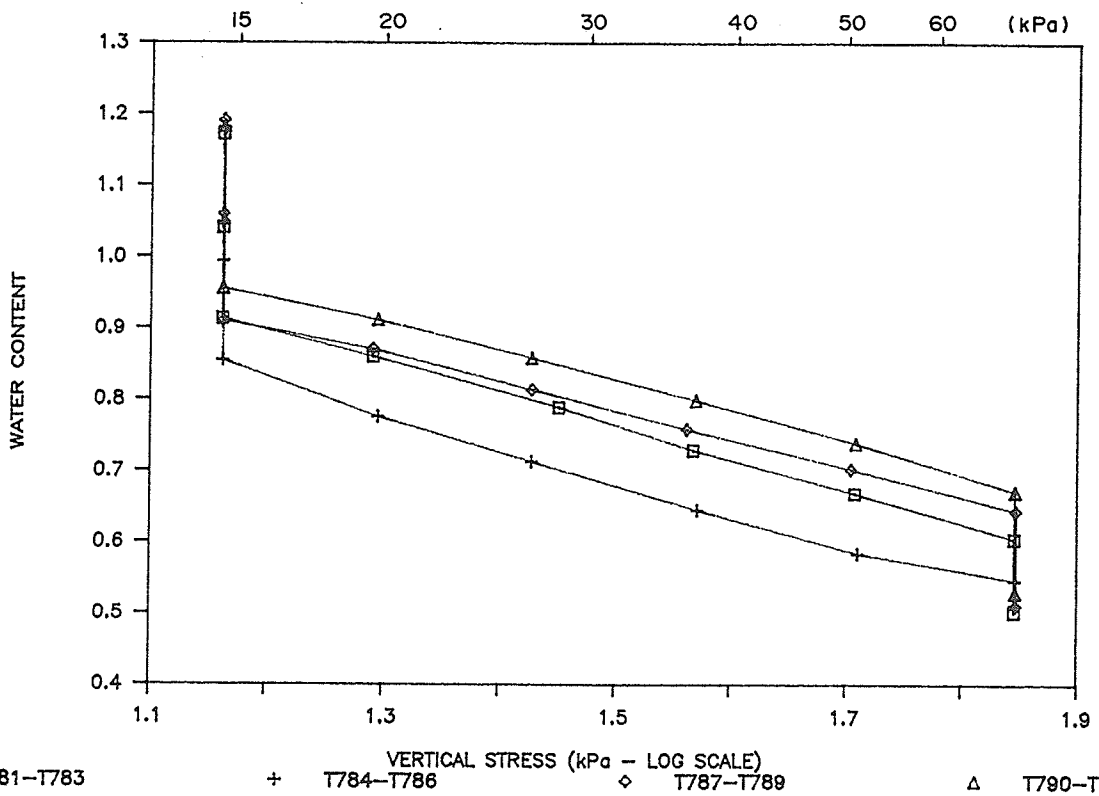
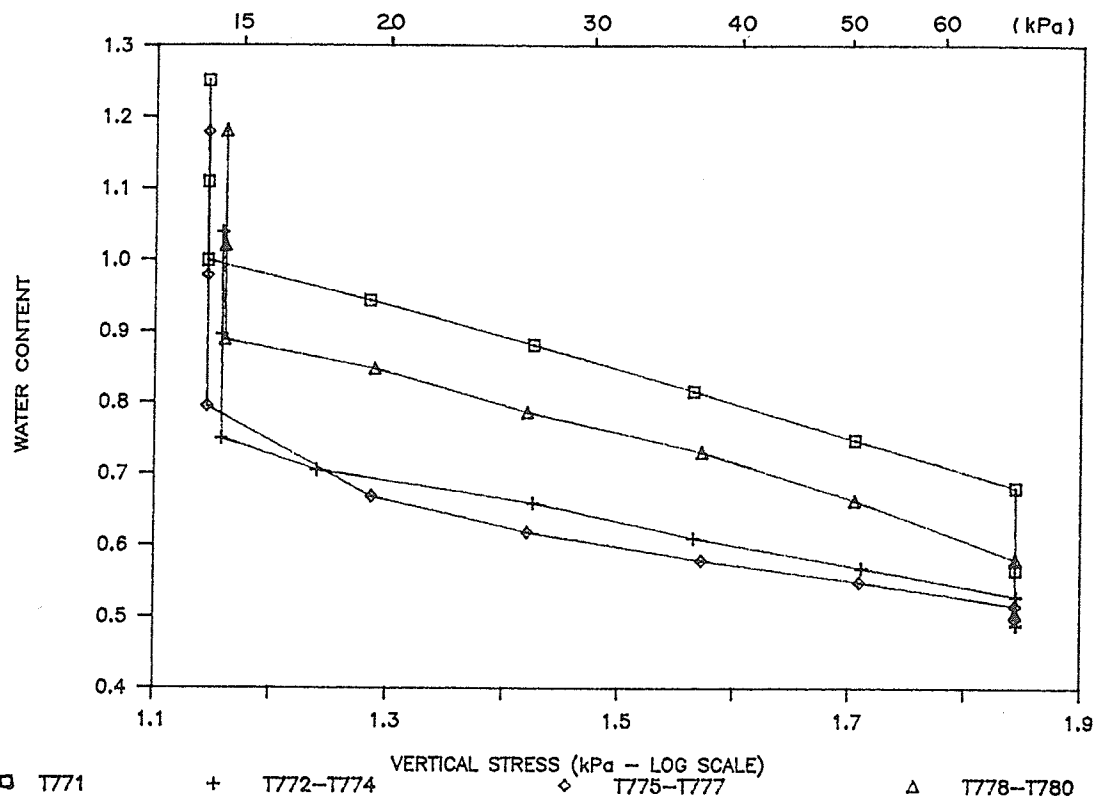


FIGURE 4.1 a,b ONE-DIMENSIONAL SLURRY CONSOLIDATION LOG ( $\sigma_v$ ) vs. w

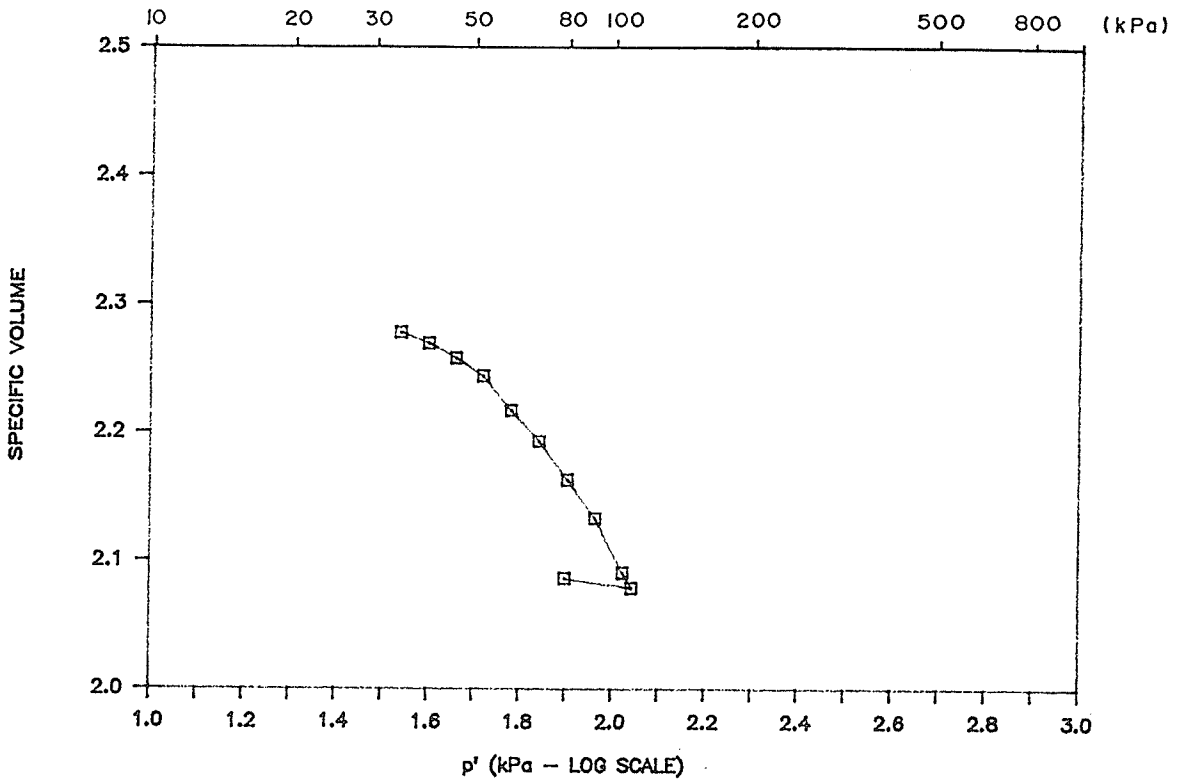
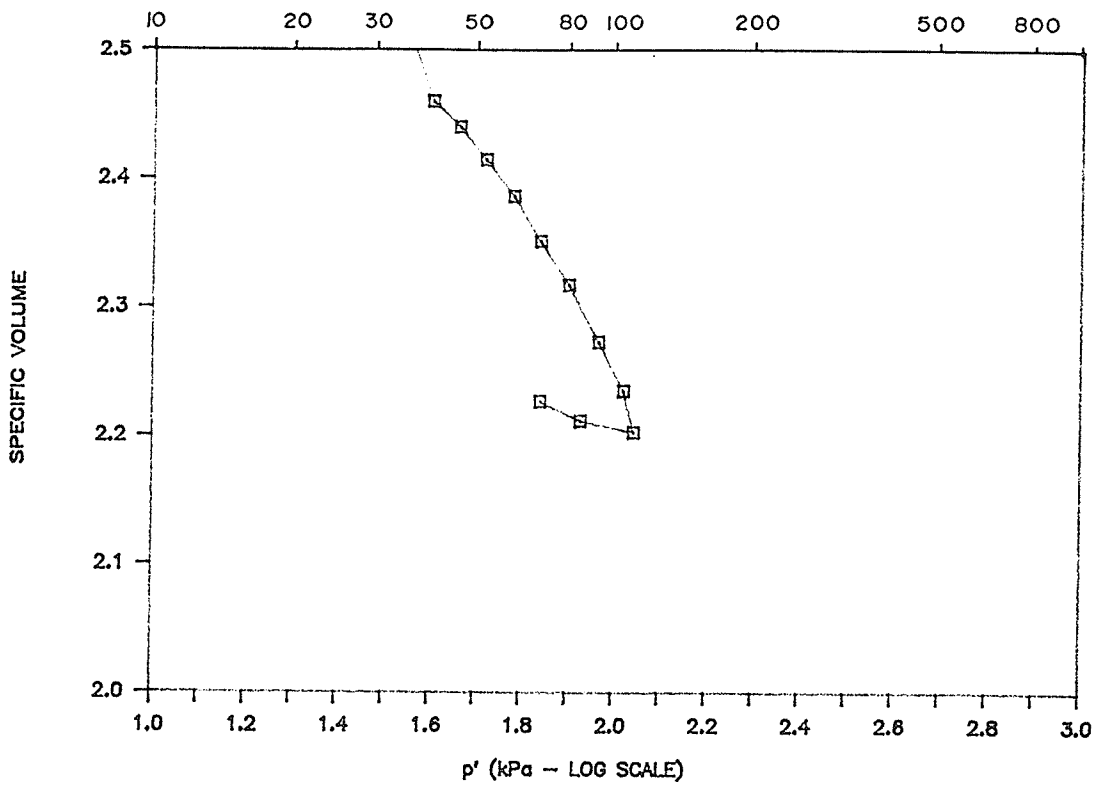


FIGURE 4.2 a,b TRIAXIAL CONSOLIDATION SAMPLES T771, T772

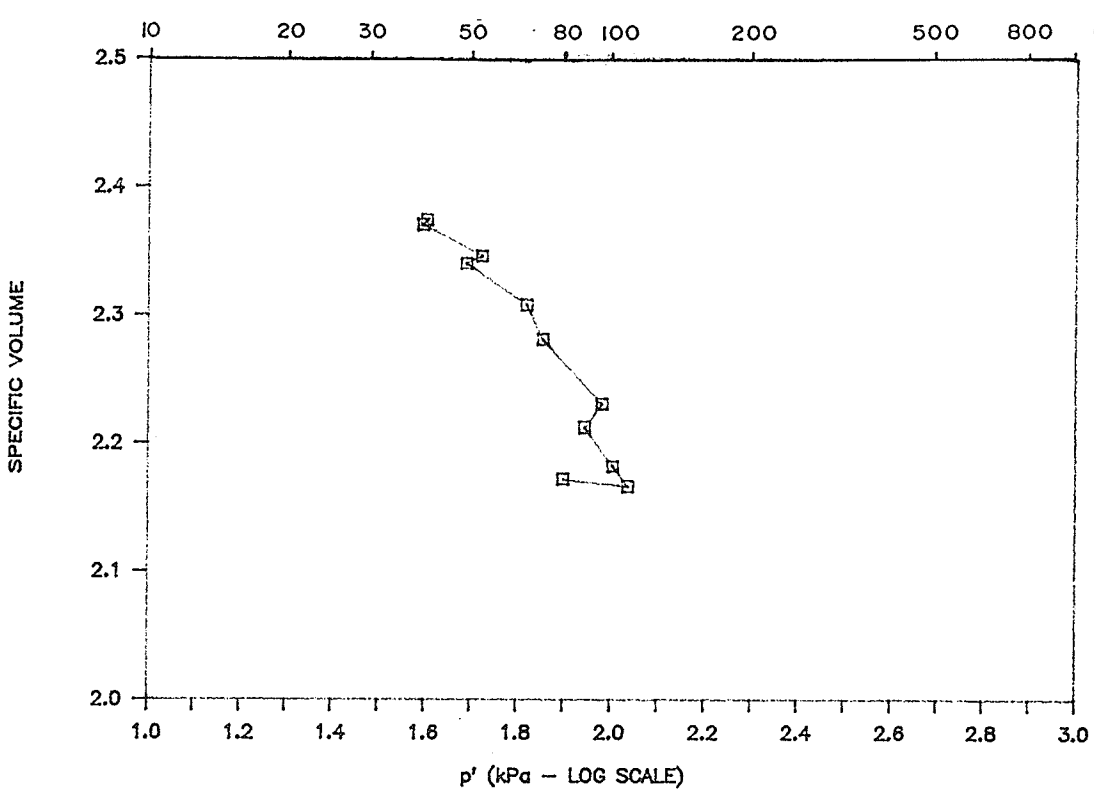
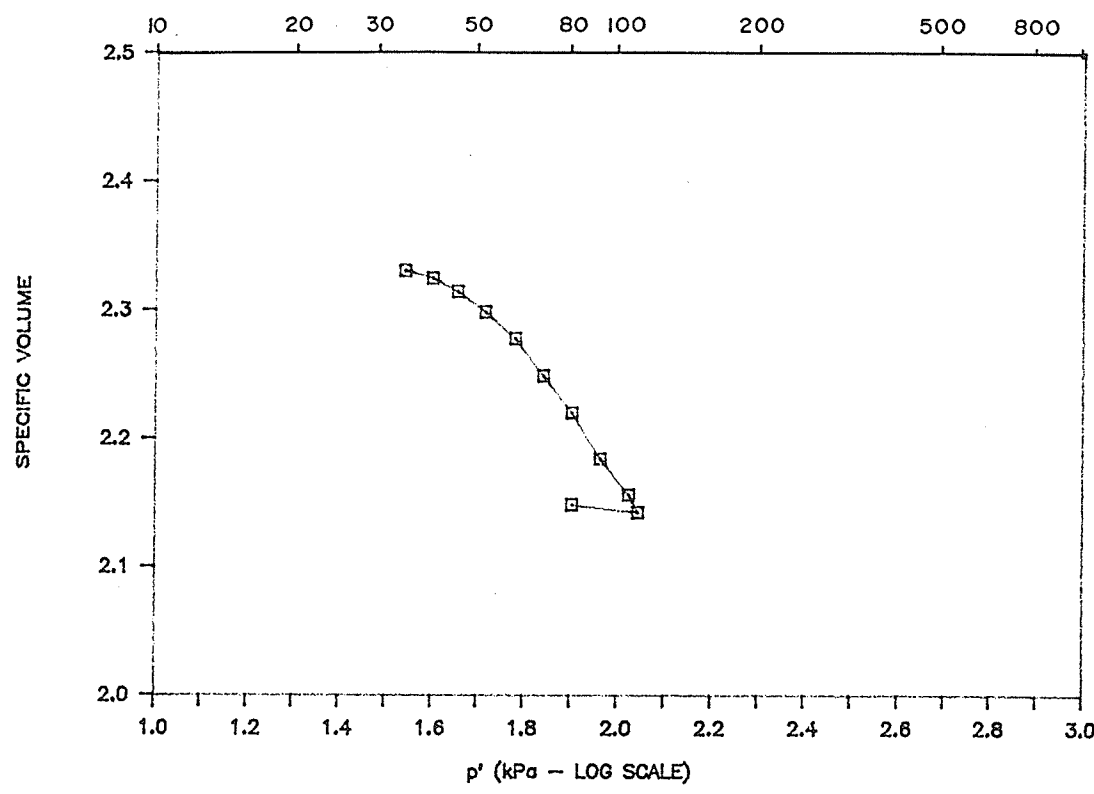


FIGURE 4.2 c,d TRIAXIAL CONSOLIDATION SAMPLES T773, T787

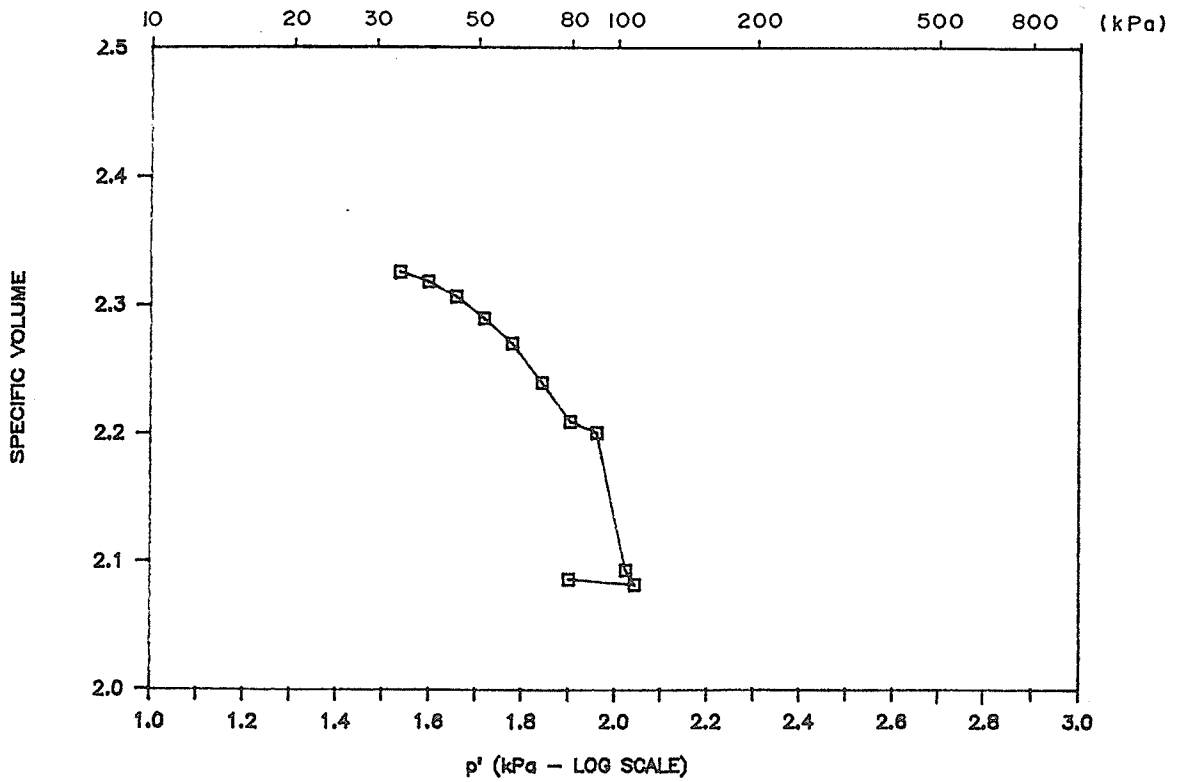
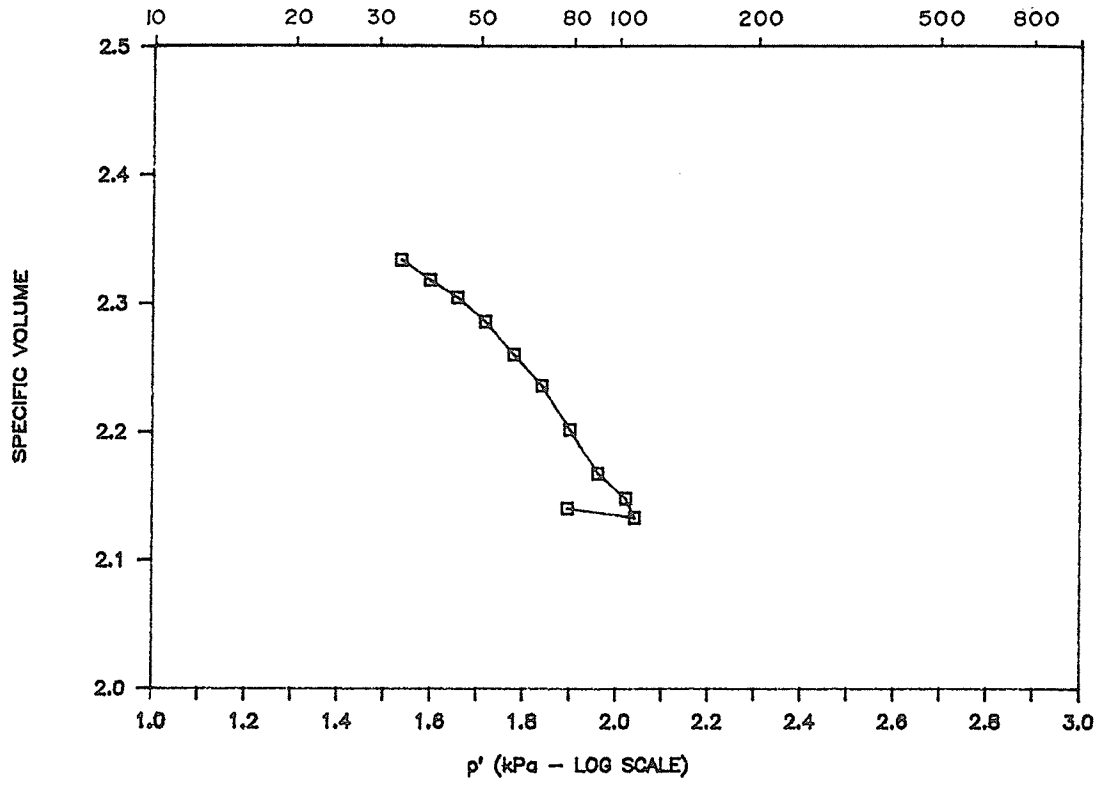


FIGURE 4.2 e, f TRIAXIAL CONSOLIDATION SAMPLES T777, T774

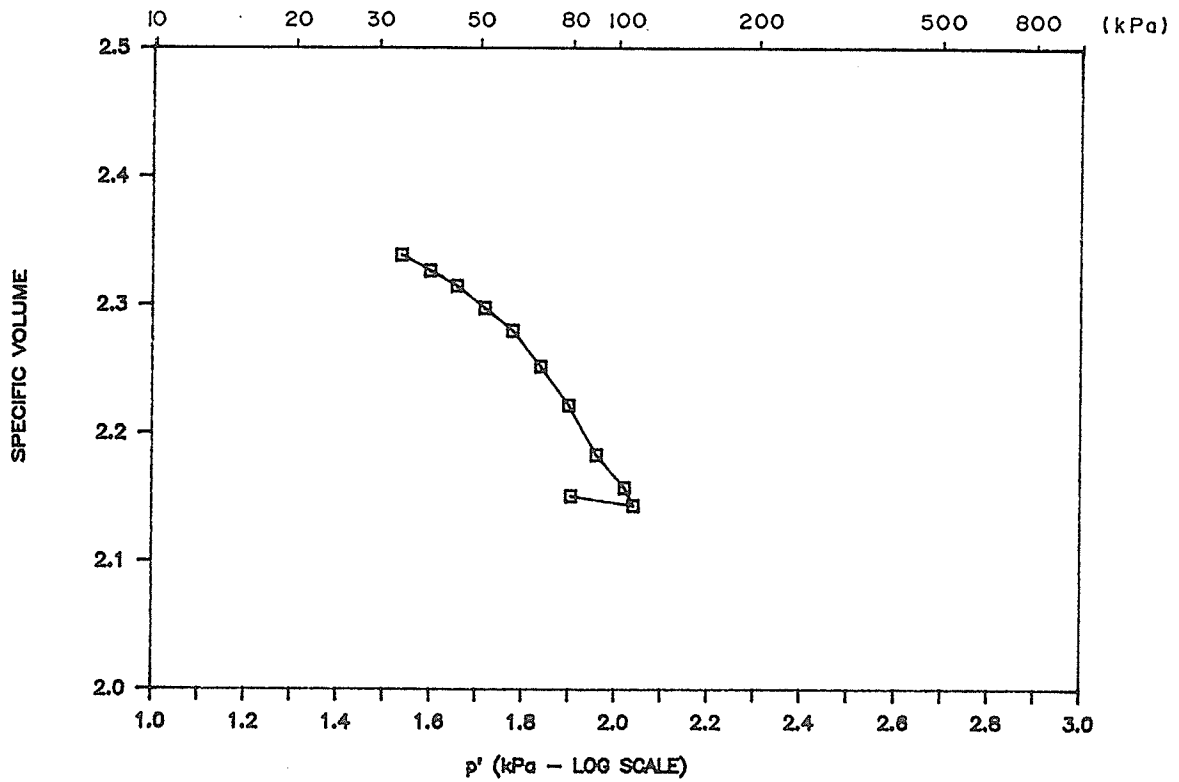
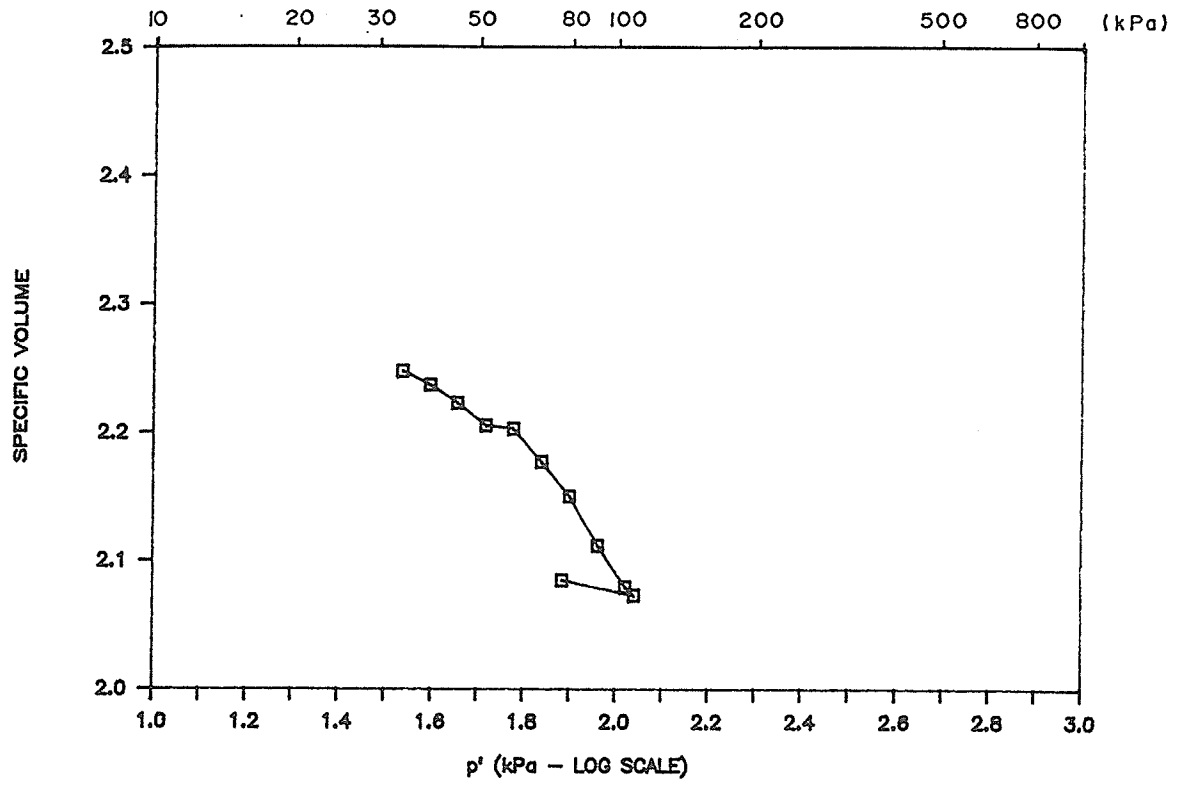


FIGURE 4.2 g,h TRIAXIAL CONSOLIDATION SAMPLES T775, T778

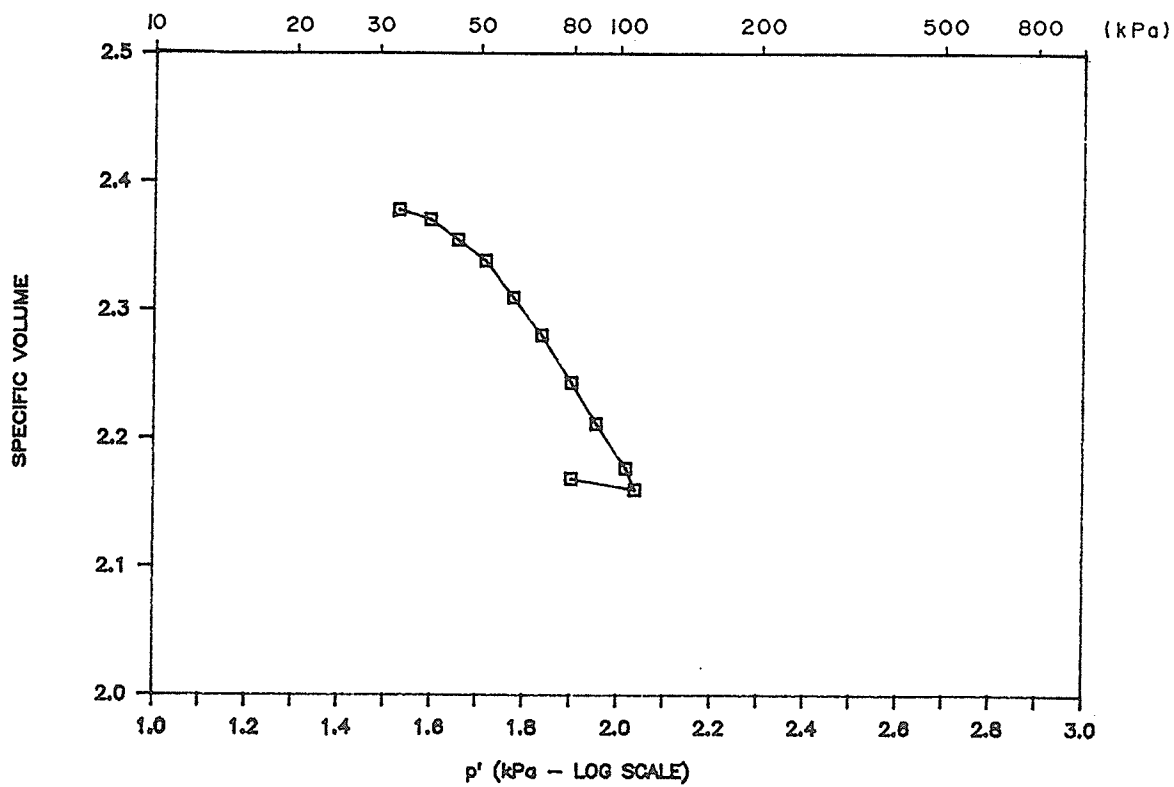
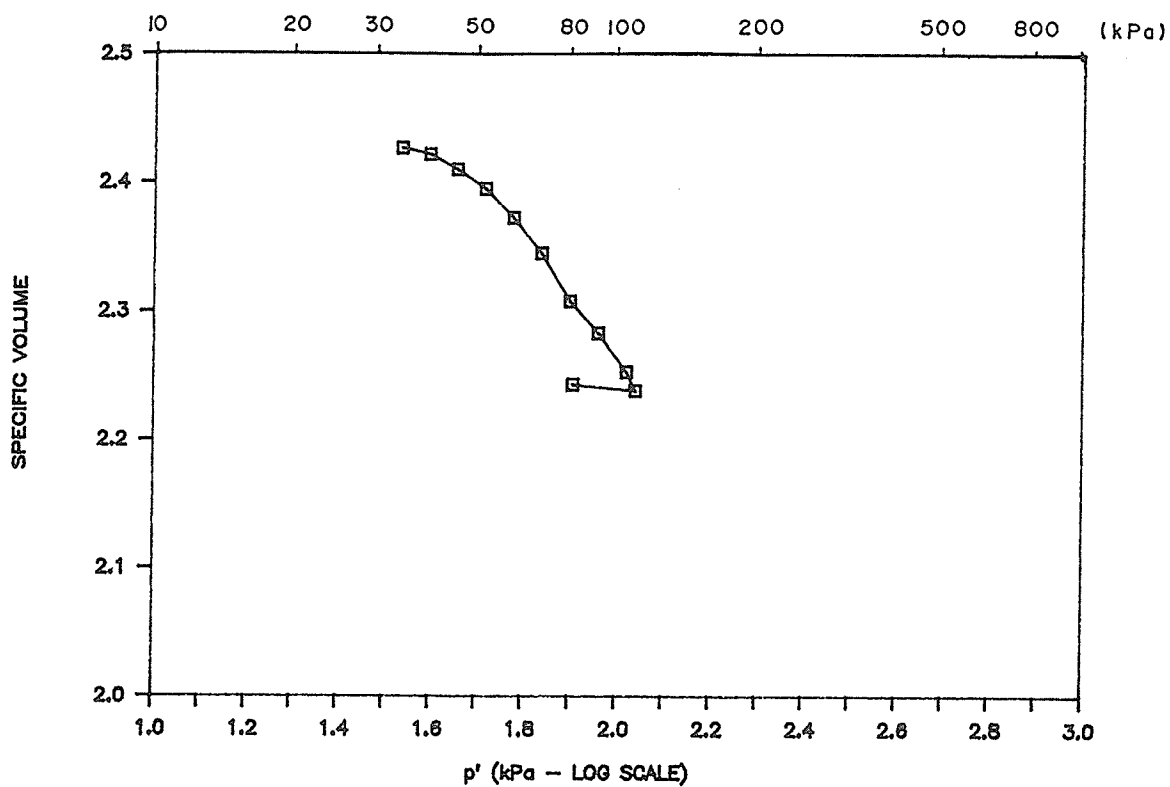


FIGURE 4.2 i,j TRIAXIAL CONSOLIDATION SAMPLES T779, T789

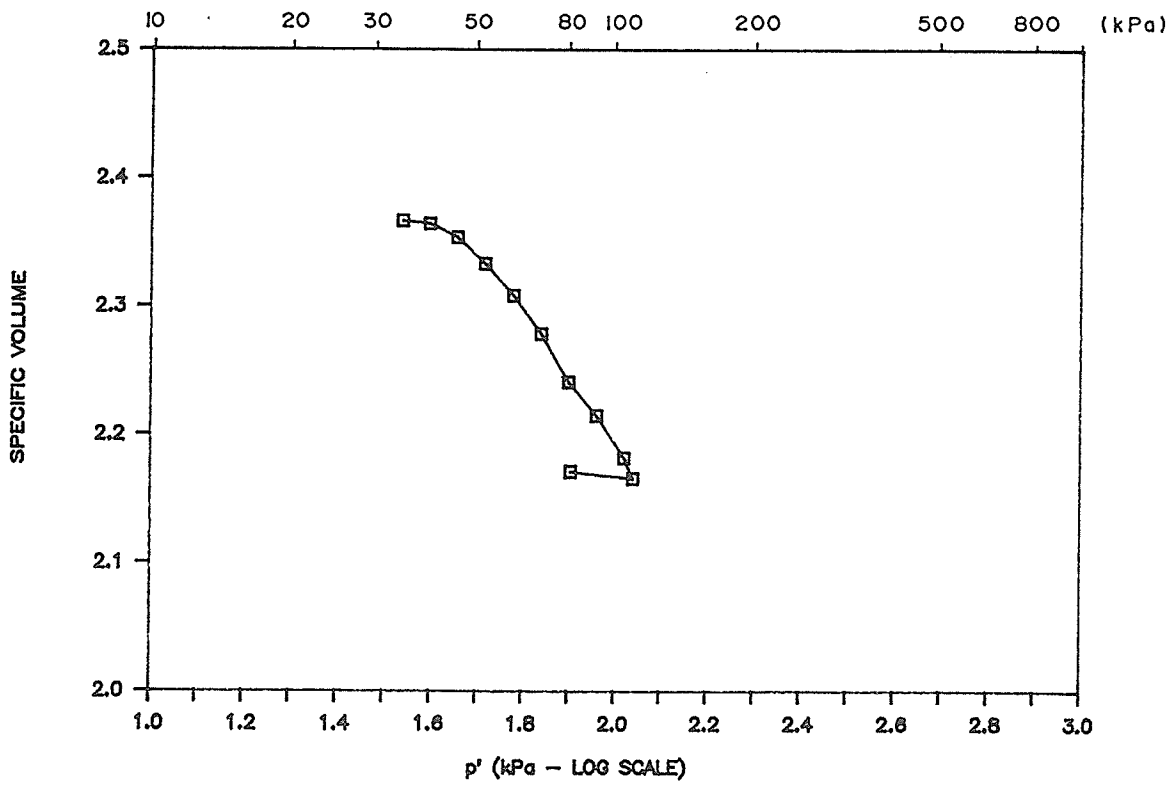
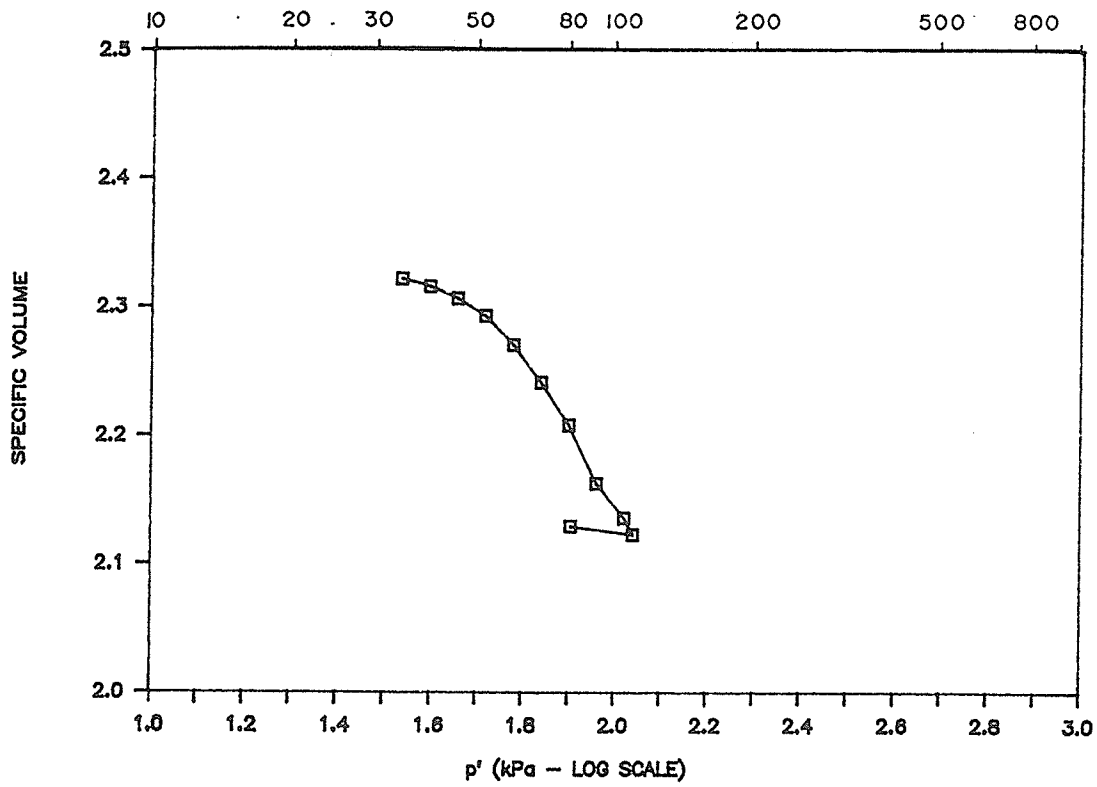


FIGURE 4.2 k,1 TRIAXIAL CONSOLIDATION SAMPLES T781, T782

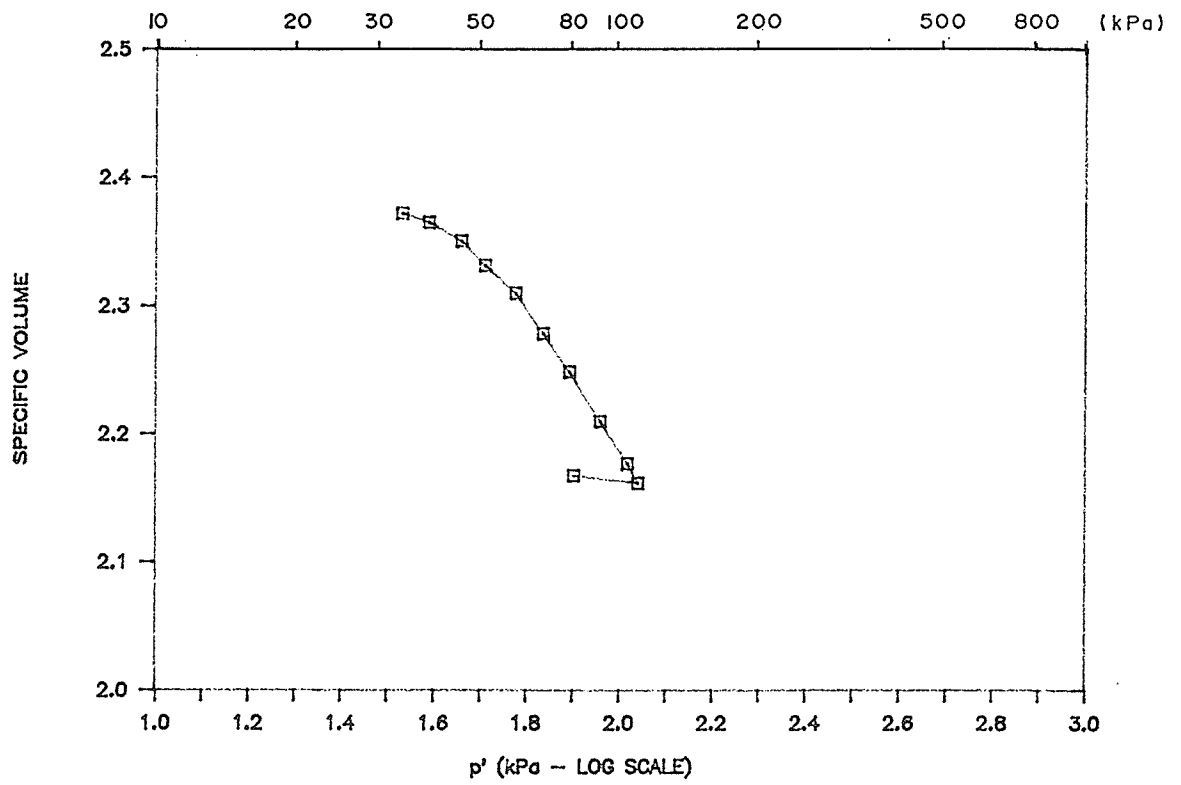
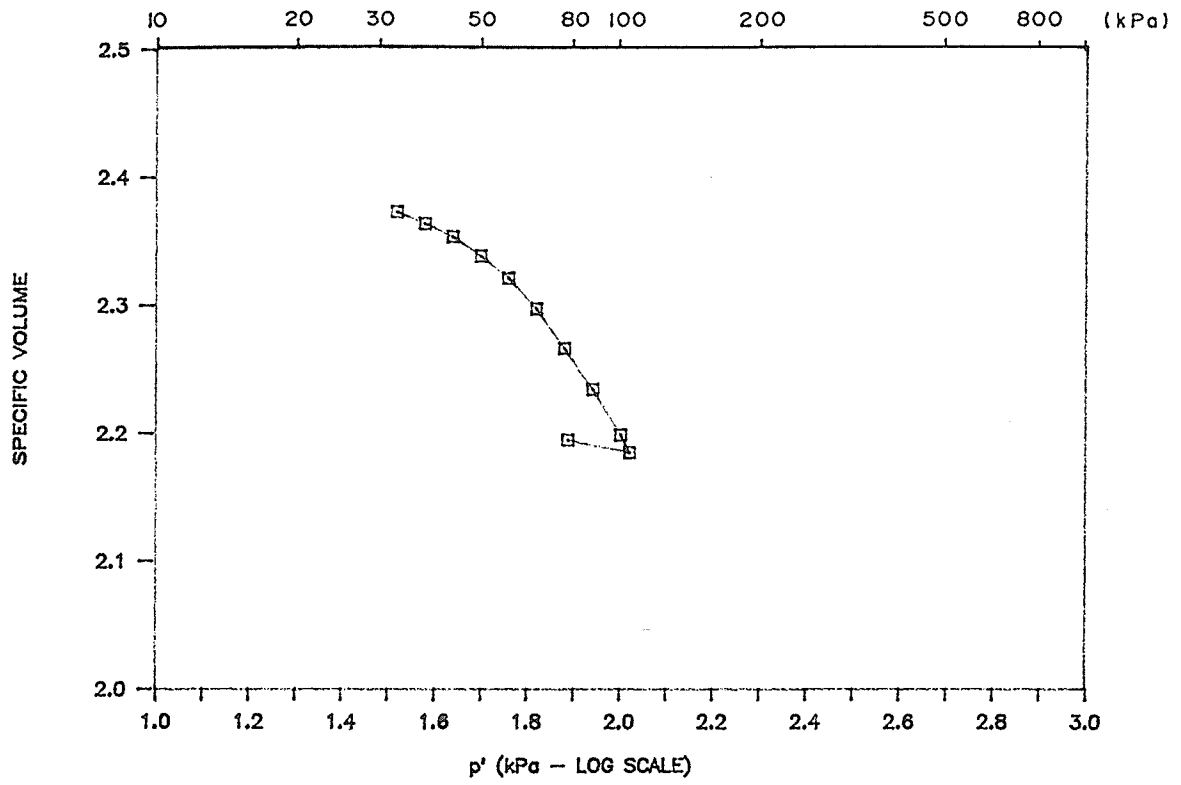


FIGURE 4.2 m,n TRIAXIAL CONSOLIDATION SAMPLES T784, T788

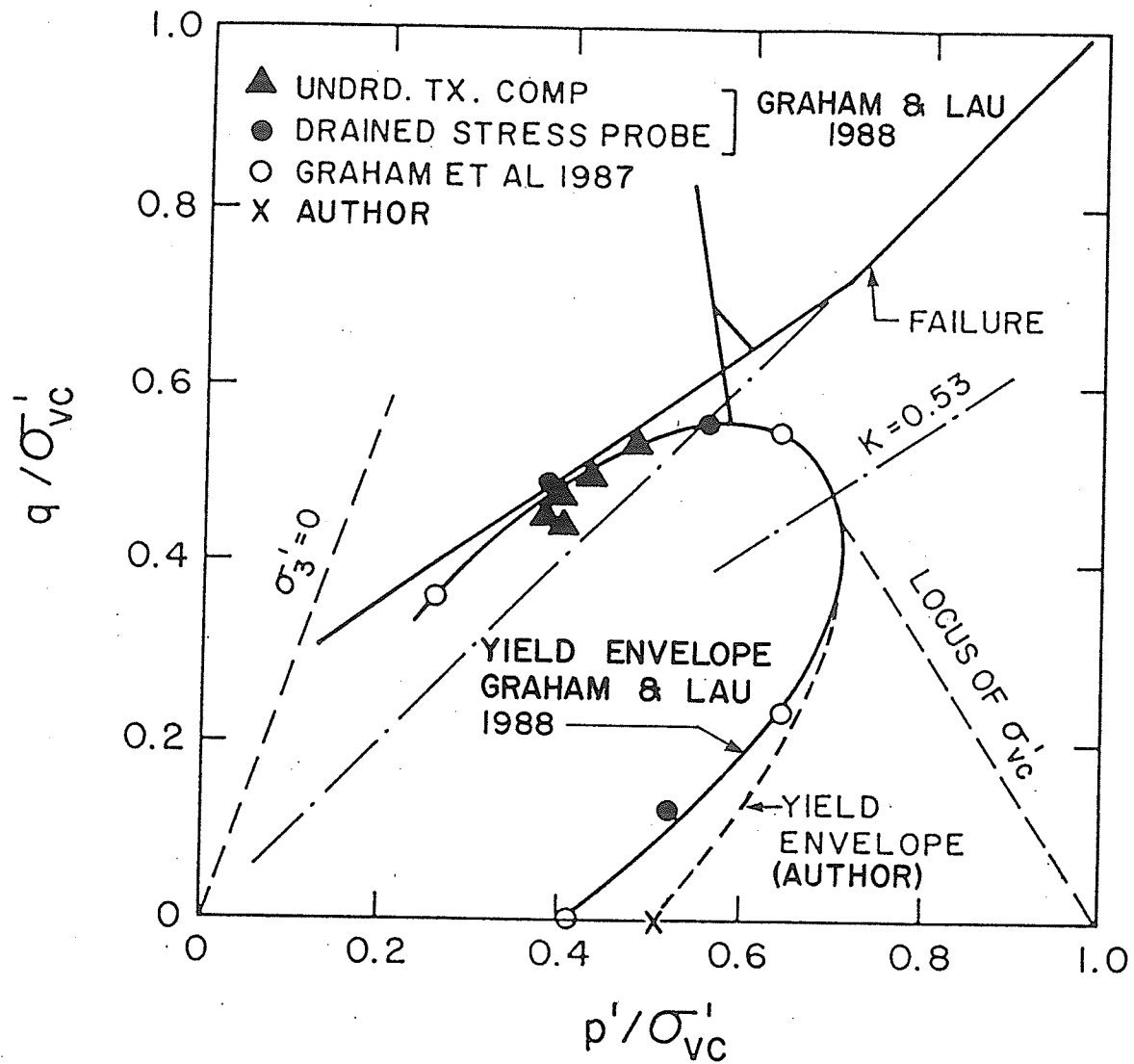


FIGURE 4.3 NORMALIZED YIELD LOCUS OF ILLITIC CLAY  
 $q$  vs.  $p'$  (GRAHAM AND LAU 1988)

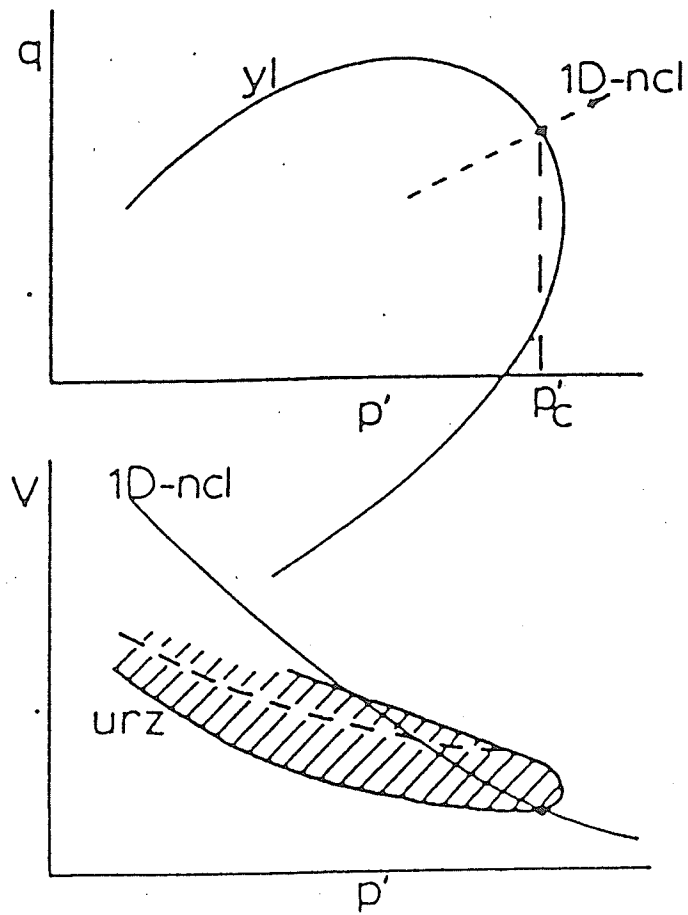


FIGURE 4.4 TYPICAL UNLOAD-RELOAD ZONE OF ANISOTROPIC CLAY  
 $v$  vs.  $\ln(p')$  (GRAHAM AND HOULSBY 1983)

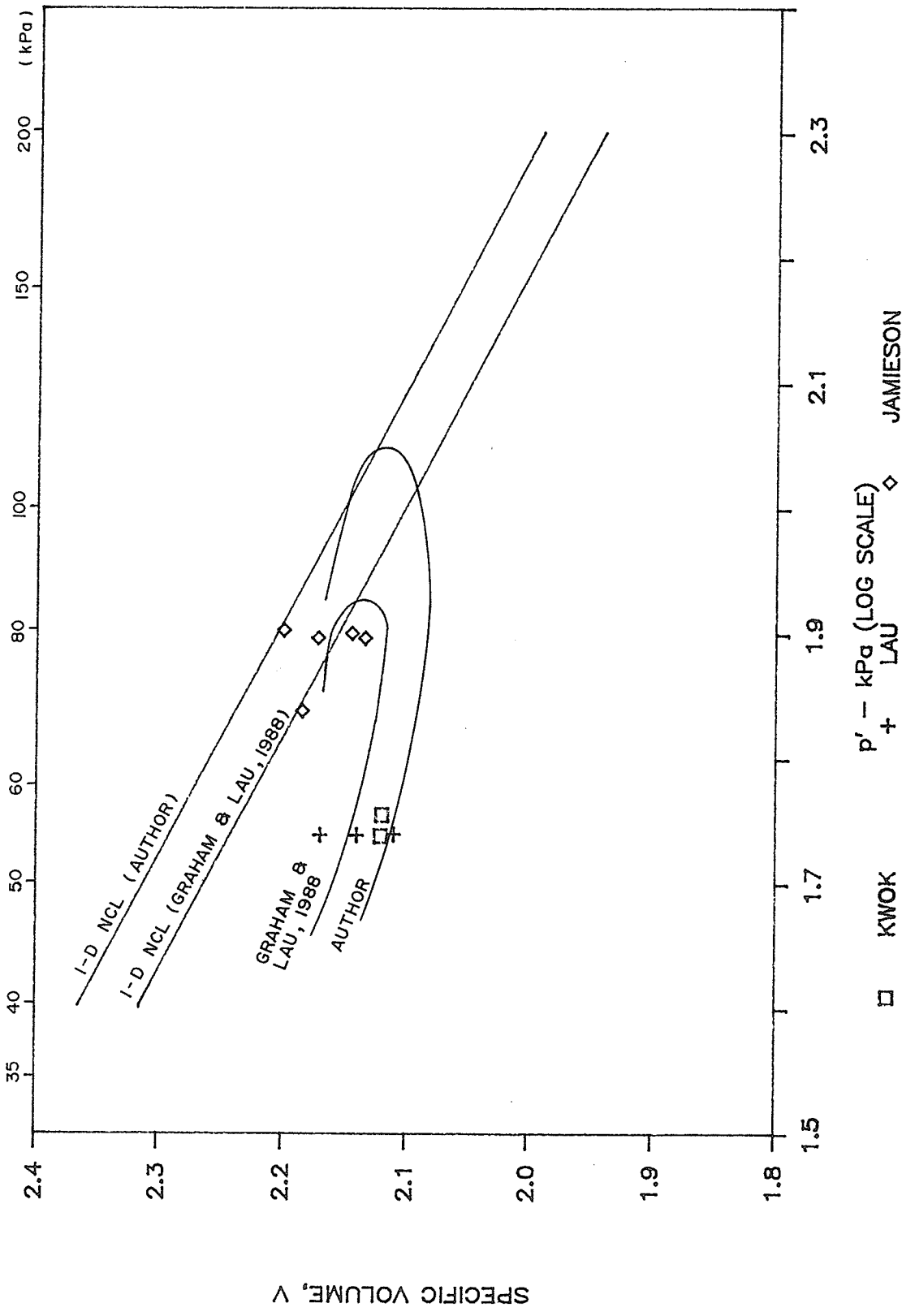


FIGURE 4.5 FINAL CONSOLIDATION POINTS FOR CONTROL SPECIMENS OF KWOK (1984), LAU (1986) AND AUTHOR IN  $v$  vs  $\log(p')$  SPACE

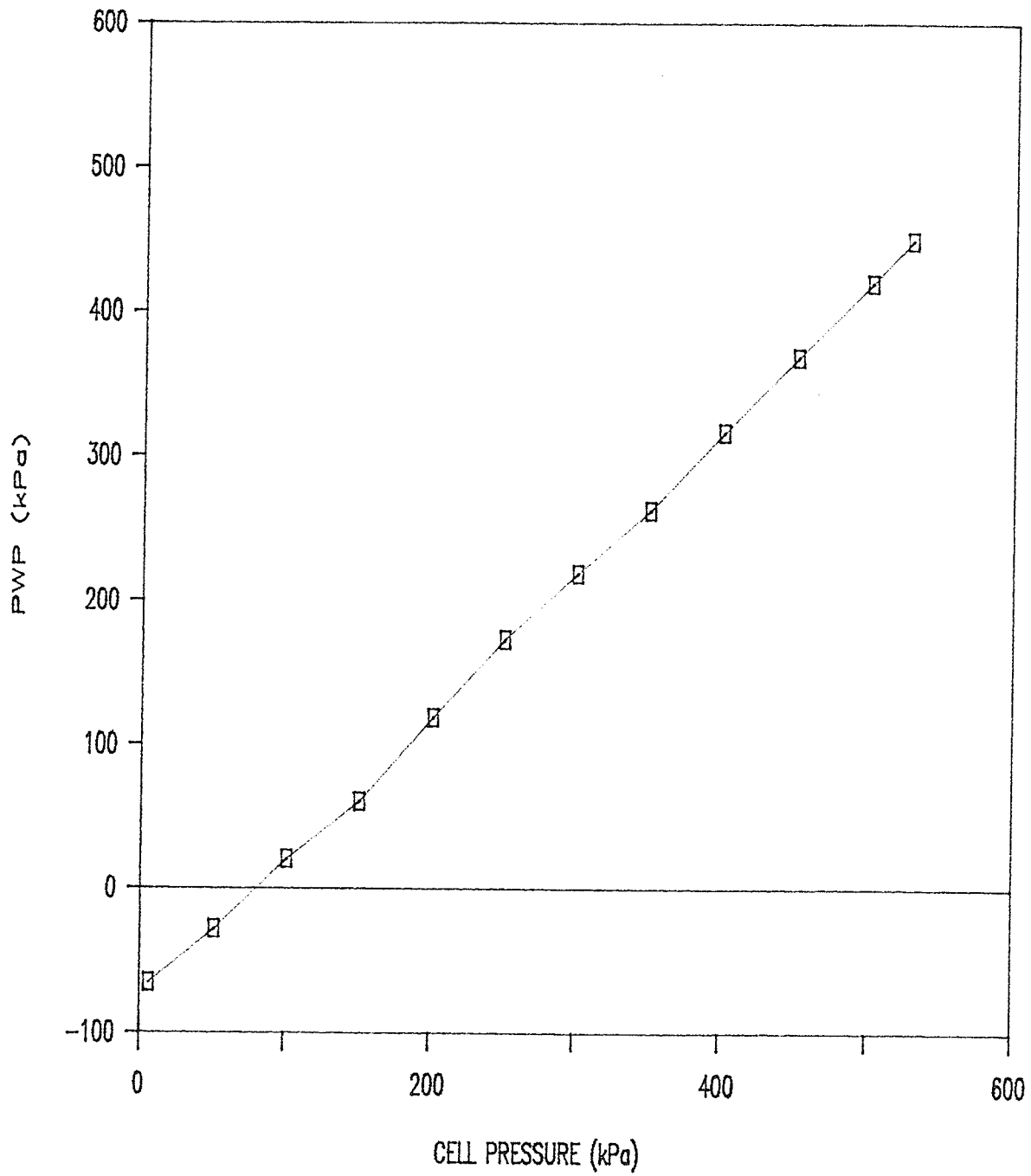


FIGURE 4.6 a POREWATER PRESSURE BEHAVIOUR DURING ISOTROPIC UNLOADING  
SAMPLE T777

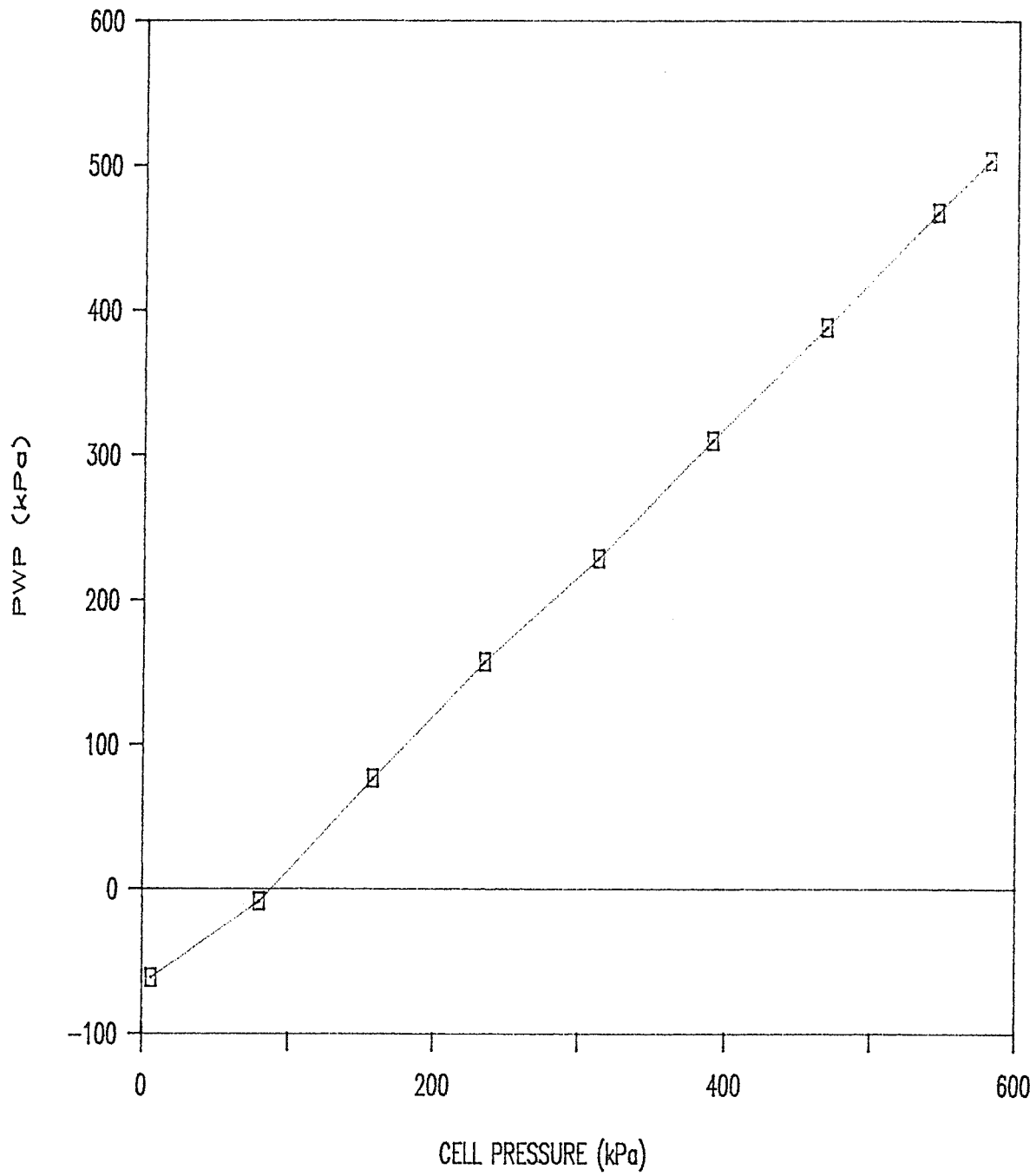


FIGURE 4.6 b POREWATER PRESSURE BEHAVIOUR DURING ISOTROPIC UNLOADING  
SAMPLE T774

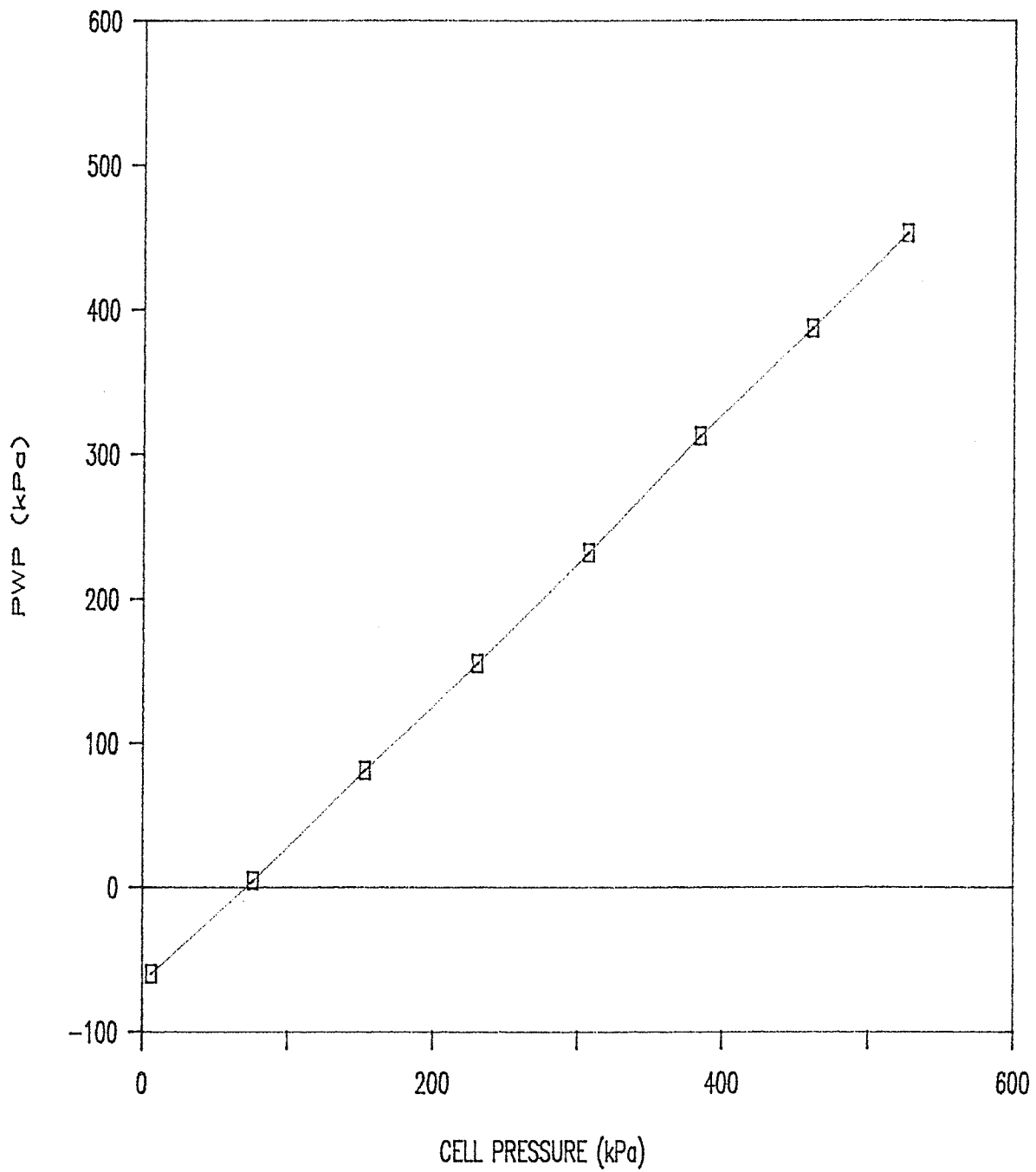


FIGURE 4.6 c POREWATER PRESSURE BEHAVIOUR DURING ISOTROPIC UNLOADING  
SAMPLE T775

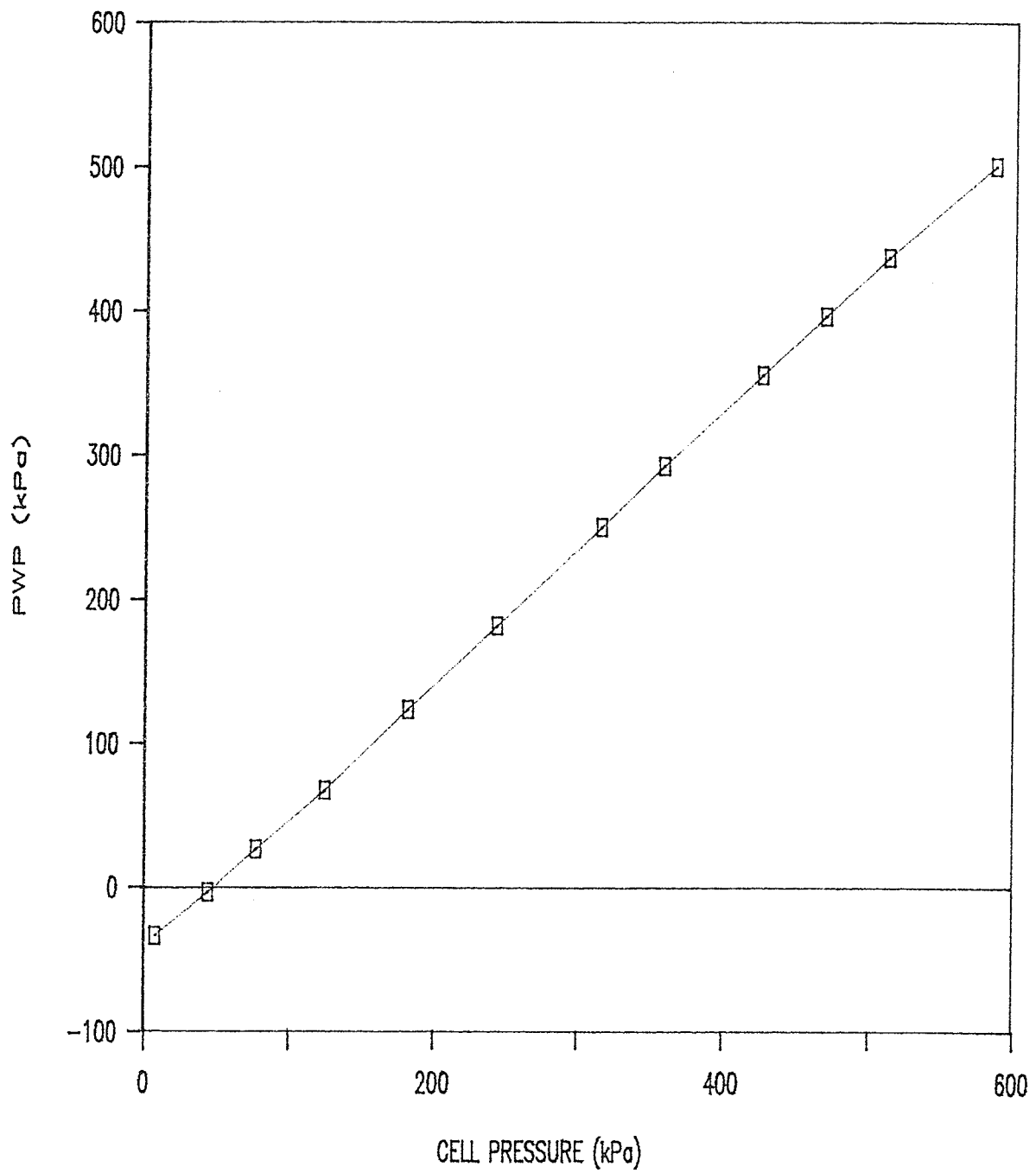


FIGURE 4.6 d POREWATER PRESSURE BEHAVIOUR DURING ISOTROPIC UNLOADING  
SAMPLE T778

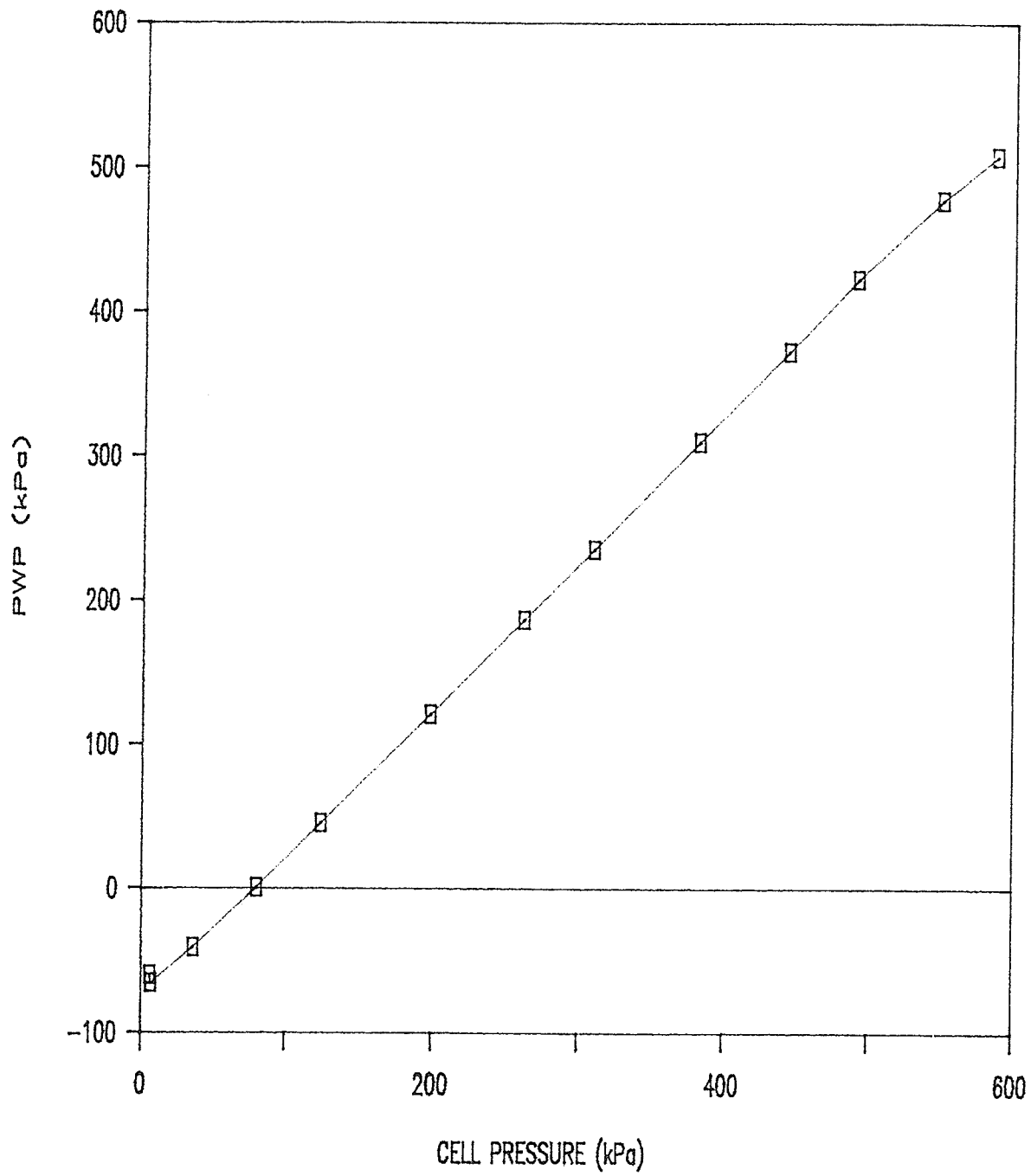


FIGURE 4.6 e POREWATER PRESSURE BEHAVIOUR DURING ISOTROPIC UNLOADING  
SAMPLE T779

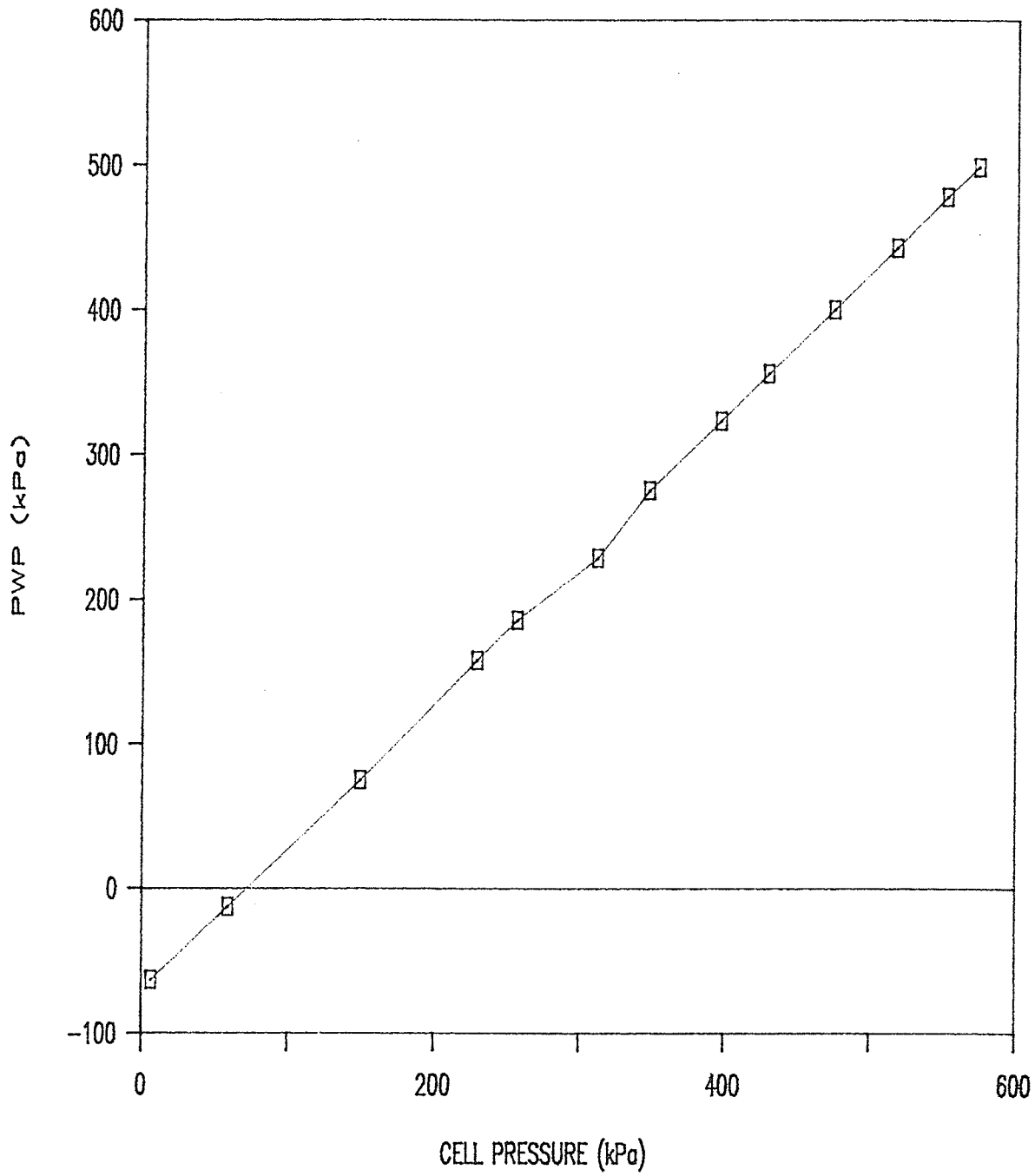


FIGURE 4.6 f POREWATER PRESSURE BEHAVIOUR DURING ISOTROPIC UNLOADING  
SAMPLE T789

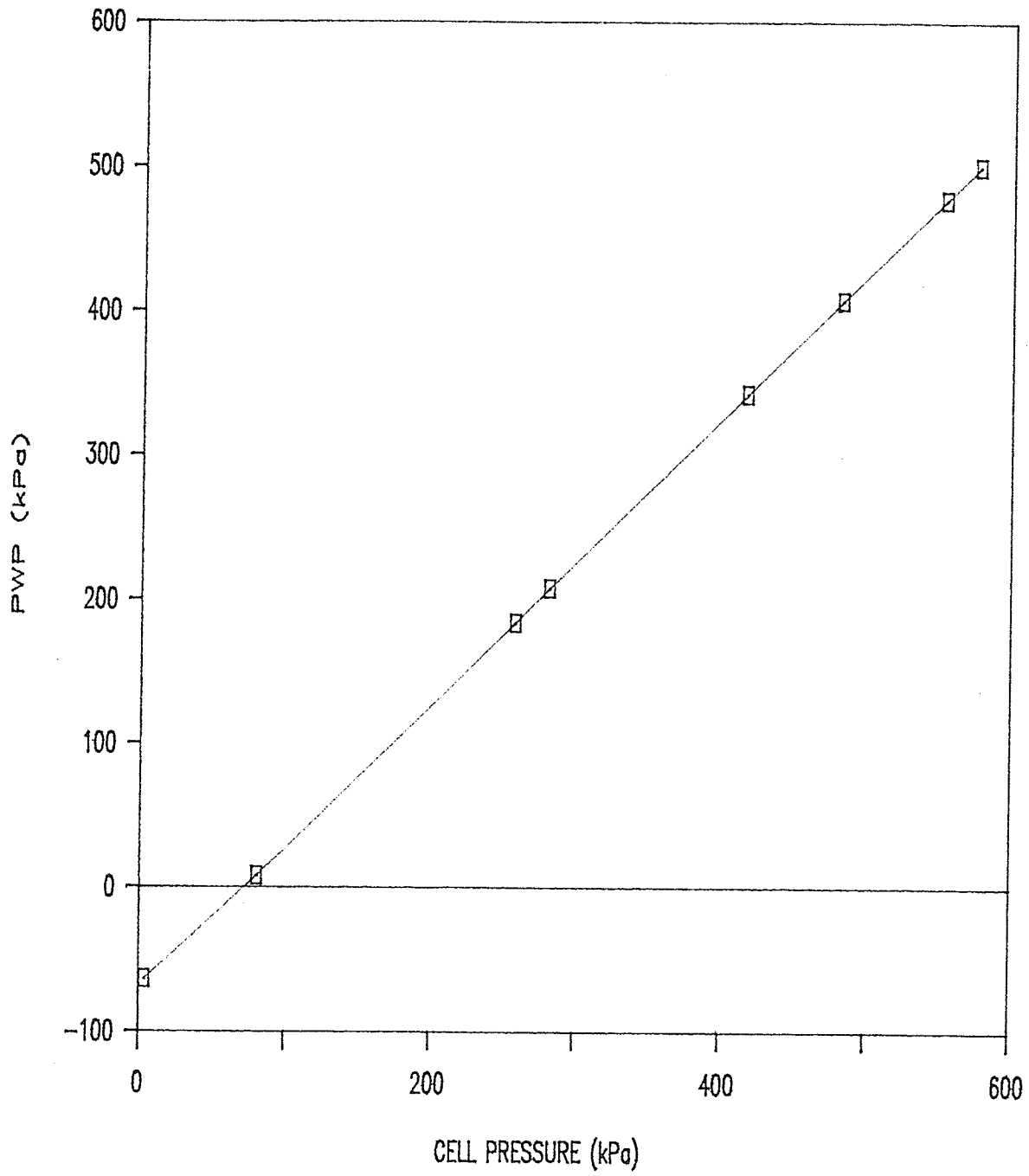


FIGURE 4.6 g POREWATER PRESSURE BEHAVIOUR DURING ISOTROPIC UNLOADING  
SAMPLE T781

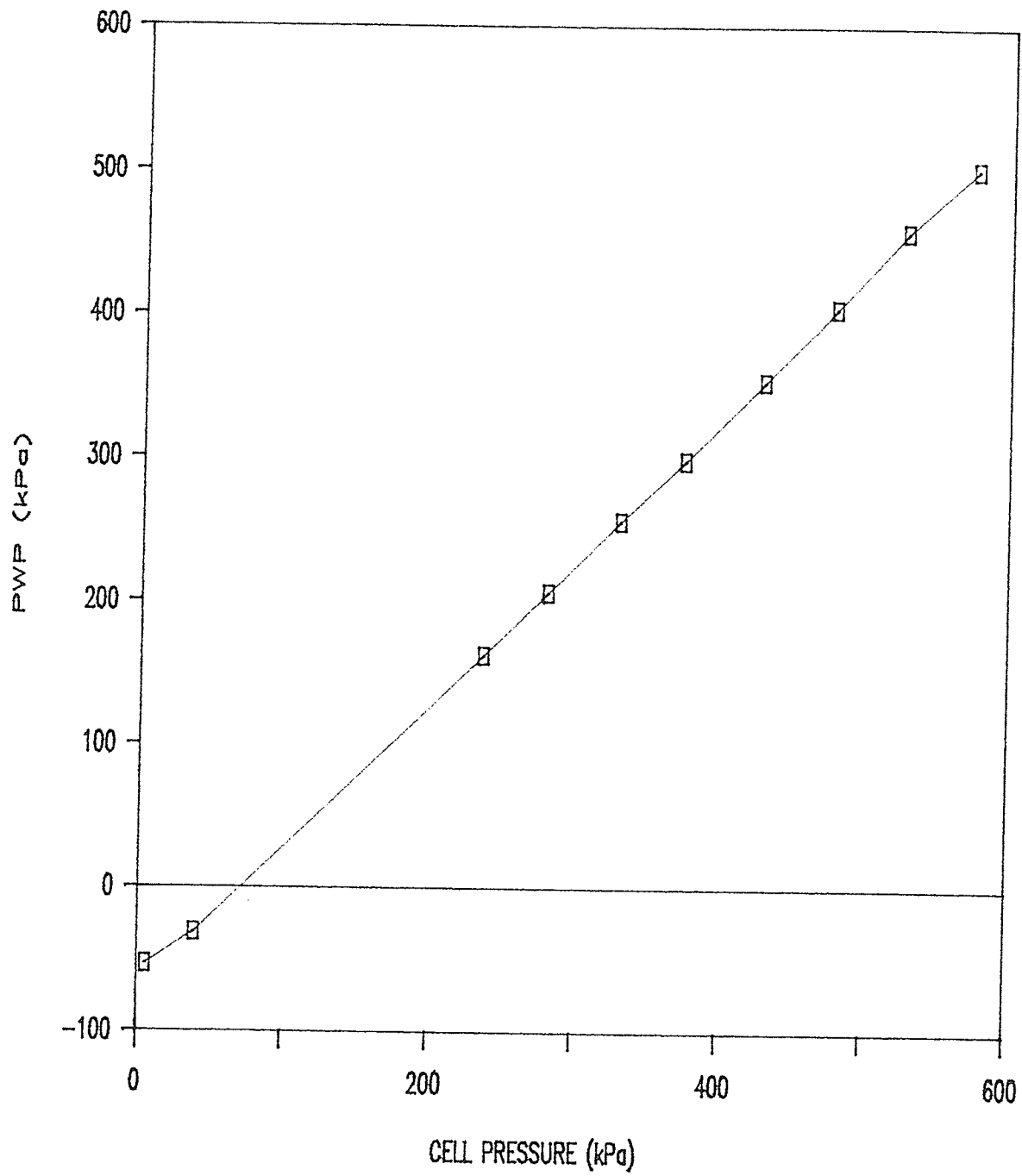


FIGURE 4.6 h POREWATER PRESSURE BEHAVIOUR DURING ISOTROPIC UNLOADING SAMPLE T782

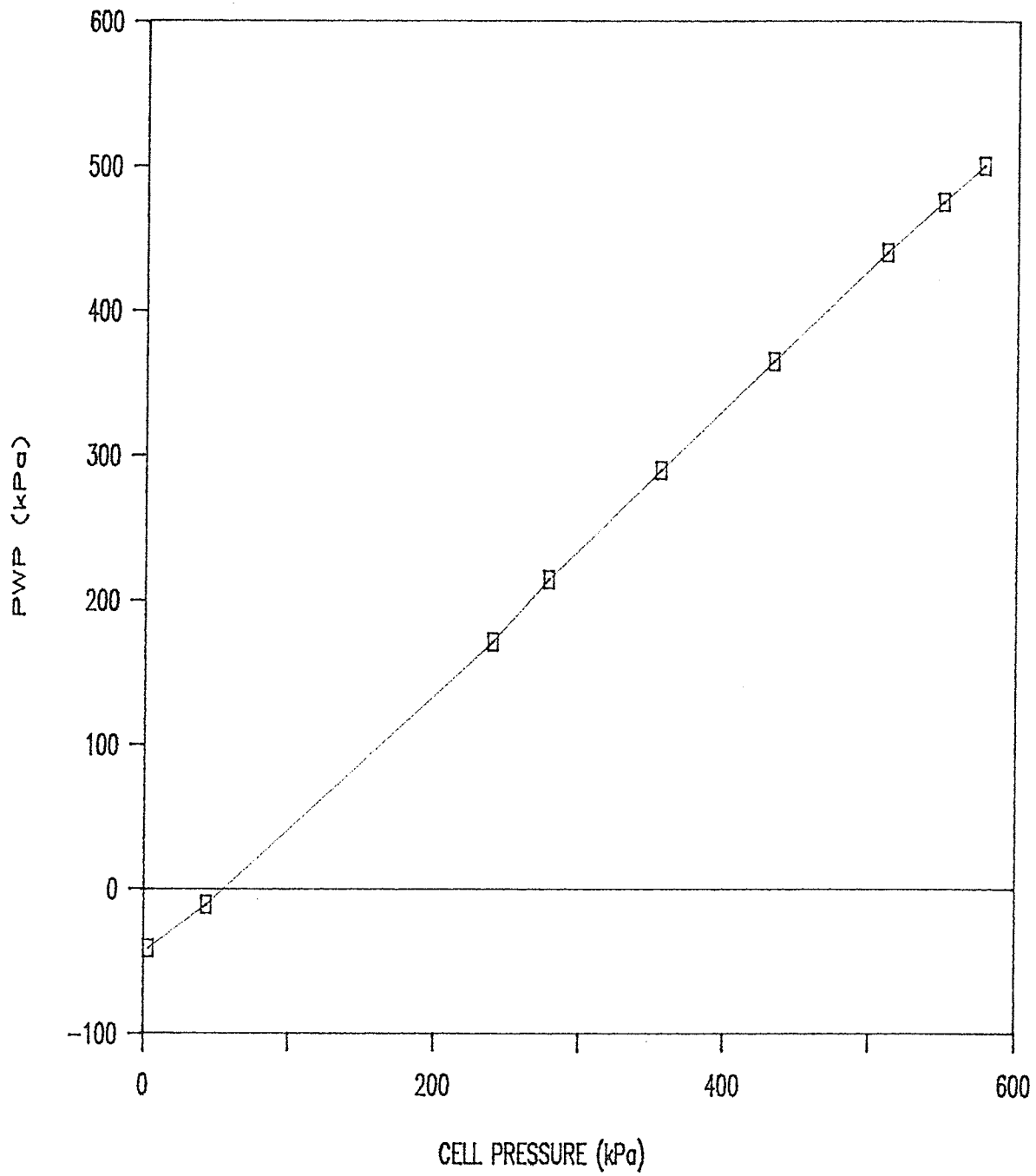


FIGURE 4.6 i POREWATER PRESSURE BEHAVIOUR DURING ISOTROPIC UNLOADING  
SAMPLE T784

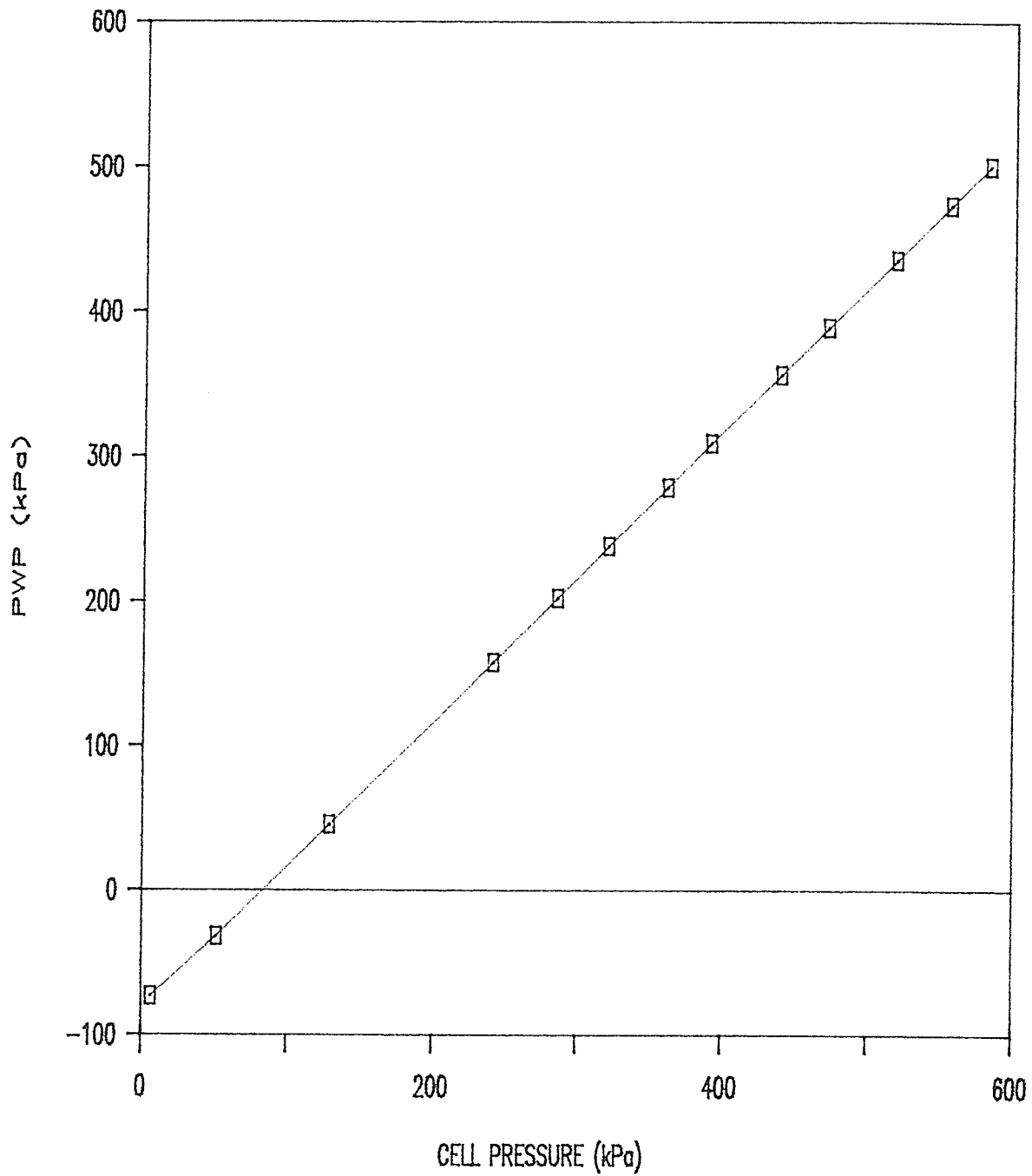


FIGURE 4.6 j POREWATER PRESSURE BEHAVIOUR DURING ISOTROPIC UNLOADING  
SAMPLE T788

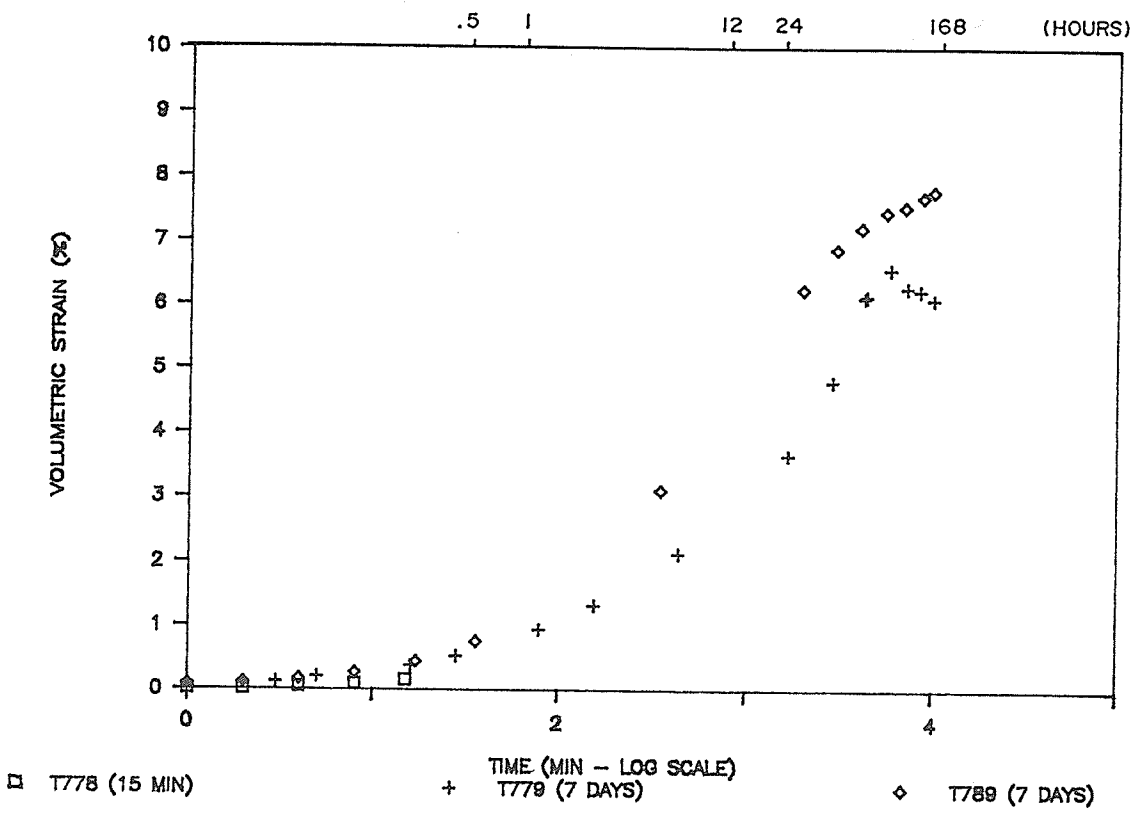
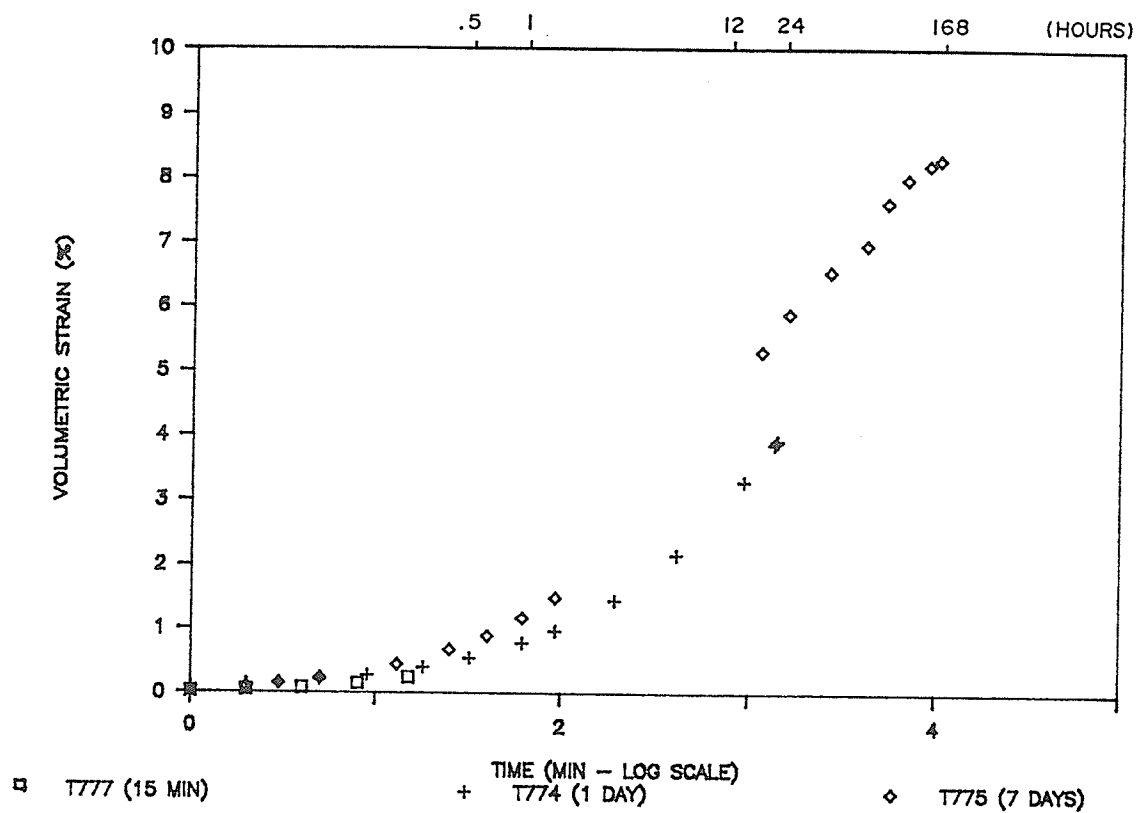


FIGURE 4.7 a,b SWELLING BEHAVIOUR DURING DRAINED STORAGE v vs. LOG (TIME)

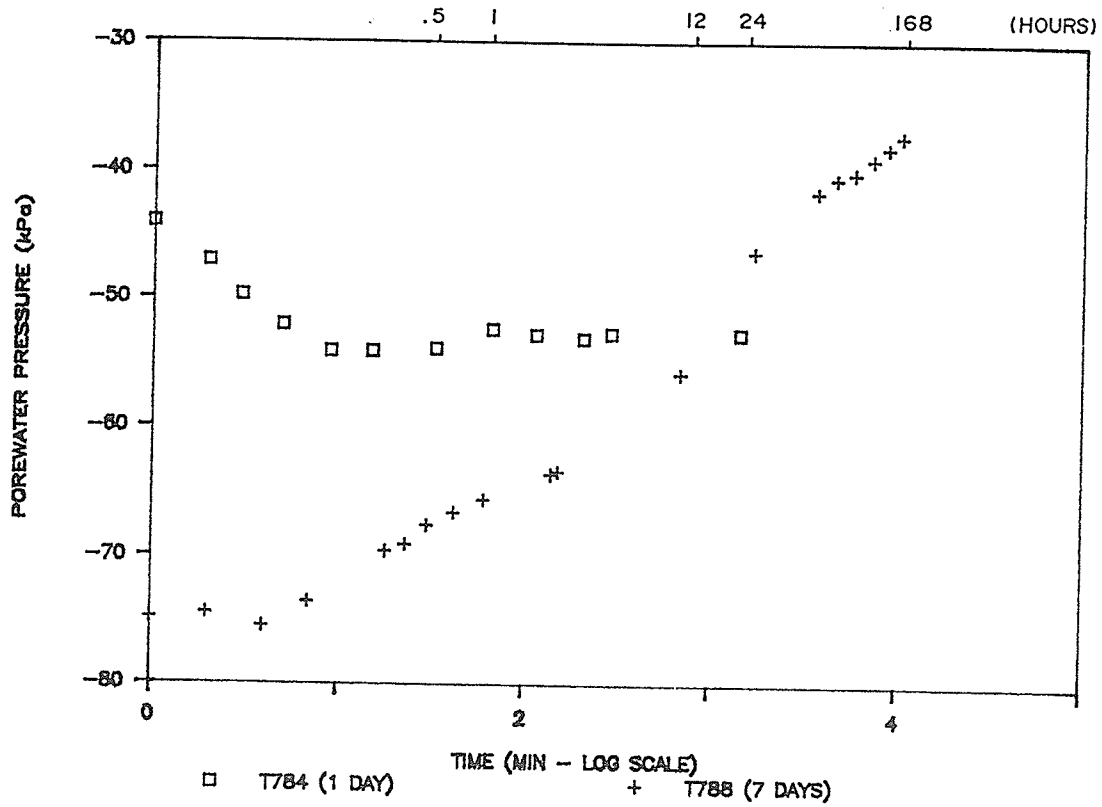
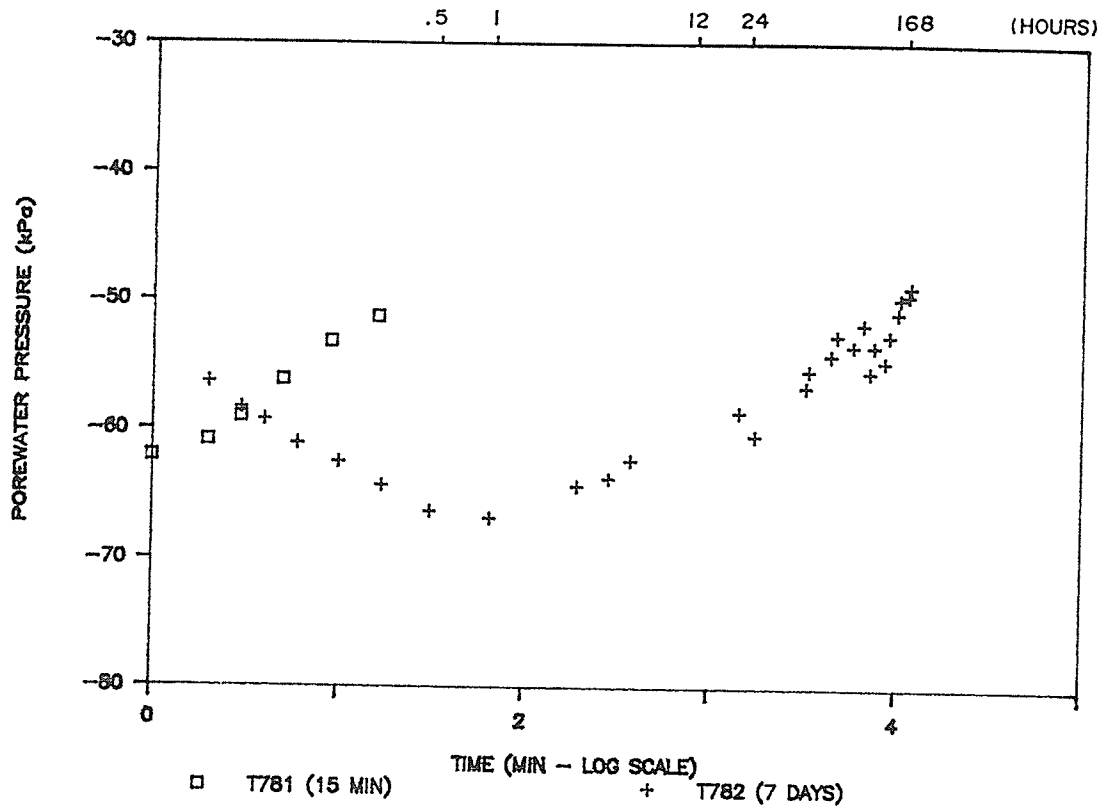


FIGURE 4.8 a,b POREWATER PRESSURE BEHAVIOUR DURING UNDRAINED STORAGE; u vs. LOG (TIME)

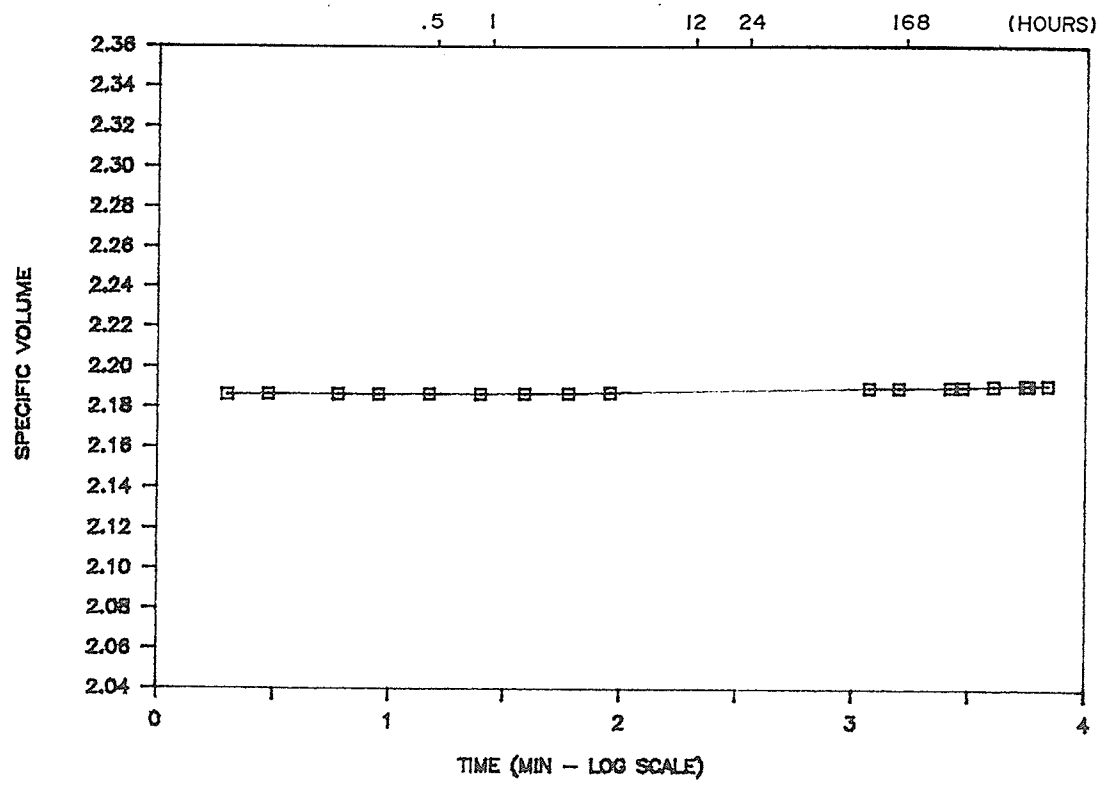
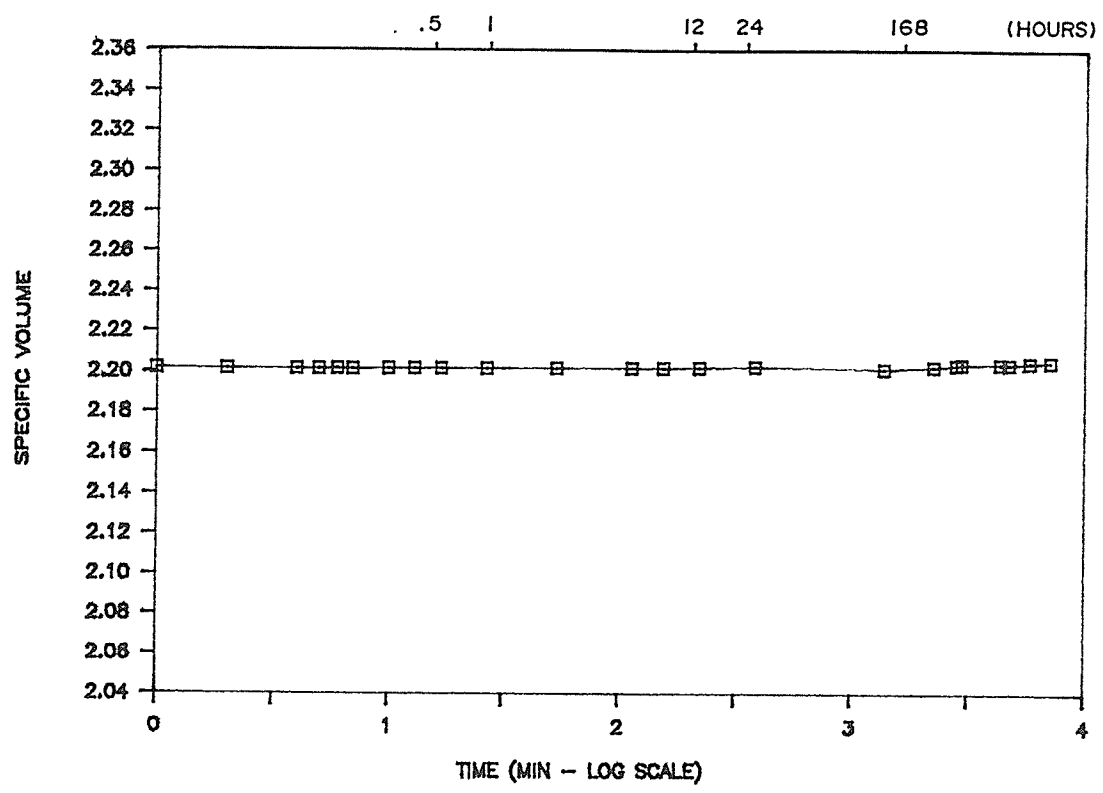


FIGURE 4.9 a,b TYPICAL VOLUMETRIC STRAINING DURING RECONSOLIDATION OF SAMPLES STORED UNDRAINED SAMPLES T784 AND T788

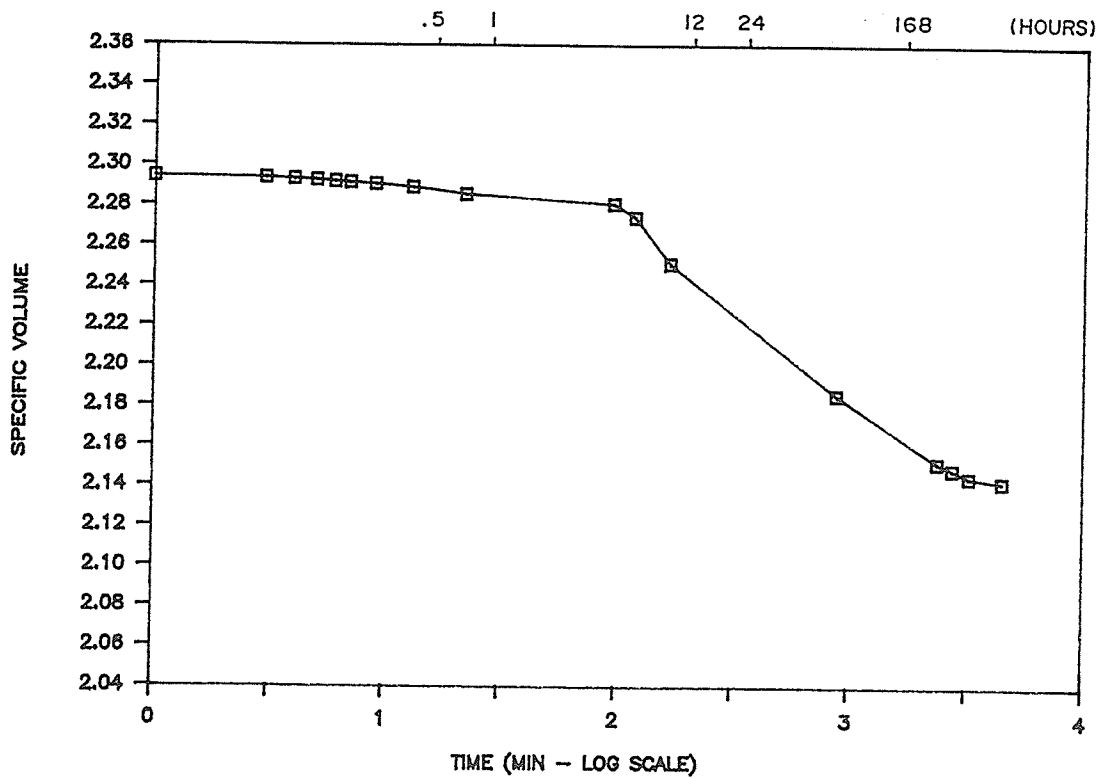
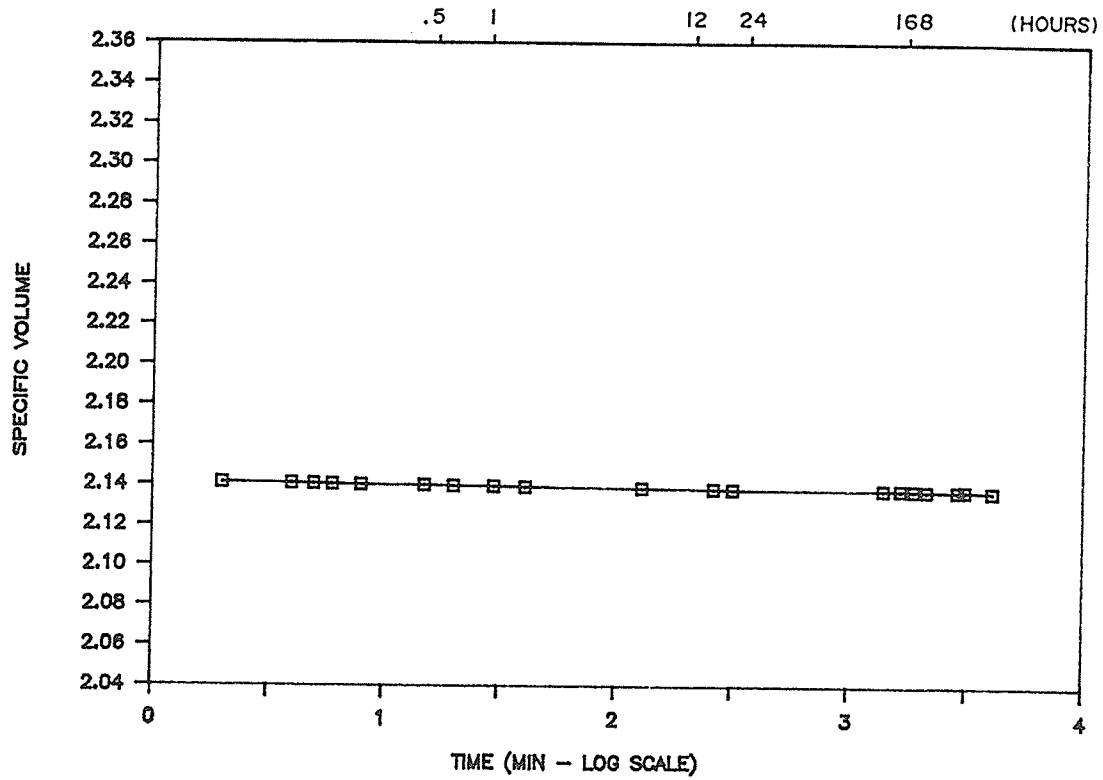


FIGURE 4.10 a,b TYPICAL VOLUMETRIC STRAINING DURING RECONSOLIDATION OF SAMPLES STORED DRAINED SAMPLES T777 AND T775

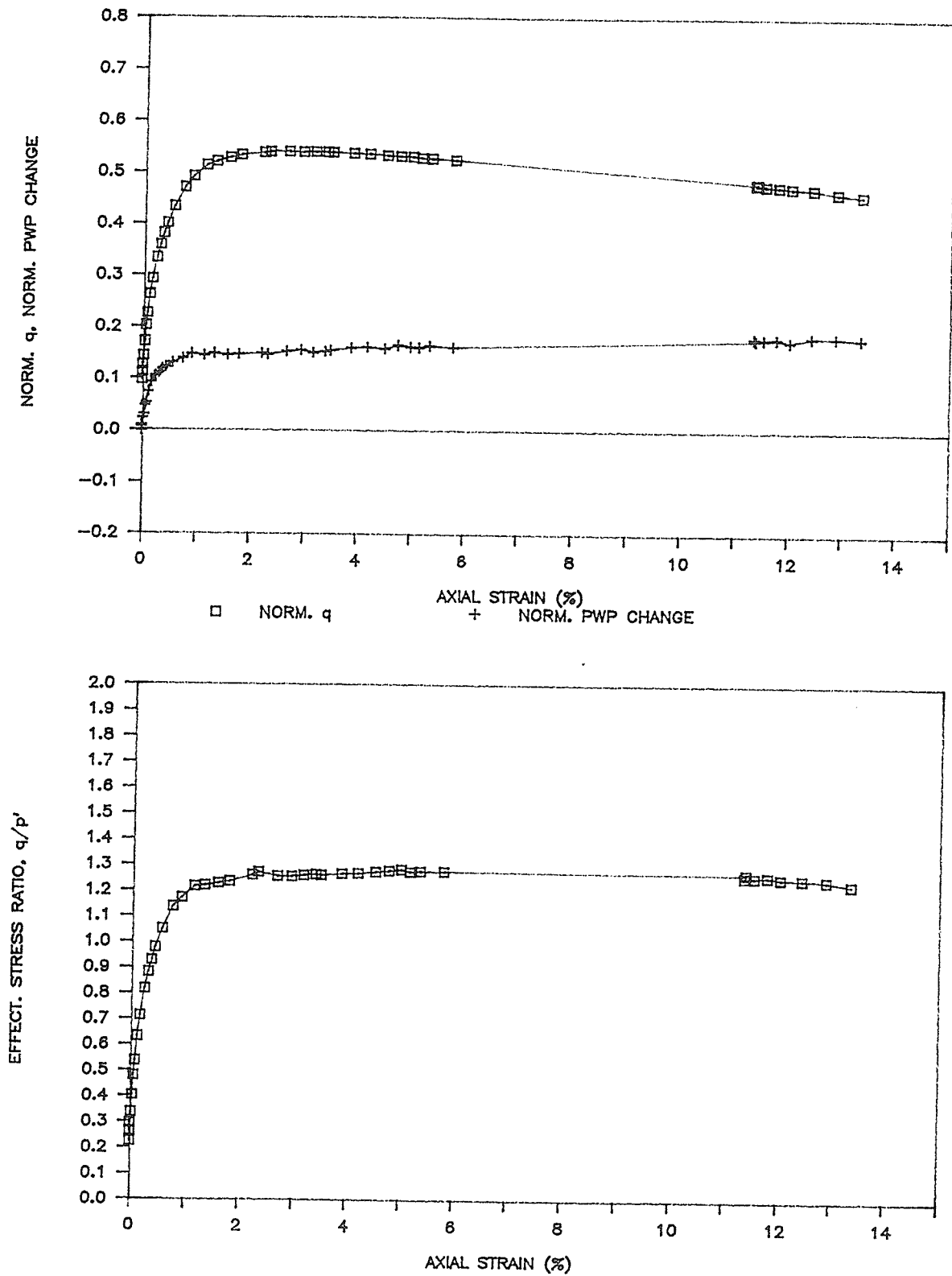


FIGURE 5.1 a,b UNDRAINED STRESS-STRAIN AND POREWATER PRESSURE RESULTS SAMPLE T771 (CONTROL SPECIMEN)

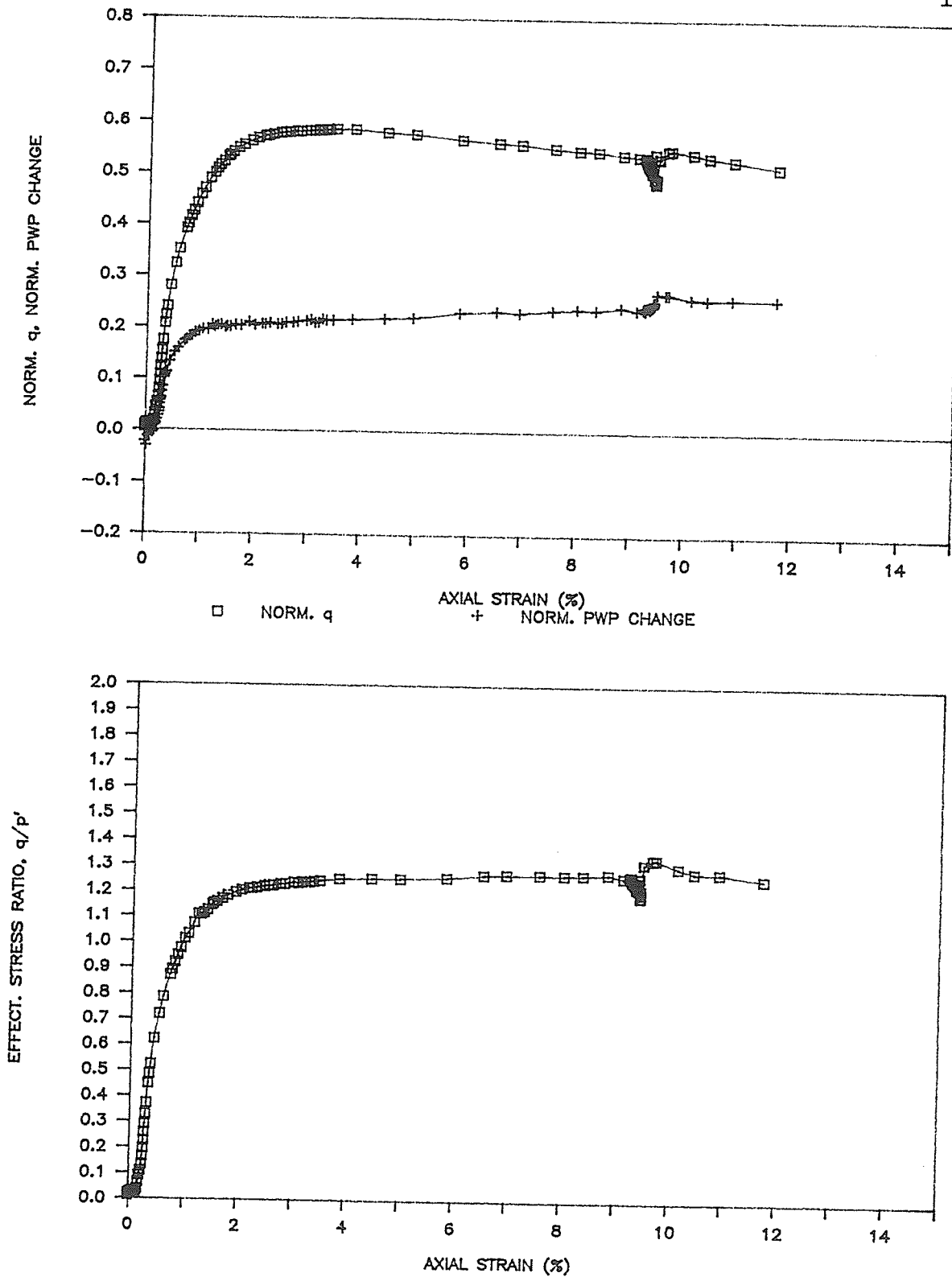


FIGURE 5.2 a,b UNDRAINED STRESS-STRAIN AND POREWATER PRESSURE RESULTS SAMPLE T772 (CONTROL SPECIMEN)

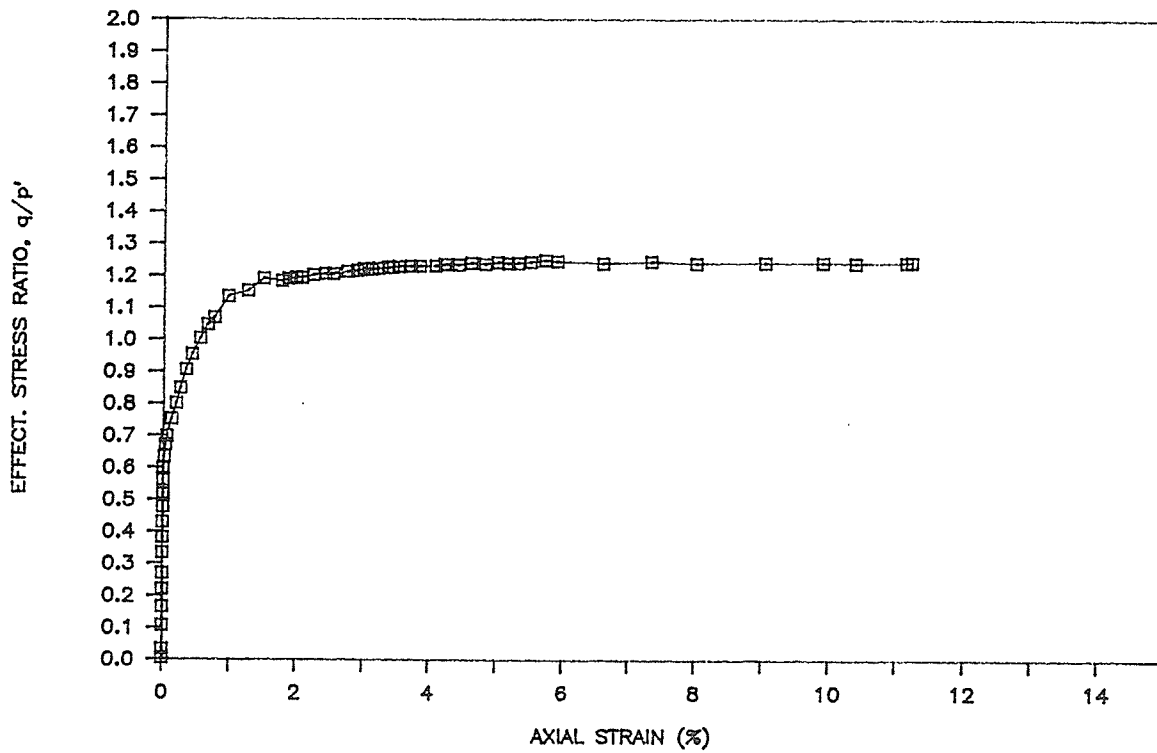
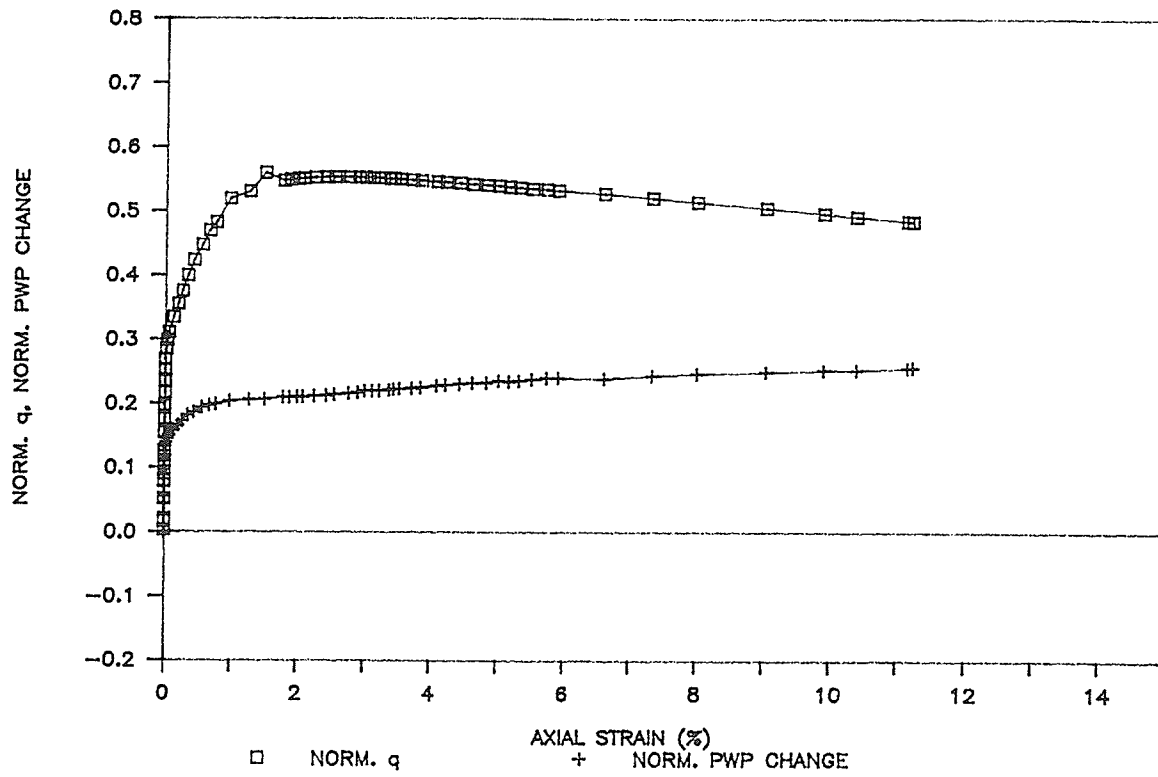


FIGURE 5.3 a,b UNDRAINED STRESS-STRAIN AND POREWATER PRESSURE RESULTS SAMPLE T773 (CONTROL SPECIMEN)

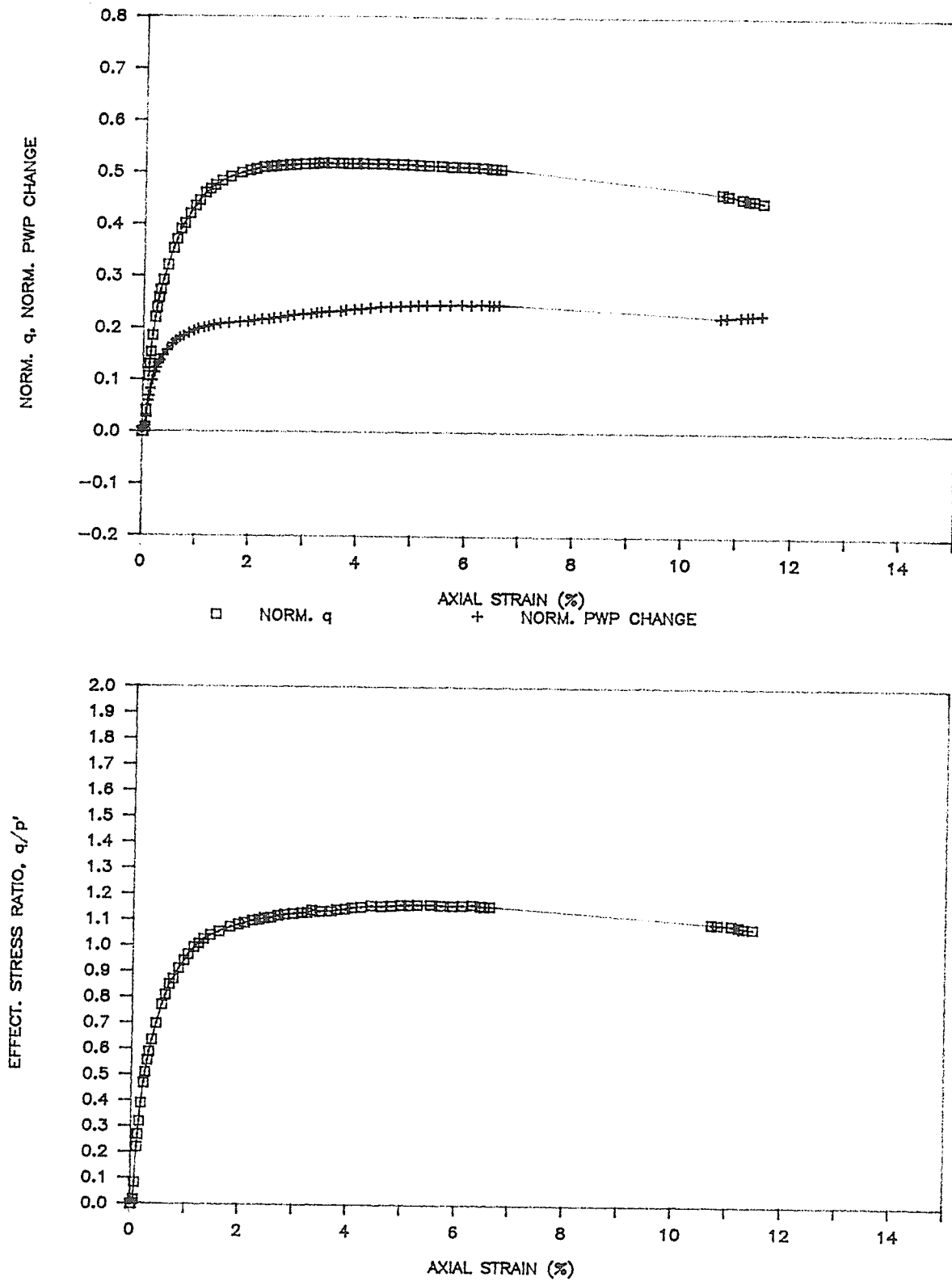


FIGURE 5.4 a,b UNDRAINED STRESS-STRAIN AND POREWATER PRESSURE RESULTS  
SAMPLE T785 (CONTROL SPECIMEN)

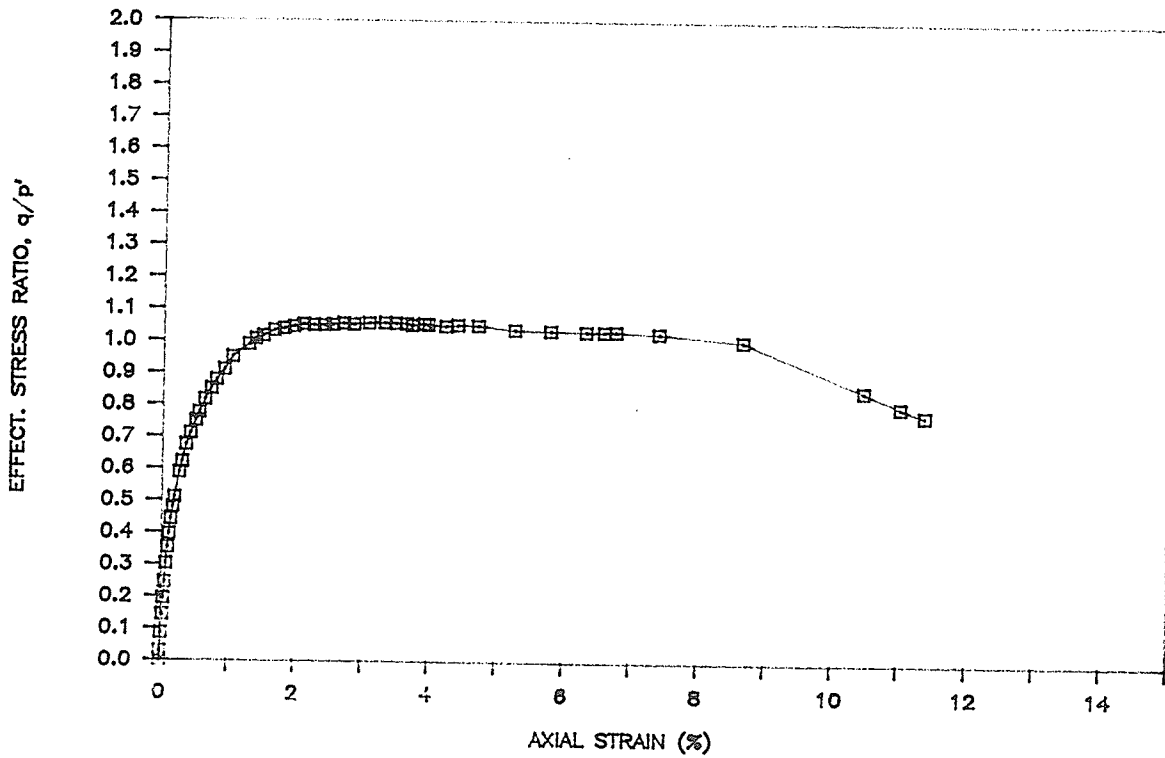
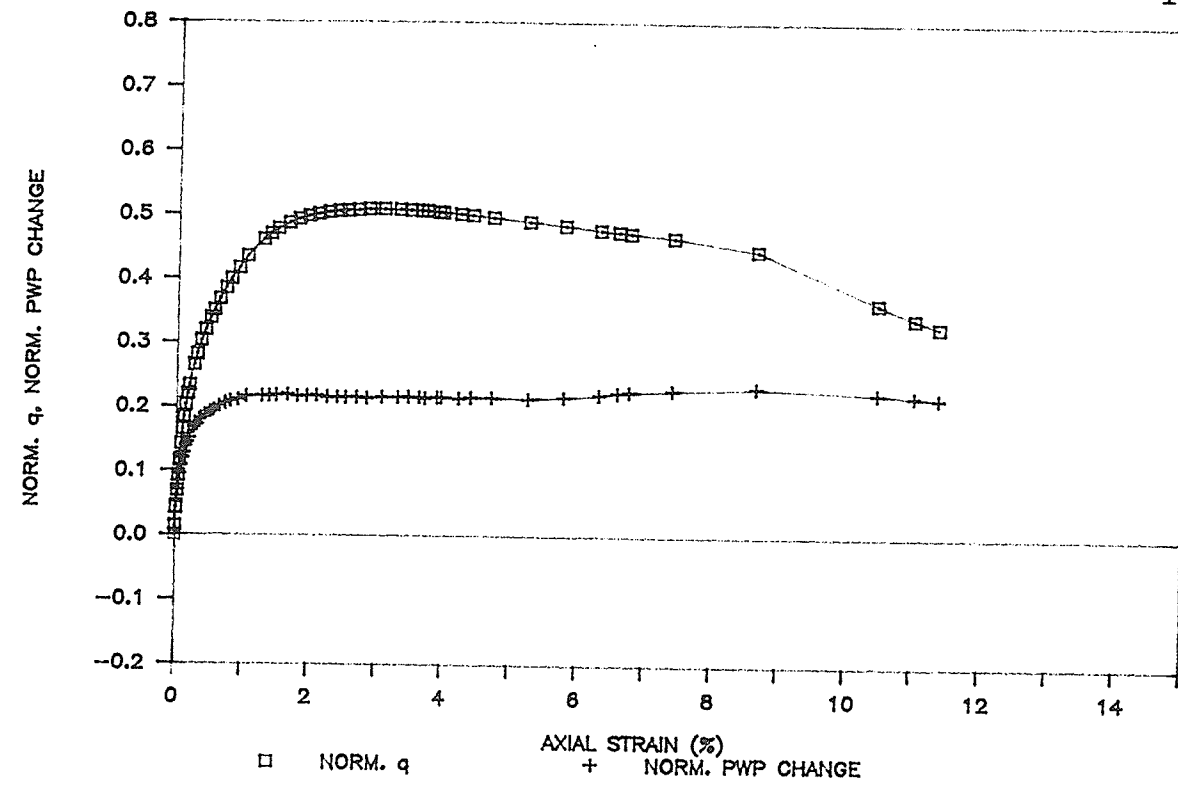


FIGURE 5.5 a,b UNDRAINED STRESS-STRAIN AND POREWATER PRESSURE RESULTS  
SAMPLE T787 (CONTROL SPECIMEN)

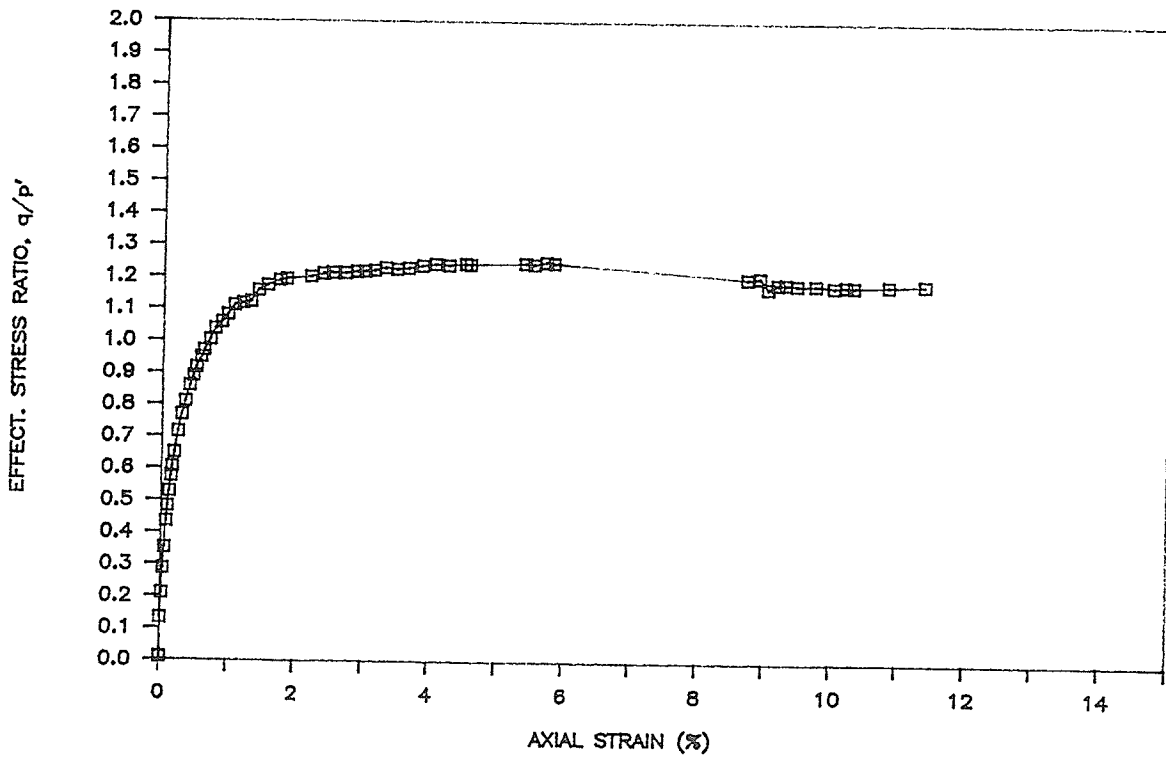
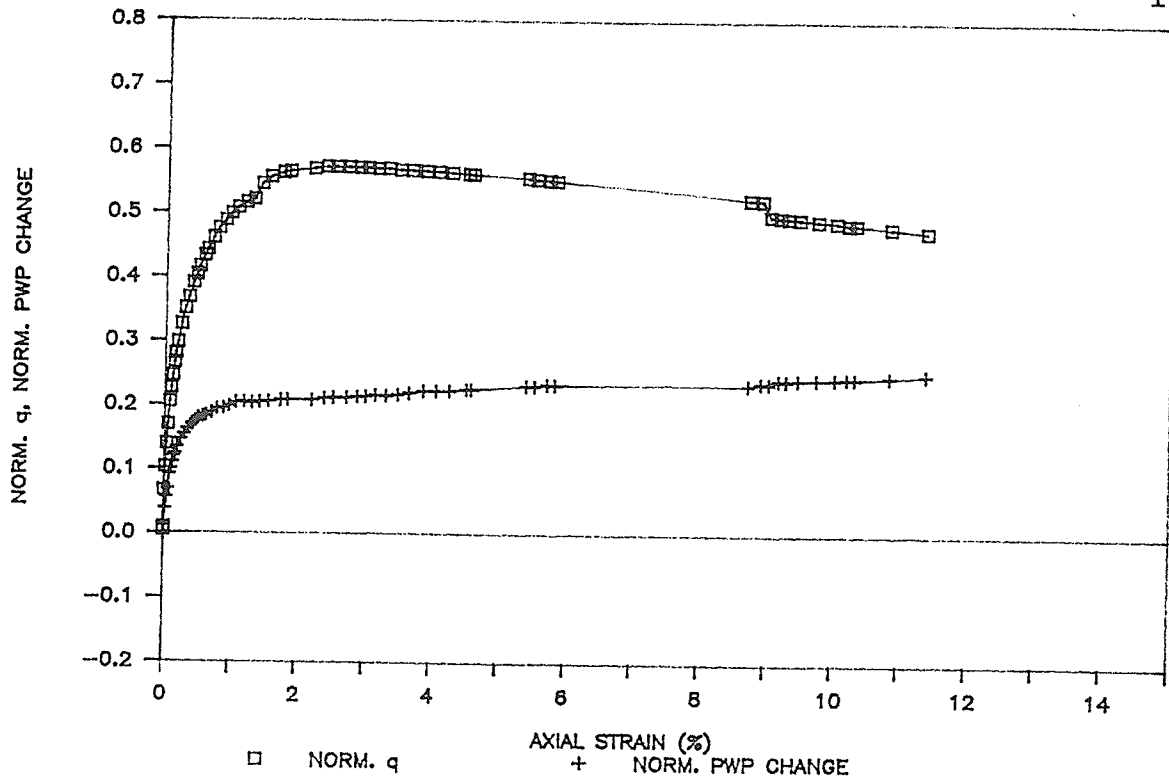


FIGURE 5.6 a,b UNDRAINED STRESS-STRAIN AND POREWATER PRESSURE RESULTS SAMPLE T777

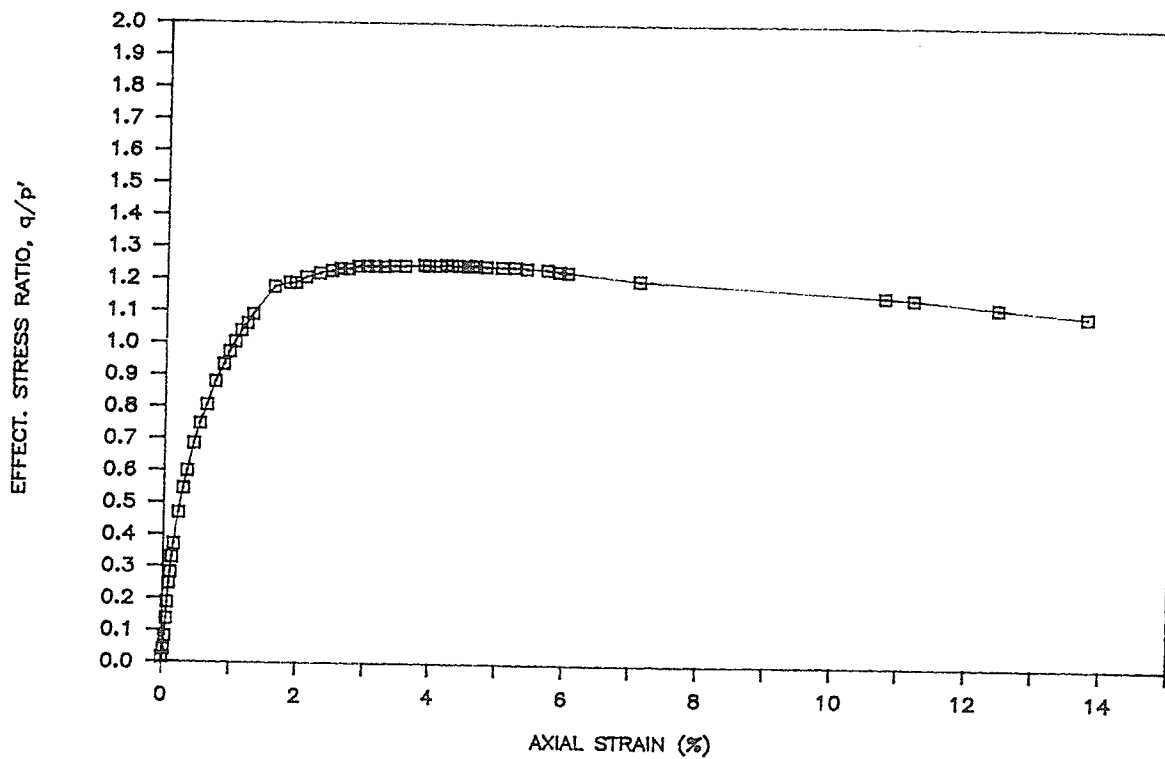
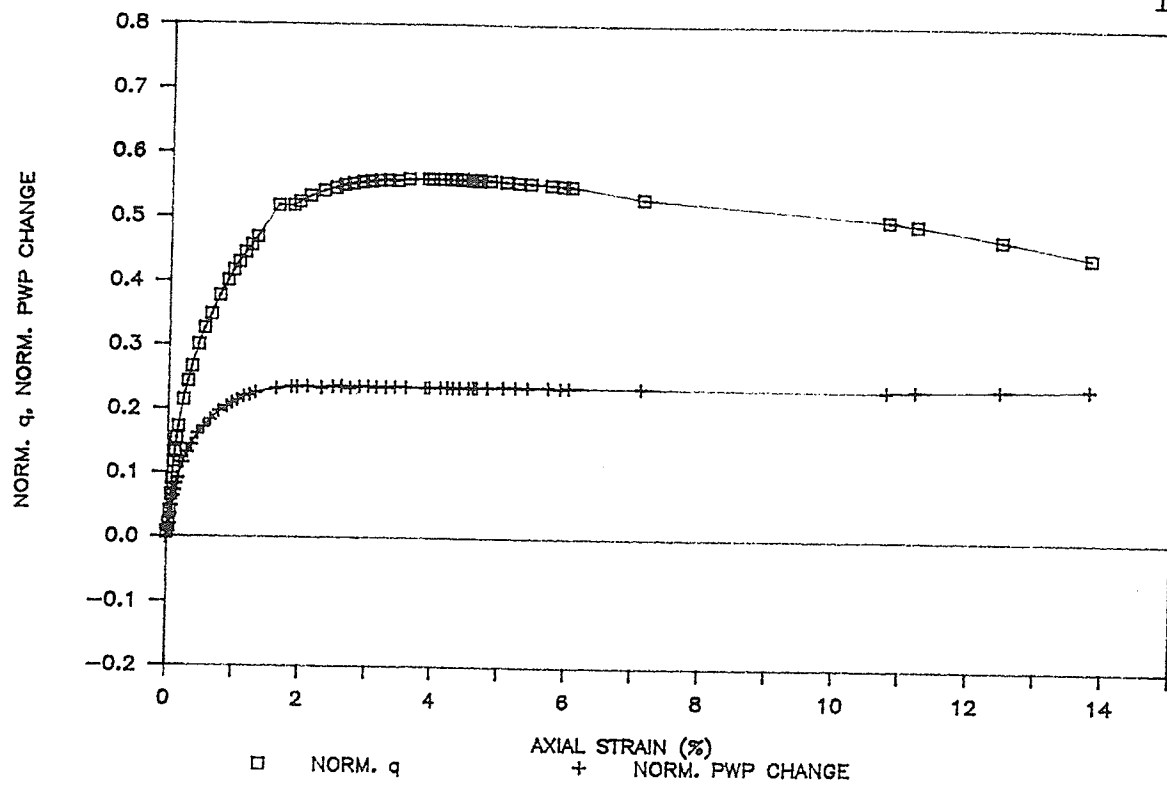


FIGURE 5.7 a,b UNDRAINED STRESS-STRAIN AND POREWATER PRESSURE RESULTS SAMPLE T774

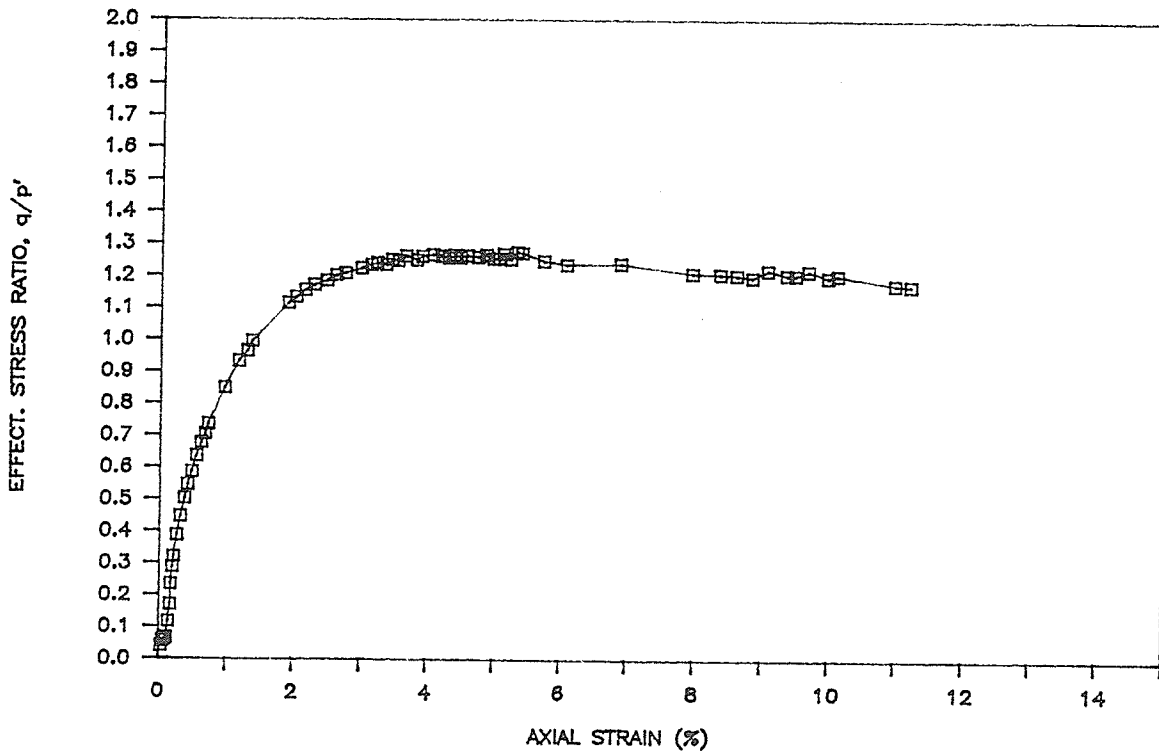
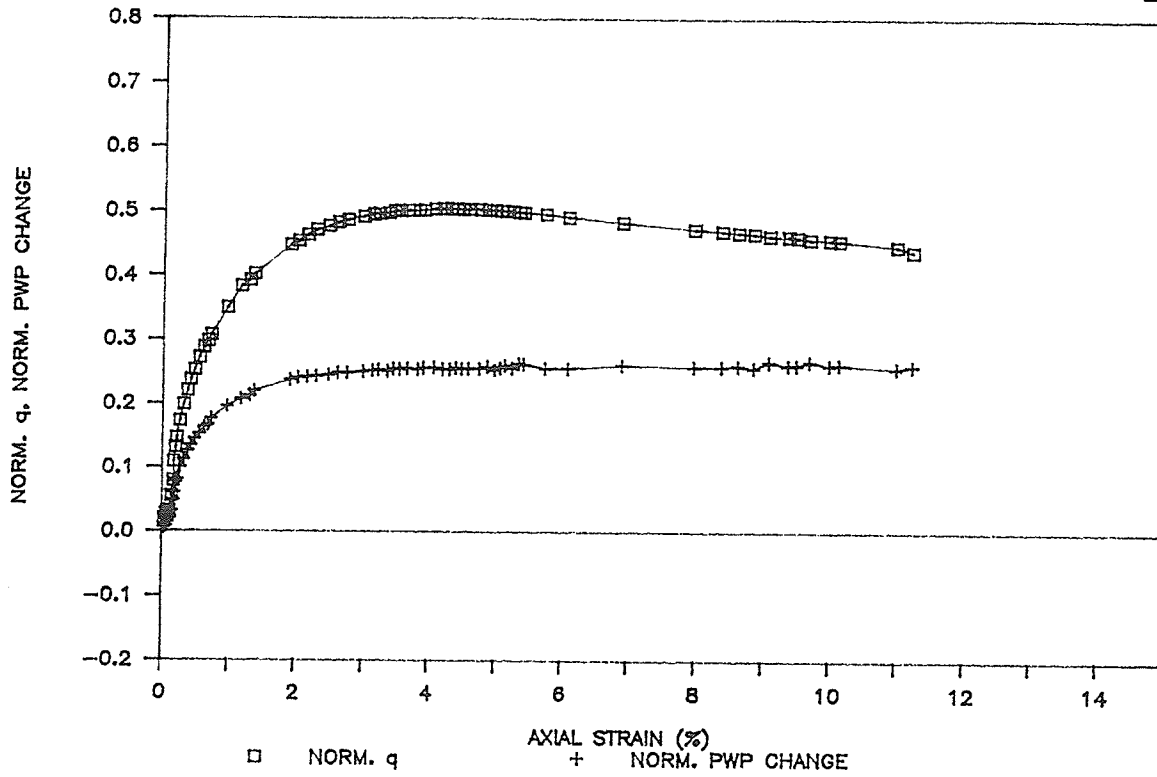


FIGURE 5.8 a,b UNDRAINED STRESS-STRAIN AND POREWATER PRESSURE RESULTS SAMPLE T775

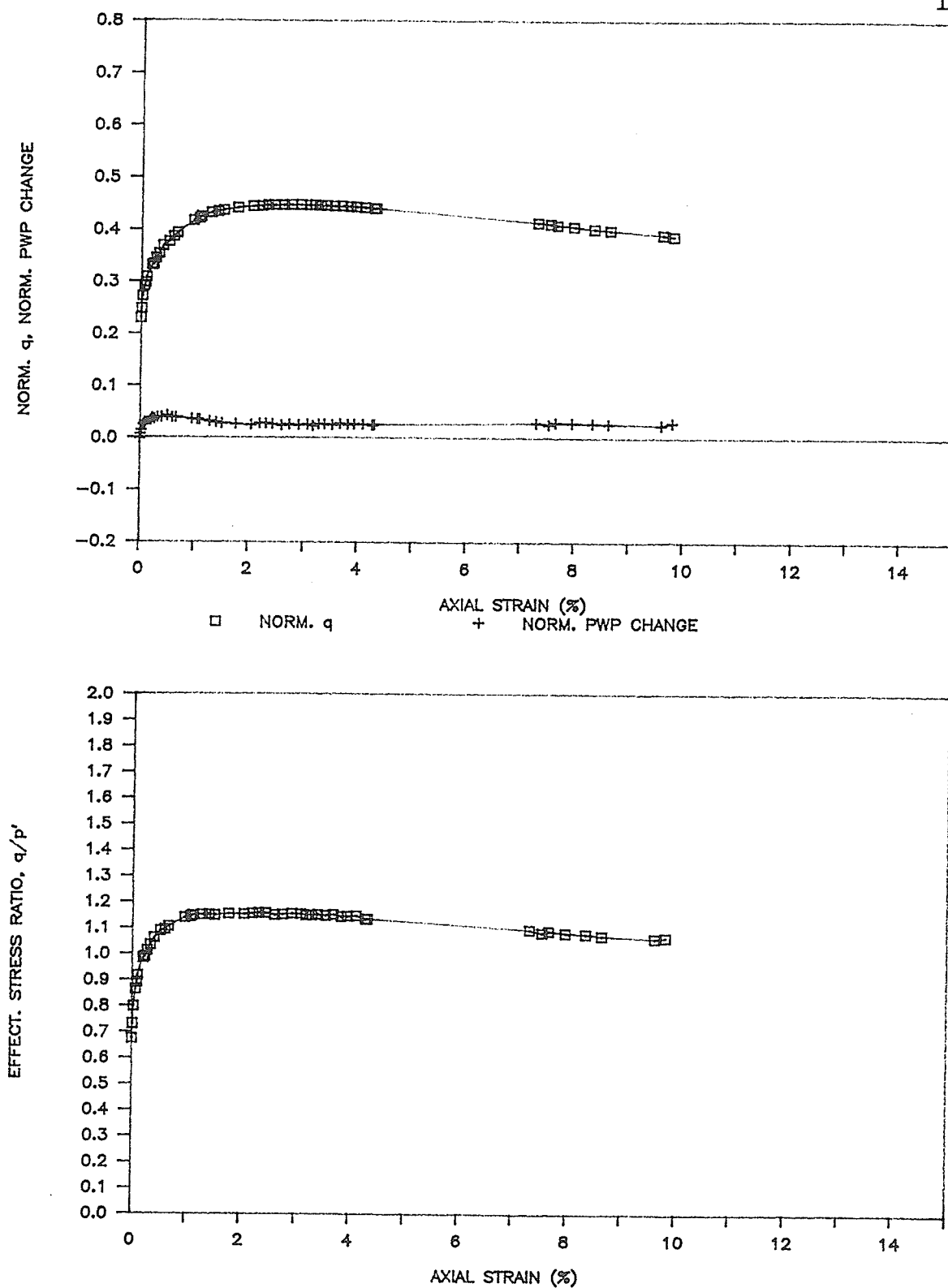


FIGURE 5.9 a,b UNDRAINED STRESS-STRAIN AND POREWATER PRESSURE RESULTS SAMPLE T778

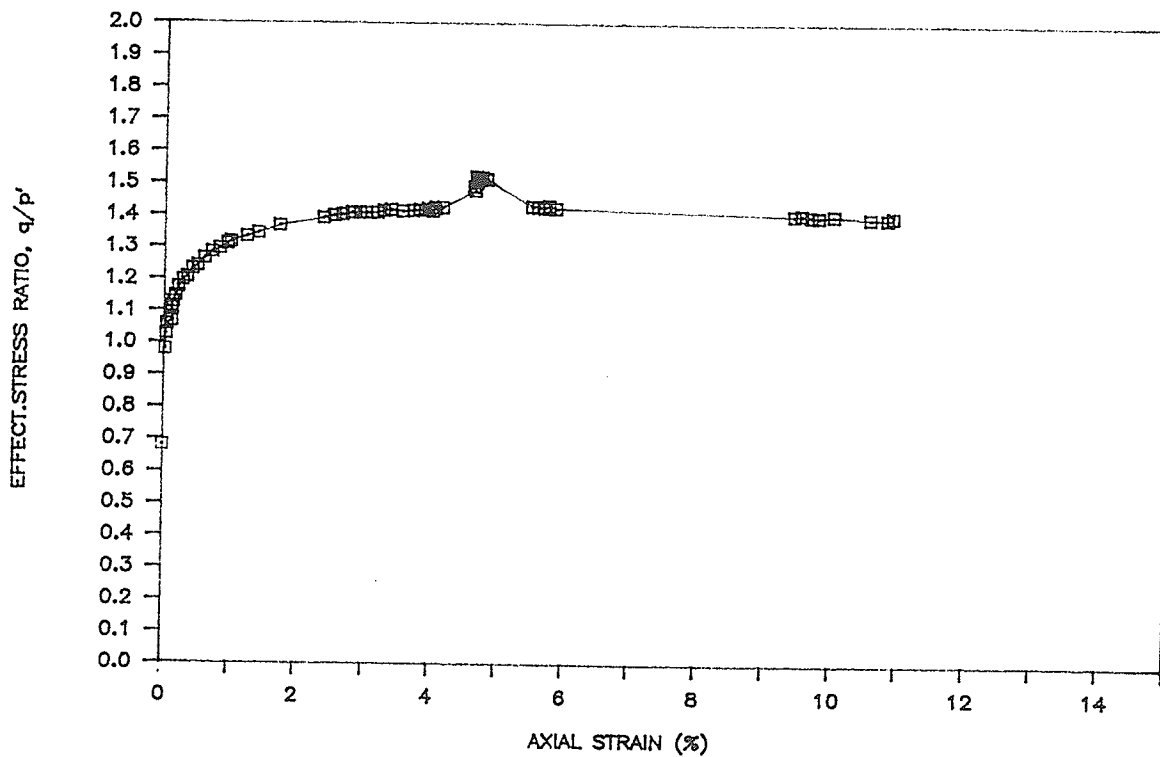
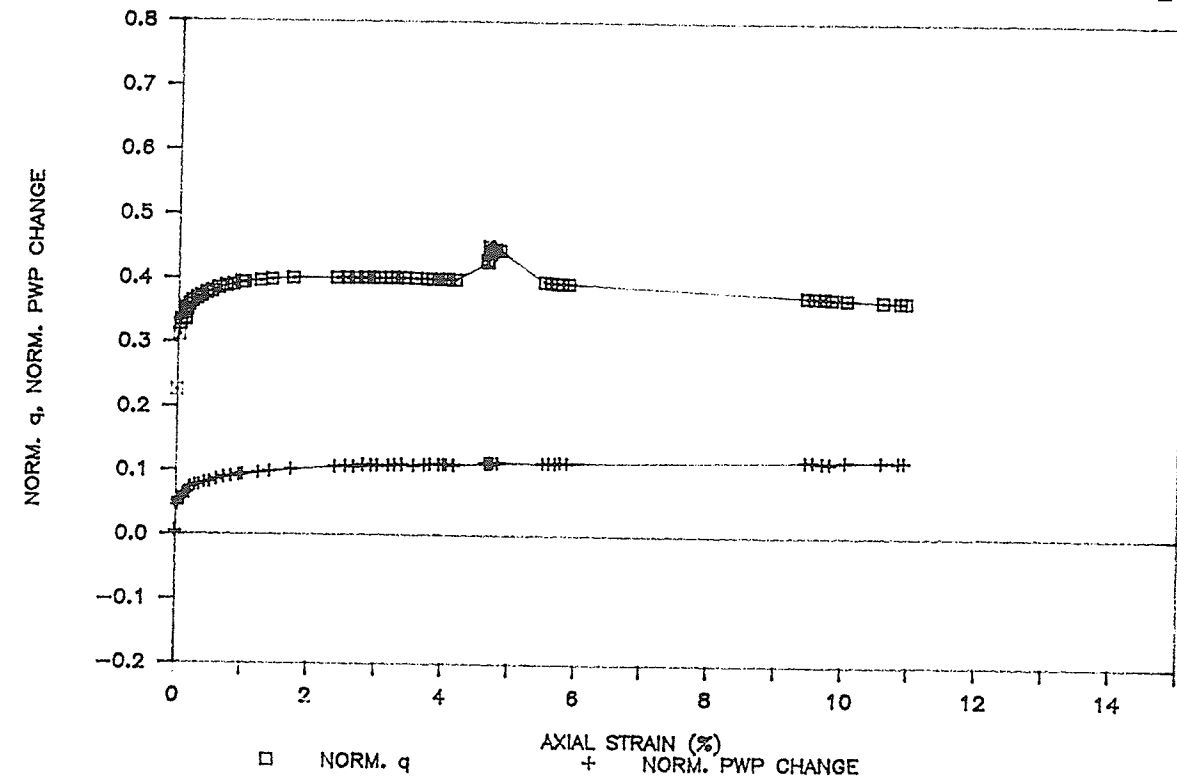


FIGURE 5.10 a,b UNDRAINED STRESS-STRAIN AND POREWATER PRESSURE RESULTS  
SAMPLE T776

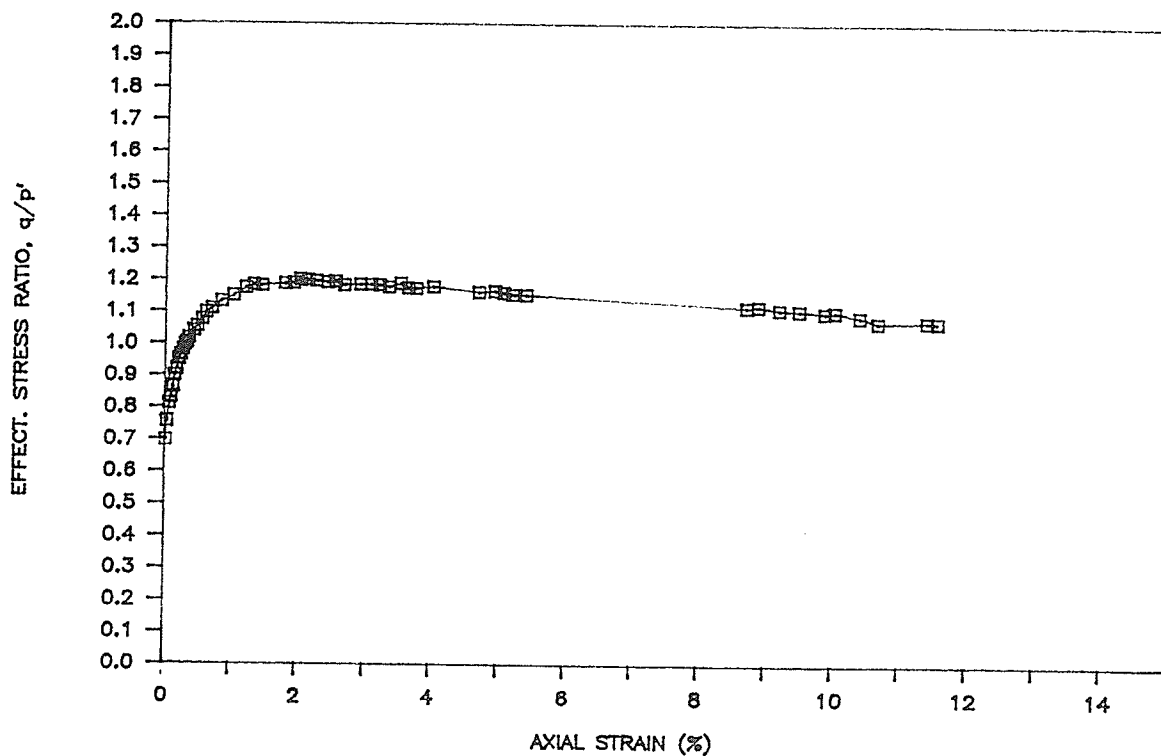
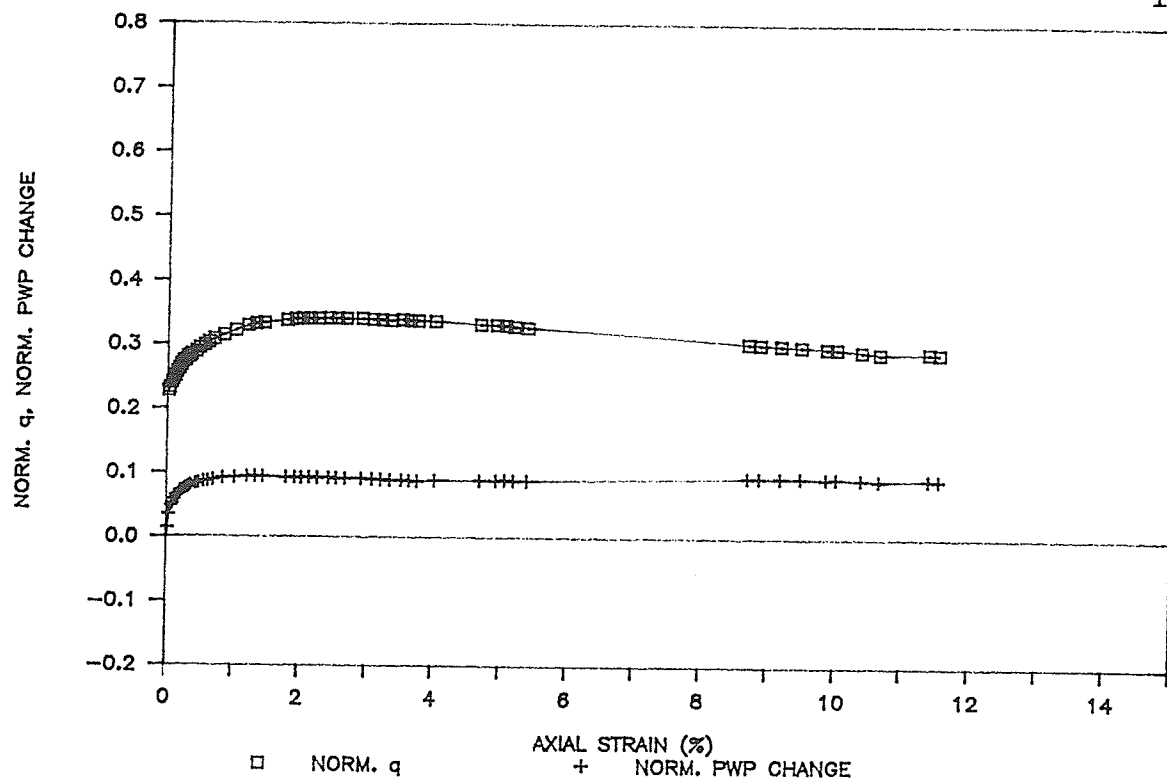


FIGURE 5.11 a,b UNDRAINED STRESS-STRAIN AND POREWATER PRESSURE RESULTS SAMPLE T779

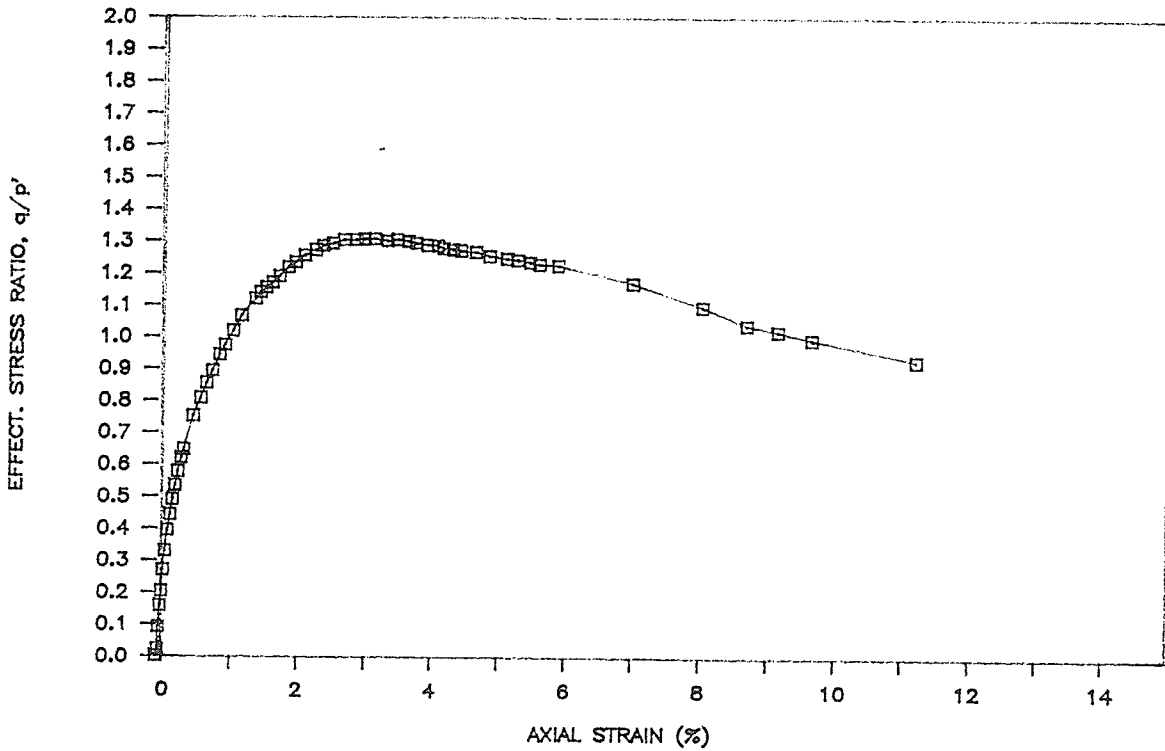
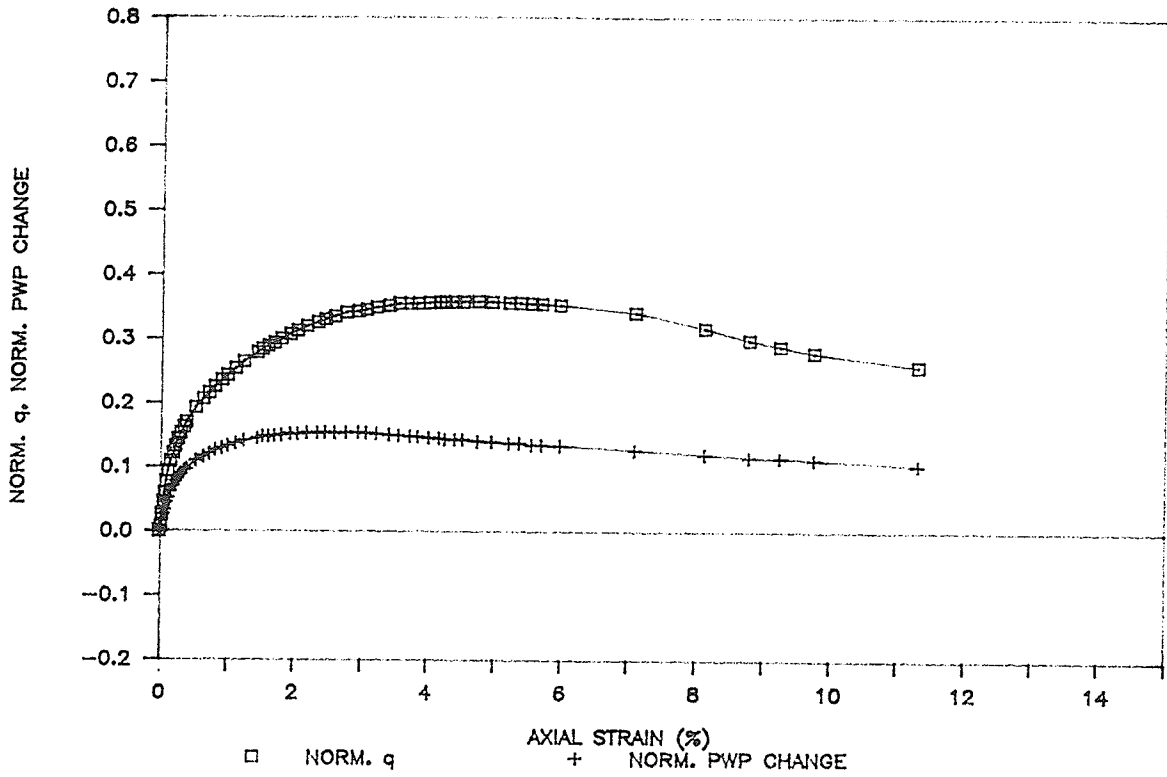


FIGURE 5.12 a,b UNDRAINED STRESS-STRAIN AND POREWATER PRESSURE RESULTS SAMPLE T789

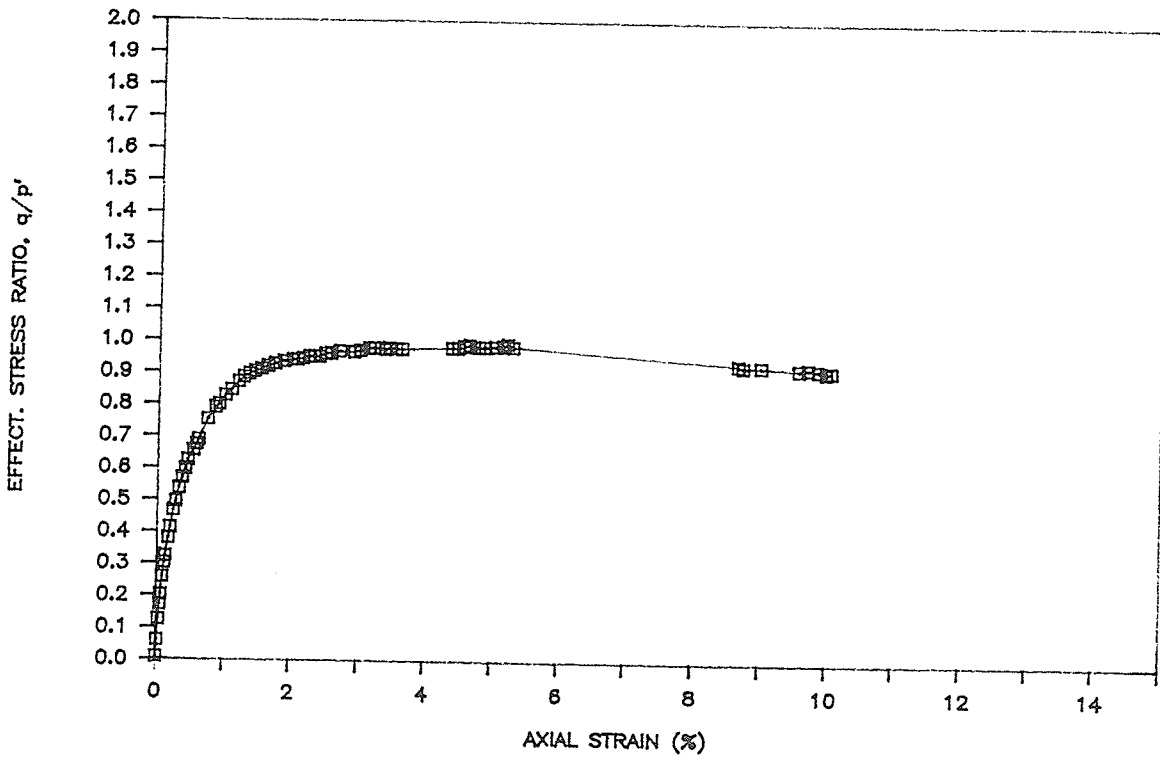
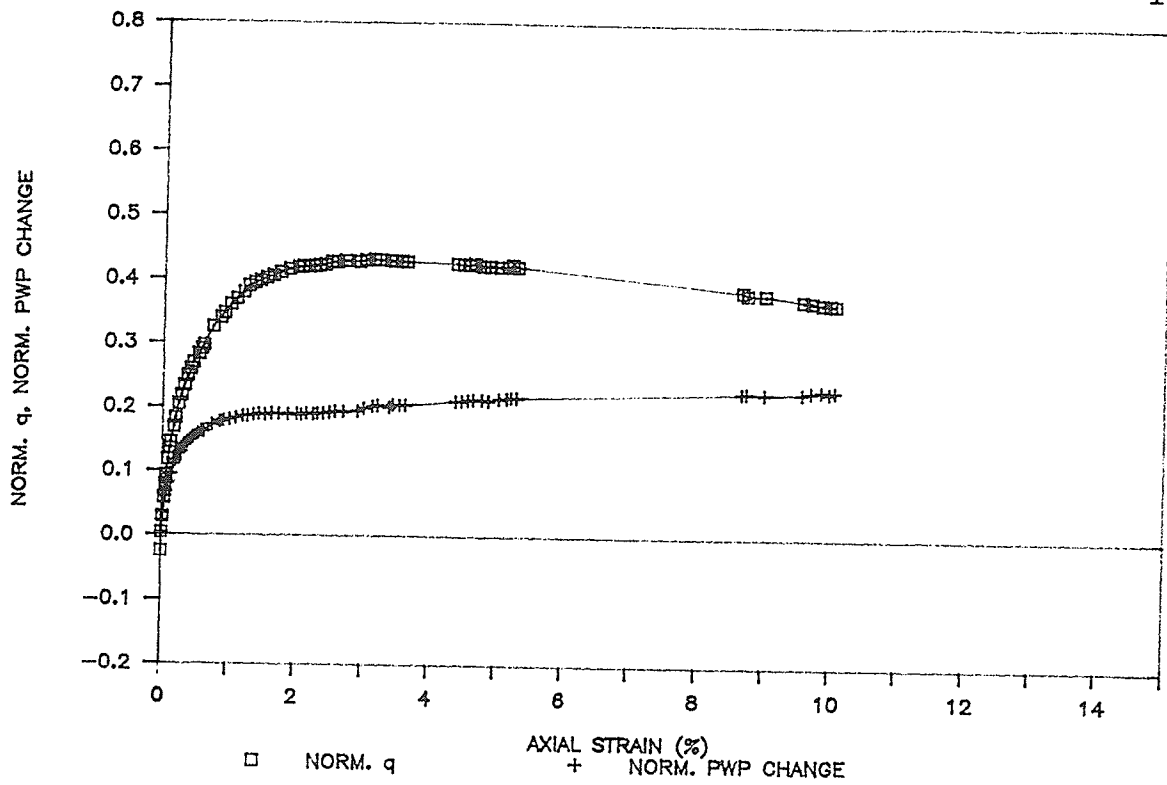


FIGURE 5.13 a,b UNDRAINED STRESS-STRAIN AND POREWATER PRESSURE RESULTS SAMPLE T781

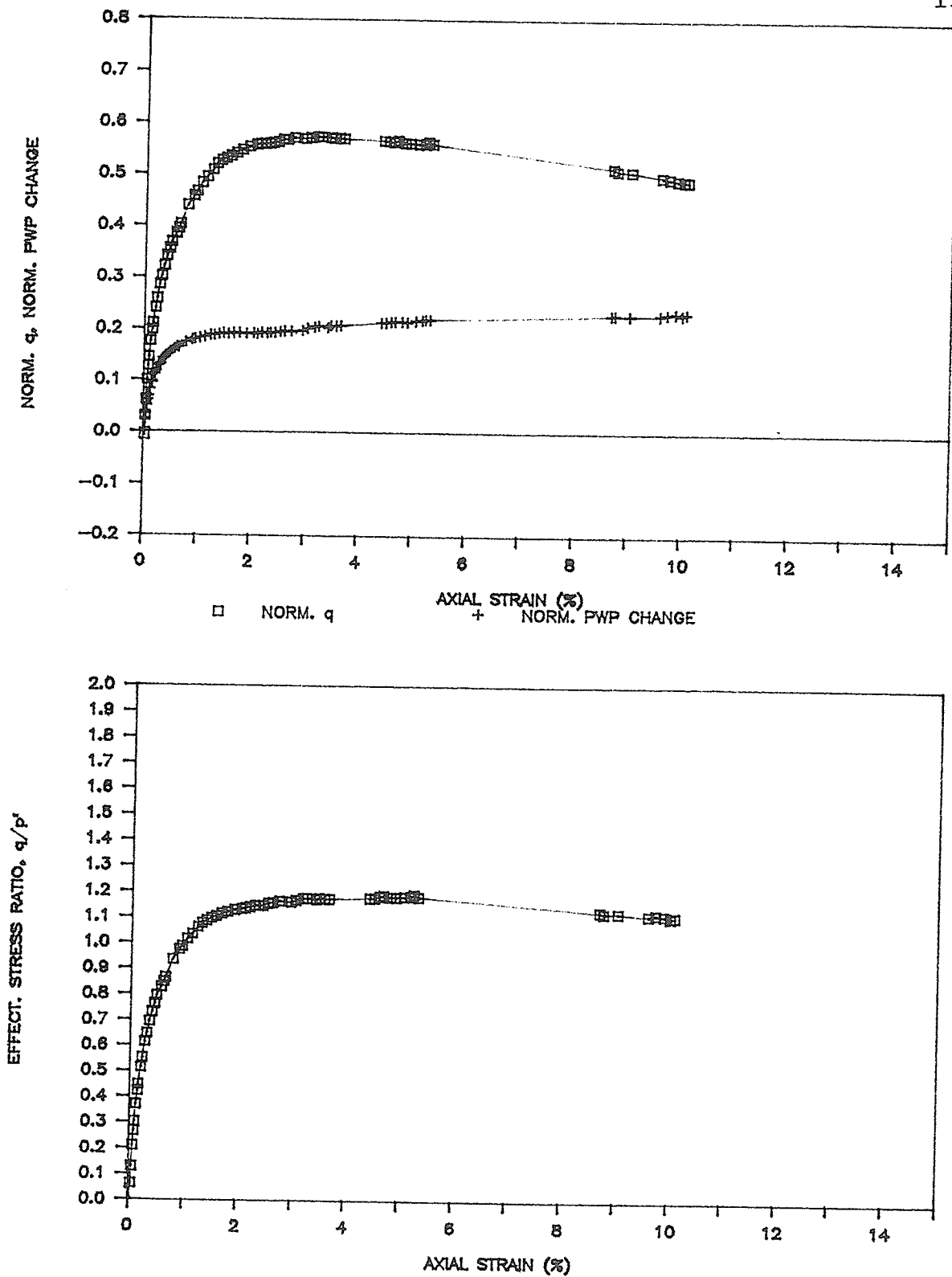


FIGURE 5.14 a,b UNDRAINED STRESS-STRAIN AND POREWATER PRESSURE RESULTS SAMPLE T781\*

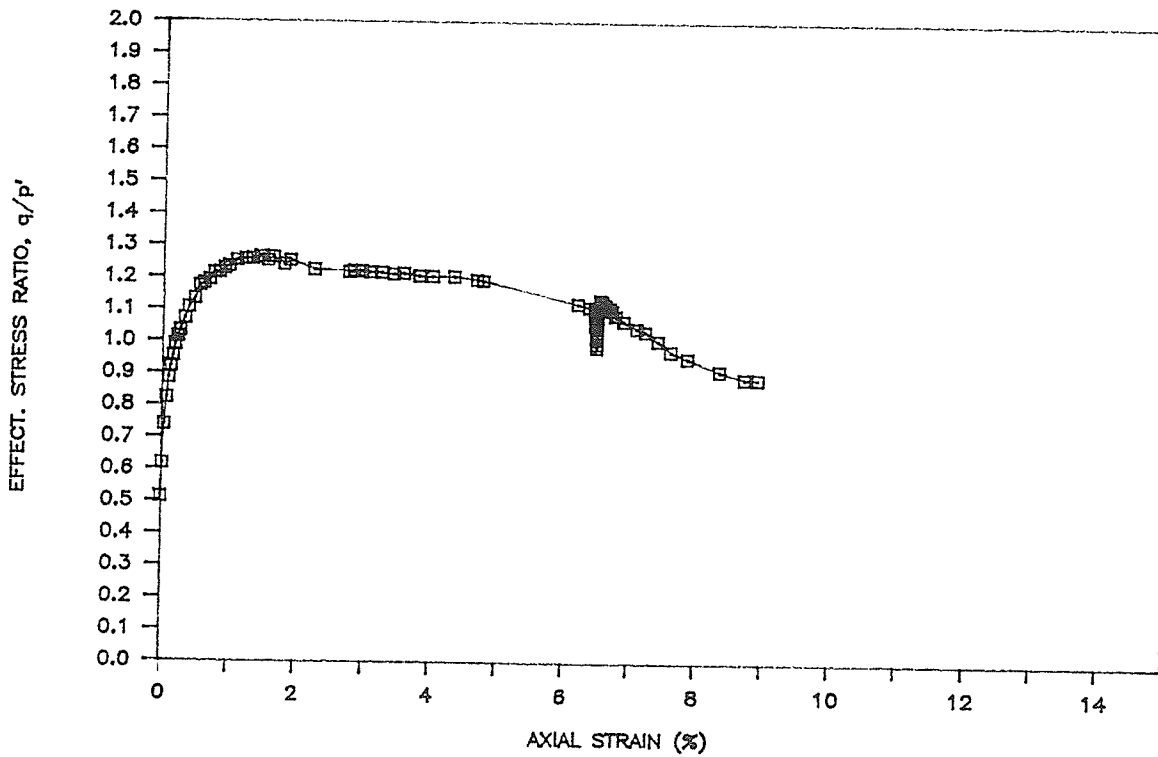
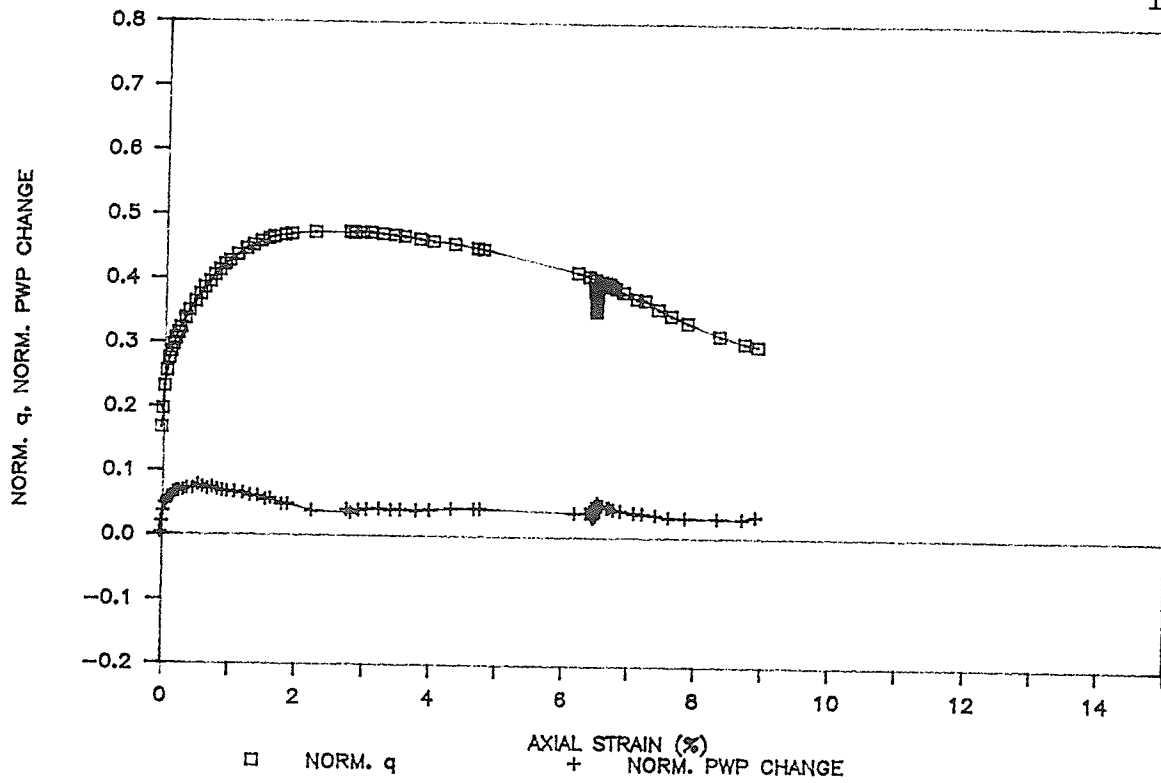


FIGURE 5.15 a,b UNDRAINED STRESS-STRAIN AND POREWATER PRESSURE RESULTS SAMPLE T782

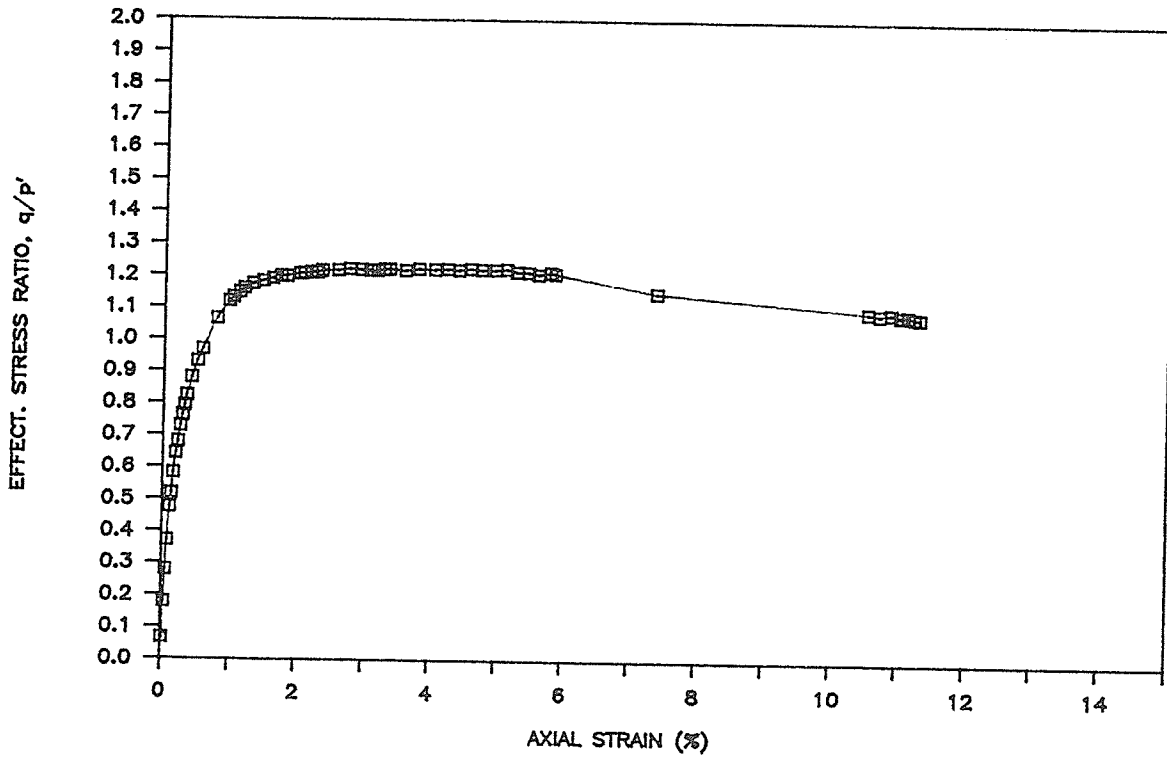
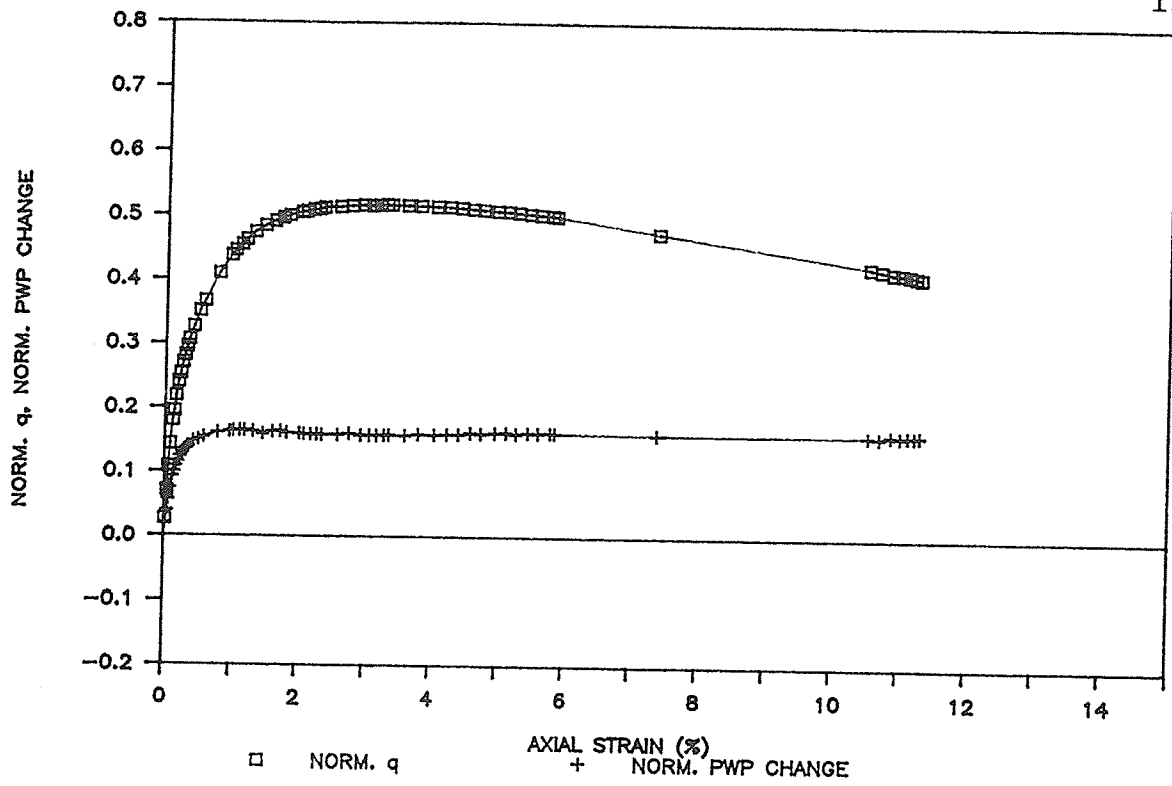


FIGURE 5.16 a,b UNDRAINED STRESS-STRAIN AND POREWATER PRESSURE RESULTS SAMPLE T784

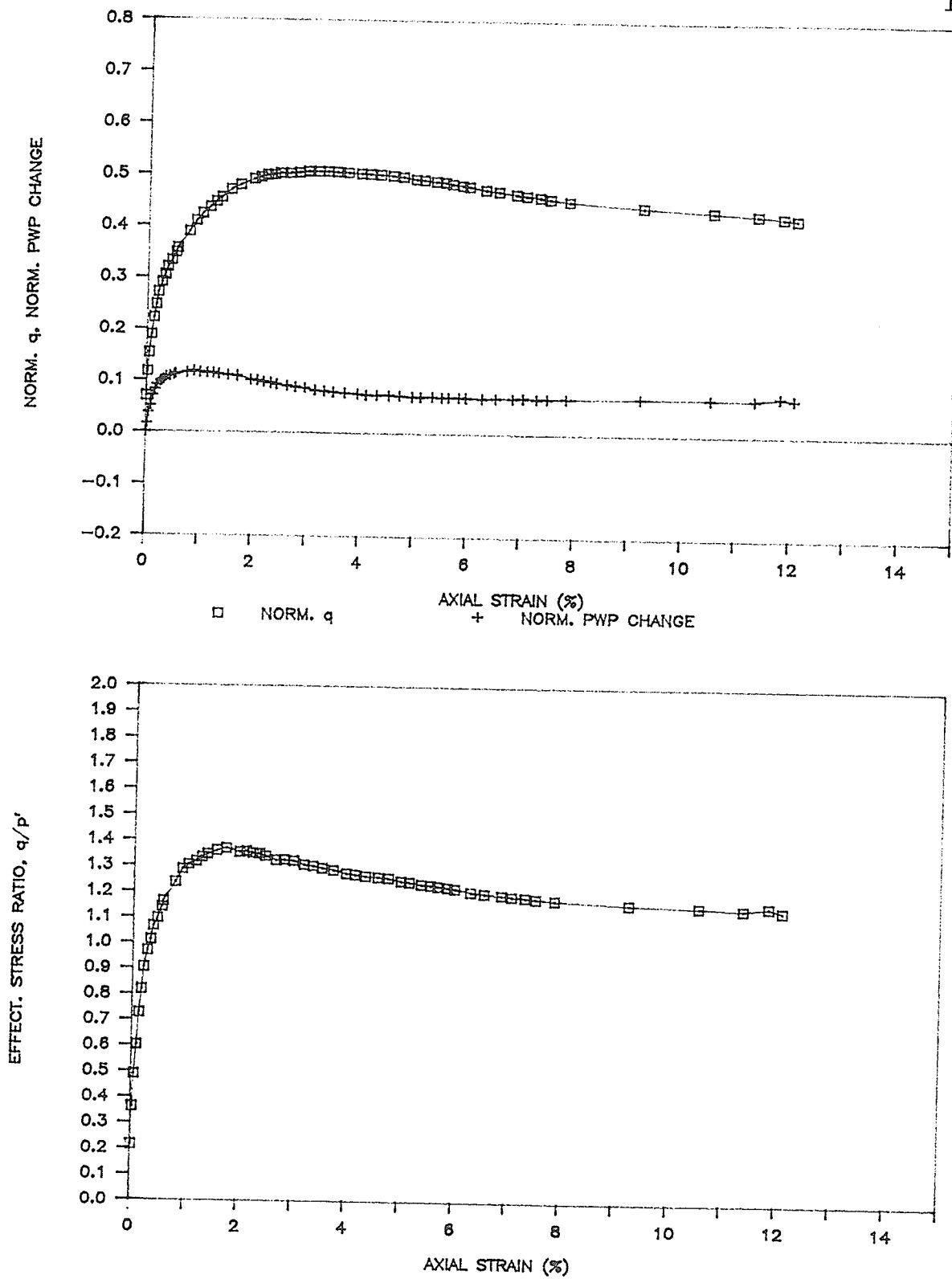


FIGURE 5.17 a,b UNDRAINED STRESS-STRAIN AND POREWATER PRESSURE RESULTS  
SAMPLE T788

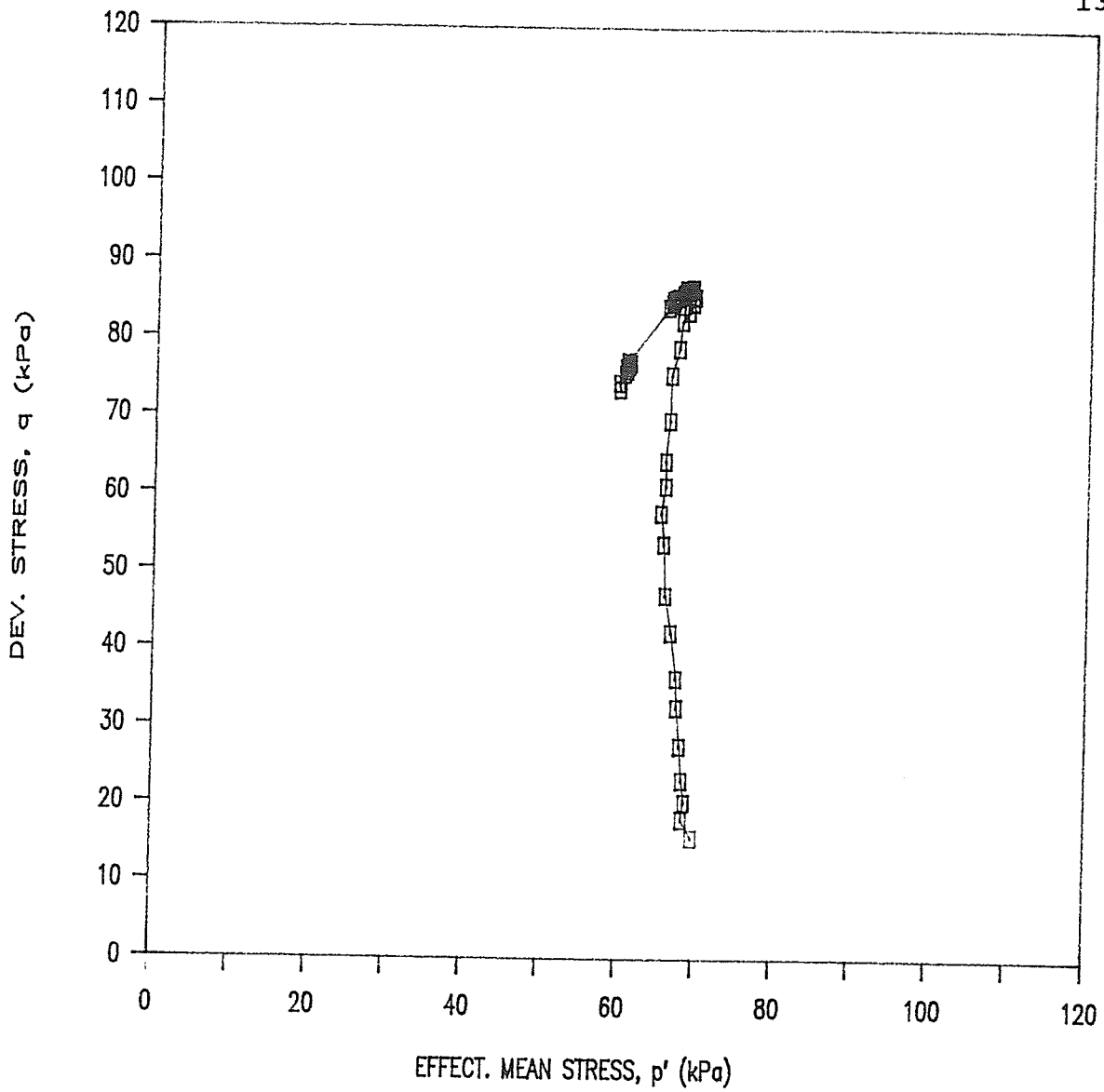


FIGURE 5.18 EFFECTIVE STRESS PATH DURING UNDRAINED SHEAR IN  $p'$  vs.  $q$  SPACE, SAMPLE T771 (CONTROL)

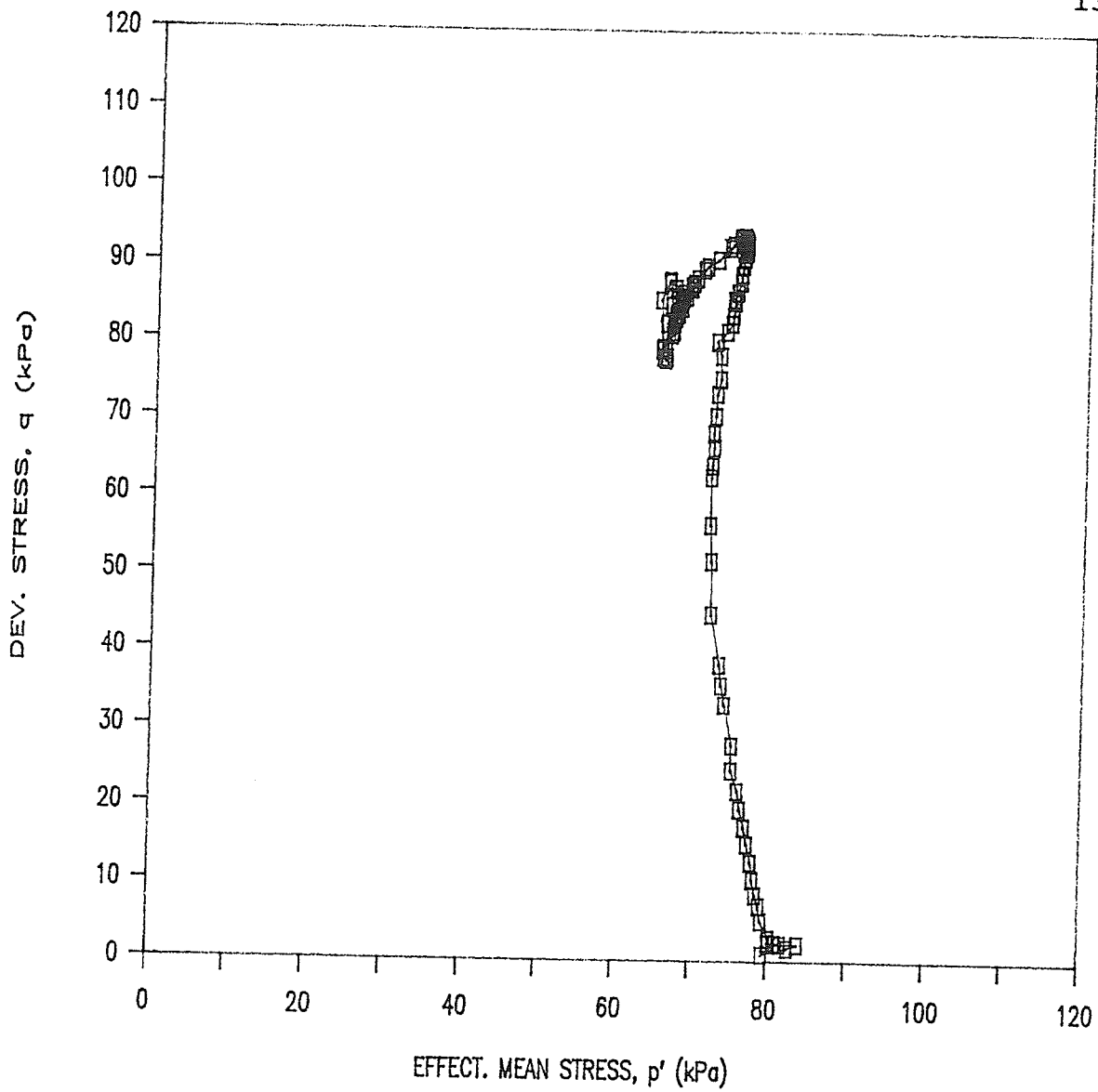


FIGURE 5.19 EFFECTIVE STRESS PATH DURING UNDRAINED SHEAR IN  $p'$  vs.  $q$  SPACE, SAMPLE T772 (CONTROL)

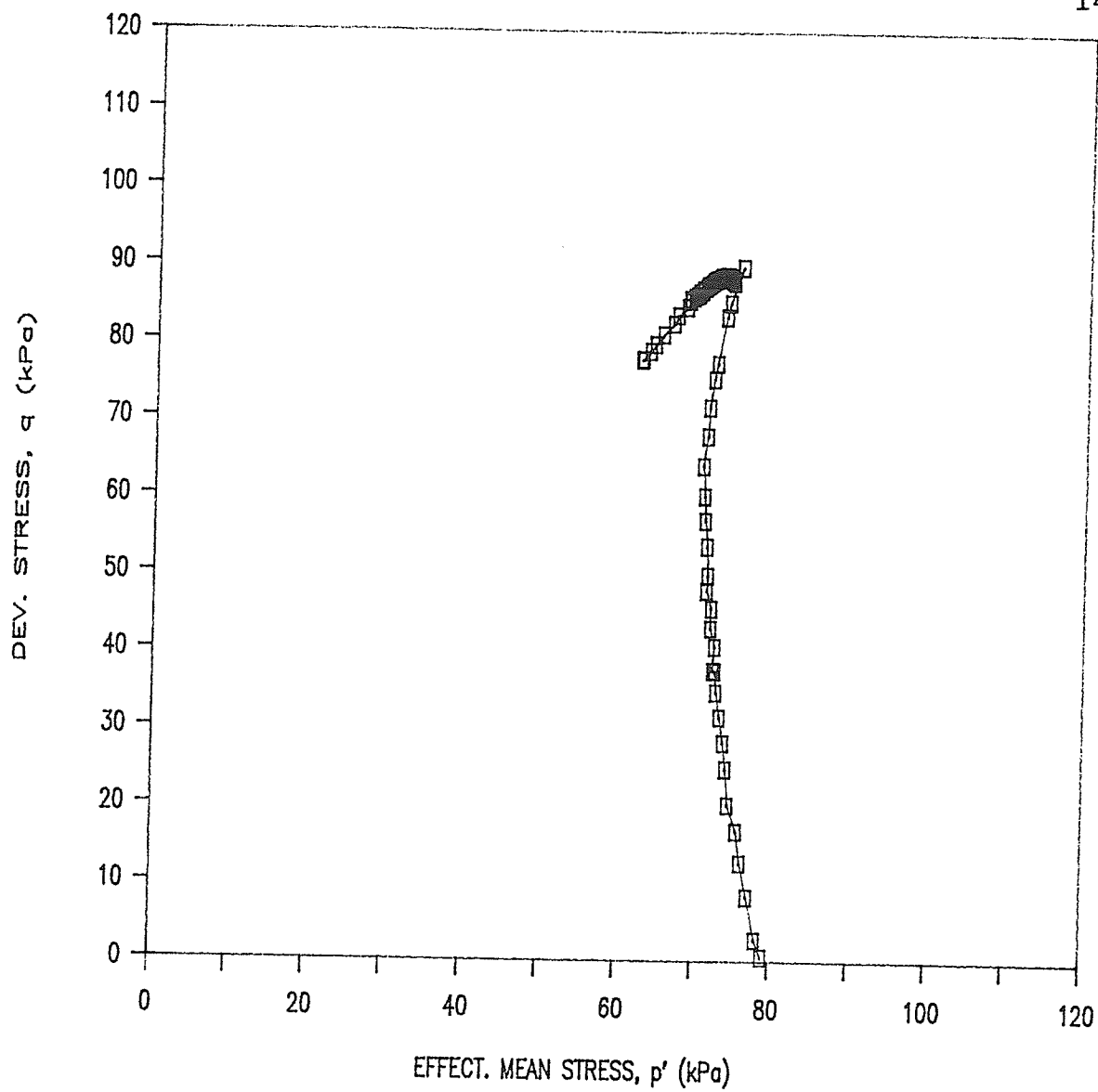


FIGURE 5.20 EFFECTIVE STRESS PATH DURING UNDRAINED SHEAR IN  $p'$  vs.  $q$  SPACE, SAMPLE T773 (CONTROL)

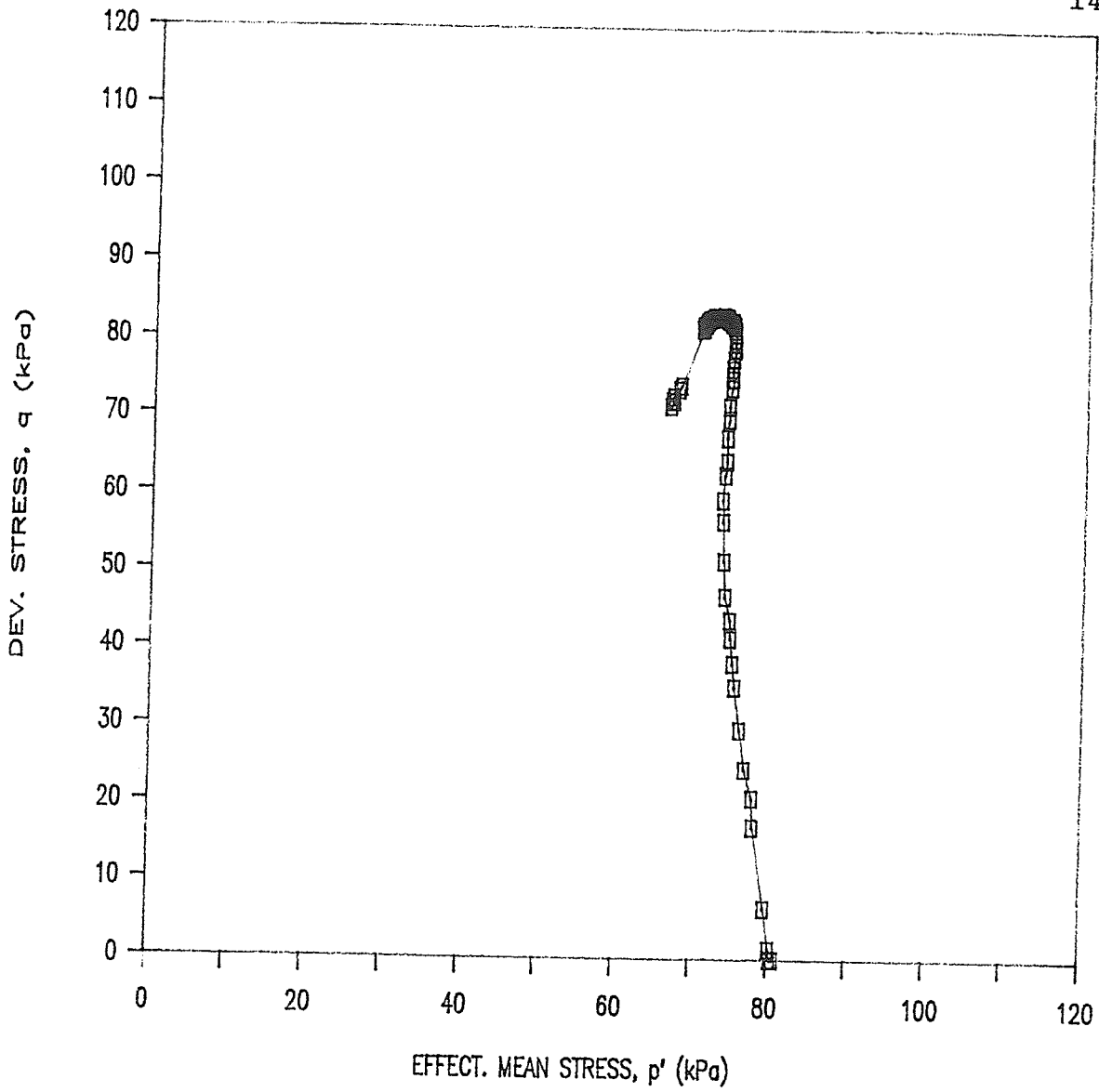


FIGURE 5.21 EFFECTIVE STRESS PATH DURING UNDRAINED SHEAR IN  $p'$  vs.  $q$  SPACE, SAMPLE T785 (CONTROL)

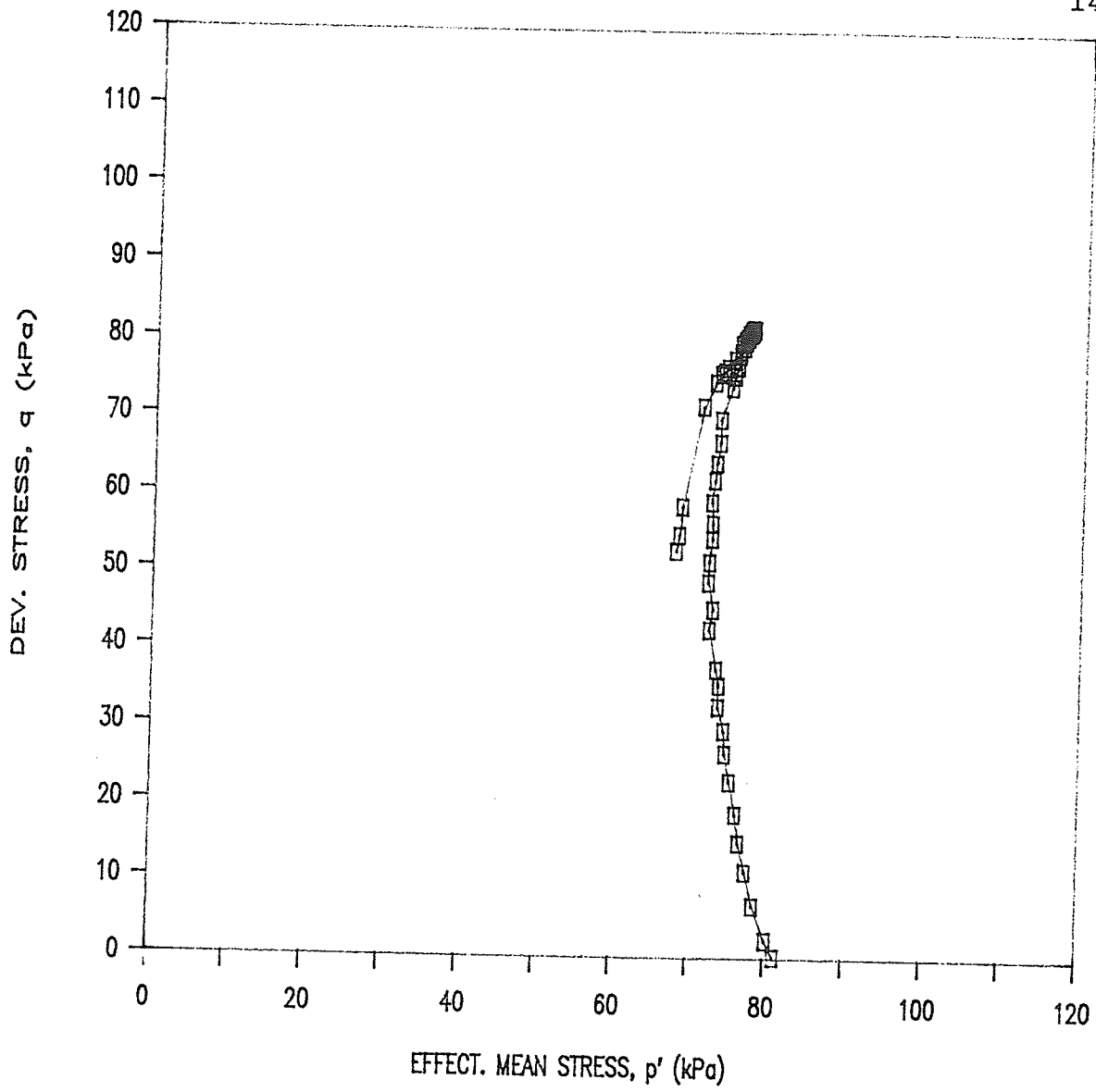


FIGURE 5.22 EFFECTIVE STRESS PATH DURING UNDRAINED SHEAR IN  $p'$  vs.  $q$  SPACE, SAMPLE T787 (CONTROL)

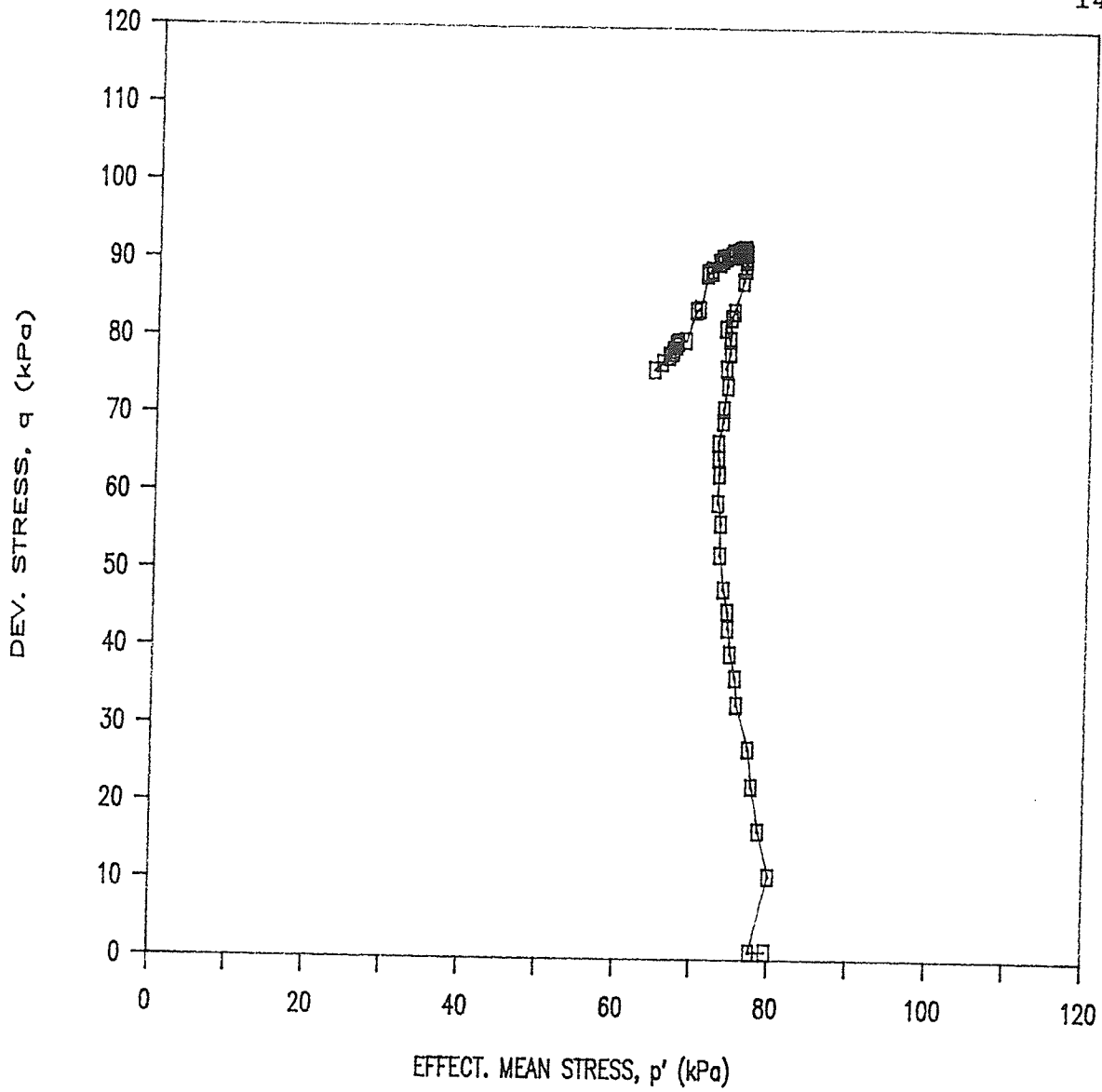


FIGURE 5.23 EFFECTIVE STRESS PATH DURING UNDRAINED SHEAR IN  $p'$  vs.  $q$  SPACE, SAMPLE T777

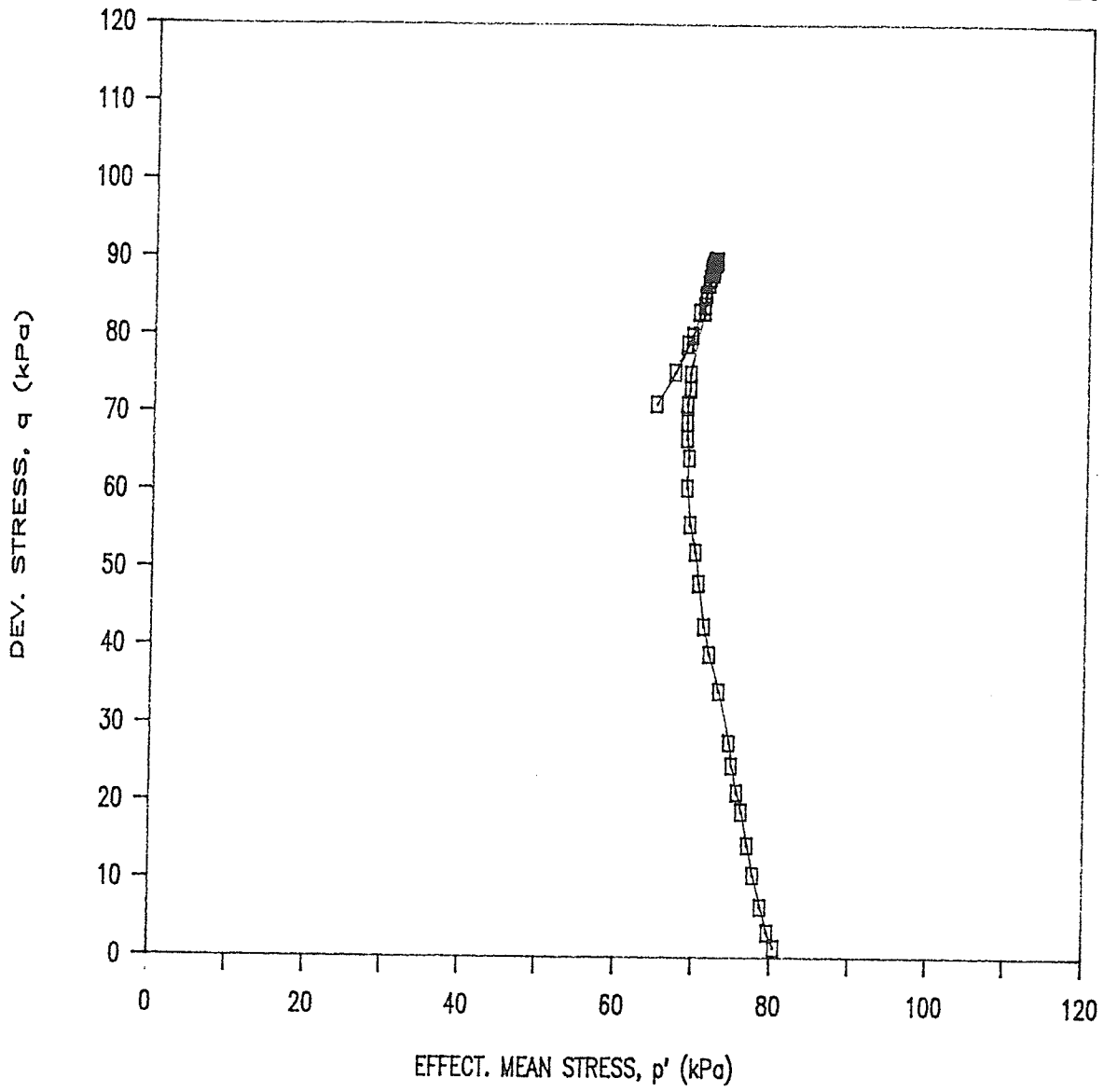


FIGURE 5.24 EFFECTIVE STRESS PATH DURING UNDRAINED SHEAR IN  $p'$  vs.  $q$  SPACE, SAMPLE T774

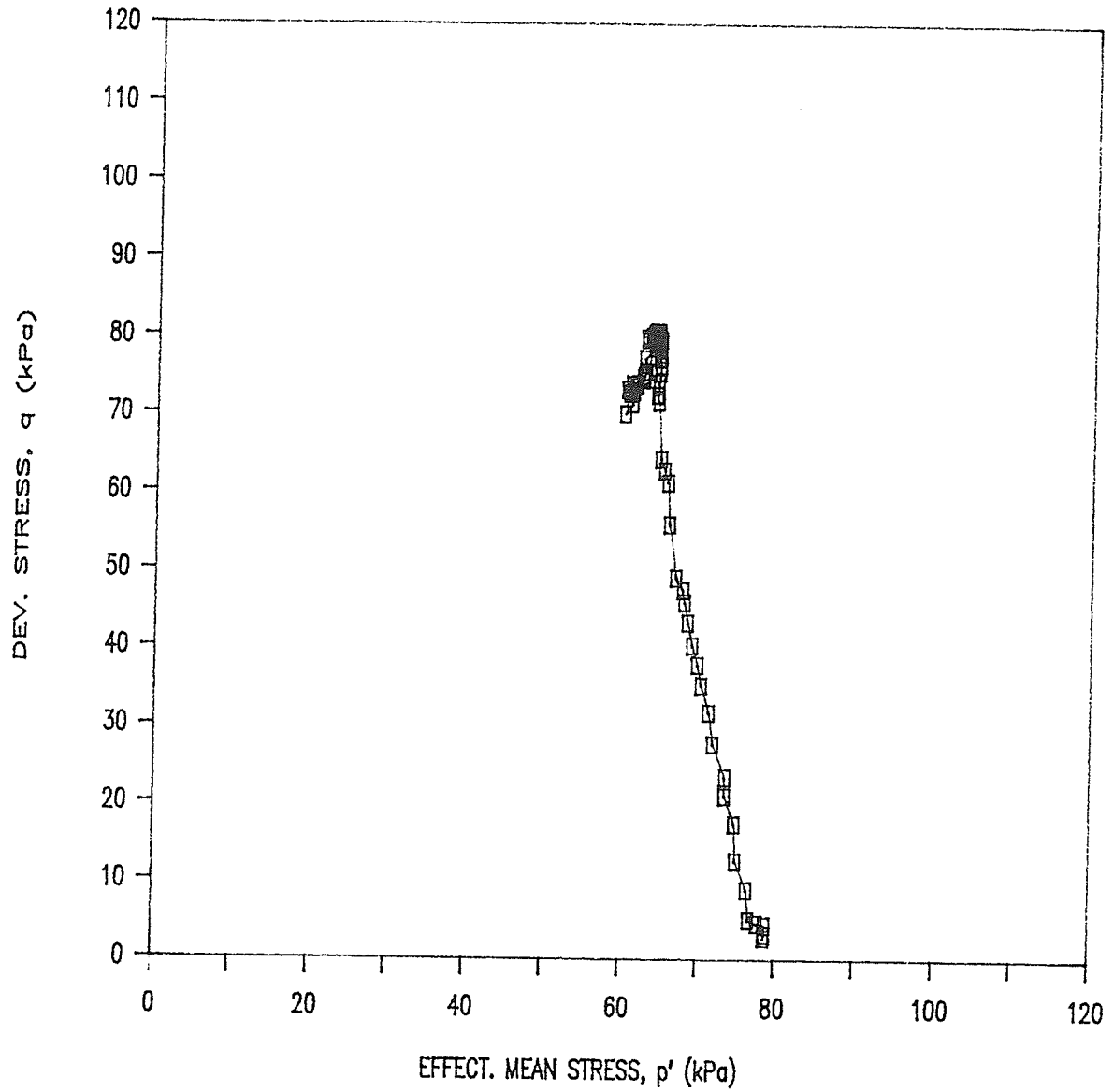
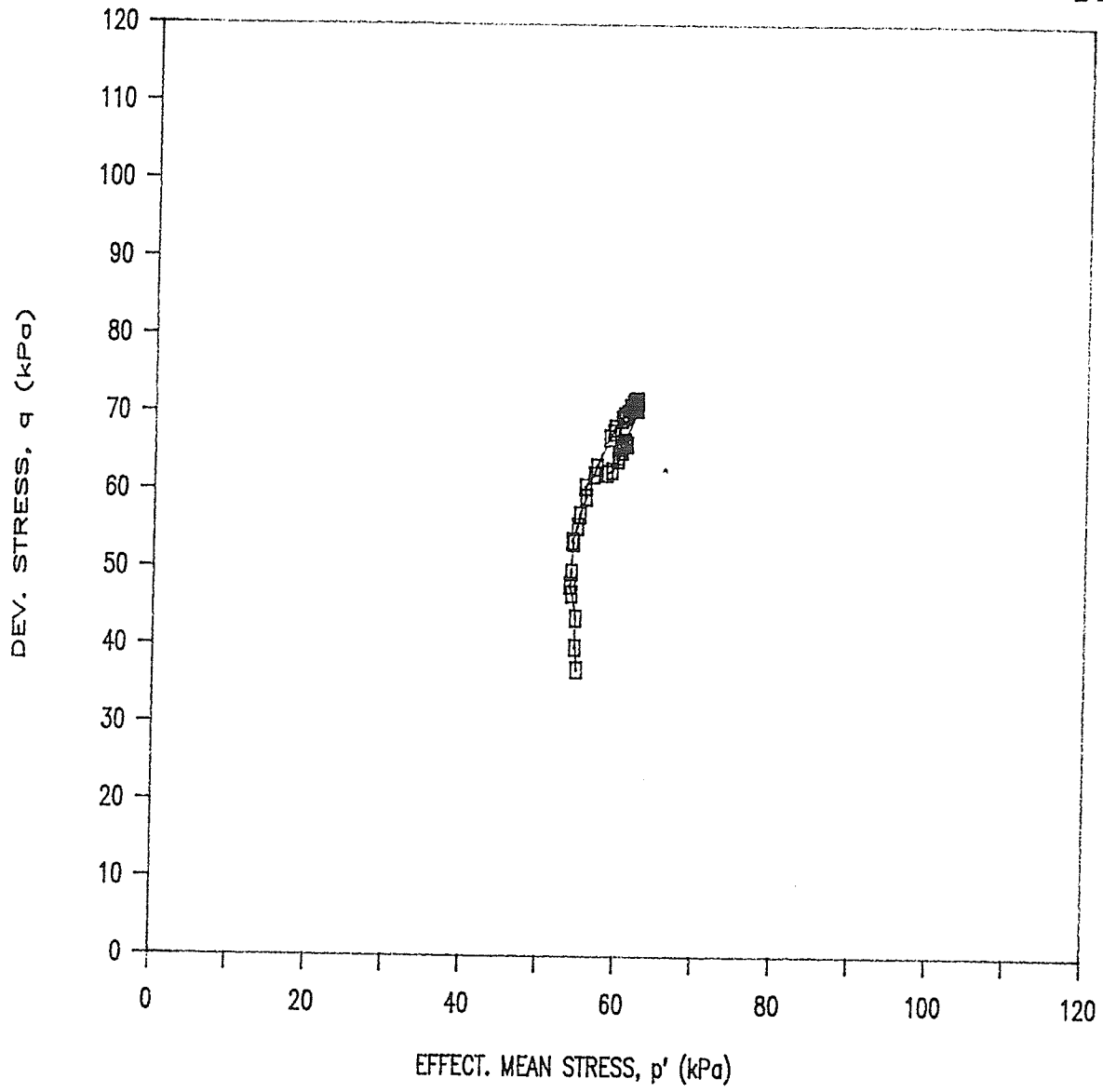


FIGURE 5.25 EFFECTIVE STRESS PATH DURING UNDRAINED SHEAR IN  $p'$  vs.  $q$  SPACE, SAMPLE T775



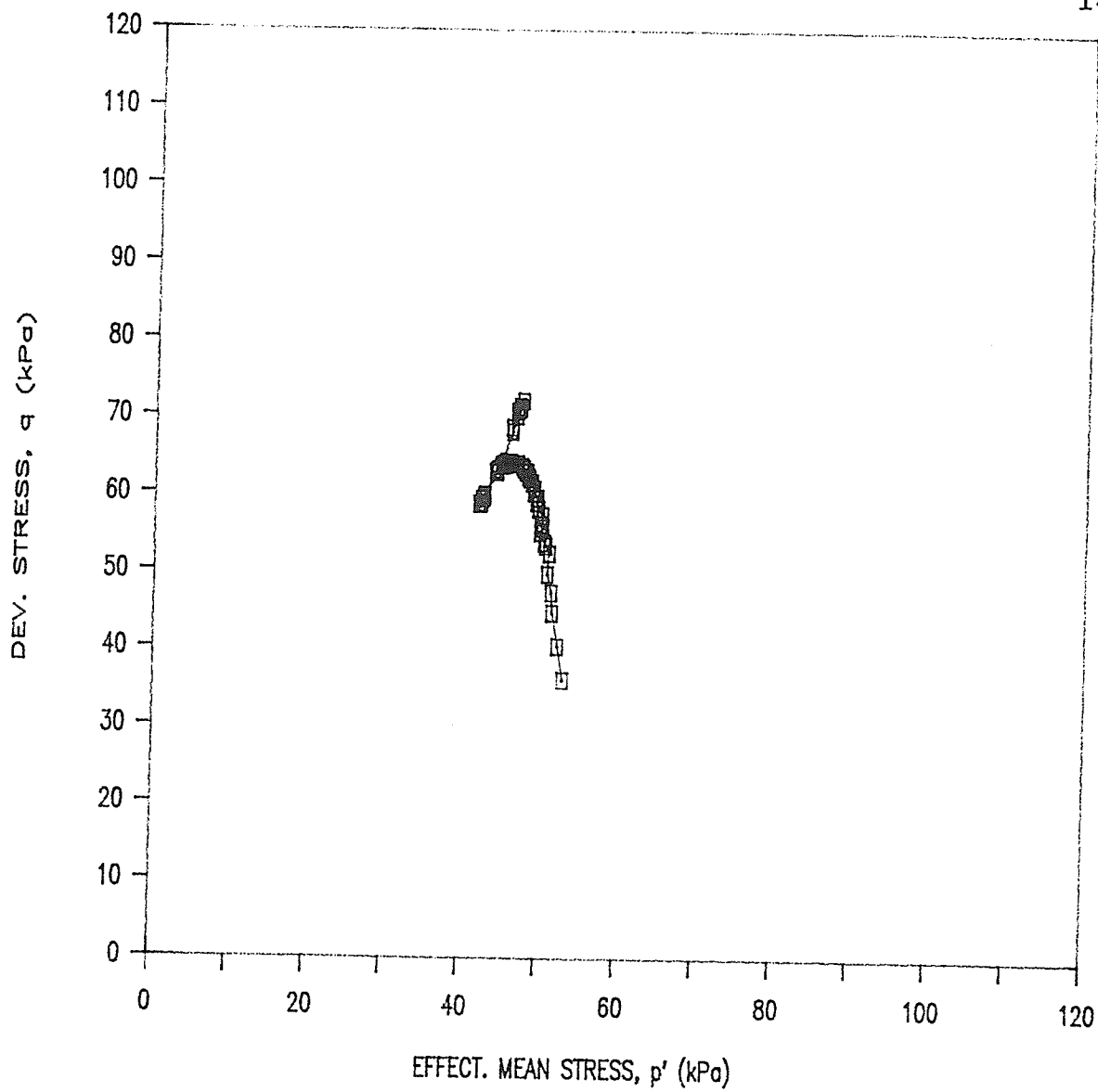


FIGURE 5.27 EFFECTIVE STRESS PATH DURING UNDRAINED SHEAR IN  $p'$  vs.  $q$  SPACE, SAMPLE T776

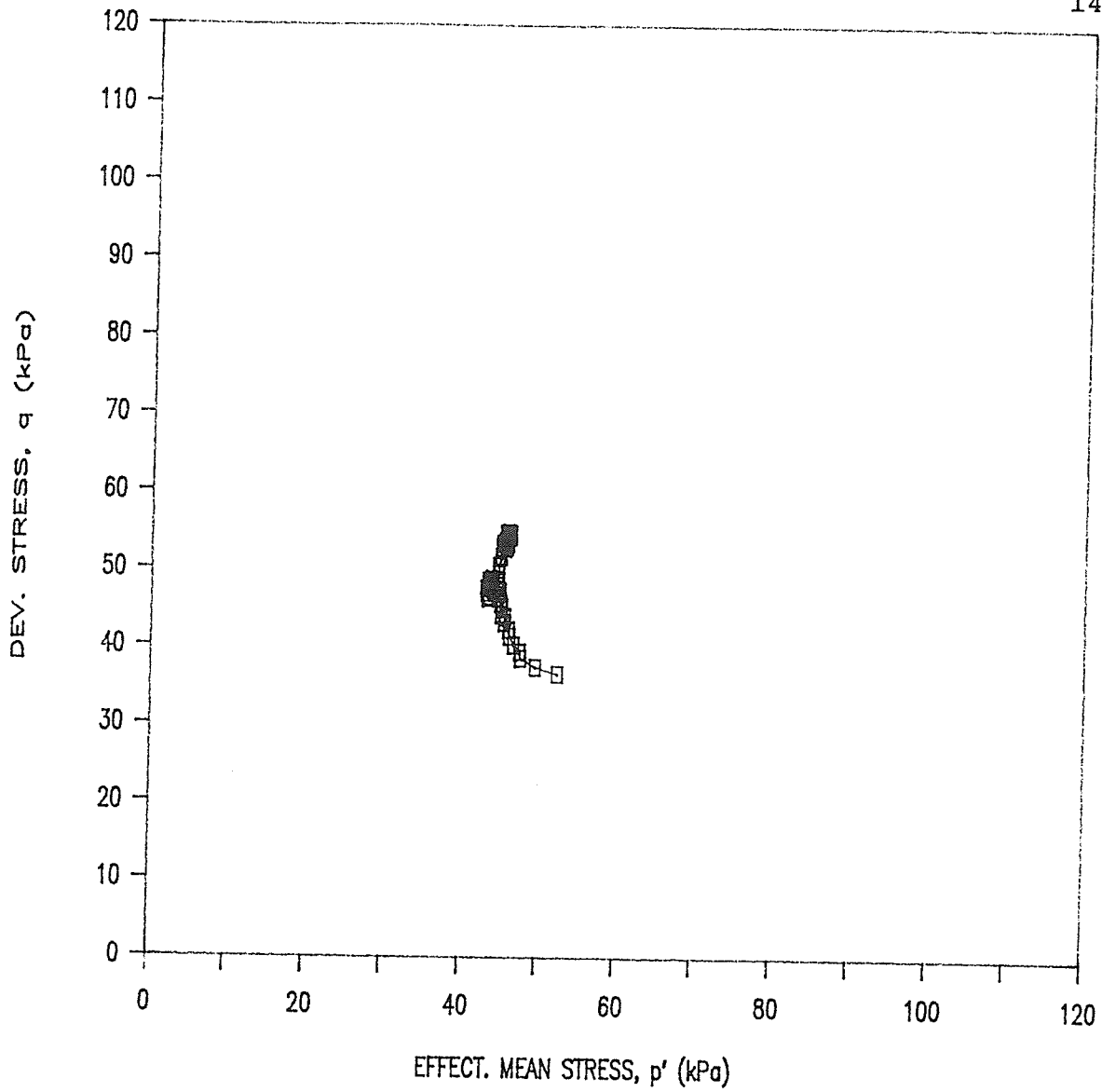


FIGURE 5.28 EFFECTIVE STRESS PATH DURING UNDRAINED SHEAR IN  $p'$  vs.  $q$  SPACE, SAMPLE T779

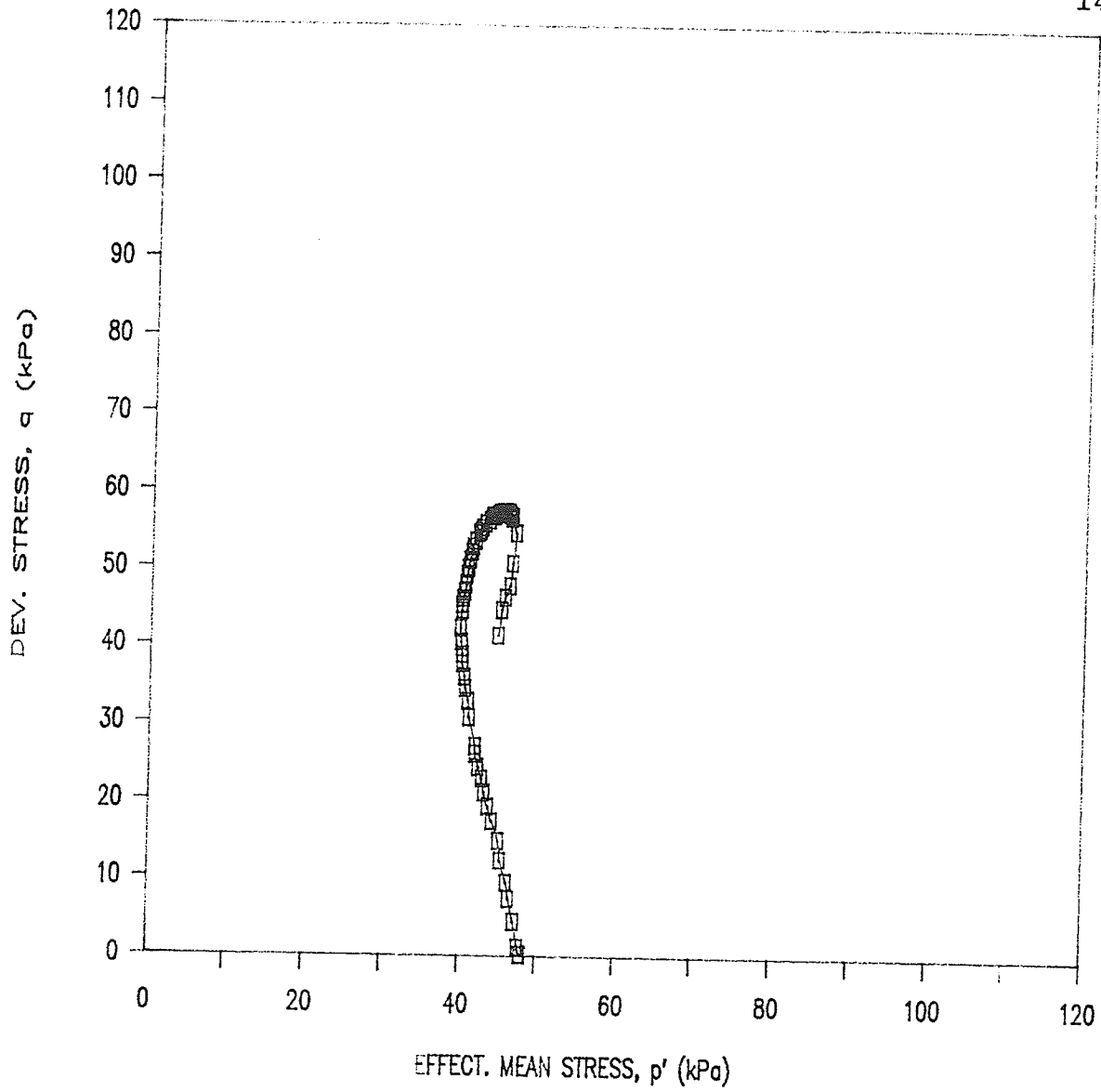


FIGURE 5.29 EFFECTIVE STRESS PATH DURING UNDRAINED SHEAR IN  $p'$  vs.  $q$  SPACE, SAMPLE T789

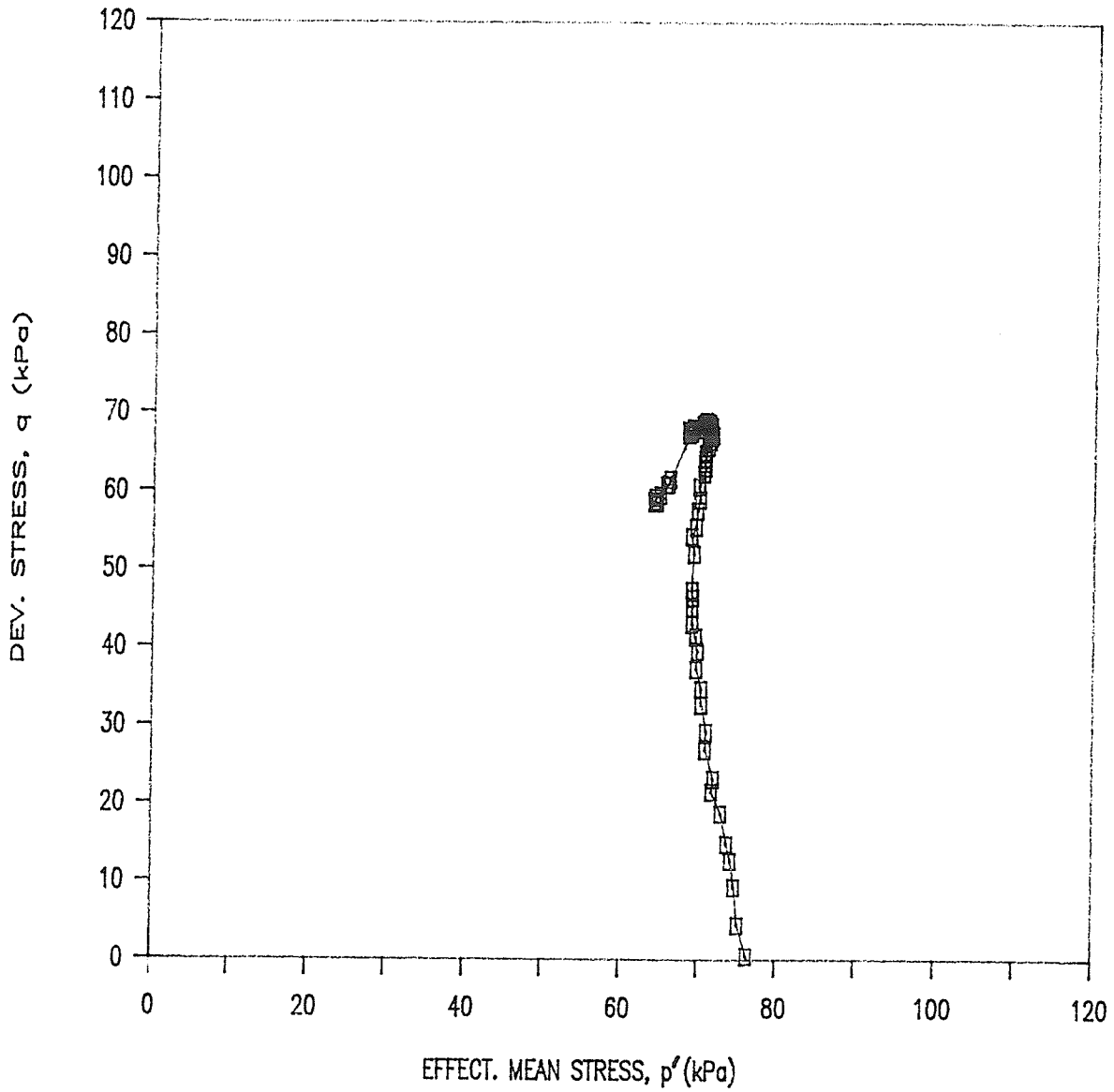


FIGURE 5.30 EFFECTIVE STRESS PATH DURING UNDRAINED SHEAR IN  $p'$  vs.  $q$  SPACE, SAMPLE T781

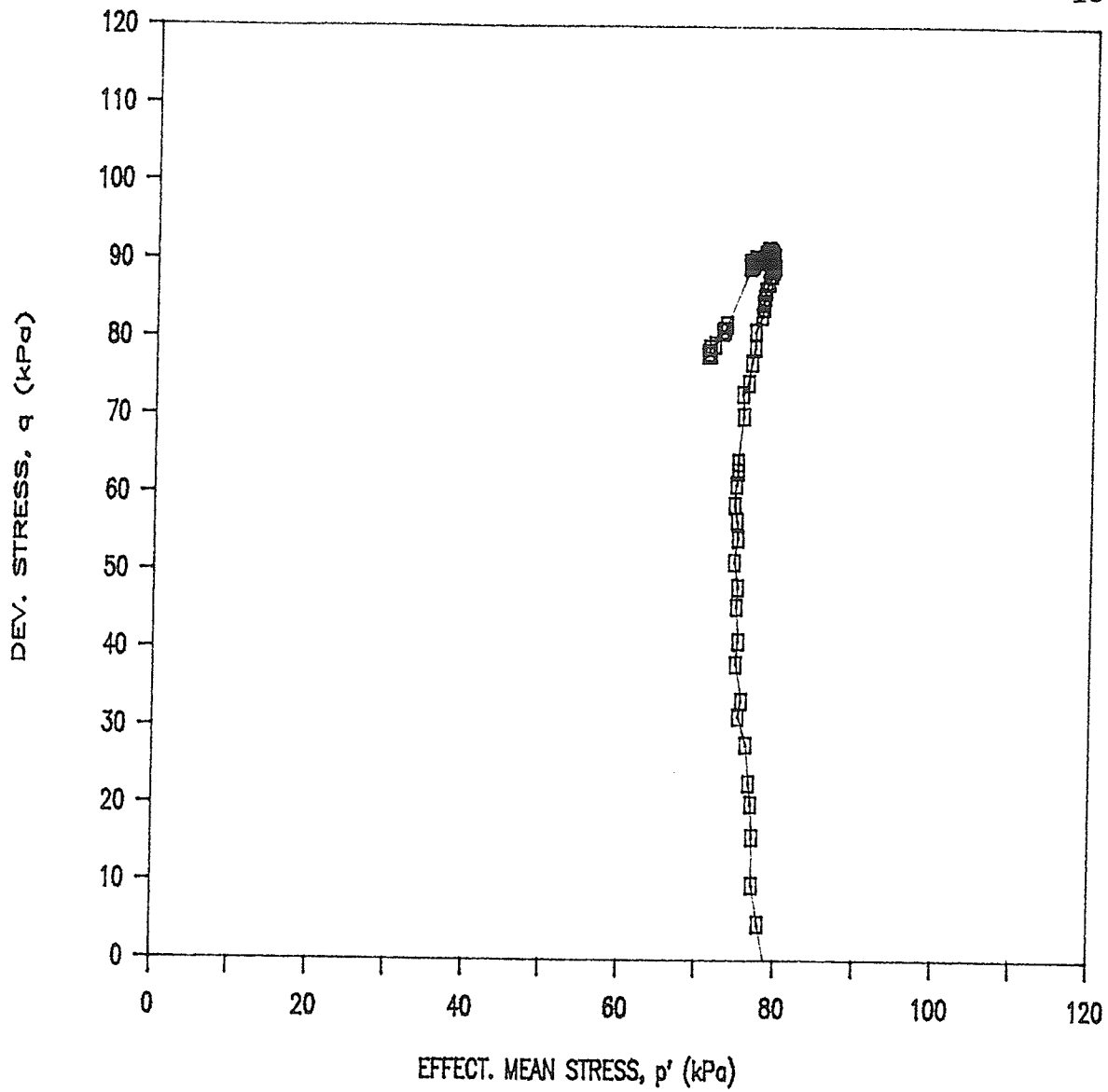


FIGURE 5.31 EFFECTIVE STRESS PATH DURING UNDRAINED SHEAR IN p' vs. q SPACE, SAMPLE T781\*

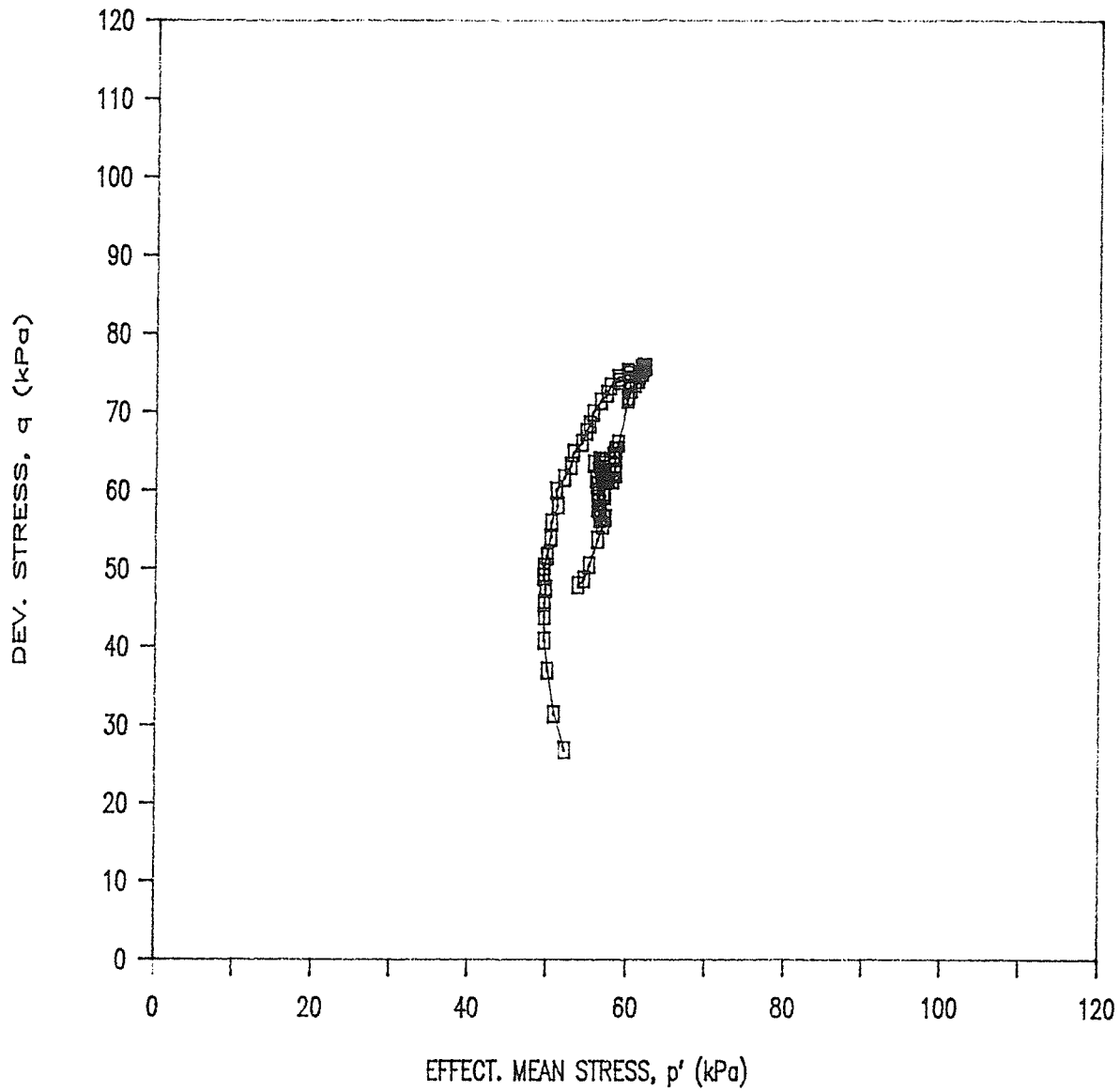


FIGURE 5.32 EFFECTIVE STRESS PATH DURING UNDRAINED SHEAR IN  $p'$  vs.  $q$  SPACE, SAMPLE T782

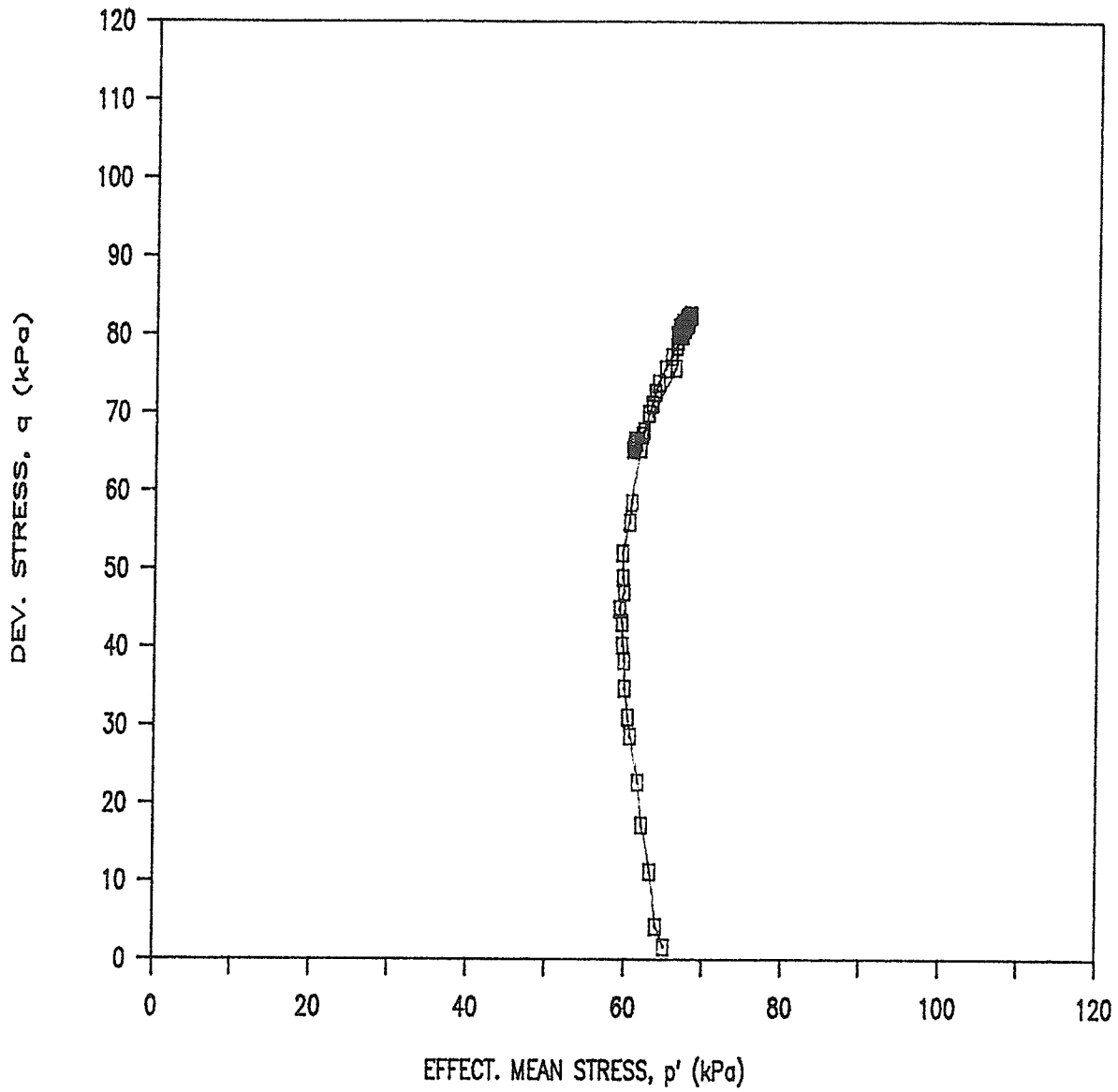


FIGURE 5.33 EFFECTIVE STRESS PATH DURING UNDRAINED SHEAR IN  $p'$  vs.  $q$  SPACE, SAMPLE T784

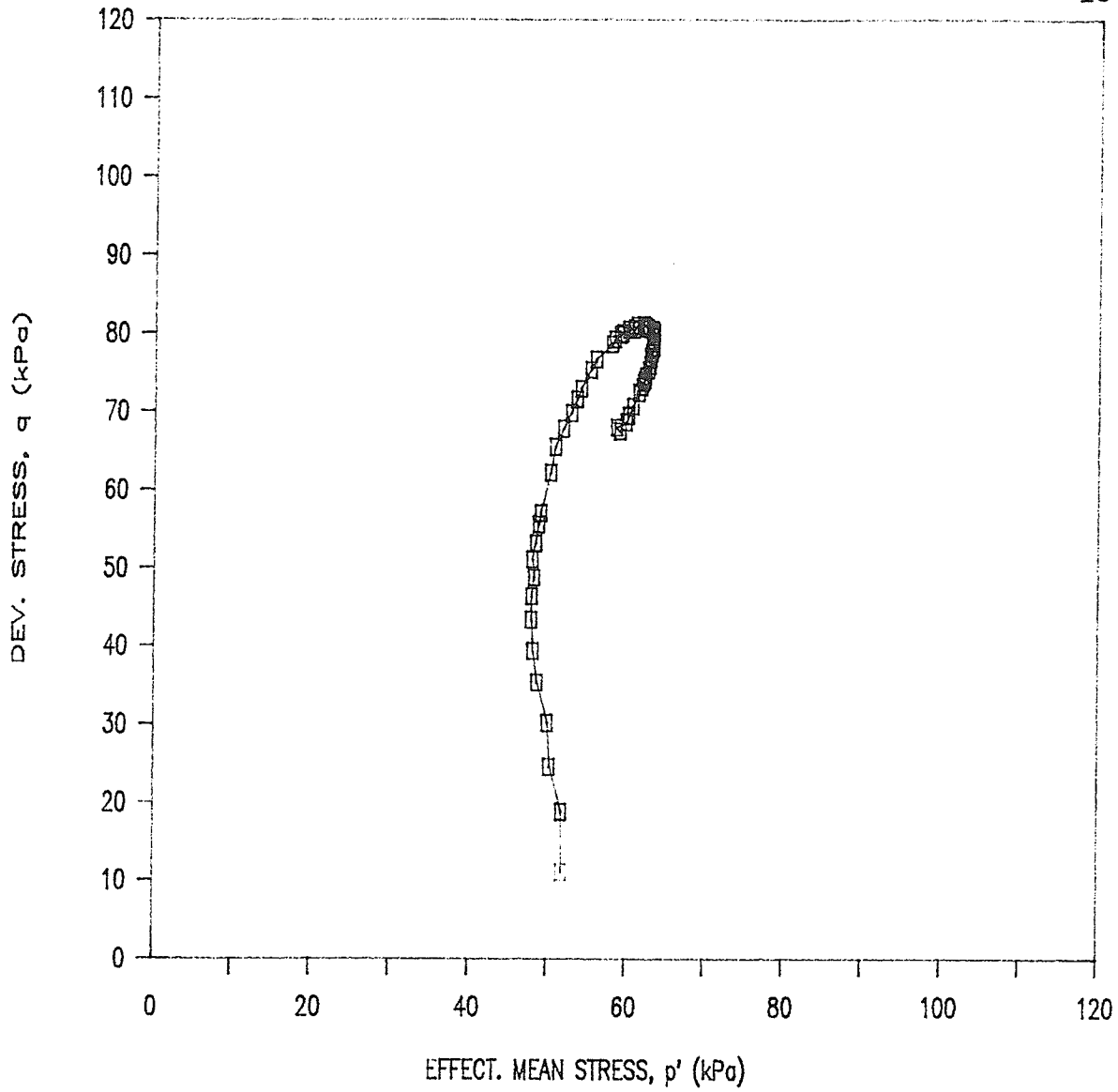


FIGURE 5.34 EFFECTIVE STRESS PATH DURING UNDRAINED SHEAR IN  $p'$  vs.  $q$  SPACE, SAMPLE T788

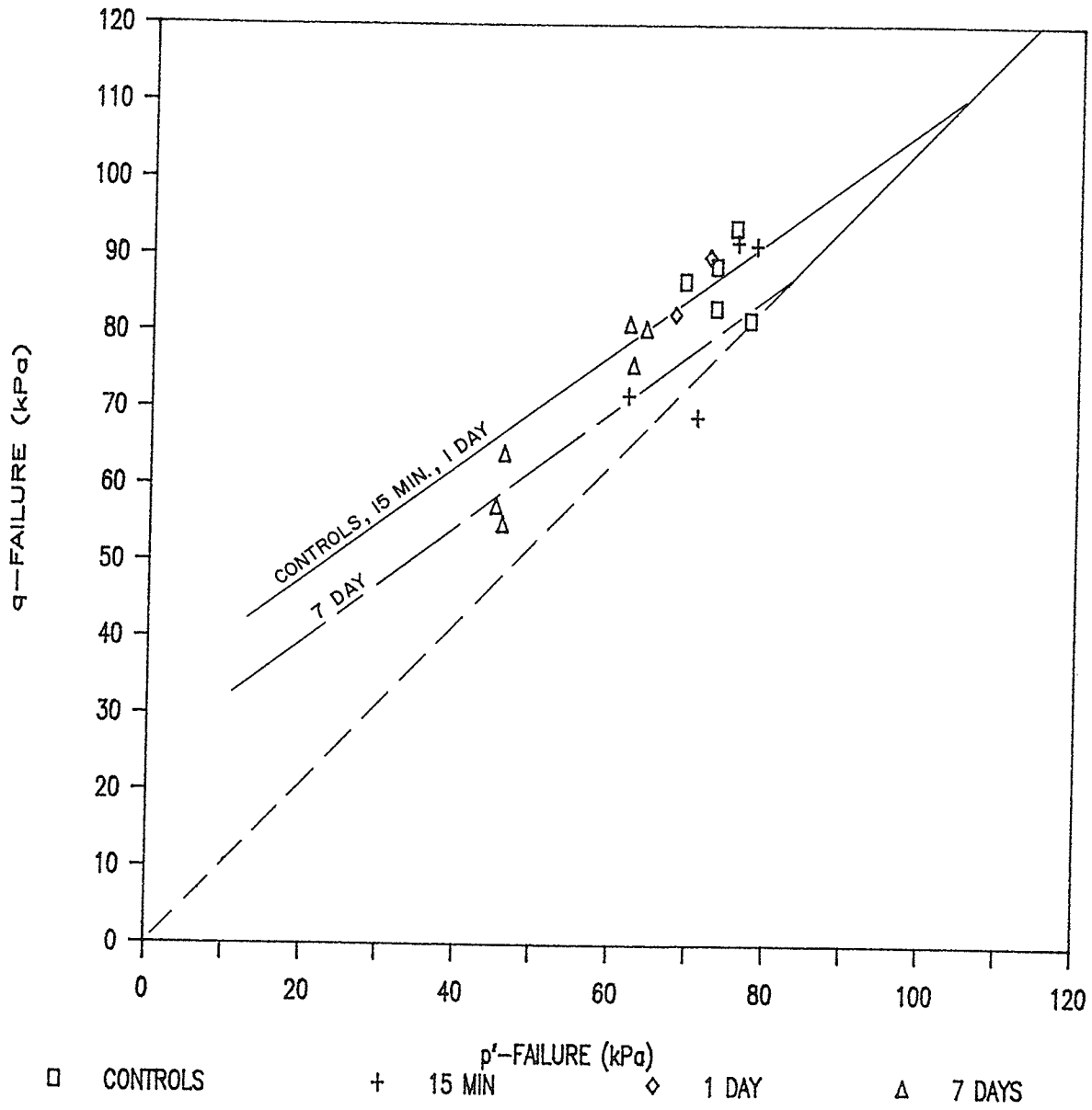


FIGURE 5.35 FAILURE ENVELOPE IN  $p'$  vs.  $q$  SPACE FOR  $\sigma_{vc}' = 160$  kPa

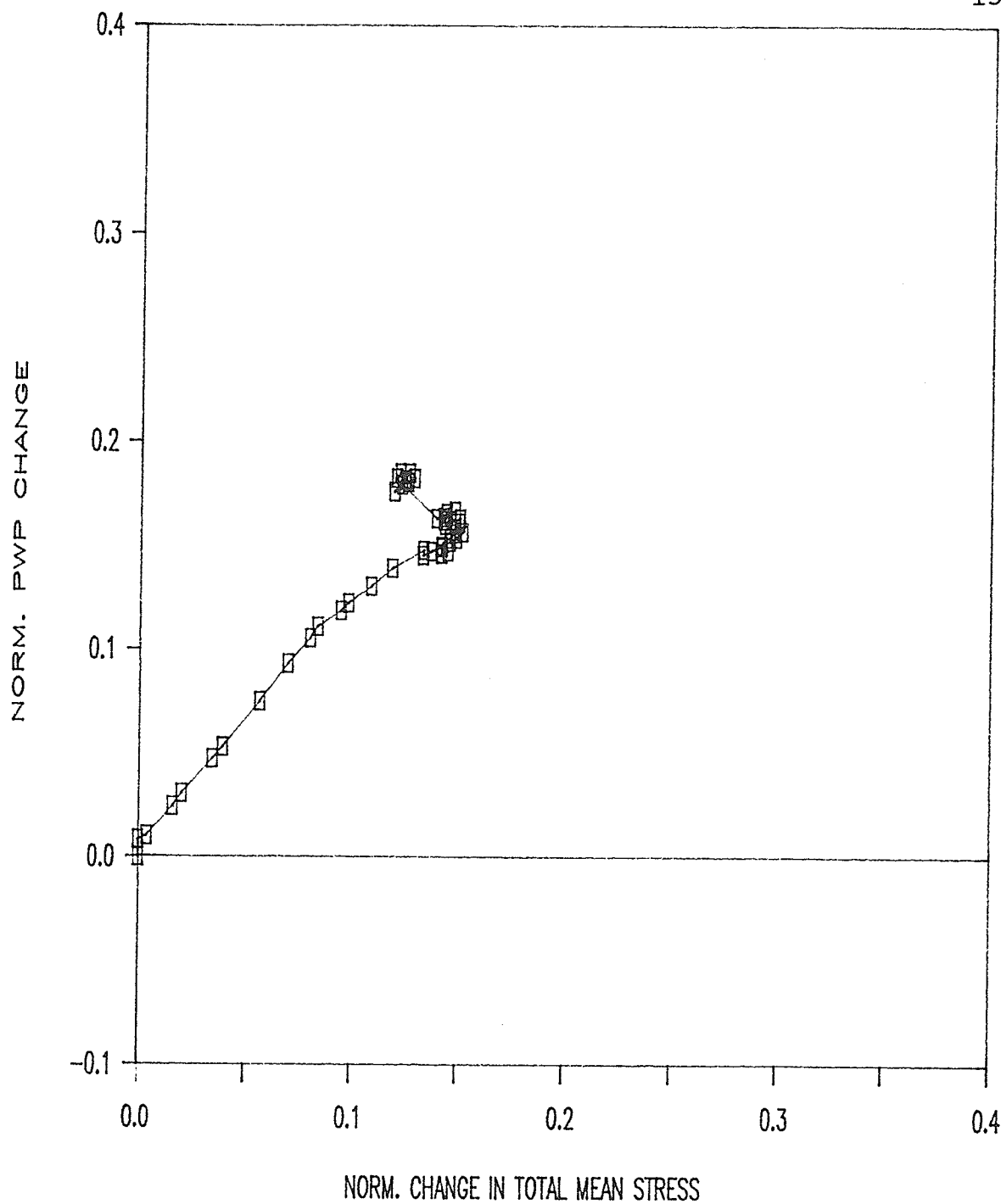


FIGURE 5.36 NORMALIZED POREWATER PRESSURE BEHAVIOUR DURING UNDRAINED SHEAR, IN  $\Delta u/\sigma_{vc}'$  vs.  $\Delta P/\sigma_{vc}'$ , SAMPLE T771 (CONTROL)

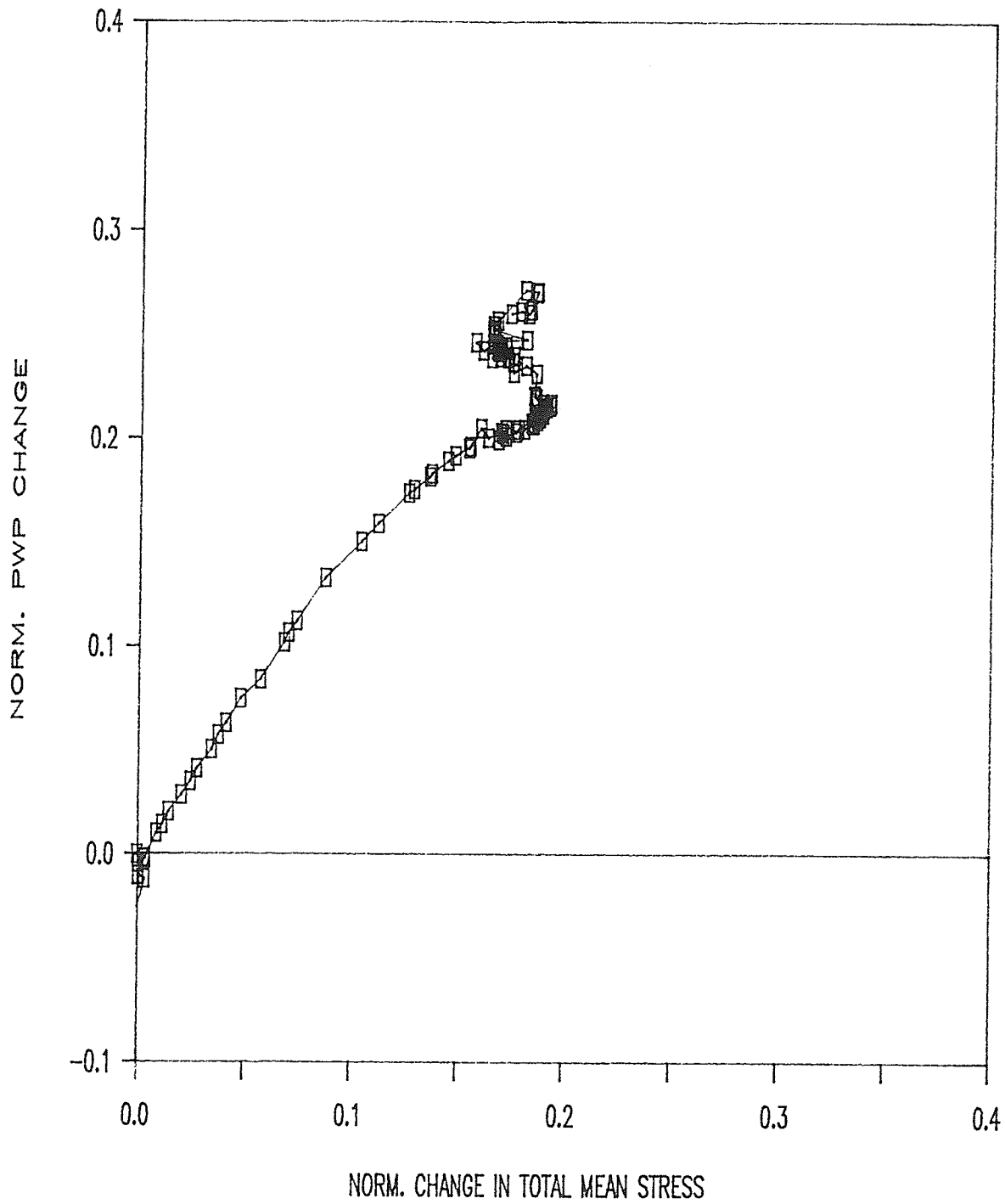


FIGURE 5.37 NORMALIZED POREWATER PRESSURE BEHAVIOUR DURING UNDRAINED SHEAR, IN  $\Delta u/\sigma_{vc}'$  vs.  $\Delta p/\sigma_{vc}'$ , SAMPLE T772 (CONTROL)

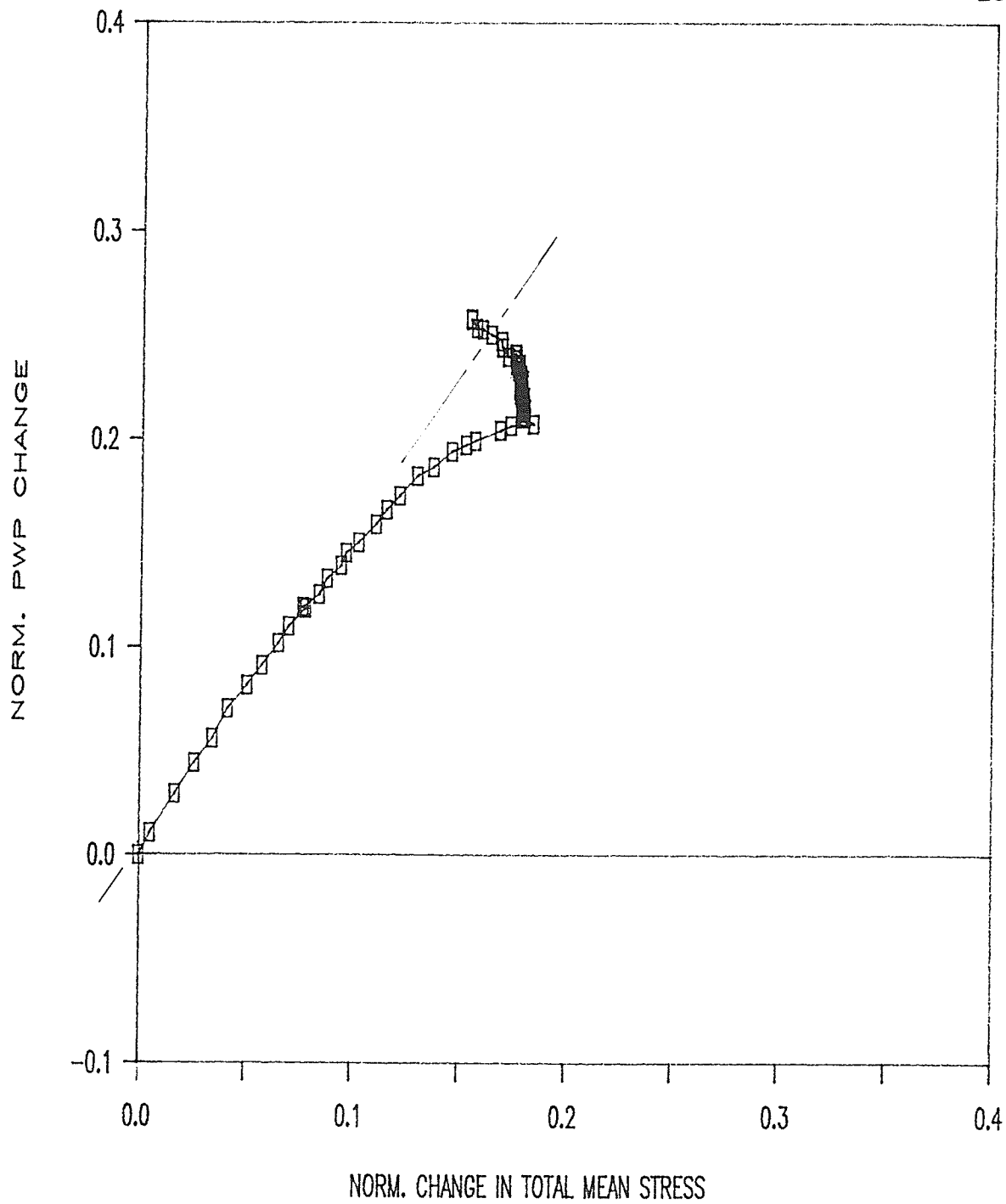


FIGURE 5.38 NORMALIZED POREWATER PRESSURE BEHAVIOUR DURING UNDRAINED SHEAR, IN  $\Delta u / \sigma_{vc}'$  vs.  $\Delta p / \sigma_{vc}'$ , SAMPLE T773 (CONTROL)

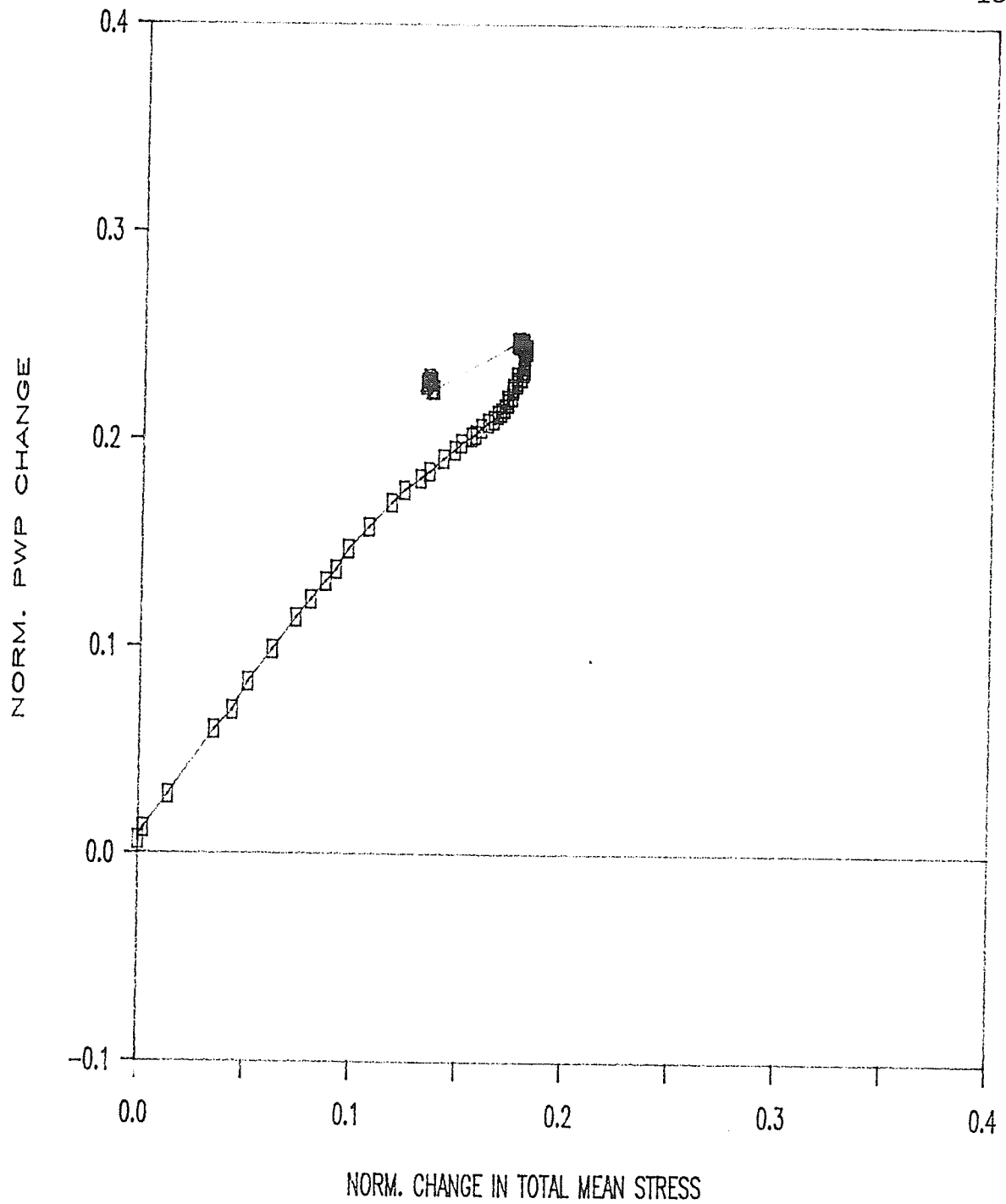


FIGURE 5.39 NORMALIZED POREWATER PRESSURE BEHAVIOUR DURING UNDRAINED SHEAR, IN  $\Delta u/\sigma_{vc}'$  vs.  $\Delta p/\sigma_{vc}'$ , SAMPLE T785 (CONTROL)

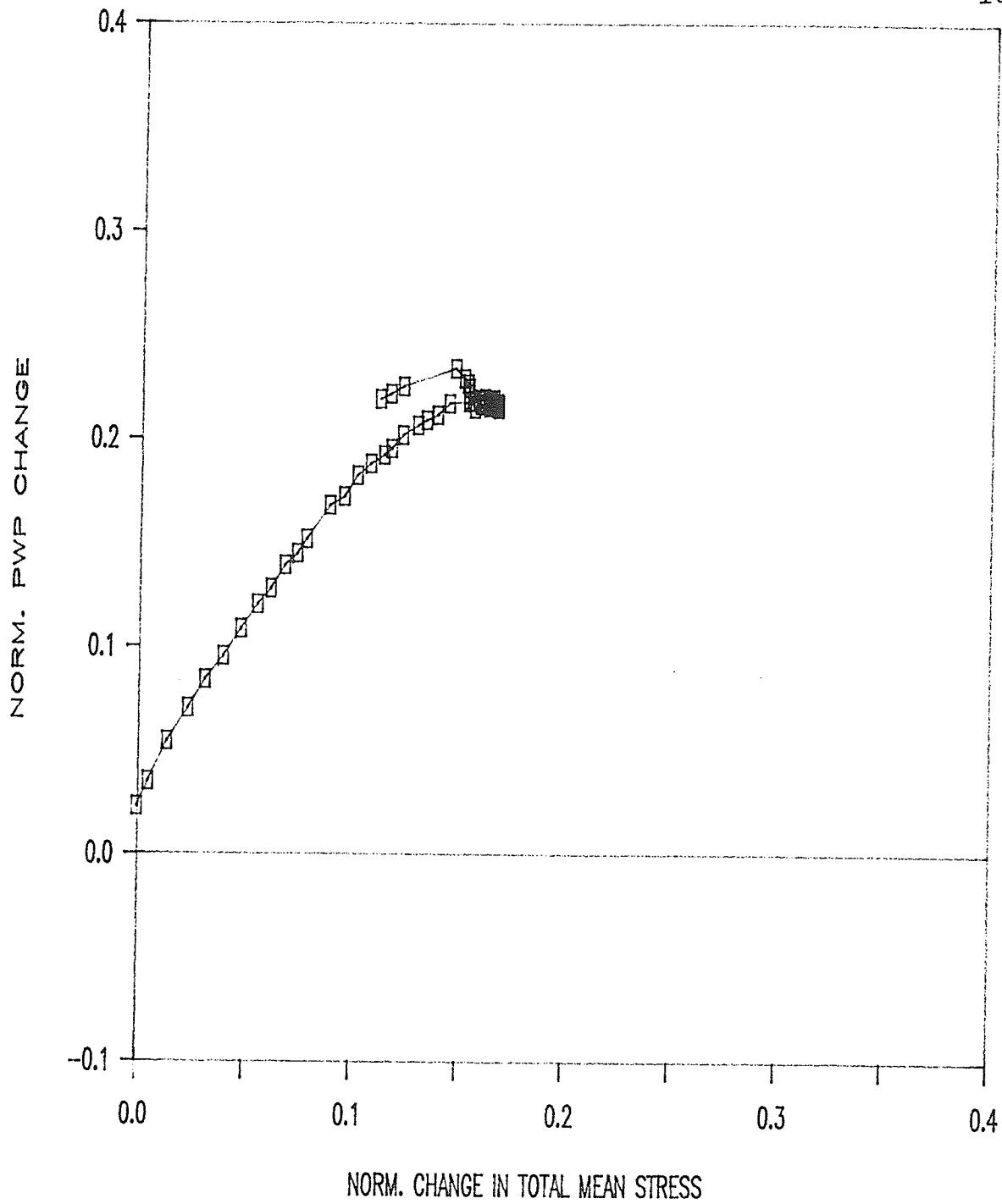


FIGURE 5.40 NORMALIZED POREWATER PRESSURE BEHAVIOUR DURING UNDRAINED SHEAR, IN  $\Delta U/\sigma_{vc}'$  vs.  $\Delta P/\sigma_{vc}'$ , SAMPLE T787 (CONTROL)

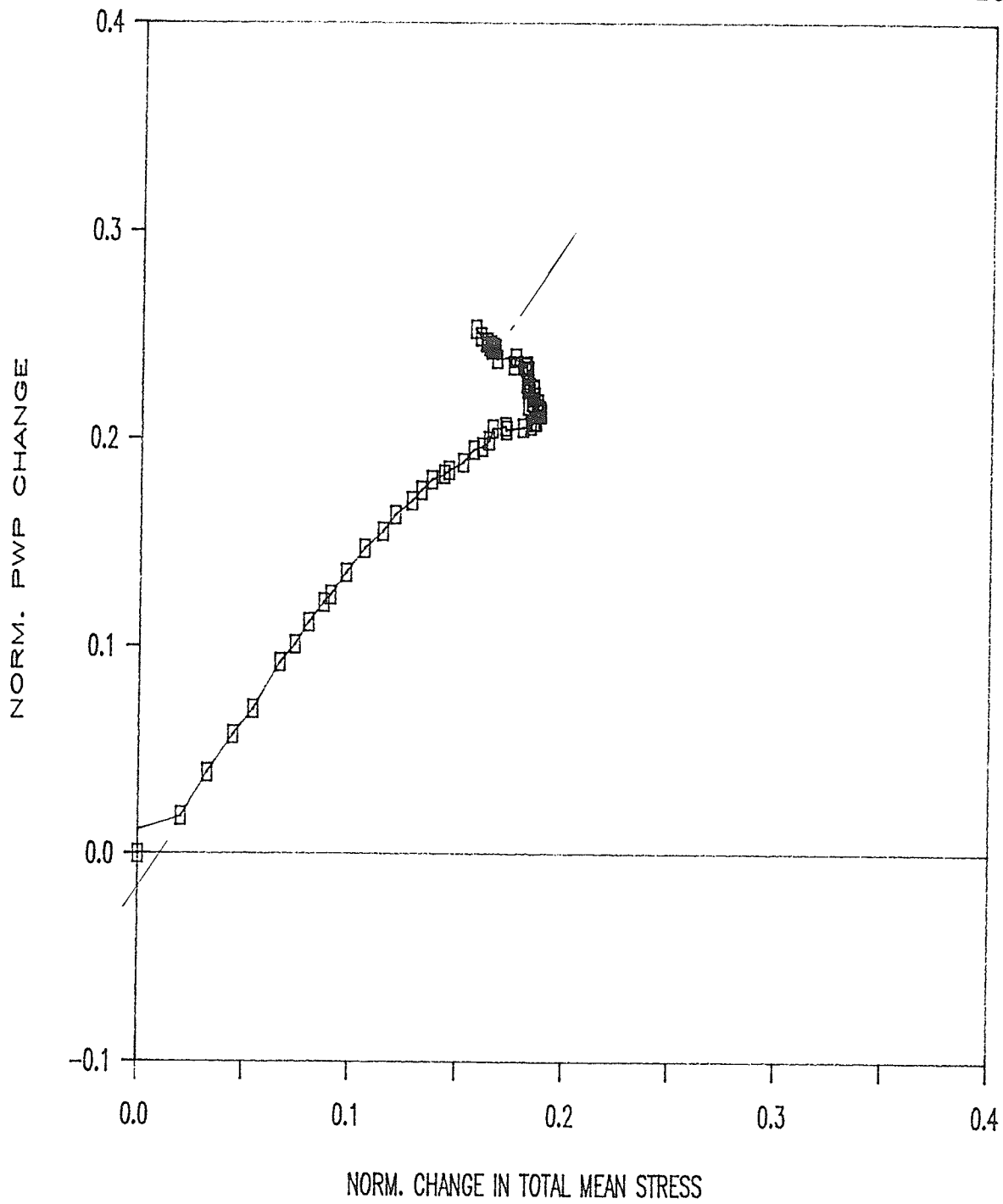


FIGURE 5.41 NORMALIZED POREWATER PRESSURE BEHAVIOUR DURING UNDRAINED SHEAR, IN  $\Delta u/\sigma'_v$  vs.  $\Delta P/\sigma'_v$ , SAMPLE T777

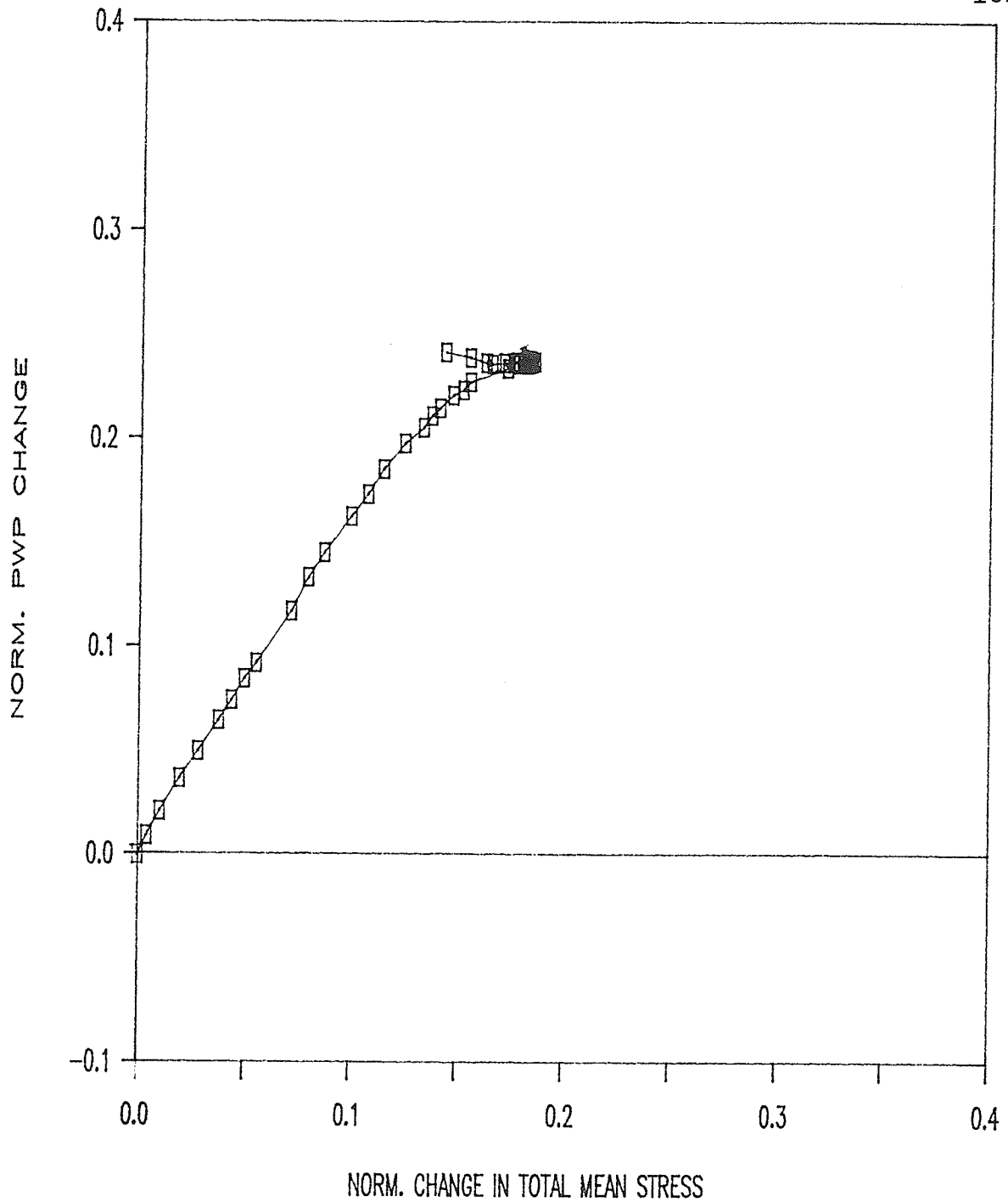


FIGURE 5.42 NORMALIZED POREWATER PRESSURE BEHAVIOUR DURING UNDRAINED SHEAR, IN  $\Delta u/\sigma_v'c$  vs.  $\Delta P/\sigma_v'c$ , SAMPLE T774

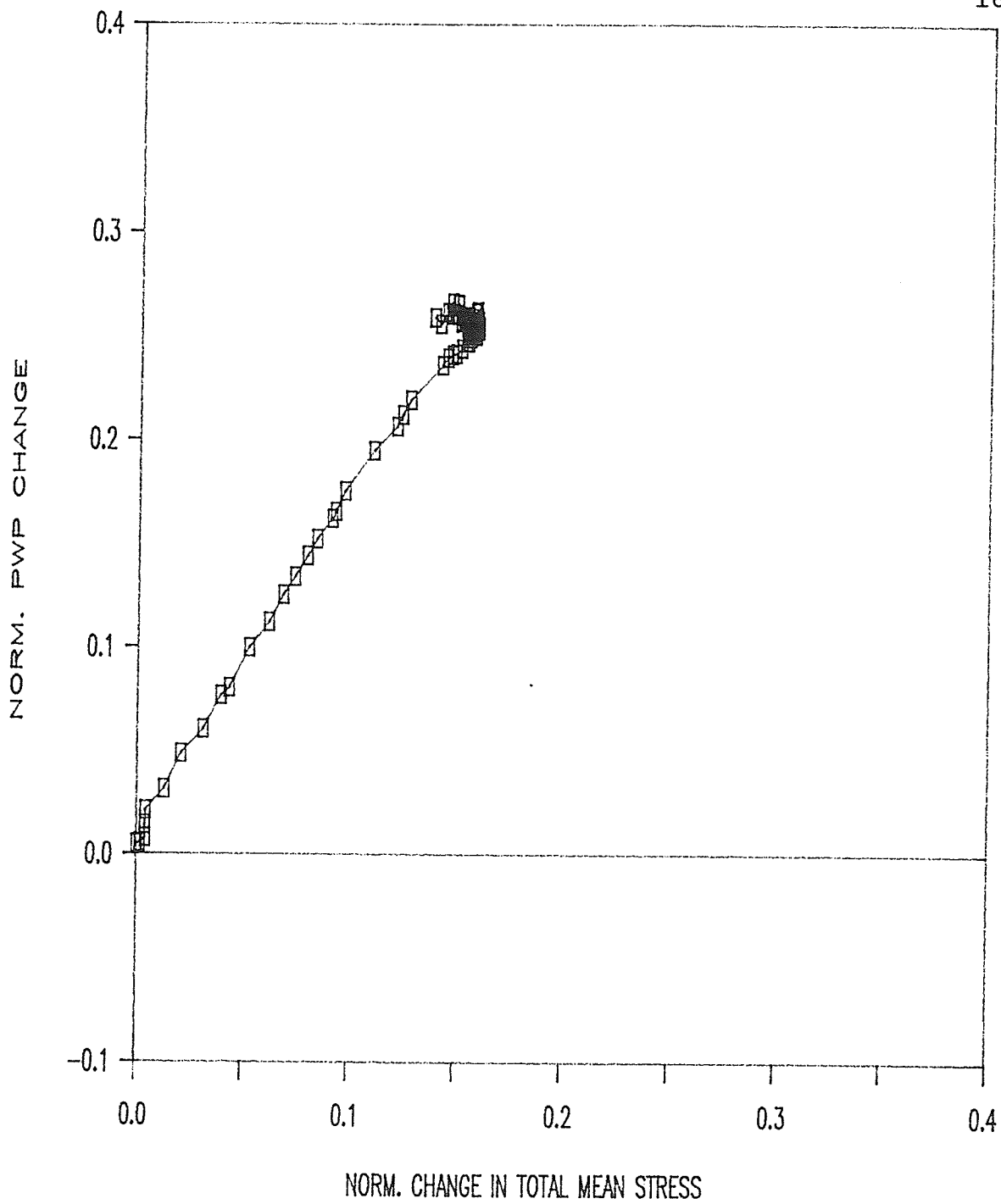


FIGURE 5.43 NORMALIZED POREWATER PRESSURE BEHAVIOUR DURING UNDRAINED SHEAR, IN  $\Delta u/\sigma_{vc}'$  vs.  $\Delta p/\sigma_{vc}'$ , SAMPLE T775

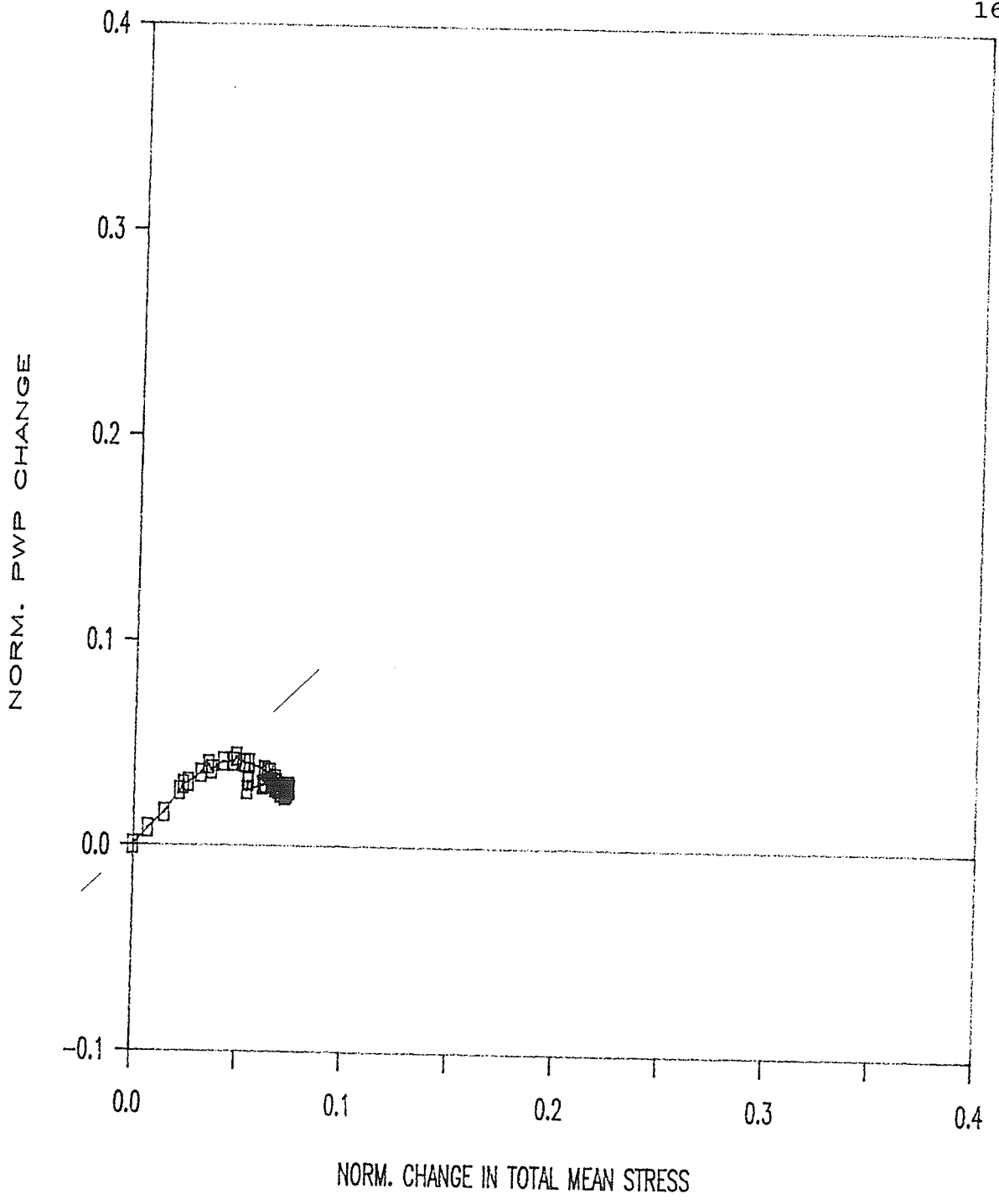


FIGURE 5.44 NORMALIZED POREWATER PRESSURE BEHAVIOUR DURING UNDRAINED SHEAR, IN  $\Delta u/\sigma'_v$  vs.  $\Delta p/\sigma'_v$ , SAMPLE T778

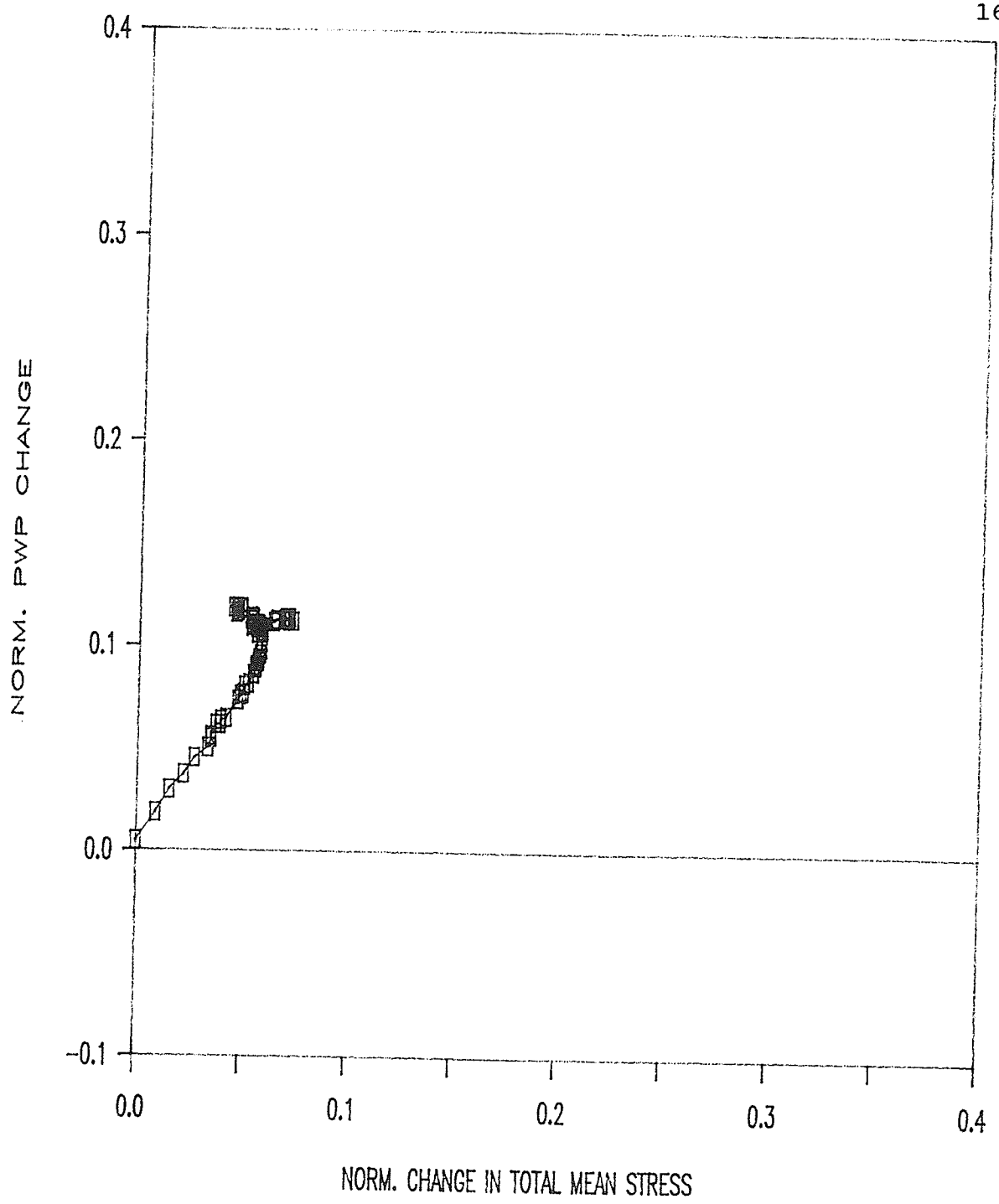


FIGURE 5.45 NORMALIZED POREWATER PRESSURE BEHAVIOUR DURING UNDRAINED SHEAR, IN  $\Delta u/\sigma_v'$  vs.  $\Delta p/\sigma_v'$ , SAMPLE T776

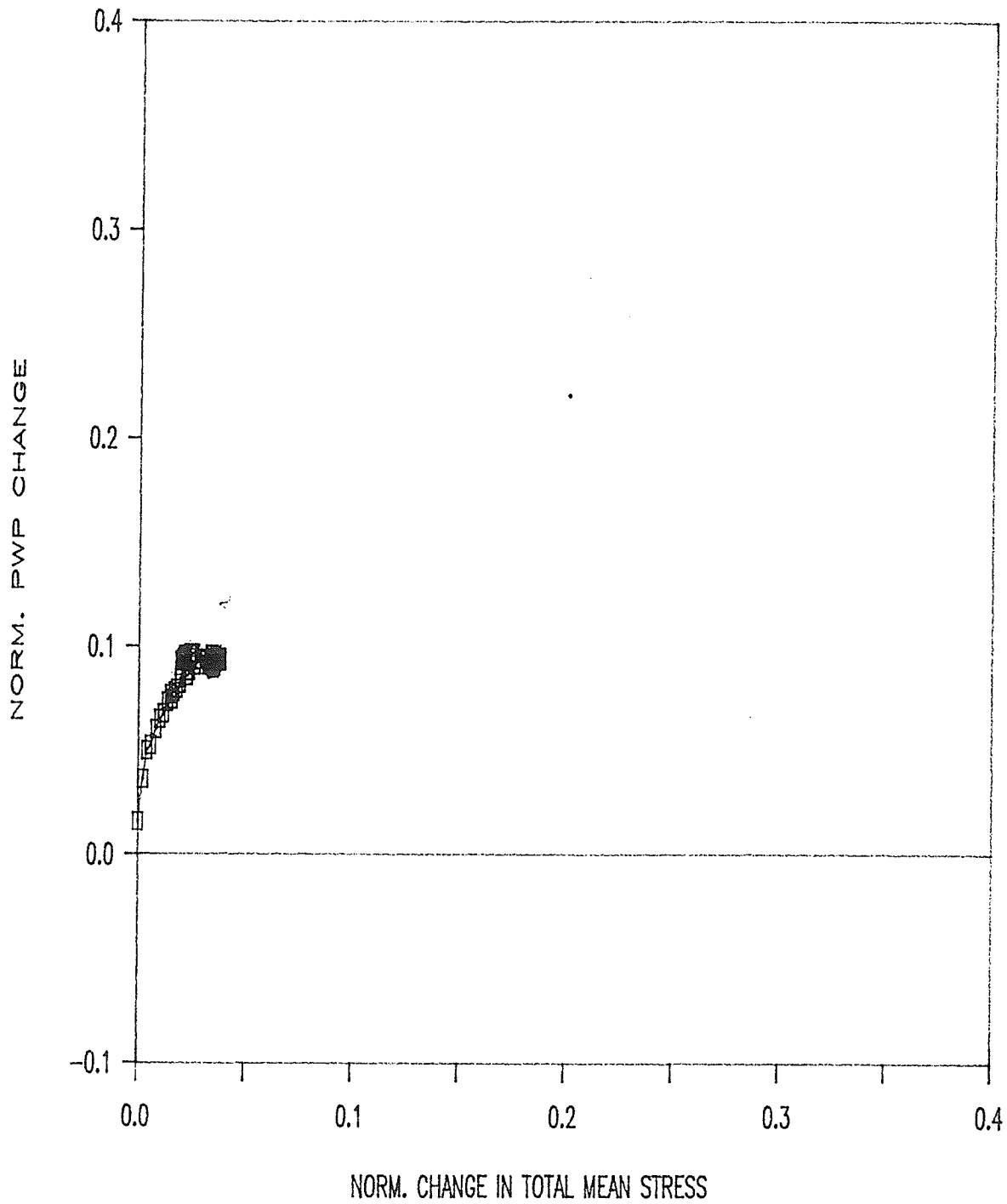


FIGURE 5.46 NORMALIZED POREWATER PRESSURE BEHAVIOUR DURING UNDRAINED SHEAR, IN  $\Delta u/\sigma_{vc}'$  vs.  $\Delta p/\sigma_{vc}'$ , SAMPLE T779

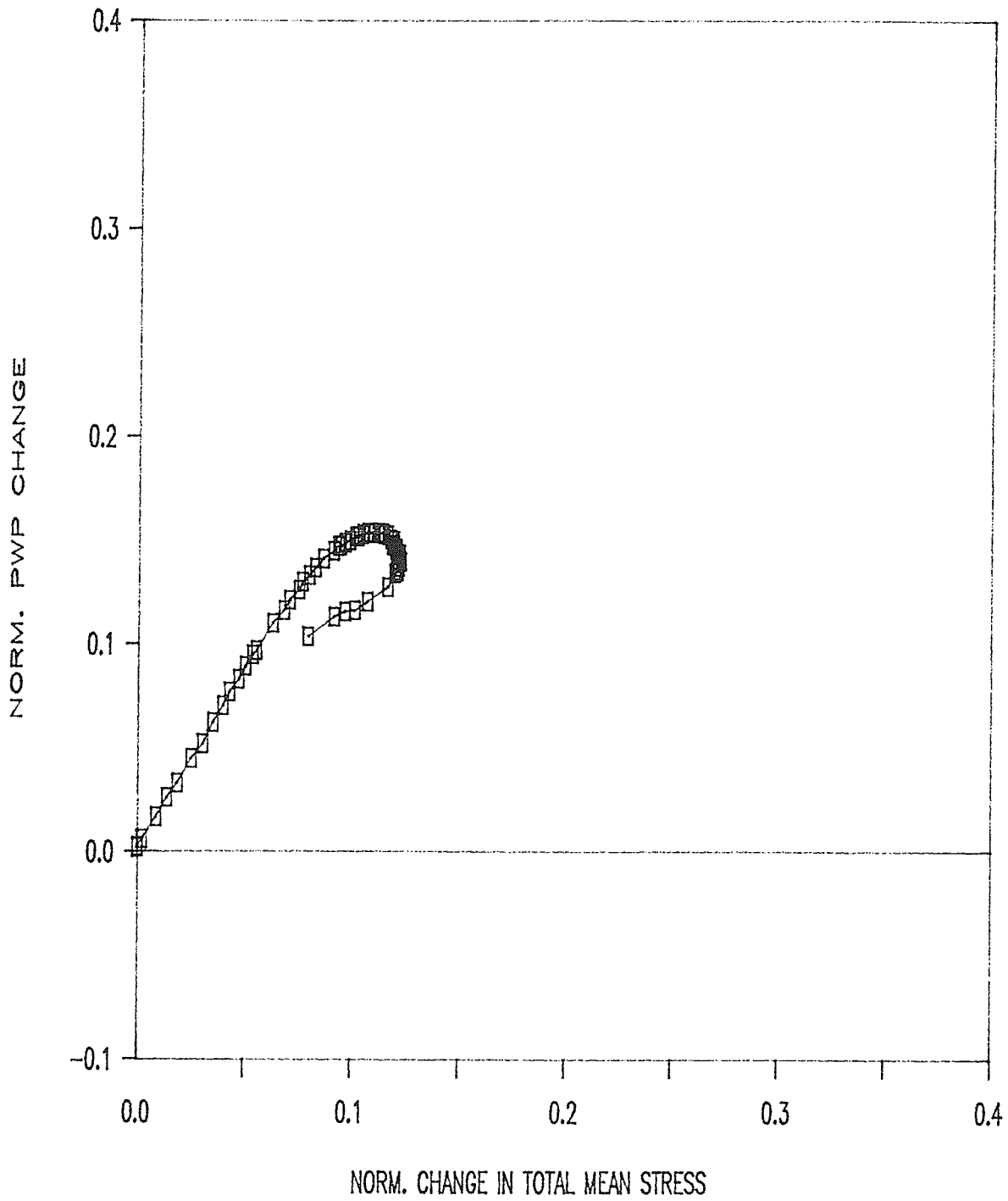


FIGURE 5.47 NORMALIZED POREWATER PRESSURE BEHAVIOUR DURING UNDRAINED SHEAR, IN  $\Delta u/\sigma'_c$  vs.  $\Delta p/\sigma'_c$ , SAMPLE T789

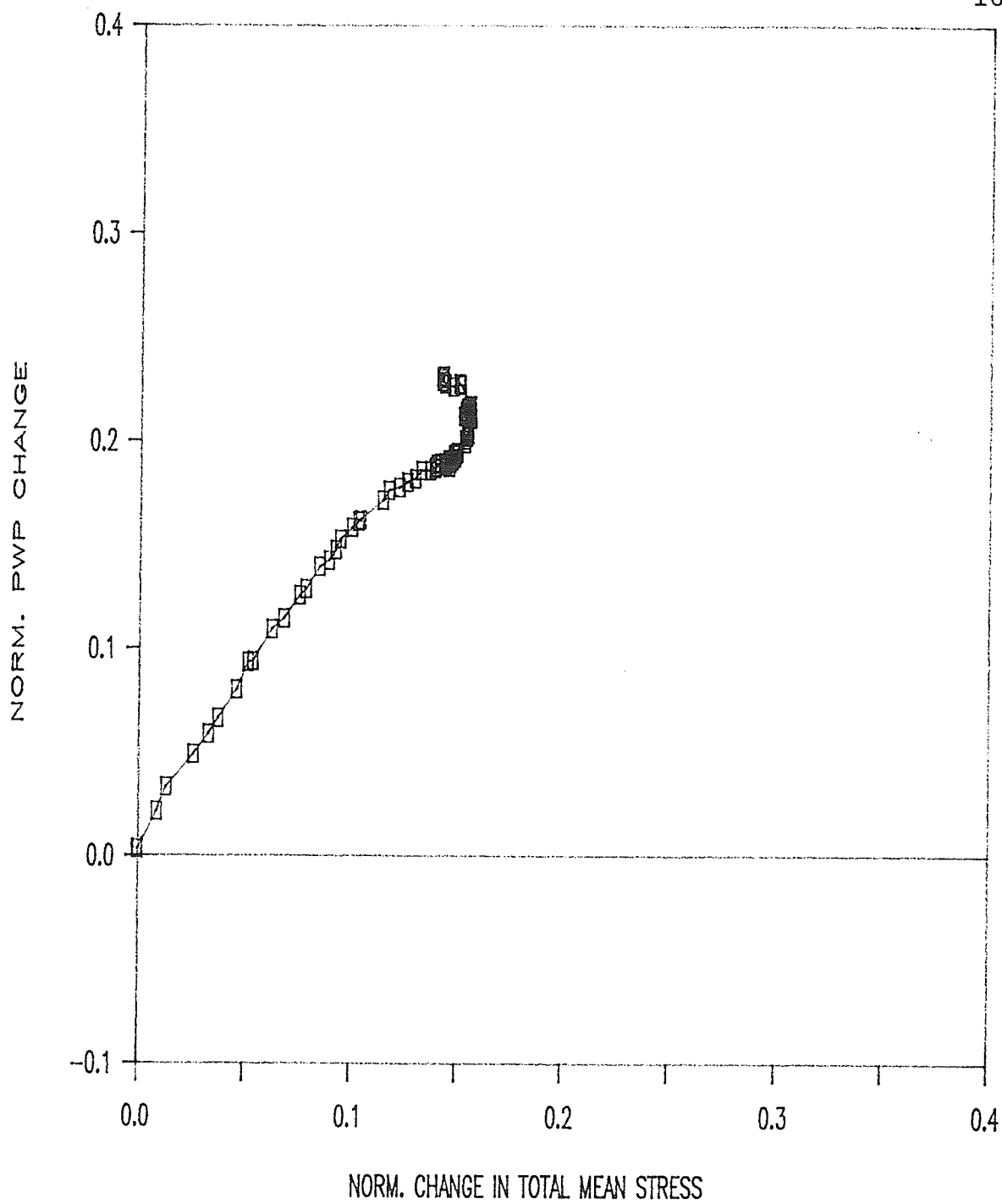


FIGURE 5.48 NORMALIZED POREWATER PRESSURE BEHAVIOUR DURING UNDRAINED SHEAR, IN  $\Delta u/\sigma'_{vc}$  vs.  $\Delta p/\sigma'_{vc}$ , SAMPLE T781

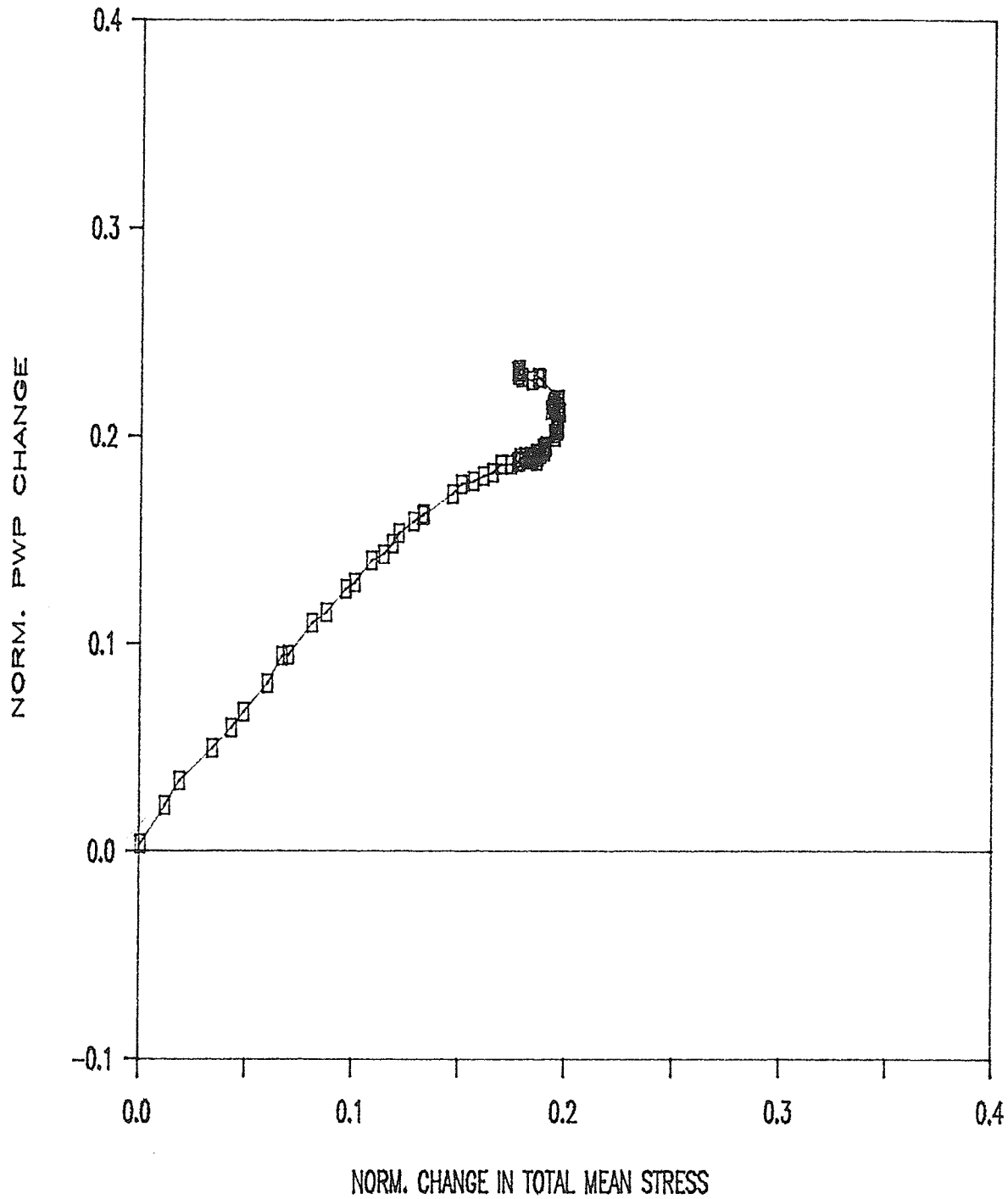


FIGURE 5.49 NORMALIZED POREWATER PRESSURE BEHAVIOUR DURING UNDRAINED SHEAR, IN  $\Delta u/\sigma'_v$  vs.  $\Delta P/\sigma'_v$ , SAMPLE T781\*

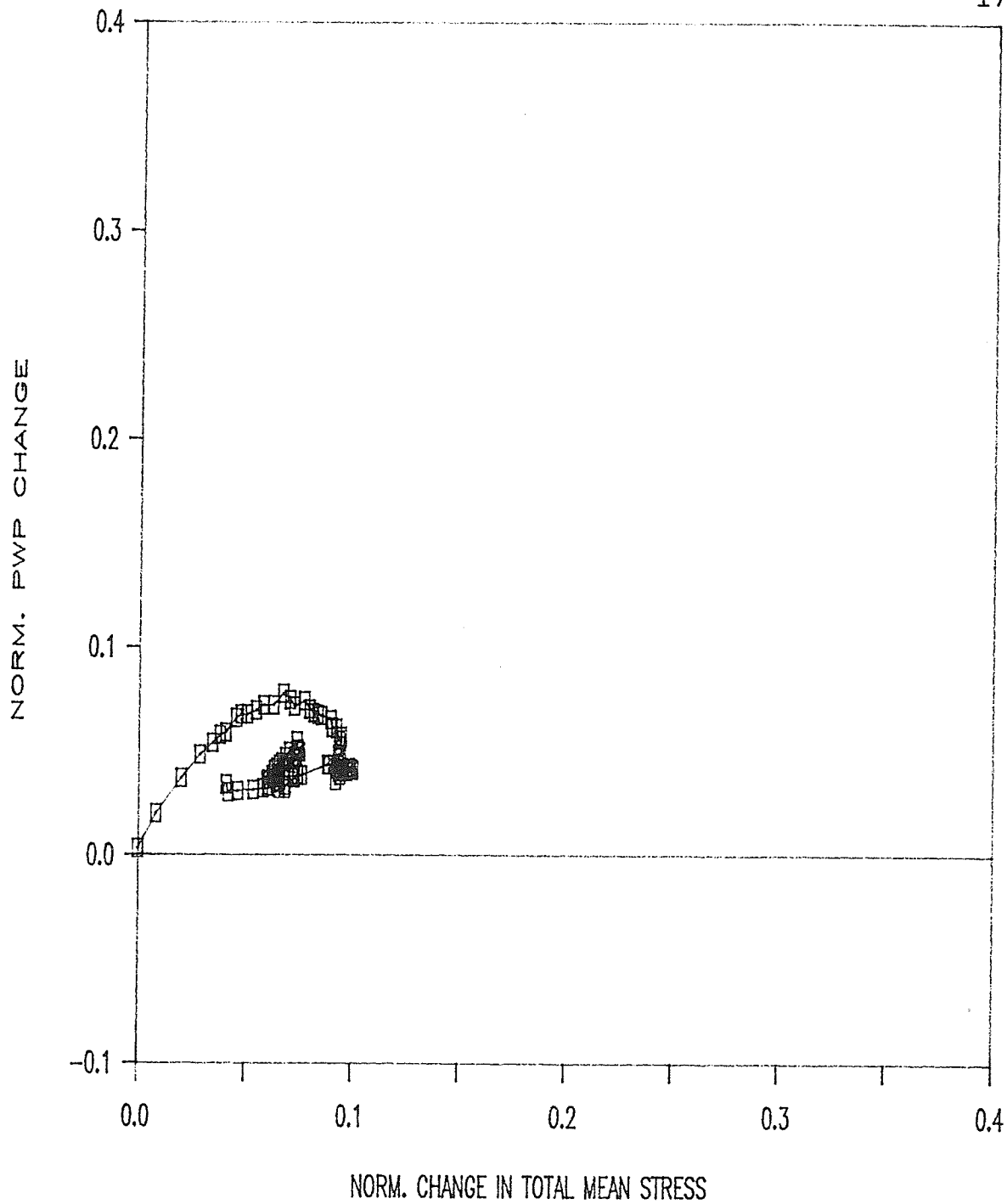


FIGURE 5.50 NORMALIZED POREWATER PRESSURE BEHAVIOUR DURING UNDRAINED SHEAR, IN  $\Delta u/\sigma_v'c$  vs.  $\Delta p/\sigma_v'c$ , SAMPLE T782

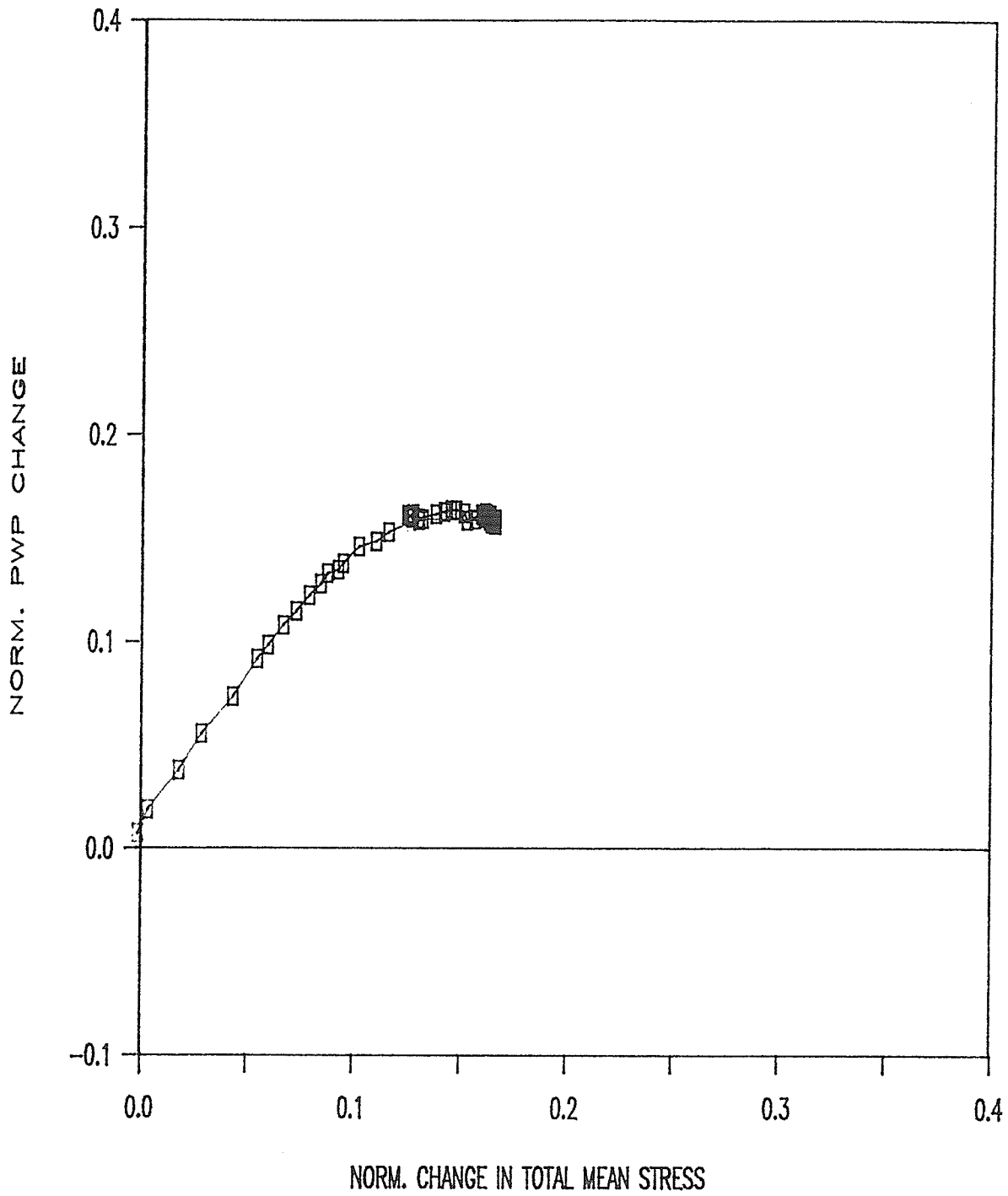


FIGURE 5.51 NORMALIZED POREWATER PRESSURE BEHAVIOUR DURING UNDRAINED SHEAR, IN  $\Delta u/\sigma_v'$  vs.  $\Delta p/\sigma_v'$ , SAMPLE T784

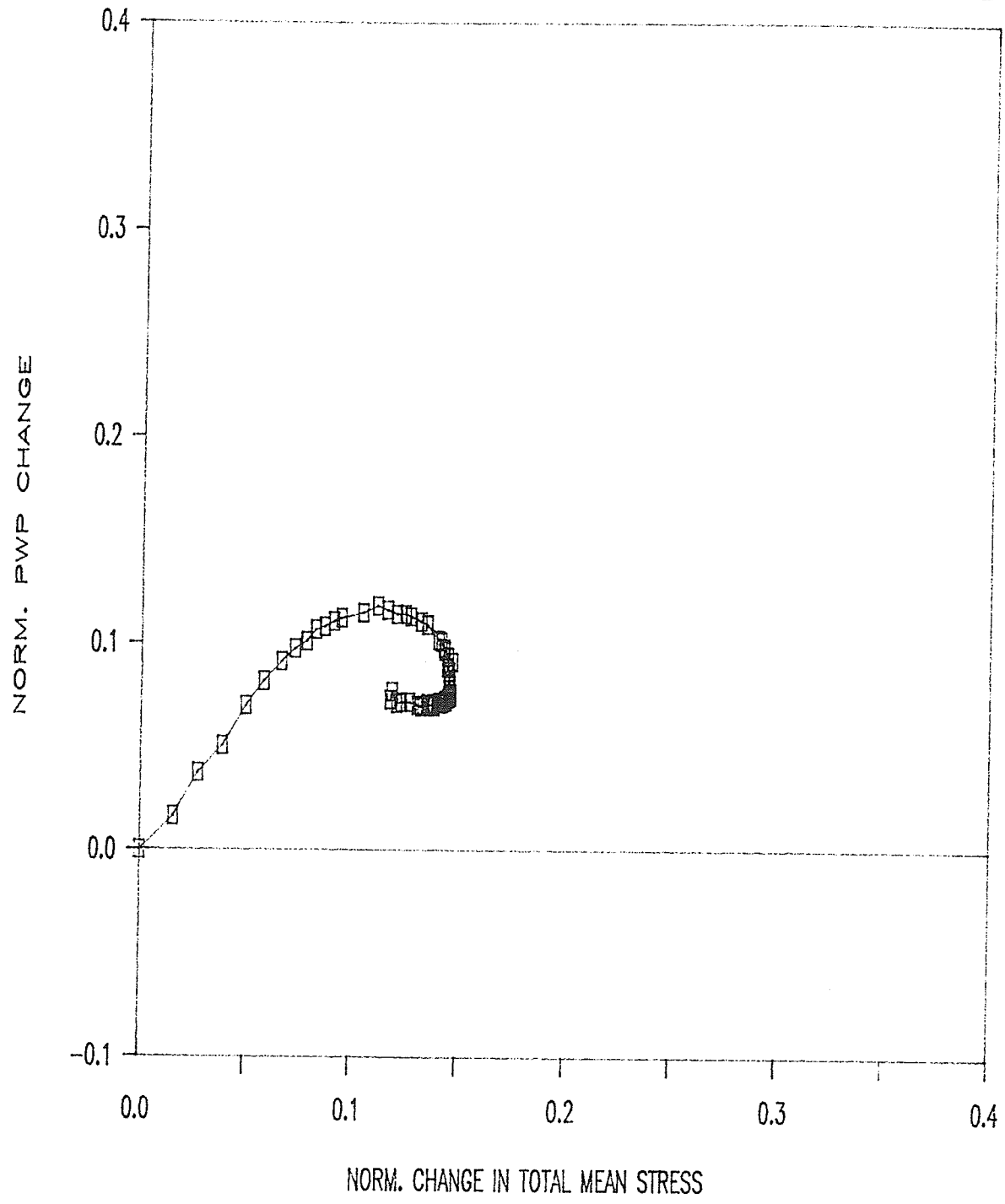


FIGURE 5.52 NORMALIZED POREWATER PRESSURE BEHAVIOUR DURING UNDRAINED SHEAR, IN  $\Delta u/\sigma_v'$  vs.  $\Delta p/\sigma_v'$ , SAMPLE T788

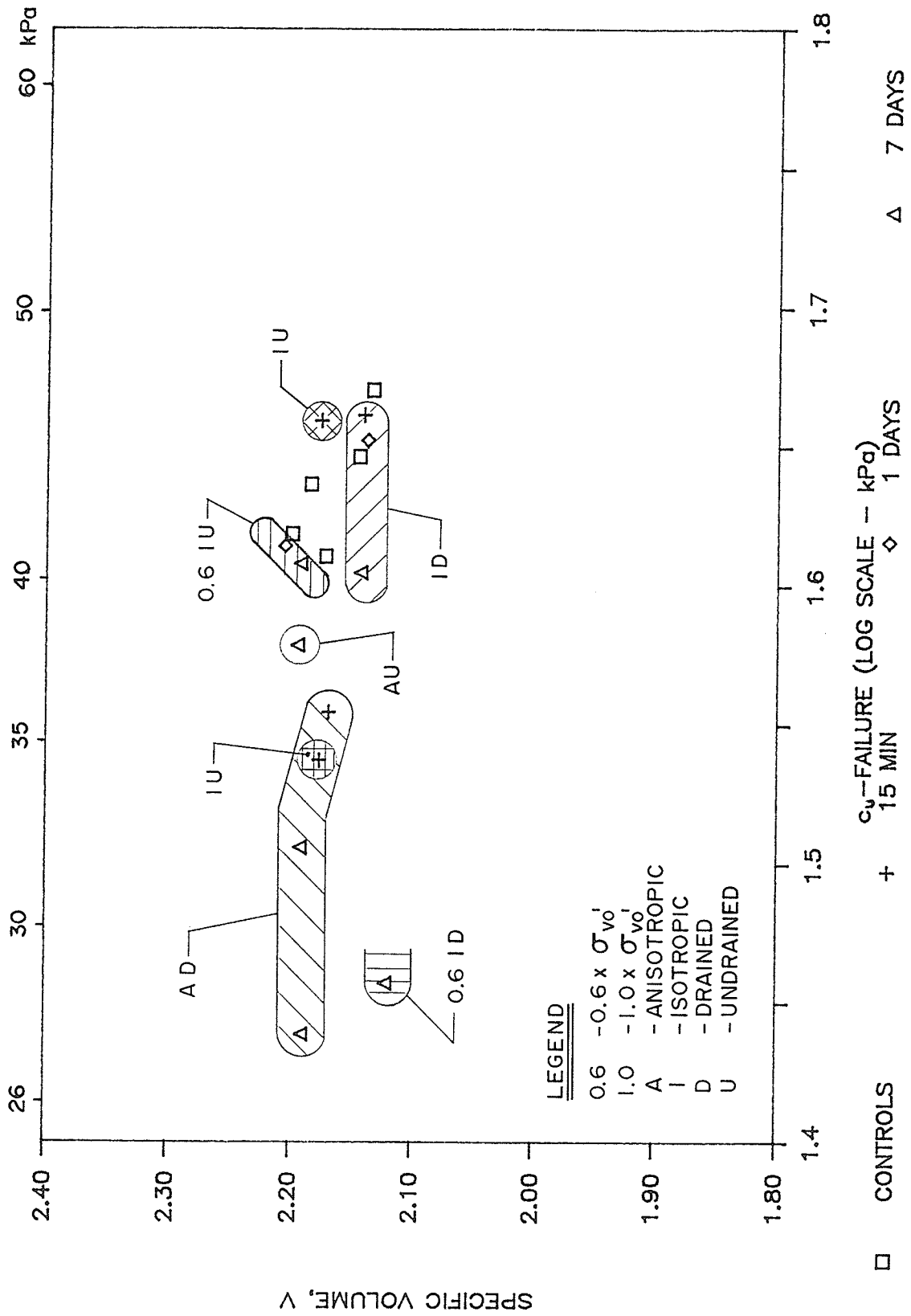


FIGURE 6.1 GRAPH OF THE UNDRAINED SHEAR STRENGTH,  $c_u$  vs. SPECIFIC VOLUME, V DURING SHEARING

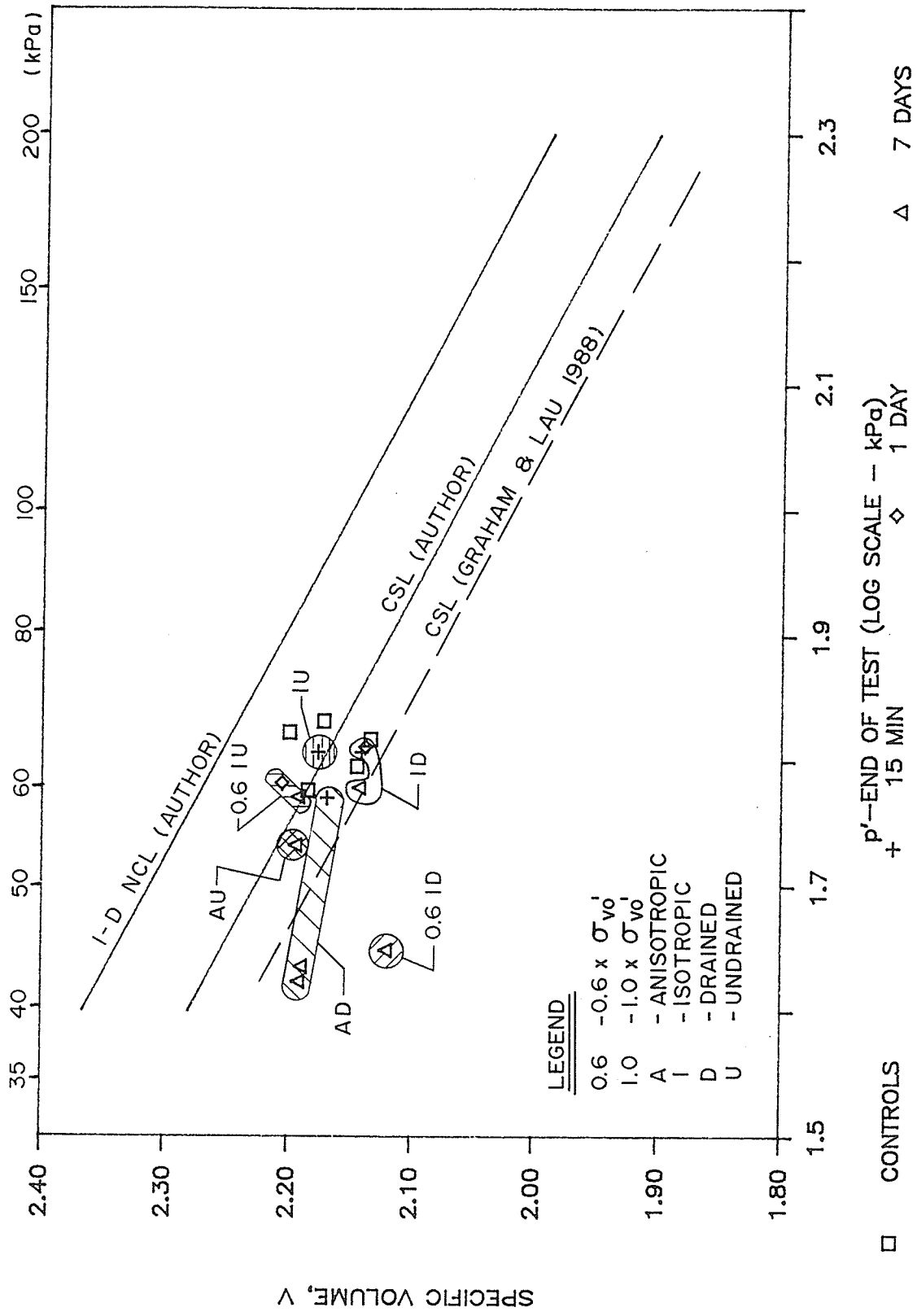


FIGURE 6.2 GRAPH OF EFFECTIVE MEAN PRESSURE,  $p'$  vs. SPECIFIC VOLUME,  $v$  AT THE END OF TEST

Appendix A

High Pressure Testing

## Appendix A - High Pressure Testing

### A.1 Introduction

As discussed in Sections 1.2 and 3.1, it was desired to initiate new technology at the University of Manitoba investigating the stress release effects associated with deep water soil sampling. Foundation piles for offshore structures are commonly placed in water depths exceeding 200 m and over 50 m into the sea bed. For proper geotechnical design, soil sampling for subsequent strength testing should be performed at these depths. To facilitate testing at these higher consolidation stresses at the University of Manitoba ( $\sigma'_v = 400$  kPa and  $u = 2000$  kPa), modifications were required to both the testing equipment and test procedures from those used in the low pressure testing portion of this thesis. These modifications as well as the results obtained will be discussed here.

### A.2 Triaxial Cell Modifications

The maximum cell pressure required for these tests was approximately 2.4 MPa. This is well above the maximum operating pressure of 1.5 MPa for the existing triaxial cells. Therefore, the capacity had to be increased. This was achieved in three basic steps. Fig. A.1 shows a schematic diagram of the high pressure triaxial cell. First, the existing clear lucite sleeve was replaced with a nickle

plated, carbon steel sleeve which has a much higher rupture strength. Secondly, the tie rods used to clamp the sleeve to the cell base were replaced with high tensile strength steel. Lastly, the connection between the rotating bushing and axial load piston housing and the top of the sleeve was made stronger. Also, a better seal was required between the the piston and the rotating bushing. A circular "wiper" seal was installed to facilitate this.

### A.3 Test Procedure Modifications

It was desired to follow the same test procedures as much as possible that were used in the low pressure testing portion of this thesis (see Section 3.2 for details) so that consistent conclusions could be made. This could be attained for the most part. However a potential problem during the unloading of confining stresses was foreseen. Fig. A.2 shows the predicted isotropic unloading curve for a sample with an in-situ stress state of  $\sigma'_v = \sigma'_h = 400$  kPa with  $u = 2000$  kPa (assuming  $\bar{B} = 1.0$ ). As can be seen, a potential negative porewater pressure of  $-400$  kPa could be induced in the specimen when the confining pressure was reduced to zero. It is believed that the water in the pore structure of the clay specimen would be able to sustain these high tension stresses. However, there is a potential for the water in the drainage leads surrounding the porewater pressure transducer to cavitate, since the cavitation point of  $-100$  kPa would be exceeded. This would lead to incorrect porewater pressure

readings. To reduce the risk of this cavitation, three modifications were implemented.

First, the pedestal base of the triaxial cell was modified so that the porewater pressure transducer could be installed immediately below the base of the test specimen, as shown in Fig. A.3. This would reduce the volume of fluid that would be subjected to the high negative porewater pressures. Secondly, it was decided to replace the water in the drainage leads with a bentonite-water slurry mixture. It was postulated that the introduction of the small clay particles would increase the tensile strength (that is, the cavitation point) of the fluid above that of pure water due to increased electromagnetic bonding. Finally, a high air entry ceramic disc was used in place of the conventional porous filter stone so that cavitation within the filter stone would not occur.

#### A.4 Results

During the triaxial consolidation, two high pressure samples were attempted (T790 and T791). Unfortunately, both were destroyed due firstly to faults in the consolidation process and secondly, to equipment failures. Each sample and its destruction will be described.

Triaxial consolidation was conducted in the same manner as for the low pressure testing, that is, a one day loading period for each consolidation stress with a constant load increment ratio of 1.29.

However, the effective stresses were approximately five times higher than that of the low pressure testing. At the end of the 6<sup>th</sup> load increment ( $p'=170.0$  kPa,  $q=116.6$  kPa, and  $u=1725$  kPa), the cell pressure was increased and the additional axial load was applied to bring the stress levels to  $p'=219.2$  kPa and  $q=150.4$  kPa. The moment that the axial load was applied, the sample (T790) was instantly sheared. It is believed that a shear failure occurred due to a continual build-up of excess porewater pressure with successive load increments. The one day time period between each stress increment was not long enough to allow for dissipation of excess porewater pressure. Fig. A.4 shows the curves of  $V$  vs.  $\log(\text{time})$  for each load increment. It can be seen that the incremental volume change for each successive load increment increased for the same time period (one day). This is evidence of porewater pressure build-up with time and eventually the undrained shear strength of the clay was exceeded, leading to an undrained shear failure.

A second specimen (T791) was then installed in the high pressure triaxial cell to again attempt the consolidation process. To help allow for dissipation of porewater pressure build-up, the confining cell pressure was increased approximately 2-3 hours prior to the addition of axial load for each load increment. Also, the volume change with time and the percent consolidation was monitored. Every second or third load increment, the sample was allowed to consolidate for an extra day or two. This provided for extra time for partial porewater pressure dissipation as well as keeping the consolidation

period as short as possible. This seemed to alleviate the problem.

However, during the night of the 8<sup>th</sup> load increment ( $p'=284.1$  kPa and  $q=193.7$  kPa), a major leak occurred around the outside of the piston. All the water in the triaxial cell and the air/water exchange tank leaked out of the cell and consequently, the confining pressure was lost. With the high axial load on the piston and no confining pressure, the sample was again sheared instantly.

It is unfortunate that these problems occurred and no positive data was obtained. Due to time constraints in the program, no more high pressure testing was attempted. While no useful results with respect to the earlier work reported in this thesis were obtained, the tests have been recorded here to place on record the work that has been done and some of the difficulties that might be encountered in future testing at high pressures.

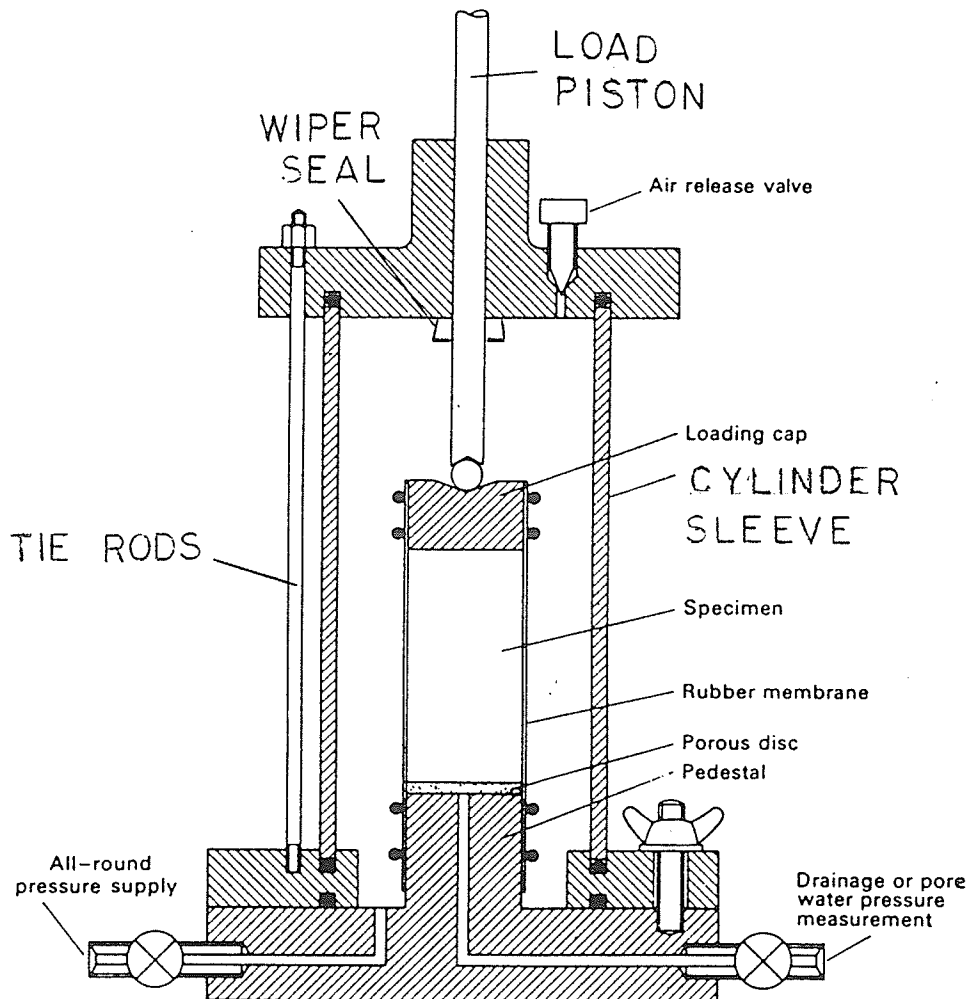


FIGURE A.1 SCHEMATIC DIAGRAM OF HIGH PRESSURE TRIAXIAL CELL  
(CRAIG 1983)

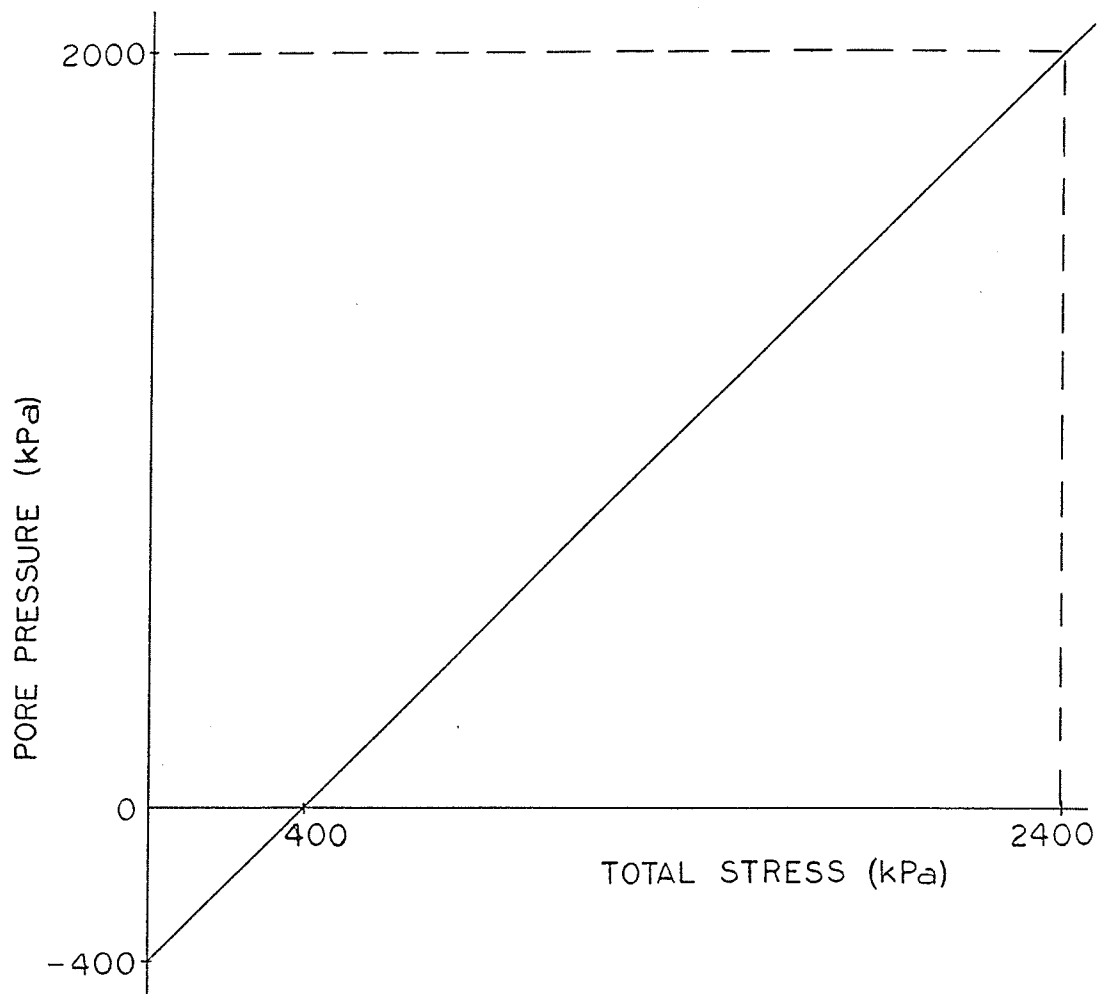
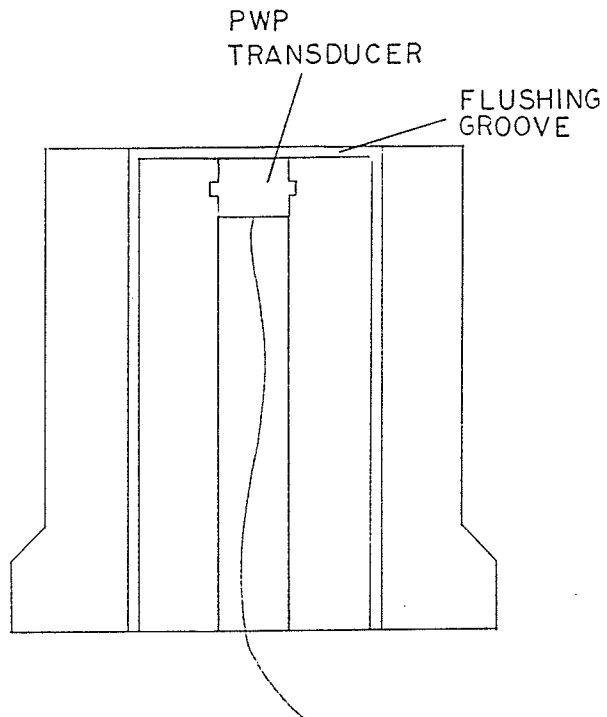
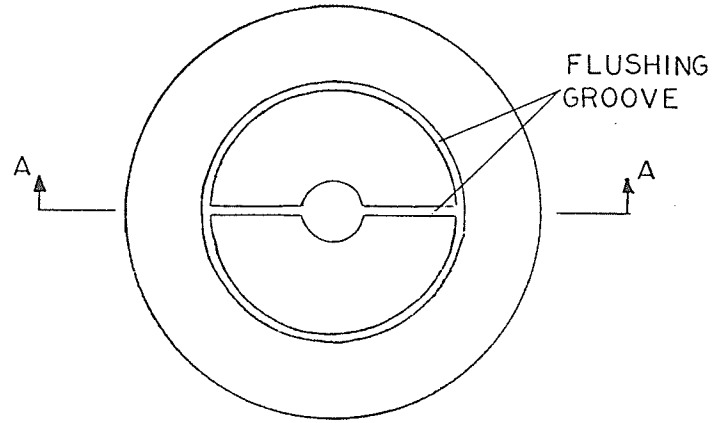


FIGURE A.2 PREDICTED ISOTROPIC UNLOADING BEHAVIOUR FOR IN-SITU STRESS STATE OF  $\sigma_v' = \sigma_h' = 400$  kPa,  $u = 2000$  kPa ( $\bar{B}=1.0$ )



SECTION A-A

SCALE



FIGURE A.3 SCHEMATIC DIAGRAM OF THE MODIFIED PEDESTAL BASE OF HIGH PRESSURE TRIAXIAL CELL

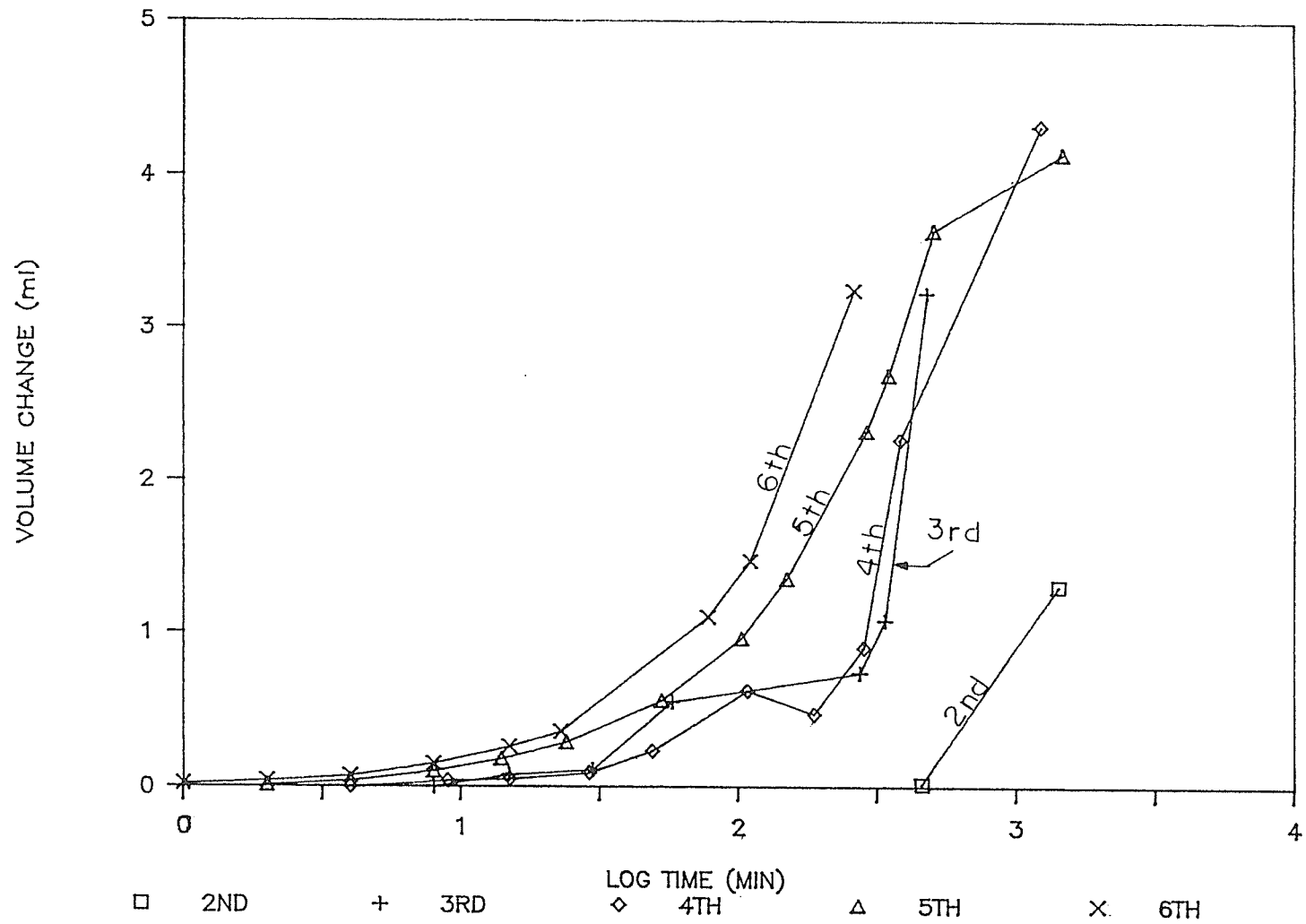


FIGURE A.4 SPECIFIC VOLUME,  $V$  vs. LOG (TIME) DURING CONSOLIDATION, SAMPLE T790